

# Near-field projection as an adaptive driver assistance system - a technical and human-oriented consideration for future traffic scenarios

**Nahfeldprojektion als adaptives Fahrerassistenzsystem - eine technische und menschenorientierte Betrachtung für zukünftige Verkehrsszenarien**

Zur Erlangung des akademischen Grades Doktor-Ingenieur (Dr.-Ing.)

Genehmigte Dissertation von Alexander Stuckert aus Moskau

Tag der Einreichung: 11. September 2023, Tag der Prüfung: 30. November 2023

1. Gutachten: Prof. Dr.-Ing. habil. Tran Quoc Khanh

2. Gutachten: Prof. Dr. rer. nat. Cornelius Neumann

Darmstadt 2023 – D17

Technische Universität Darmstadt



TECHNISCHE  
UNIVERSITÄT  
DARMSTADT

Electrical Engineering and  
Information Technology  
Department

Laboratory of Adaptive  
Lighting Systems and Visual  
Processing

Near-field projection as an adaptive driver assistance system - a technical and human-oriented consideration for future traffic scenarios

Nahfeldprojektion als adaptives Fahrerassistenzsystem - eine technische und menschenorientierte Betrachtung für zukünftige Verkehrsszenarien

Accepted doctoral thesis by Alexander Stuckert

Date of submission: 11. September 2023

Date of thesis defense: 30. November 2023

Darmstadt 2023 – D17

Technische Universität Darmstadt

Bitte zitieren Sie dieses Dokument als:

URN: urn:nbn:de:tuda-tuprints-263988

URL: <http://tuprints.ulb.tu-darmstadt.de/26398>

Jahr der Veröffentlichung auf TUprints: 2023

Dieses Dokument wird bereitgestellt von tuprints,  
E-Publishing-Service der TU Darmstadt

<http://tuprints.ulb.tu-darmstadt.de>

[tuprints@ulb.tu-darmstadt.de](mailto:tuprints@ulb.tu-darmstadt.de)

Die Veröffentlichung steht unter folgender Creative Commons Lizenz:

Namensnennung – Weitergabe unter gleichen Bedingungen 4.0 International

<https://creativecommons.org/licenses/by-sa/4.0/>

This work is licensed under a Creative Commons License:

Attribution–ShareAlike 4.0 International

<https://creativecommons.org/licenses/by-sa/4.0/>



---

## Erklärungen laut Promotionsordnung

### § 8 Abs. 1 lit. c PromO

Ich versichere hiermit, dass die elektronische Version meiner Dissertation mit der schriftlichen Version übereinstimmt.

### § 8 Abs. 1 lit. d PromO

Ich versichere hiermit, dass zu einem vorherigen Zeitpunkt noch keine Promotion versucht wurde. In diesem Fall sind nähere Angaben über Zeitpunkt, Hochschule, Dissertationsthema und Ergebnis dieses Versuchs mitzuteilen.

### § 9 Abs. 1 PromO

Ich versichere hiermit, dass die vorliegende Dissertation selbstständig und nur unter Verwendung der angegebenen Quellen verfasst wurde.

### § 9 Abs. 2 PromO

Die Arbeit hat bisher noch nicht zu Prüfungszwecken gedient.

Darmstadt, 11. September 2023

---

Alexander Stuckert



---

# Abstract

---

The present work deals with the fundamental consideration of optical parameters for designing a projection system for near-field projections based on perceptual-physiological criteria to enable a user-oriented and technology-independent design of the projection system. For this purpose, different psychophysical tests on resolution and brightness perception of near-field projections investigated the parameters and dependencies in seven participant tests.

Therefore, the testing on resolution perception shows that for a near-field projection at a maximum distance of 5 m from the vehicle, the resolution requirements for dynamic representations (25 pixels per degree (ppd)) are almost just half as high as for static symbols or texts (40 ppd) in the mesopic adaptation level, which in the studies is between  $0.5$  and  $2 \text{ cd m}^{-2}$ . In addition, DIN 1450 [1] recommends compliance, as non-compliance with this standard leads to increased resolution requirements due to the influence of projection size and text type, especially for safety-relevant near-field projections. From the psychophysical tests performed and the perceived resolution requirements for near-field projections, it is finally possible to conclude the resolution of the microdisplay to evaluate the current technology in this respect. State of the art shows that the resolution requirements of the subject studies are already achieved with a DMD or LCoS system for near-field projections, and a  $\mu$ LED microdisplay still requires 2.5 times the resolution for dynamic projections.

The tests on brightness perception show various influences on the perception of near-field projections based on psychophysical data. A significant influence of adaptation environment on the threshold of contrast perception is present between mesopic ( $\approx 0.6 \text{ cd m}^{-2}$ ) and photopic (above  $210 \text{ cd m}^{-2}$ ) adaptation luminances. In addition, the influence of projection content, whether a near-field projection is symbol-based or text-based, impacts the perception of the near-field projection since, at reaction times of 600 to 650 ms, the symbol-based near-field projection has lower detection contrast thresholds. Furthermore, compared to a static representation of the same projection content in the mesopic region, a dynamic projection shows a 38% lower detection contrast threshold, providing better detectability in safety-critical situations in urban road traffic. Finally, the dependence of the recognition contrasts on the position of the near-field projection in the peripheral visual field was also determined.

The perception tests' results and the projections' associated illuminance levels create a model that defines the necessary illuminance level of the projected object for direct or peripheral viewing of a near-field projection as a function of the ambient lighting level. This model can determine for each environmental condition the necessary illuminance of the projection for a detection probability of 90% and the resulting characteristics of the projector. Furthermore, this model evaluates the current state of the art and assesses the limitations of the available technologies for near-field projections using a user-oriented model, such as that an LCoS projection system is only sufficient for projections at night and in illuminated streets. In contrast, if the brightness increases thrice, a DMD projection system guarantees visibility during dusk and dawn.



---

# Zusammenfassung

---

Die vorliegende Arbeit beschäftigt sich mit der grundlegenden Betrachtung optischer Parameter für die Gestaltung eines Projektionssystems für Nahfeldprojektionen anhand wahrnehmungsphysiologischer Kriterien, um eine nutzerorientierte und technologieunabhängig Gestaltung des Projektionssystems zu ermöglichen. Dazu werden in insgesamt sieben verschiedenen Studien unterschiedliche psychophysikalische Tests zur Auflösungs- und Helligkeitswahrnehmung von Nahfeldprojektionen durchgeführt.

So zeigen die Untersuchungen zur Auflösungs- und Helligkeitswahrnehmung, dass für eine Nahfeldprojektion, die maximal 5 m vom Fahrzeug entfernt ist, die Auflösungsanforderungen für dynamische Darstellungen (25 Pixel pro Grad (ppd)) ca. halb so hoch sind wie für statische Symbole oder Texte (40 ppd) im mesopischen Adaptionsbereich, der in den Untersuchungen zwischen 0,5 und 2  $\text{cd m}^{-2}$  liegt. Darüber hinaus wird die Einhaltung der DIN 1450 [1] empfohlen, da die Missachtung dieser Norm speziell für sicherheitsrelevante Nahfeldprojektionen zu erhöhten Auflösungsanforderungen hinsichtlich des Einflusses von Projektionsgröße und Textart führt. Aus den durchgeführten psychophysischen Tests und den wahrgenommenen Auflösungsanforderungen für Nahfeldprojektionen kann schließlich auf die Auflösung des Bildgebers geschlossen werden, um die aktuelle Technologie diesbezüglich zu bewerten. Der Stand der Technik zeigt, dass die Auflösungsanforderungen der Probandenstudien bereits mit einem DMD- oder LCoS-System eines Nahfeldprojektors erreicht werden und ein  $\mu\text{LED}$ -Mikrodisplay Projektor noch die 2,5-fache Auflösung für eine dynamische Projektion benötigt.

Die Untersuchungen zur Helligkeitswahrnehmung zeigen verschiedene Einflüsse auf die Wahrnehmung von Nahfeldprojektionen. Ein signifikanter Einfluss der Adaptionsumgebung auf die Schwelle der Kontrastwahrnehmung liegt zwischen mesopischen ( $\approx 0.6 \text{ cd m}^{-2}$ ) und photopischen (über  $210 \text{ cd m}^{-2}$ ) Adaptionsleuchtdichten vor. Zusätzlich hat der Einfluss des Projektionsinhaltes, ob eine Nahfeldprojektion symbol- oder textbasiert ist, einen Einfluss auf die Wahrnehmbarkeit der Nahfeldprojektion, da bei Reaktionszeiten von 600 bis 650 ms die symbolbasierte Nahfeldprojektion niedrigere Kontrastschwellen aufweist. Außerdem weist eine dynamische im Vergleich zu einer statischen Darstellung desselben Projektionsinhaltes im mesopischen Bereich eine um 38 % niedrigere Detektionskontrastschwelle auf, was eine bessere Erkennbarkeit in sicherheitskritischen Situationen im städtischen Straßenverkehr gewährleistet. Zusätzlich wurde die Abhängigkeit der Detektionskontraste von der Position der Nahfeldprojektion im peripheren Gesichtsfeld ermittelt.

Die Ergebnisse der Wahrnehmungsstudien und die damit verbundenen Beleuchtungsstärken der Projektionen werden verwendet, um ein Modell zu erstellen, das in Abhängigkeit von der vorhandenen Umgebungsbeleuchtung die notwendige Beleuchtungsstärke des projizierten Objekts für die direkte oder periphere Betrachtung einer Nahfeldprojektion definiert. Dieses Modell bestimmt je Umgebungsszenario die notwendige Beleuchtungsstärke der Projektion für eine Detektionswahrscheinlichkeit von 90 % und die daraus resultierenden Projektoreigenschaften. Darüber hinaus ist es mit Hilfe dieses Modells möglich, den aktuellen Stand der Technik zu bewerten und die derzeitigen Einschränkungen der verfügbaren Technologien für Nahfeldprojektionen anhand eines nutzerorientierten Modells zu beurteilen, wie z.B. dass ein LCoS-Projektionssystem nur für Projektionen bei Nacht und bei beleuchteten Straßen ausreicht, während ein DMD-Projektionssystem bis zu dreimal heller sein müsste, um eine Sichtbarkeit in der Dämmerung zu garantieren.



---

# Acknowledgements

---

The tests and results in this thesis were conducted from 2020 to 2023 at the BMW Group and the Laboratory of Lighting Technology in Darmstadt to acquire a Doctoral degree in Electrical Engineering and Information Technology from the Technical University of Darmstadt. In this section, I want to thank and acknowledge the ones who made this thesis possible by supporting me over the last few years.

First of all, I owe my deepest gratitude to my supervisor Prof. Dr.-Ing. habil. Tran Quoc Khanh supported me in creating the steps needed to fulfill the goals of this thesis. His advice in automotive lighting, psychological testing, and analysis of photometric parameters have been fundamental for the success of this thesis. Additionally, I am deeply grateful to Prof. Dr. rer. nat. Cornelius Neumann for his agreement to be the second referee during the doctoral examination phase following the thesis submission.

Furthermore, I want to thank my supervisor Dr. Alexander Totzauer for his advice and discussions on and besides thesis-related topics and his support during the whole process of writing this thesis.

Special thanks go to Tabea for her valuable support during the participant tests and assistance in the collaborative scientific contributions. Further, thanks go to Philipp, Richard and Andra for all the support and encouragement besides the academic side and to Denise for all the inspiring discussions. Moreover, I appreciate the help of all colleagues of the BMW Group or at the Technical University of Darmstadt, students, and subjects for their participation and support in many conducted tests.

Last but not least, this thesis would not have been possible without the support of my parents, Roman and Inna, my partner, Finja, and my friends over the last few years for backing me up at all times and accompanying me on this journey.





---

# Contents

---

<b>1. Introduction and motivation</b>	<b>1</b>
<b>2. Literature review</b>	<b>7</b>
2.1. Comparison of projection technologies . . . . .	7
2.1.1. Micro-electro-mechanical devices . . . . .	8
2.1.2. Liquid crystal based microdisplays . . . . .	9
2.1.3. Direct-emitting active matrices . . . . .	9
2.1.4. Summary of the digital projectors' comparison . . . . .	10
2.2. Applications in the automotive industry . . . . .	10
2.3. Human visual system and perceptual psychophysics . . . . .	13
2.3.1. The human eye and its perceptual mechanisms . . . . .	14
2.3.2. Perception and psychophysics . . . . .	17
2.3.3. Subjective influence on perception . . . . .	19
2.4. Research related to resolution requirements . . . . .	20
2.4.1. Resolution requirements influenced by personal factors . . . . .	20
2.4.2. Resolution requirements influenced by external factors . . . . .	22
2.5. Research related to contrast perception . . . . .	26
2.5.1. Fundamentals of contrast perception . . . . .	26
2.5.2. Evaluation of the state of the art in near-field projections . . . . .	29
2.6. Summary of the literature review . . . . .	32
2.7. Identified research questions . . . . .	33
<b>3. Experimental set-up and technical aspects for the definition of resolution requirements of near-field projections</b>	<b>35</b>
3.1. Characterization of the projection surface . . . . .	35
3.1.1. Selection of the experiment scenarios . . . . .	39
3.1.2. Determination of the resolution on the projection surface . . . . .	41
3.2. Experimental setup . . . . .	44
3.3. Test parameters . . . . .	46
3.3.1. Static projection content . . . . .	46
3.3.2. Dynamic projection content . . . . .	49
3.3.3. Research participant collectives . . . . .	50
3.4. Summary of the experimental setup . . . . .	50
<b>4. Experiment results and derived resolution requirements of near-field projections</b>	<b>53</b>
4.1. Influence factors on resolution aspects for near-field projections . . . . .	53
4.1.1. Ambient lighting . . . . .	54
4.1.2. Viewing distance . . . . .	56
4.1.3. Projection content . . . . .	56
4.1.4. Projection size . . . . .	57



4.1.5. Animation speed . . . . .	58
4.2. Summary of the resolution requirements for near-field projections . . . . .	59
4.3. Discussion and guidance for the resolution requirements of near-field projections . . . . .	61
<b>5. Experiment for the definition of contrast perception</b>	<b>63</b>
5.1. Characterization of the test setup . . . . .	63
5.1.1. Luminance coefficient and reflection of different projection surfaces . . . . .	64
5.2. Experimental setup . . . . .	67
5.3. Test parameters . . . . .	69
5.3.1. Selection of projection content . . . . .	69
5.3.2. Contrast perception with direct viewing direction . . . . .	71
5.3.3. Contrast perception of dynamic near-field projection . . . . .	73
5.3.4. Contrast perception in the peripheral field of view . . . . .	74
5.3.5. Subjective evaluation of contrasts . . . . .	74
5.3.6. Research participant collectives . . . . .	75
5.4. Summary of the experimental setup . . . . .	76
<b>6. Contrast and illuminance requirements for near-field projections</b>	<b>79</b>
6.1. Influence factors on detection contrast with direct viewing direction . . . . .	79
6.1.1. Ambient lighting . . . . .	80
6.1.2. Viewing distance . . . . .	82
6.1.3. Projection content . . . . .	82
6.1.4. Animation speed . . . . .	84
6.1.5. Projection surface . . . . .	85
6.1.6. Definition of projector illuminance for foveal detection . . . . .	85
6.2. Contrast perception in peripheral field of view . . . . .	88
6.2.1. Detection contrast . . . . .	88
6.2.2. Disturbing contrast . . . . .	91
6.2.3. Projector illuminance in the peripheral field of view . . . . .	92
6.3. Summary of the contrast and illuminance requirements for near-field projections . . . . .	94
<b>7. Summary and outlook</b>	<b>97</b>
<b>Bibliography</b>	<b>103</b>
<b>A. Additional material for the resolution tests</b>	<b>115</b>
A.1. Materials for the PGS and DDS tests . . . . .	115
A.2. Materials for the SP and FR tests . . . . .	117
A.3. Materials for the DP test . . . . .	119
A.4. Questionnaire analysis . . . . .	120
A.4.1. Projection content for near-field projections . . . . .	121
A.4.2. Aspects for high quality near-field projections . . . . .	122
A.4.3. Perception of the animation speed of the dynamic near-field projections . . . . .	124
A.4.4. Additional material for the questionnaire analysis . . . . .	125
<b>B. Additional analysis for resolution aspects of near-field projections</b>	<b>127</b>
B.1. Logistic regression analysis for resolution aspects . . . . .	127
B.2. Statistical analysis for dependencies of resolution aspects . . . . .	130

---

<b>C. Additional material for the contrast and perception tests</b>	<b>133</b>
C.1. Measurements for characterizing the test setup . . . . .	133
C.2. Measurements for the luminance coefficient and reflection of the surface materials . . . . .	135
C.3. Analysis of the perception test of the various surface materials . . . . .	136
C.4. Materials for the test procedure for direct and peripheral viewing of near-field projections . . .	138
C.5. Detailed illuminance, luminance and Weber contrast measurements for the contrast perception tests . . . . .	140
<b>D. Additional analysis for contrast and brightness perception testing of near-field projections</b>	<b>147</b>
D.1. Statistical analysis for dependencies of contrast perception testing . . . . .	147
D.2. Additional analysis for direct viewing of near-field projections . . . . .	148



---

# List of Figures

---

1.1. Illustration of the worldwide death rates for different road user categories . . . . .	1
1.2. Data of a data analysis performed in Darmstadt, Germany, between 2006 and 2019 . . . . .	2
1.3. Graphical illustrations and photos display near-field projections for safety-relevant scenarios. . . . .	3
1.4. Decision-making mechanism for vulnerable RUs in traffic situations . . . . .	4
1.5. Visualization of this thesis's structure . . . . .	5
2.1. Illustration of the basic structure of a digital projector . . . . .	7
2.2. Overview of the area-based modulation technologies . . . . .	8
2.3. Illustration of projections' around the vehicle . . . . .	11
2.4. Overview of the use cases for near-field projections . . . . .	12
2.5. Distribution of cones and rods on the retina of the human eye . . . . .	14
2.6. Dark adaptation . . . . .	15
2.7. Influence factors on visual acuity . . . . .	17
2.8. Process in the visual system for perception . . . . .	18
2.9. Illustration of an example of contrast threshold testing and its psychometric analysis . . . . .	19
2.10. Plots from Gittings and Fozard [101] represent visual acuity . . . . .	21
2.11. Comparison of median logMAR values for visual acuity . . . . .	23
2.12. Examples of testing methods for dynamic visual acuity (DVA) . . . . .	24
2.13. Comparison of different resolution qualities . . . . .	25
2.14. Illustration of the luminance dependency related to the object size . . . . .	27
2.15. Detection probability of a test stimulus as a function of eccentricity . . . . .	28
2.16. Distribution of the contrast detection probability depending on the eccentricities in the field of view . . . . .	29
2.17. Picture of actual participant testing and luminance measurement . . . . .	30
3.1. Illustration of different test patterns for visual acuity testing . . . . .	35
3.2. Schematic of the simple optical structure of a human eye and the constellation of an observer who is looking with a foveal vision on the illustrated small detail . . . . .	36
3.3. Testing algorithm and picture of the used setup in the pre-test . . . . .	38
3.4. Pictures of the luminance measurements for the PGS and DDS in the pre-test . . . . .	39
3.5. Schematic visualization of the pre-test derived from Schiller [130] . . . . .	42
3.6. Characterization of the minimal resolution under different ambient illuminances . . . . .	43
3.7. Experimental setup for resolution requirements testing . . . . .	44
3.8. Picture of the setup with a test-vehicle . . . . .	45
3.9. Symbol- and text-based projection content for the PGS and DDS tests . . . . .	47
3.10. Symbol- and text-based projection content for the SP and FR tests . . . . .	48
3.11. Display of the text-based testing pattern for the SP and FR tests . . . . .	48
3.12. Design-orientated projection content was used for the DS test. . . . .	49

4.1. Logistic regression of the symbol-based projection under the consideration of dependencies for ambient lighting . . . . .	54
4.2. Logistic regression of the design-based projection under the consideration of dependencies for viewing distance . . . . .	58
5.1. Detailed illustrations for the luminance coefficient measurements . . . . .	64
5.2. Weber contrast curves for the various projection surfaces of the squared test target projection at 1 m viewing distance . . . . .	66
5.3. Different ambient scenarios for contrast perception testing . . . . .	68
5.4. Symbol- and text-based projection content for the perception testing, including a photo of the setup including a text-based projection . . . . .	70
5.5. Overview of the contrast curves for the presented stimuli (symbol and text) . . . . .	71
5.6. The setup for the evaluation of the contrast perception in the direct and peripheral field of view	72
5.7. Luminance images of the symbol- and text-based projection content in PGS at 1 m . . . . .	72
6.1. Logistic regression fitted for the Weber contrasts, including data points of the detection probability	80
6.2. Logistic regression fitted for the Weber contrasts for mesopic vision with the variation of projection content . . . . .	83
6.3. Relationship of ambient illuminance and the projection's object illuminance . . . . .	86
6.4. Logistic regression of the Weber contrast for the mesopic and photopic setting depending on the eccentricities in the peripheral field of view . . . . .	89
6.5. The relationship of the perceived Weber contrasts threshold values for different eccentricity levels	91
6.6. The relationship of the Likert scale evaluation of various Weber contrasts levels the peripheral field of view . . . . .	92
6.7. Relationship of the projection's object illuminance for direct viewing and the peripheral field of view . . . . .	93
6.8. Relationship of ambient illuminance and the projection's object illuminance in the peripheral field of view . . . . .	93
7.1. Various data inputs are processed by several algorithms for applying adaptive near-field projection as a driver assistance system. . . . .	101
A.1. Illustration of the introduction text for the participants used in the PGS and DDS tests in German.	115
A.2. Illustration of the questionnaire used in the PGS and DDS tests in German. . . . .	116
A.3. Illustration of the introduction text for the participants used in the SP and FR tests in German.	117
A.4. Illustration of the questionnaire used in the SP and FR tests in German. . . . .	118
A.5. Illustration of the introduction text for the participants used in the DP test in German. . . . .	119
A.6. Illustration of the questionnaire used in the DP test in German. . . . .	120
A.7. Boxplot of the projection content of the DP test . . . . .	121
A.8. Boxplot of the aspects for high-quality near-field projections of the DP test . . . . .	123
A.9. Boxplot of the subjective perception of the animation speed of near-field projections of the DP test	124
A.10.Boxplot of the subjective perception of the animation speed of near-field projections is pleasant of the DP test depending on the age groups . . . . .	125
A.11.Visual acuity of the SP test participants compared to the literature by Owsley et al. [147] for 20 to 59 year old participants . . . . .	126
B.1. Logistic regression of the text-based projection under the consideration of dependencies font style	127
B.2. Logistic regression of the size perception of the symbol-based projection in the SP test . . . . .	128

B.3. Logistic regression of the size perception of the text-based projection in the SP test . . . . .	128
B.4. Logistic regression of the regular and italic projection in the SP and FR testing for 1 m viewing distance . . . . .	129
C.1. Burn-in time of the projector used in the tests . . . . .	133
C.2. Illuminance surface plot for a white projection . . . . .	134
C.3. Illuminance surface plot for a black projection . . . . .	134
C.4. Appearance of the materials used for the luminance coefficient measurements and perception tests are listed above. The pictures are taken from a viewing distance of 1 m in the DLS. . . . .	135
C.5. Weber contrast curves for the various projection surfaces of the squared test target projection at 5 m viewing distance . . . . .	136
C.6. Burn-in time of the ambient lighting used in the tests for DLS . . . . .	137
C.7. Introduction text for the participants used in the contrast perception testing in German . . . . .	138
C.8. Introduction text for the participants used in the subjective contrast evaluation testing in German	139
C.9. Luminance measurement of the symbol-based projection content in PGS at 1 m and 5 m . . . . .	143
C.10.Luminance measurement of the text-based projection content in PGS at 1 m and 5 m . . . . .	144
C.11.Luminance measurement of the symbol-based projection content in PGS in the threshold region	144
C.12.Luminance measurement of the text-based projection content in PGS in the threshold region .	145
C.13.Luminance measurement of the symbol-based projection content in DLS at 1 m and 5 m . . . . .	146
C.14.Luminance measurement of the text-based projection content in DLS at 1 m and 5 m . . . . .	146
D.1. Logistic regression of the Weber contrast for the photopic setting . . . . .	148
D.2. Overview of the eight stimuli presented for the illuminance levels . . . . .	148
D.3. Overview of the eight stimuli presented for the illuminance levels . . . . .	148
D.4. Overview of the eight stimuli presented for the Weber contrast . . . . .	149
D.5. Logistic regression curves and data points of the detection probability percentages for the various environmental scenarios . . . . .	149
D.6. Logistic regression fits and data points for the detection probability percentages of the various environmental scenarios . . . . .	149
D.7. Logistic regression of the projection's illuminance for the mesopic setting . . . . .	150





---

# List of Tables

---

1.1. Shares of accidents for vulnerable RUs depend on the location of the accidents and depending on the time of the day. The statistics for the USA focus solely on pedestrians [3], whereas the numbers for Germany include pedestrians and cyclists [4]. All numbers in the table are in percent. . . . .	2
2.1. Comparison of digital area-based modulated projectors characteristics for the automotive sector regarding resolution, contrast, and optical efficiency [34, 13, 14, 37, 38] . . . . .	10
2.2. Comparison of the near-field projector prototypes for DMD or LCoS solution and comparable data of headlamp projectors with $\mu$ LED as a correspondence with the related literature indicated in the table cells. . . . .	13
2.3. Interaction of the receptor types results in different types of vision and depends on the adaptation luminance [30, 31]. The overview is retrieved from Gross [31]. . . . .	15
2.4. Literature review related to resolution aspects, including test parameters and possible impact aspects such as external and personal factors. Table 2.3 indicates different levels of vision. . .	32
2.5. Summary of the literature review related to contrast perception, including test parameters and possible impact aspects such as external and personal factors. Table 2.3 indicates different levels of vision. . . . .	33
3.1. List of the used gap sizes on the projection surface in mm and as multiple of 1' depending on the participant's viewing distance of either 1 m or 3 m to the projection area. . . . .	39
3.2. Measured luminance levels for viewing distance of either 1 m or 3 m to the projection in the PGS or DDS. The measurements relate to a 2.93 mm thick lines with a 5.35 mm gap size. . . .	40
3.3. List of resulting Weber contrasts $C_{Weber}$ in the pre-test depending on the viewing distance (1 m or 3 m) and the scenario (PGS or DDS). . . . .	41
3.4. Perceived detail size on the ground for a 90 % threshold level evaluated by the participants for the line pair projected under different adaptation luminance levels (PGS and DDS) defined in mm and as a multiple of one angular minute by applying equation 3.6. . . . .	44
3.5. Summary of the variation of viewing distances and the resulting viewing angles assuming a person's height of 1.72 m [125] for all conducted studies in Chapter 3 and 4. . . . .	49
3.6. List of the subject collectives' characteristics for all participants of the tests for defining the resolution requirements of near-field projections. The characteristics consist of the number of subjects $N$ , the age of the subjects, including the standard deviation of the age in every collective, the age range in every test, the number of females or males, and the proportion of visual aid usage. . . . .	50
3.7. Summary of the variation of the executed tests involving the characteristics for the ambient illuminance levels, ambient luminances on the street's surface, and the perceived Weber contrast of the projected content on the street. . . . .	51

4.1. Results for the perceived resolution on the projection surface for a 90 % threshold level fitted by the logistic function for the symbol-based projection content under different adaptation luminance levels defined in pixels per degree ( <i>ppd</i> ). The numbers in brackets indicate the confidence intervals of 95 %, with the lower bound as the left number and the higher bound as the right number for the three distances and two ambient lighting levels tested in the PGS and DDS. . . . .	55
4.2. Resolution on the projection surface for a 90 % threshold level fitted by the logistic function for the symbol- and design-based projection content under different viewing distances defined in pixels per degree ( <i>ppd</i> ). The numbers in brackets indicate the confidence intervals of 95 %, with the lower bound as the left number and the higher bound as the number on the right for the DDS and DP tests. . . . .	59
4.3. The participants evaluated the resolution requirements on the projection surface for a 90 % threshold level fitted by the logistic regression for the symbol-, text- and design-based projection content under different adaptation luminance levels and various viewing distances defined in pixels per degree ( <i>ppd</i> ). The numbers in brackets indicate the confidence intervals of 95 %, with the lower bound as the left number and the higher bound as the number on the right of the perceived resolution on the street under the consideration of the characteristics displayed in Table 3.7. . . . .	60
5.1. Overview of the reflection <i>S</i> classification according to the CIE [133] for the five measured surface materials of asphalt, white panel, rubber, white leather and brown leather for the PGS and DDS. All materials are diffusely scattering $S < 0.4$ . . . . .	65
5.2. Detection contrasts extracted from Figure 5.2 for a 90 %-threshold level of the fitted data for a 1 m viewing distance of the five projection surfaces: asphalt, rubber, white panel, and brown and white leather. . . . .	67
5.3. Calculated viewing angles in horizontal and vertical direction from the distances 1 m and 5 m for the symbol- and text-based projections. An exemplary eye height of 168 cm was used for the calculation, which relates to an average German person [125]. . . . .	70
5.4. Summary of the used parameters in the subjective evaluation of perceived contrasts in the peripheral field of view like projection content, grayscale levels, Weber contrast range in the mesopic environment at a viewing distance of 5 m, the examined eccentricities and the display time of the near-field projection during testing. . . . .	75
5.5. List of the participants collectives' characteristics for all participants of the contrast perception tests. The parameters are the participants's number <i>N</i> , the participants' age, the age's standard deviation in every collective, the age range, the number of females or males, and the visual aid usage in %. . . . .	76
5.6. Overview of the variation of the executed tests of direct or peripheral viewing and the dynamics' influence involving the characteristics for the projection content, viewing distance, eccentricities in the peripheral view, projections' display time, and dynamics. The used grayscale levels of the projection and the perceived Weber contrasts for 1 m and 5 m viewing distance are also listed. . . . .	77
6.1. Results for the perceived Weber contrast on the projection surface for a 90 % threshold of the logistic function for the symbol- and text-based projection for two adaptation luminances ( $L_{\text{Background}} \approx 0.6 \text{ cd m}^{-2}$ , $L_{\text{Background}} \approx 235 \text{ cd m}^{-2}$ ). The numbers in the bracket indicate the confidence intervals of 95 %, with the lower bound (left number) and the higher bound (right number) for two viewing distances and two adaptation scenarios. . . . .	80

6.2.	Chi-square analysis defines the statistical effects of the ambient luminance influence responsible for a mesopic and photopic vision for 1 m and 5 m viewing distance for a symbol- and text-based projection. . . . .	81
6.3.	Values of the continuous logistic regression fit determine the 90 % detection contrast for the symbol-based projection with the representations of dynamic with 3 Hz for a duration of 2 s, static representation for 350 ms, and static for 2000 ms under mesopic and photopic vision at a viewing distance of 1 m. . . . .	84
6.4.	Results for projector's illuminance levels of the psychophysical testing on the projection surface for a 90 % threshold of the logistic function for the symbol-based projection for two adaptation luminances ( $L_{\text{Background}} \approx 0.6 \text{ cd m}^{-2}$ , $L_{\text{Background}} \approx 235 \text{ cd m}^{-2}$ ). The numbers in the bracket indicate the confidence intervals of 95 %, with the lower bound (left number) and the higher bound (right number) for two viewing distances and two adaptation scenarios. . . . .	85
6.5.	The table includes the extracted luminous flux of Table 2.2 and the calculated object illuminance by the equation 6.2 with the assumed projection size analog to the symbol-based projection of $A_{\text{projection}} = 0.62 \text{ m} \cdot 0.41 \text{ m}$ . Additionally, the inverse relationship of equation 6.3 concludes the maximal ambient illuminance for the illuminated projection to be detectable. . . . .	87
6.6.	Ambient illuminance levels, according to Kloppenburg [169], are ordered from high to low ambient illuminance levels. . . . .	87
6.7.	90 % Weber contrast threshold levels determined for the mesopic and photopic vision for the symbol and text-based projection. The Weber contrasts per eccentricity of either 0, 5, 10, 20, or 30 degrees are displayed with the 95 % confidence intervals (lower and upper bound in the brackets). . . . .	89
6.8.	Chi-square analysis defines the statistical effects of various eccentricities of the projection located in the peripheral field of view at a viewing distance of 5 m for mesopic and photopic testing environments. The Table also includes the related effect size (Cramer's V). . . . .	90
6.9.	The table includes the extracted luminous flux of Table 2.2 and the calculated object illuminance by the equation 6.4 with the assumed projection size analog to the symbol-based projection of $A_{\text{projection}} = 0.62 \text{ m} \cdot 0.41 \text{ m}$ . Additionally, the inverse relationship of equation 6.4 concludes the maximal ambient illuminance for the illuminated projection to be detectable by peripheral vision. . . . .	94
A.1.	Projection sizes of the SP and FR tests displayed in the resulting viewing angle (vertical and horizontal) of the participants with an average German person's height [125] in degrees. The participant is either 1 m or 3 m apart from the projection area. . . . .	118
A.2.	MANOVA with the Wilks test for the near-field projection contents displayed in Figure A.7 under the consideration of influence factors such as age and previous knowledge for the DP test. . . . .	122
A.3.	MANOVA with the Wilks test for aspects of high-quality for near-field projections displayed in Figure A.8 under the consideration of age as an influencing factor for the DP test. . . . .	123
A.4.	MANOVA with the Wilks test for the perception of the animation speed of the projected content, which refers to Figure A.7, under the consideration of influence factors such as age and previous knowledge for the DP test. . . . .	125
A.5.	ANOVA regarding the animation speed perception if the displayed design-orientated animation in the DP test gave a pleasant feeling to the participants while observing the animation. . . . .	125
B.1.	Chi-square analysis defines the statistical effects of viewing distance, ambient lighting, and projection content for PGS and DDS tests. The Table also includes the related effect size (Cramer's V). . . . .	130

B.2.	Chi-square analysis defines the statistical effects of viewing distance, projection size, and projection content for the SP test. The Table also includes the related effect size (Cramer's V).	131
B.3.	Chi-square analysis defines the statistical effects of the projection content of either the comparison of the symbol- and text-based projection and the two various fonts (regular and italic) for the SP and FR tests. The Table also includes the related effect size (Cramer's V).	131
C.1.	Measured target illuminance $E_{\text{target}}$ and luminance $L_{\text{target}}$ to obtain the luminance coefficient $q$ of equation 5.2 for the PGS and DDS.	135
C.2.	Calculated luminance coefficient $q$ for the measuring angles $\gamma$ of $0^\circ$ and $63.5^\circ$ to obtain the reflection $S$ with equation 5.2 for the PGS and DDS.	135
C.3.	Weber contrasts perceived in the pre-test for the perception of illuminance levels on various projection surfaces.	136
C.4.	Detection contrasts for a 90 %-threshold level of the fitted data in Figure 5.2 for a 5 m viewing distance of the five projection surfaces: asphalt, rubber, white panel, and brown and white leather.	137
C.5.	Used grayscale intensities with the resulting illuminances and Weber contrasts of the <b>symbol-based projections</b> in the <b>PGS</b> at viewing distances of 1 m and 5 m. Weber contrasts marked with a dash are not measured since these contrasts are not relevant to the conducted tests.	140
C.6.	Used grayscale intensities with the resulting illuminances and Weber contrasts of the <b>text-based projections</b> in the <b>PGS</b> at viewing distances of 1 m and 5 m. Weber contrasts marked with a dash are not measured since these contrasts are not relevant to the conducted tests.	141
C.7.	Used grayscale intensities with the resulting illuminances and Weber contrasts of the <b>symbol-based projections</b> in the <b>DLS</b> at viewing distances of 1 m and 5 m. Weber contrasts marked with a dash are not measured since these contrasts are not relevant to the conducted tests.	142
C.8.	Used grayscale intensities with the resulting illuminances and Weber contrasts of the <b>text-based projections</b> in the <b>DLS</b> at viewing distances of 1 m and 5 m. Weber contrasts marked with a dash are not measured since these contrasts are not relevant to the conducted tests.	143
D.1.	Chi-square analysis defines the statistical effects of projection content, and viewing distance, for mesopic and photopic testing environments. The Table also includes the related effect size (Cramer's V).	147
D.2.	Chi-square analysis defines the statistical effects of projection's display mode in 1 m viewing distance for mesopic and photopic testing environments. The mode 3 Hz relates to the dynamic display of the projection for 2 s, and the other two variations are in static mode for either 350 ms and 2000 ms projection's display duration.	147

---

# Index of Abbreviations

---

<b>AI</b>	Artificial Intelligence
<b>CIE</b>	Commission Internationale de l'Éclairage
<b>DDS</b>	Dusk and Dawn Scenario
<b>DLS</b>	Daylight Scenario
<b>DMD</b>	Digital Micromirror Device
<b>DP</b>	Dynamic Projection
<b>DVA</b>	Dynamic Visual Acuity
<b>dpi</b>	Dots Per Inch
<b>FR</b>	Font Relation
<b>GPS</b>	Global Positioning System
<b>HD</b>	High Definition
<b>HMI</b>	Human-Machine-Interface
<b>LC</b>	Liquid Crystal
<b>LCD</b>	Liquid Crystal Display
<b>LCoS</b>	Liquid Crystal on Silicon
<b>LED</b>	Light-Emitting Diode
<b>MEMS</b>	Micro-Electro-Mechanical Systems
<b>PGS</b>	Parking Garage Scenario
<b>ppd</b>	Pixel Per Degree
<b>PWM</b>	Pulse Width Modulation
<b>RU</b>	Road User
<b>S</b>	Reflection behavior
<b>SP</b>	Size Perception
<b>SVA</b>	Static Visual Acuity

---

<b>USA</b>	United States of America
<b>VA</b>	Visual Acuity
<b>WHO</b>	World Health Organisation

# 1. Introduction and motivation

When developing new lighting systems, the human being and his visual system should be the focus of the development. Human well-being, safety, and performance can increase the application of lighting technology - particularly evident in road traffic. Here, lighting or signaling systems significantly influence traffic safety during the day and at night. Cars incorporate several lighting functions like headlights to ensure that the driver has a clear view of the traffic and a sufficiently illuminated foreground at night to perform the driving task safely. Additionally, signaling systems such as tail, brake, or daytime running lights increase the vehicle's visibility and indicate dangerous situations to other traffic members.

Nevertheless, according to the World Health Organisation (WHO) [2], road traffic is the eighth leading cause of death worldwide no matter what age and even ranked the number one reason for the age group of 5 to 29 years old traffic members. In order to improve future traffic, it is necessary to understand current traffic scenarios and to identify critical or safety-relevant situations. Thus, it is necessary to understand which road users (RUs) are at risk and which conditions have led to these safety-critical situations in traffic. The global status report on road safety from 2018 by the WHO compares the various regions worldwide, showing the distribution of traffic fatalities by mode of transport in Figure 1.1 [2].

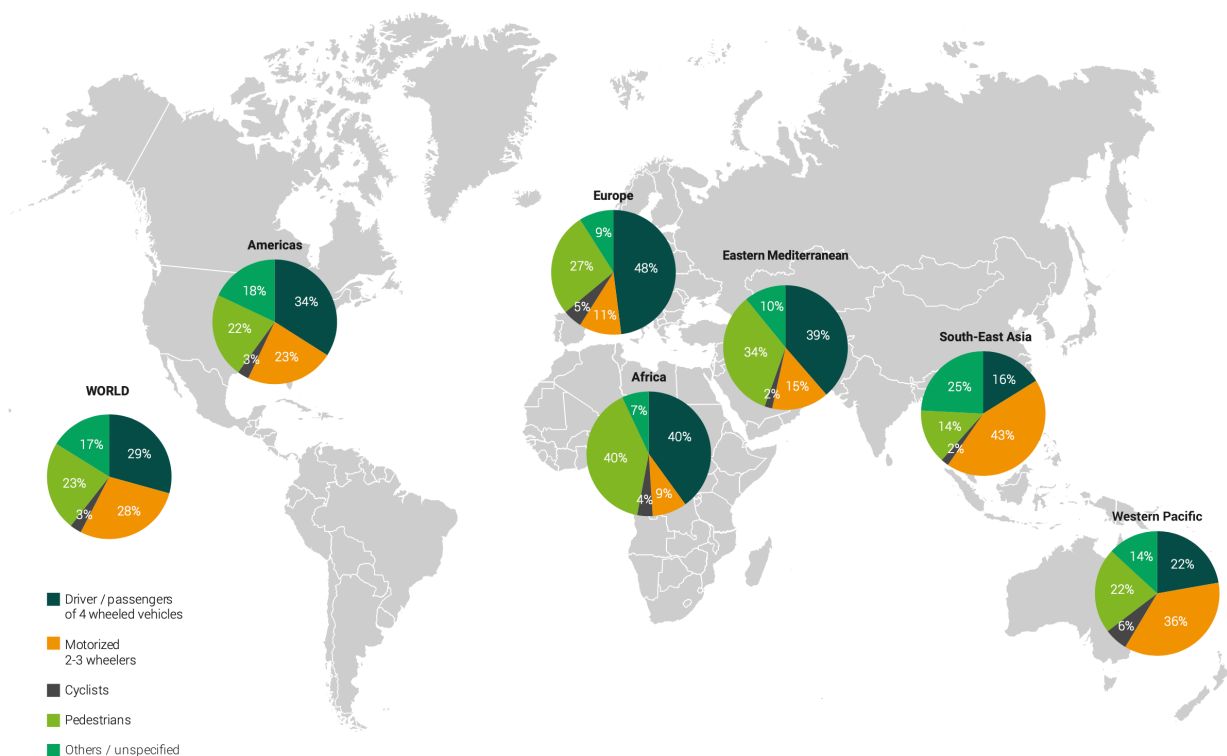


Figure 1.1.: Illustration of the worldwide death rates for different road user (RU) categories per region. The RU categories include vehicle's driver and passengers, motorized 2-3 wheeled vehicles, cyclists, pedestrians, and others, retrieved from the WHO report [2].

Figure 1.1 illustrates clearly that, except for South-East Asia, the percentage shares of traffic fatalities among vulnerable RUs, here the pedestrians and cyclists, ranges from 25 to 44 % worldwide. Averaging the global distribution, Figure 1.1 on the left shows that vulnerable RUs account for 26 % of all traffic fatalities, and the WHO indicates a share of 56 % [2], as they have included motorized 2-3 wheelers in their definition of vulnerable RUs due to poorer protection and lower road safety compared to four-wheeled vehicles. However, an exemplary comparison between the United States of America (USA), located on the North American continent, and Germany, as a possible representative of Europe, illustrates the complexity and variability of accident patterns in Table 1.1.

Table 1.1.: Shares of accidents for vulnerable RUs depend on the location of the accidents and depending on the time of the day. The statistics for the USA focus solely on pedestrians [3], whereas the numbers for Germany include pedestrians and cyclists [4]. All numbers in the table are in percent.

	Urban	Rural	Daylight	Dusk and dawn	Night
<b>USA</b>	83.8	15.43	19.36	6.16	74.48
<b>Germany</b>	69.3	24.9	71.59	4.8	23.6

By looking at the accident locations in detail (Table 1.1), parallels are visible between the two countries for RU accidents in urban areas, 83.8 % of which occur in the USA and 69.3 % in Germany. In the USA in 2021, 76.81 % of accidents occur on open roads and 22.82 % at intersections, while in urban areas, collisions with turning or crossing vehicles are more frequent in Germany (30.6 %) than in the USA (22.82 %). [3, 4] A striking difference is that in the USA, about 75 % of accidents involving pedestrian accidents occur at night due to, e.g., limited visibility for the driver or a possible lack of distance estimation, especially for elderly drivers who are an essential target group due to the continuously aging population [3, 5, 6]. Further, Germany has an accident share of 71.59 % involving vulnerable RU injuries and fatalities to cyclists or pedestrians happening during the day and 77.22 %, if looking solely at hazards in German urban areas [4]. Singer et al. underline the overall statistics with detailed protocols from Darmstadt in Germany, where 70 % of the analyzed accidents in the urban area of Darmstadt was during daylight (see Figure 1.2 in the middle) [7].

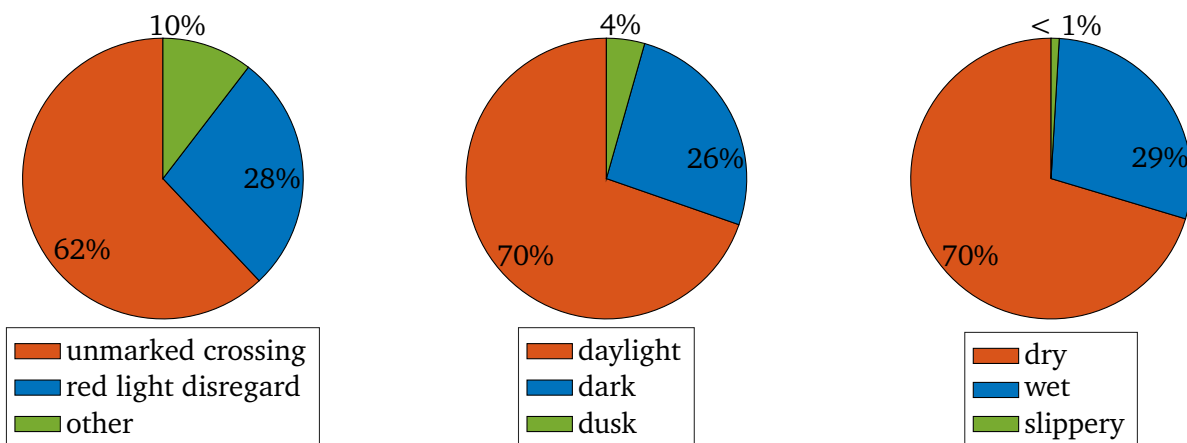


Figure 1.2.: Data of a data analysis performed in Darmstadt, Germany, between 2006 and 2019 for accidents where the pedestrian is the cause. In total, the analysis displays  $N = 432$  protocols for the cause of the accident (on the left), light conditions (in the middle), and road conditions for the accident (on the right). The data is retrieved from the contribution of Singer et al. [7].



The number of analyzed accidents in the contribution of Singer et al. refers to just accidents where the pedestrian causes the accident in the urban area, since in the future, urban traffic will be one of the last remaining nonautomated RUs because Singer et al. consider a reduction of the vehicle caused accidents due to the introduction of automated vehicles. Within the 432 analyzed hazards, the most common accident cause is a concealed pedestrian who steps on the road. [7] Therefore, focusing on projection-based accident prevention is necessary since displayed messages on the car's body are not visible for concealed RUs. The data of Singer et al. in Figure 1.2 (on the left) are also comparable to the data in the USA since the central location, or cause of an accident is an interaction at an unmarked crossing in 62% of all accidents followed by 28% of red light disregard. [7] However, in the USA, the unmarked crossing occurs 20% likelier [3]. Furthermore, Figure 1.2, on the right, considers the road conditions, where 70% of accident occurs in dry conditions [7].

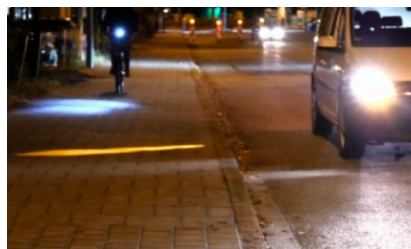
With the steady progress of urbanization and the associated population growth in cities, traffic density in urban areas is increasing. Whereas in 2010, about 70% of the American population lived in cities, the population in urban areas also gained popularity worldwide. [8, 9, 10] This development again underscores the need for technologies to mitigate safety-critical situations. Increasing urbanization will lead to further conflict between vehicles and vulnerable RUs in urban areas if the automotive industry does not seek a solution.

Focusing on the other group of vulnerable RUs - the cyclists, the rate of deaths increased in 15 countries worldwide between 2010 and 2019, including not only Germany, Denmark, and Norway, with increases of less than 30%, but also the USA, Israel, and Argentina, with increases of over 30% to 130%, which highlights the need for explicit consideration of accidents involving cyclists [11]. Especially in Germany, the total number of bicycles now reaches 81 million - statistically, almost every German now owns one bike, no matter if motorized or not [12]. The mentioned data reflects the growing popularity of cycling in the urban area.

Therefore, despite the various vehicle lighting systems, such as headlights, brake lights, or turn indicators, the data presented in this section (Figures 1.1 and 1.2 and Table 1.1) shows a need for action worldwide. Therefore, further innovative lighting systems need investigation and development - one possibility is to project information in traffic situations to other RUs. Besides headlight projections in the direction of travel [13, 14, 15, 16, 17, 18], projections around the vehicle are playing an increasingly important role, not only for design purposes but to reduce safety-critical situations as displayed in Figures 1.3a, 1.3b and 1.3c [19, 20, 21, 22, 23, 24, 25, 26, 27]. Some progress for the automotive application is already made for applying such projections, e.g., communicating a turning vehicle to an approaching cyclist using not only the conventional turn indicator but a near-field projection to display the intention like in Figures 1.3a and 1.3b [19, 20, 24, 25]. As displayed in Figure 1.3, the industry already considers the usage of near-field projections for safety-critical situations in darkness. However, it covers only 13.23% of all bicycle accidents (injured and killed) in a German city [4]. Dusk and daylight need consideration to reduce accidents in urban traffic effectively worldwide.



(a) Graphical illustration displays near-field projections of the vehicle's side and back [20].



(b) Picture displays a confrontation of a cyclist with a vehicle's projected turn indicator [25].



(c) Picture displays a cyclist's view on a confrontation with a projected turn indicator [25].

Figure 1.3.: Graphical illustrations and photos display near-field projections for safety-relevant scenarios.

Figures 1.3b and 1.3c show different lighting scenarios in urban traffic at night. In addition to the headlights of one's own or other vehicles, stationary street lighting likewise contributes to the lighting situation. The European standard EN 13201 [28], therefore, defines different lighting classes for urban areas, according to which the street lighting is designed depending on parameters such as the street's traffic density or speed limit. Consequently, there is no actual dark/ unlit situation for using near-field projections in urban areas because there will always be stray lights from vehicles or stationary street lighting at night.

Moreover, not only the environmental factors influence the conflict situation, but also personal factors of the vulnerable RU simultaneously. If considering, for example, a pedestrian crossing the street, which is a reason for a significant share of accidents (76.81 % in USA [3], and 62 % in Darmstadt, Germany [7]), and from an ethnographic point of view, crossing conflicts arise from the individual tendencies of a pedestrian, which influence the decision-making, as shown in Figure 1.4 [29]. Rothmüller et al. derive several other influence factors, besides the environmental factors which determine the intersection but also the factors which are hard to predict for every person, such as the knowledge about the intersection, the influence of the culture or the current mindset which affects the decision, e.g., for crossing the road. Figure 1.4 illustrates the possible RU decision-making mechanism in traffic situations. [29]

Therefore, Figure 1.4 emphasizes, even more, the design of a user-oriented technology to prevent and reduce conflict situations in urban traffic, which leads to the development of a projection system based on psychophysical tests, incorporating, to some extent, some of the personal factors and not only based on analytical or best practice approaches.

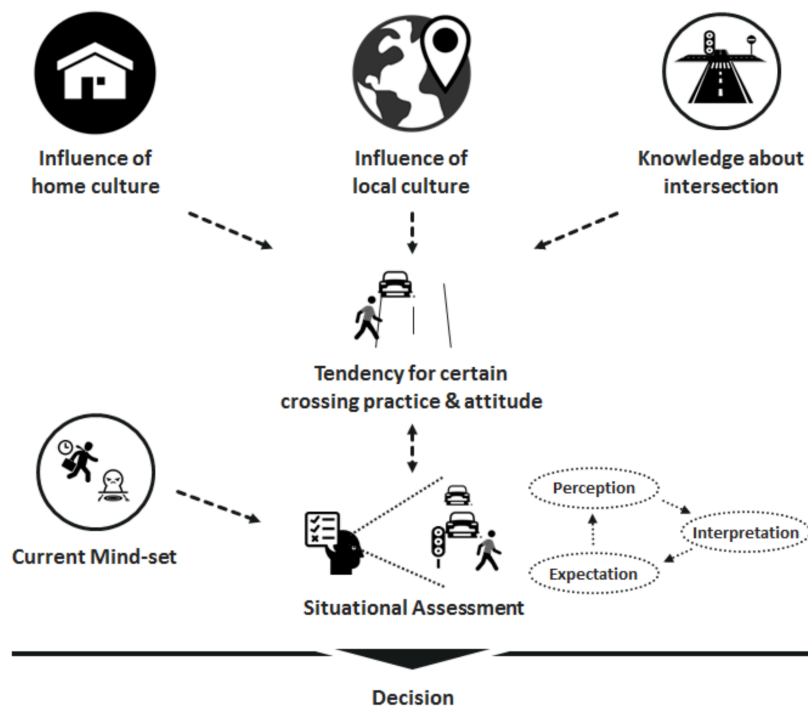


Figure 1.4.: Decision-making mechanism for vulnerable RUs like a pedestrian in traffic situations with the possible influencing factors for the chosen decision, retrieved from Rothmüller et al. contribution [29].

All mentioned facts considered, the urge for near-field projections becomes evident not just for design-orientated purposes but significantly for safety-critical situations when a vehicle interacts with vulnerable RUs. Considering the effect of higher urbanization rates where the conflict situations of a vehicle with other RUs

will increase in numbers. The statistics show a clear tendency for action to harm the conflicts and reduce the number of accidents in urban areas worldwide. Possible examples include a concealed pedestrian attempting to cross the street, as evaluated by Singer et al. statistics [7], or a cyclist riding in the same direction as a vehicle, even though the vehicle will turn (see Figures 1.3a and 1.3b). The differences between several countries indicate the need for near-field projections visible at night and day to prevent safety-critical hazards for pedestrians or cyclists. Especially, considering the increasing urbanization and therefore the stationary street lighting as defined in the European standard EN 13201 [28] dim vision, which creates a transition process between night and daytime vision will be dominant in cities [30, 31]. Ultimately, the vision type responsible within the ambient setting mainly influences humans' perception in general and of near-field projections no matter the situation. Besides, personal factors influence the perception of the RU in traffic, as illustrated in Figure 1.4.

Moreover, this thesis considers a user-orientated design of near-field projections to define and predict the technological characteristics of near-field projectors by examining psychophysical testing to prevent and reduce accidents. Therefore, the psychophysical testing needs to focus on the visibility under various conditions of the near-field projections, such as dusk and dawn and during night and daylight. Projection-based communication has an exemplary advantage compared to display-based methods since safety-relevant projections can address road users (RUs) by placing the projection directly in the field of view of the RUs. Therefore, this thesis focuses on the design of digital projection-based systems and technologies to have the possibility to address each RU individually. Human perception plays an essential role since objective parameters, such as the projection on the road, play a significant role in different ambient brightness levels, as accident analyses show in Table 1.1. Furthermore, the relationship of visibility of the projected content, which can be symbol- or text-based, needs detailed investigations and is equally important considering the resolution of digital projections. Digital projections will be the core technology for near-field projectors in the future to gain design freedom to display static and animated content around the vehicle. Figure 1.5 shows the structure of the thesis.

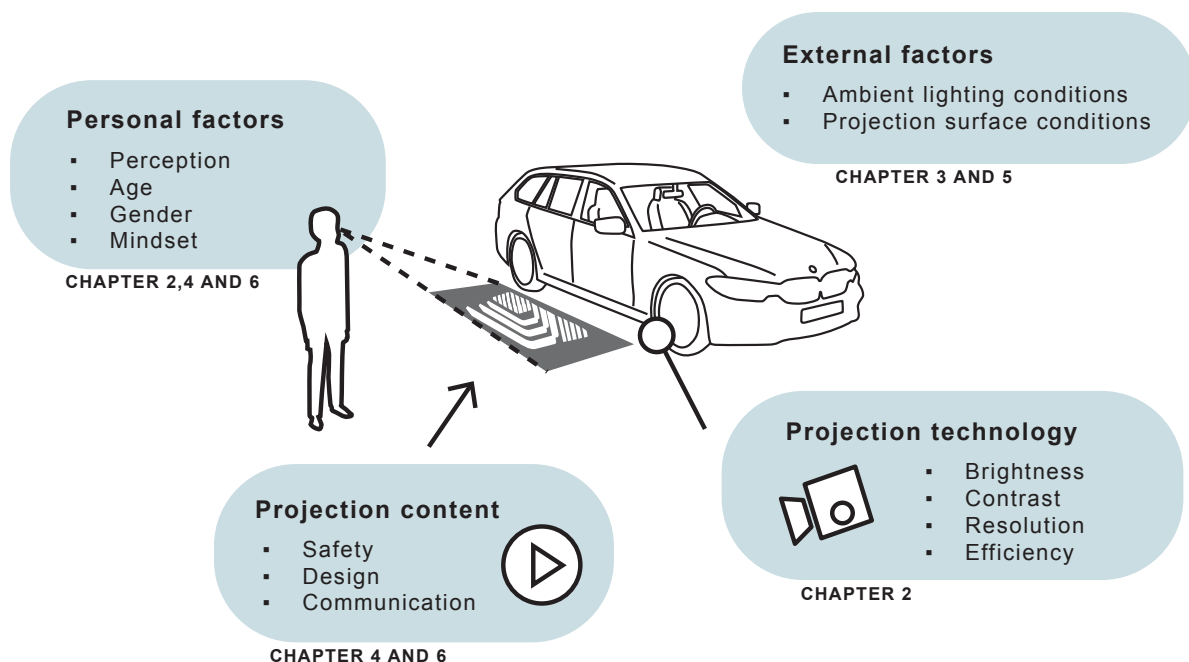


Figure 1.5.: Visualization of this thesis's structure indicates the related chapters of each aspect. The BMW G31 serves as a model for the vehicle's contours in the sketch [32].

---

In order to define and derive the contrast, brightness and resolution of near-field projections as a function of the ambient brightness and other perception-relevant variables such as viewing distance or projection size, the results of seven studies are evaluated and analyzed. Chapter 2 first explains the state of the art with the fundamentals of projection technologies and current prototypes of near-field projectors. Furthermore, Chapter 2 describes the state of research on the perception of visual acuity in general and contrast and brightness perception in the automotive application. From the literature review in Chapter 2, the research questions of this thesis are derived. Chapter 3 describes the theoretical considerations and participant testing design on resolution requirements. The following Chapter 4 analyses and defines the resolution requirements for near-field projections. Further, Chapter 5 determines the environmental conditions for the field tests on the detection perception, ensuring the tested parameters' validation. Thus, the contrast and brightness perception results define the perception-based parameters and their application to the projection technology to determine the brightness of the near-field projections in Chapter 6. Moreover, the outcomes of Chapters 4 and 6 create a basis for a user-orientated near-field projector design. Finally, Chapter 7 summarizes the thesis and gives a conclusion and an outlook.

---

## 2. Literature review

---

In this section, the standard technologies used for digital projectors today, such as Digital Micromirror Device (DMD), Liquid Crystal Display (LCD), Liquid Crystal on Silicon (LCoS), or  $\mu$ -Light-Emitting Diode ( $\mu$ LED) microdisplays, are listed and characterized in detail for the application area of near-field projection and the possible special features of every technology for each field of application in the automotive sector. It defines a near-field projection and how it differs from the other application areas in the automotive industry. Therefore, a derivation serves for the further work procedure as a basis for the execution of participant testing and the according interpretation. In addition, the state of the art of research on the perceptual-psychological fundamentals of the visual system, visual acuity perception, brightness perception, and subjectively perceived glare in dark and bright environments, which occur in road traffic, is defined. Further, an overview of current research on near-field projections defines the different aspects of engagement for near-field projection. These findings derive the research questions and relevant participant tests, which are a part of the proceeding thesis.

### 2.1. Comparison of projection technologies

This section compares several projector technologies, focusing on a digital projector with a microdisplay, creating the projecting image on the screen (Figure 2.1) [33, 34, 35, 36]. Typical applications for projectors are in offices, in theaters, at home, or as a portable unit for displaying work- or entertainment-related content on various sizes and shapes of screens [36]. Nowadays, projectors are getting popular in the automotive sector for the usage of projections created by headlamps [13, 14, 37, 38] or as near-field projections which are projected around the vehicle within 5 m distance to the vehicle [19].

Figure 2.1 displays the basic structure of a digital projector, including a light source, like LED or laser, that provides the light, illumination optics, which directs the light and converts the light beam matching to the shape and aspect ratio of the microdisplay with homogeneous light distribution [33, 34, 35].

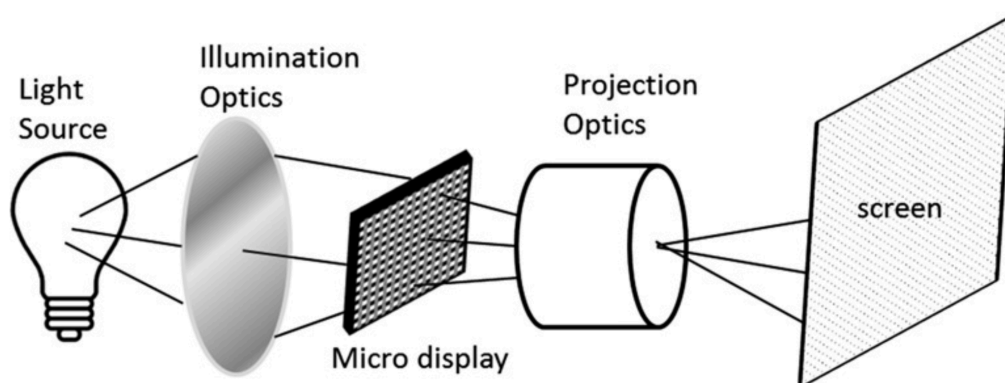


Figure 2.1.: Illustration of the basic structure of a digital projector including the light source, illumination optics, micro display, projection optics and the resulting image on the screen [33].

The microdisplay generates the image, which has different methods of creating the digital image depending on the microdisplay's technology, like DMD, LCD, LCoS, or  $\mu$ LED [33, 34, 35]. After the microdisplay, the light proceeds through the projection optics and projects the created microdisplay image with an enlarging factor depending on the projection optics so the resulting image on the screen meets the application's requirements. For applying projection-based human-machine interfaces (HMIs) in the automotive sector, the screen surface is asphalt or any other street material that appears in urban and rural environments [21, 22].

To differentiate the possible projector technologies, several researchers did an overview separating projection technologies into area-based modulation, displayed exemplary in Figure 2.2, such as DMD (Figure 2.2a), LCD (Figure 2.2b), LCoS, or LED matrices, also including  $\mu$ LED microdisplays (Figure 2.2c) or modulation of the light beam, like scanning methods with exemplary micro-electro-mechanical systems (MEMS) [13, 14, 38, 15]. Further, area-based modulation technologies are under consideration since that kind of projector is already acknowledged in the automotive sector for headlamp systems and near-field projectors. Additionally, an evaluation of pixel-based resolution aspects is possible.

Therefore, this literature review lists the advantages and disadvantages of such area-based modulated projection systems like DMD, LCD, LCoS, and  $\mu$ LED involving general literature and specific literature for automotive qualified projection systems focusing on system's characteristics like resolution aspects, projector's brightness, optical efficiency, and others.

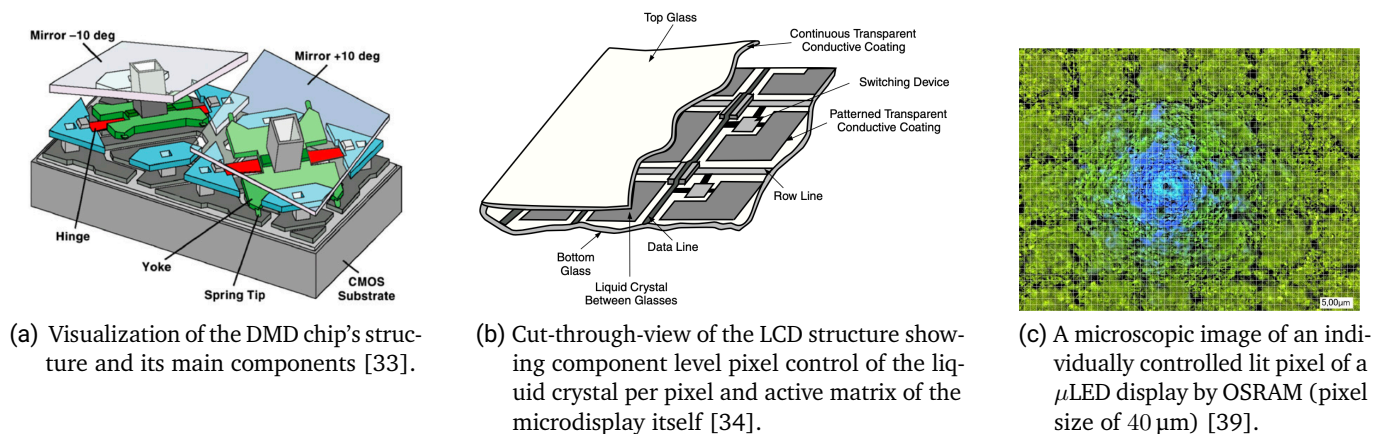


Figure 2.2.: Overview of the area-based modulation technologies, such as DMD, LCD, and  $\mu$ LED, as a schematic illustration or as a microscopic picture.

This overview is an excerpt of the currently progressing development and research. It serves as a basis for presenting the different types of area-modulated projections. This work focuses mainly on the characteristics of the microdisplay, which influence the projector's design with the corresponding characteristics [33]. Additionally, it is necessary to concentrate on an user-oriented design of such systems and not on detailed aspects such as efficiencies of sub-domains of the illumination or projection path, as introduced by Brennesholtz and Stupp [34] for modeling the projector's lumen output, and the resulting design of either projection optics or illumination optics if needed.

### 2.1.1. Micro-electro-mechanical devices

Micro-electro-mechanical devices such as DMD are part of area-based or light-beam modulation technologies and are a reflective projection solution [33, 14, 15]. When focusing on the area-based modulation, the projection's grayscales are created by the on (incident light reflects into the projection optics - mirror position:



---

+12°)/ off (incident light is deflected into a light absorber - mirror position: -12°) duty cycle for every micro-mirror/ pixel, displayed in Figure 2.2a. Additionally, multiplexing multiple light sources enable the creation of an RGB-colored image. [33, 34, 35, 40, 41]

Presuming a high brightness and high-quality projection are demanded. In that case, a 3-chip system, where every color channel (RGB) gets its own DMD chip, is a solution to reduce the rainbow effect, which displays at the edges of contours, compared to a one-chip system [33, 34, 36]. In the automotive sector, a 3-chip solution will not be the first choice of a near-field projector, mainly if focusing on monochrome digital projections, as mentioned by Rosenauer et al. [20]. With a 3-chip solution, the module size and the cost of the projector will increase due to the higher number of illumination optics and the required module's size before the projection optics [20, 42, 23].

One of the limitations of DMD projectors is the time-multiplexing of the mirror state, which restricts the peak of the luminance output to 70 % of the maximal luminance in the system resulting from the tilting angle limitations of 12°. So, the grayscale level of the DMD is affected by this limitation, too [34, 35]. Additionally, as mentioned before, a rainbow effect caused by the refresh rate of the DMD mirrors for one-chip solution affects the imaging quality [33, 34, 36]. Nevertheless, there are concepts for RGB compact projectors with a one-chip application [42, 23, 43]. All these restrictions, including the optical efficiency of about 20 %, do not harm the development of such projectors for the automotive sector, so there are several prototypes and solutions in the market [20, 42, 23, 43, 44].

### 2.1.2. Liquid crystal based microdisplays

Two possibilities exist for a liquid crystal (LC)-based microdisplay - LCD or LCoS [45]. The incident light either passes through the LC microdisplay, displayed in Figure 2.2b, or reflects on the LCoS, which has a reflective silicon backplane [33, 34, 35, 45]. LC-based microdisplays only transmit longitudinal light waves, which requires a polarization converter in the illumination optics and reduces the light by 50 % [33, 34, 35].

Looking at the boundaries of an LC-based projector, a reflective LCoS projector results in lower contrast due to an increasing incident angle [46]. Other limitations of LC-based microdisplays relate to the light polarization before the image generation to create a projection which results in a decrease of the possible image contrast, too [33, 34, 35, 38]. However, LC-based projectors have higher light collection efficiency than DMD projectors, so the lumen output ratio with the same light source would be higher with similar color performance and power consumption [33, 47]. Additionally, LCoS has a smaller pixel pitch of 4.25  $\mu\text{m}$  [45]; what is the nonluminous area between two neighboring pixels, compared to a DMD with a pitch of 7.26  $\mu\text{m}$  [41] for a similar sized microdisplay. Therefore, an LCoS has a higher resolution of 1920 x 1080 pixels than 864 x 480 pixels of a DMD [45, 41]. Consequently, the demanded application can cause a higher preference for a projector with a higher resolution, so single pixels are not apparent to the observer. Similar to DMD projectors, LC-based projectors can be built with a one- or three-chip solution to improve image quality, but it is crucial to align the three stacked images of the three-chip solution to avoid convergence [33, 34].

LCD projectors are used in the automotive sector in high-resolution headlights [14, 48] and near-field projections [21] and provide an alternative to DMD projectors.

### 2.1.3. Direct-emitting active matrices

Another technology to create projectors is to use direct-emitting active matrices or LED arrays, which combine the light source itself with the microdisplay, so there is no need for an illumination optic which results in a simplification of Figure 2.1 to just a microdisplay with a projection optics [13, 14, 39, 49, 50, 51]. The active matrices can consist of  $\mu\text{LEDs}$  as a light source with a pixel size below 50  $\mu\text{m}$  with a pixel pitch of less than 20  $\mu\text{m}$ , which has its limits depending on the photo-lithographic processes [52, 47].

Compared to the other two introduced technologies in Sections 2.1.1 and 2.1.2, the active matrices are not a subtractive microdisplay, which needs a light source that is always on and redirects the unnecessary light into an absorber, but it is an additive technology, which creates light in a pixel where it is needed. The active matrices solution can also dim each pixel with a pulse width modulation (PWM) as known from conventional LED light sources [34, 13, 14, 15, 37].

Therefore, additive technologies such as  $\mu$ LED microdisplays have the advantage that these kinds of projectors are more efficient since no polarization is needed, nor the light source has to be entirely on the whole time when the projector is powered [34, 13, 14, 37, 49]. This advantage is remarkable when symbols or projections, which do not use the whole chip size, are projected. Moreover, additive projectors can reach higher contrasts before the projection optics due to partly turned-off pixels. However, in the end, the projection optics will influence the projected image. [13, 14, 38, 49]

Nevertheless, compared to the other two projector technologies (DMD or LC-based), additive projectors have lower resolution when using  $\mu$ LED active matrices since the pixel sizes are significantly bigger. Also, as displayed in Figure 2.2c, some stray light can occur in  $\mu$ LED microdisplays from one pixel in on-state and the other being off due to the Fresnel effect, which causes some artifacts leaving the projection optics [38, 47].

In the automotive sector, such active-matrices projectors are already present for high-resolution headlamps with a resolution of 16,000 to 25,600 pixels per headlamp [53, 54].

#### 2.1.4. Summary of the digital projectors' comparison

Finally, Table 2.1 presents a qualitative overview, which summarizes the advantages and disadvantages mentioned and displays this summary based on the previously mentioned literature. Thus, the summary includes aspects of the area-modulated digital projection technologies as follows in terms of resolution, contrast, and efficiency:

Table 2.1.: Comparison of digital area-based modulated projectors characteristics for the automotive sector regarding resolution, contrast, and optical efficiency [34, 13, 14, 37, 38]

Parameter	DMD	LCoS	LCD	$\mu$ LED
Resolution	high	high	medium	low
Contrast	medium	low	low	high
Optical efficiency	low	low	low	high

Regardless of the technology and maturity level, an increasing interest in projection-based technologies in the automotive industry is evident. With this in mind, the next section will focus on projectors used in the automotive sector and give an overview of different applications for digital projections around the vehicle.

## 2.2. Applications in the automotive industry

A possible background for applying projections in the automotive context is the high interest in research for external HMI for automated vehicles (AVs). The HMI establishes communication between an AV and another road user (RU) with static messages, which display symbol -or text-based projections on the street's surface, a display surface on the vehicle, or a dynamic message with an animation integrated into the illustration. So, vehicle manufacturers and research institutes develop various HMI designs and technologies. However, in this work, the focus is on projection-based HMIs.



Most researches focus on VR- or monitor-based field tests to investigate the fundamental of future communication with projection-based systems and the necessary characteristics [55, 56, 57, 58, 59, 24, 60]. Moreover, car manufacturers outline projection-based HMI systems to communicate the vehicle's information, which is either informative or safety-relevant, or an intention to other RU [61, 62, 63, 64, 65]. Clear visibility of the projection-based HMI in the RU's field of view [56, 57] and positive feedback in the questionnaire-based evaluations compared to other HMI technologies present advantages and prospects for the application of a near-field projection or by projecting information from the headlamps on the street as a projection-based HMI [13, 14, 38, 57].

However, two use cases for projection-based HMIs in the automotive context are defined, and Figure 2.3 displays the location and the premises: near-field, which is within 5 m around the vehicle [19], so the projected message on the ground can be assigned to a vehicle in the urban traffic, or high-resolution headlamp projections for ADB or symbol projection located in 10 to 25 m from the vehicle's front [13, 38]. This work focuses on the projections in the near-field of the vehicle, thus not going further into the projections from the headlamps, which other publications have already considered in more detail [13, 14, 37, 38, 15, 39, 40, 51, 16, 66, 67, 68, 17, 18, 69, 70].

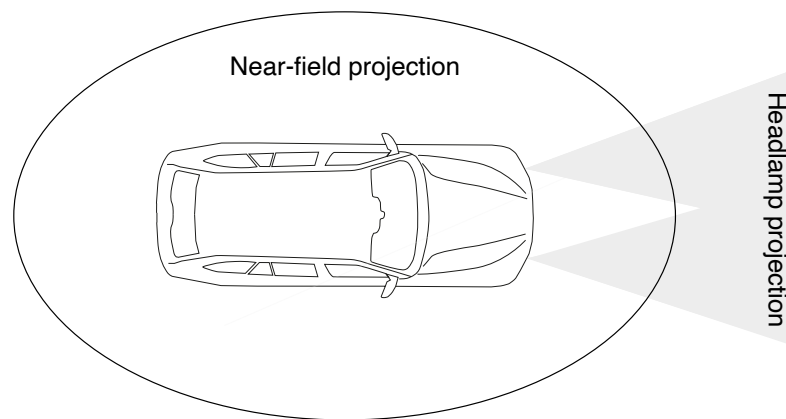


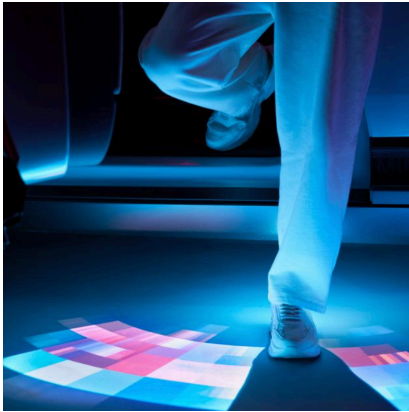
Figure 2.3.: Illustration of projections around the vehicle for either near-field projections which are not further than 5 m away from the vehicle and will be projected within the indicated circle [19] or headlamp projections for ADB or symbol projection in 10 to 25 m [13, 38]. The BMW G31 serves as a model for the vehicle's contours in the sketch [32].

Nevertheless, there is already some research work for near-field projections and prototypes for digital near-field projectors with a DMD or LC-based microdisplay to display the proof of concept for the automotive circumstances, such as to miniaturize the projector's size and to integrate the projector into the vehicle's architecture [20, 21, 42].

For projecting near-field projections around the vehicle, as shown in Figure 2.3, within a 5 m projection distance around the vehicle, it is essential to determine which possible applications are of interest for automotive projections. Figure 2.4 classifies three categories, which are possible use cases for near-field projections [19, 23, 21, 22, 24, 25, 26]: Welcome- or goodbye scenarios, safety-relevant scenarios, and in a scenario used as a communication medium.

Welcome, or goodbye scenarios may include logo projections of the brand, personalized messages, and illustrations like the owner's name during the welcome scenario (displayed in Figure 2.4a) [20, 19, 64, 71].

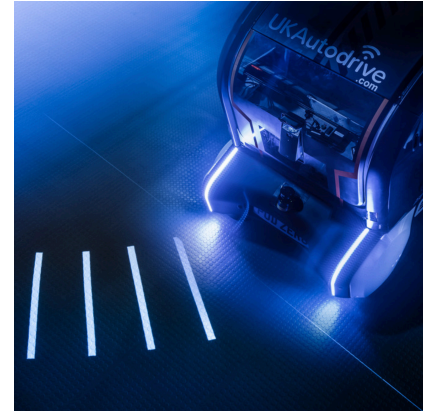
Near-field projections for safety-relevant scenarios can display an extended turn signal projected onto the ground (Figure 2.4b) or warnings for hazardous situations in urban traffic, like a pedestrian entering the street while covered behind an obstacle. Moreover, e.g., a vehicle warns cyclists with a near-field projection in the cyclist’s field of view about an intended turn, which significantly defuses this critical safety situation [20, 61, 62, 65, 25, 24, 26].



(a) Display the use case of the welcome or goodbye scenario of the MINI Concept Aceman, where an interactive light carpet appears when an user approaches the vehicle or while leaving the vehicle as displayed [64].



(b) Illustration of a safety-relevant projection with the example of a projected turning indicator, which shall warn or make another RU aware of a turning vehicle by projecting the amber arrow into the RU’s field of view [72].



(c) Example of a projection for communication purposes. Here, especially the indication of the intended direction in an area without road markings to indicate the intended action of the automated concept car [62].

Figure 2.4.: Overview of the use cases for near-field projections: 2.4a displays a welcome and goodbye scenario; 2.4b illustrates an example of a safety-relevant projection; 2.4c shows possible use case of vehicle’s intention communication.

Figure 2.4c illustrates the usage of projections as a communication medium, which researchers are currently investigating. However, possible use cases could be communicating the vehicle’s intention in deadlock situations [55, 56, 57, 58, 73].

Near-field projection content differs in the mode of display. On the one hand, a static near-field projection displays non-moving graphics, whether symbol- or text-based [19, 71]. On the other hand, dynamic near-field projections, which are digital projectors and not limited to one or several static patterns, can also project video content and, therefore, can vary in the customization (e.g., graphics and color) and be updated [20, 21, 22, 42, 23, 64, 25]. Especially the second category, which focuses on digital projectors, is the main focus of this work and combines the previously established area-based microdisplay projector technologies for implementation in the automotive sector for near-field projections.

Therefore it is crucial to show which characteristics the projectors for a near-field application have based on the released information from academics or the commercial market. Furthermore, it is essential to understand a  $\mu$ LED microdisplay’s possibilities or enhancements, even though no known high-resolution prototype for near-field projection is yet to be released. Therefore, comparable data, such as resolution, contrast ratio, or optical efficiency, are compared from automotive projector prototypes. With this background, the data are summarized in Table 2.2 and represent the current state of the art of projectors for near-field projections, corresponding to the automotive demands and requirements, e.g., the temperature or the module size.

Table 2.2 confirms Table 2.1 qualitative data according to the literature evaluation, mainly focusing on high-resolution headlamp projections for area-modulated technologies, which also applies to the near-field

projections. Thus it is evident that the resolution of the DMD (414720 pixels [41]) and LCoS (921600 pixels [45]) systems are significantly higher than that of  $\mu$ LED (25600 pixels [39]).

Table 2.2.: Comparison of the near-field projector prototypes for DMD or LCoS solution and comparable data of headlamp projectors with  $\mu$ LED as a correspondence with the related literature indicated in the table cells.

Parameter	DMD	LCoS	$\mu$ LED
Resolution in pixel	588 x 330 [20] or 864 x 480 [41]	1280 x 720 [45]	80 x 320 [53]
on: off Contrast	400:1 [42]	100:1 [21]	500:1 [51]
Optical efficiency in %	$\sim$ 20 [20]	$\sim$ 15 [48]	33 [51] - 48 [53]
Luminous flux in lm	25 - 120 [42]	27 [21]	800 [51]

Furthermore, equation 2.1 defines the contrast range that the projector achieves and calculates contrast by dividing the on-luminance  $L_{on}$  (white image) by the off-luminance  $L_{off}$  (black image) [34]:

$$C = \frac{L_{on}}{L_{off}} \quad (2.1)$$

The data of Table 2.2 shows that the  $\mu$ LED microdisplay can achieve higher contrast values (500:1) for the technology-related contrast, followed by the DMD (400:1) and the LCoS (100:1); thus, the trends of Table 2.1 overlap with the physical values of the prototypes for near-field projectors. The system's overall optical efficiency of a  $\mu$ LED projector (approx. 48%) is almost up to two times better than that of a DMD ( $\sim$ 20%) or LCoS projector ( $\sim$ 15%), partly due to the elimination of illumination optics and the additive projection technique what Section 2.1.3 described in detail. Therefore, the  $\mu$ LED projector allows a higher luminous flux than the other two projection technologies (see Table 2.2). However, this value must be considered cautiously, as just the DMD investigation displays the necessary power consumption with 3 W for 25 lm to 10 W for 120 lm [42], the other two projection technologies do not specify the corresponding power consumption for the luminous flux values. Therefore, whether these three examples operate in the same power range is uncertain.

### 2.3. Human visual system and perceptual psychophysics

Besides, a technological investigation of the near-field projector and its influence on the parameters for near-field projections requires a detailed investigation based on a user-orientated perspective. It is necessary to consider the projection at the component level (Section 2.1) - the projector itself - and at a perceptual level of consideration that includes the user's needs and perception. These two domains interact with each other and describe the projector with an user-oriented design in terms of resolution and contrast or other necessary parameters. In the perceptual design of the component, not only do the components' mechanisms play a role but also influences from the outside world, such as the ambient luminance or the characteristics of the road surface like roughness, reflectance, or if the street surface is wet [21, 22, 42]. The environmental influences interact with humans and affect the visual system, the resulting perception of contrast thresholds or visual acuity, and subjective perceptions of interfering influences such as glare [74, 75, 30, 76, 77].

Therefore, besides the application-specific considerations for projections in the automotive context, the following sections deal with the state of the art of research on the perceptual-physiological fundamentals of the visual system and human perception, including the aspects of vision like visual acuity or contrast perception.

Additionally, tests related to visual tasks or for subjective and objective evaluation of stimuli (in this case, projections) are presented, which will serve as a basis for comprehending the participant tests conducted in the following chapters.

### 2.3.1. The human eye and its perceptual mechanisms

The demands on the visual system's flexibility and performance are high. When considering visual information from the environment, recognition is made between several essential physiological functions of the eye. These include the discrimination of luminance and color differences and the perception of shapes [75, 30, 76, 77, 78, 31]. This thesis focuses on white projections and does not consider color differentiation further. The topic of the human eye is extensive, so this thesis focuses on the essential aspects, including the eye's adaptation and response to light stimuli, especially when the human eye needs to adapt to different luminance levels of the environment. Another aspect is visual acuity, which allows seeing details and differs depending on the adaptation luminance.

The retina contains two types of receptors, cones and rods, in which incoming light initiates a biochemical conversion of the visual pigments and creates a receptor potential [30, 31], displayed in Figure 2.5. The cones are responsible for photopic vision and color vision and divide themselves into the S, M, and L cones. Here, the S (425 nm) stands for short, the M (530 nm) for medium, and the L (560 nm) for long, indicating the wavelength range with the highest sensitivity in each case [30]. The dominant wavelengths differ depending on the literature, but more or less are identical [30, 31, 79]. The cones have up to 300 times lower light sensitivity of the rods when they are active [79].

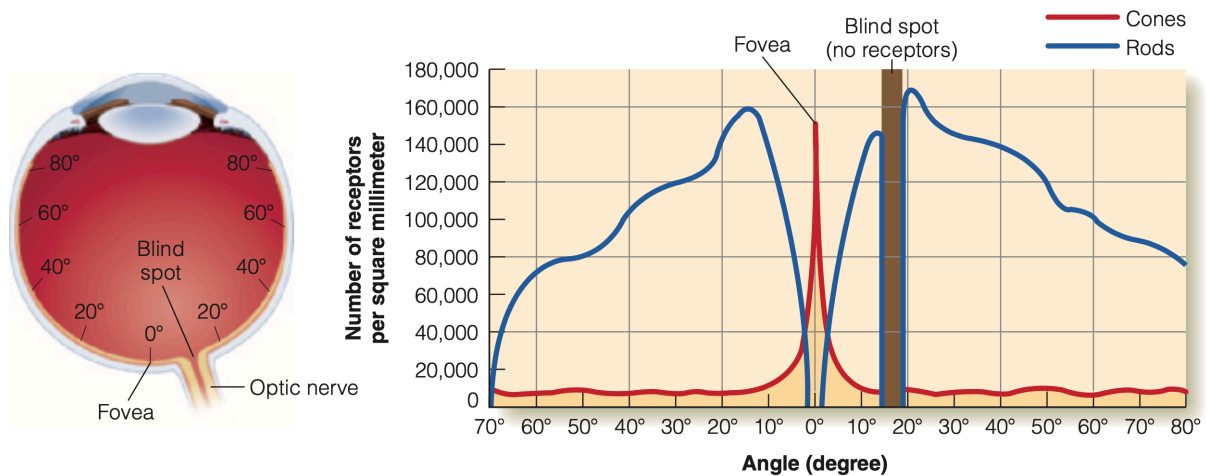


Figure 2.5.: Distribution of cones and rods on the retina of the human eye, while cone density, illustrated in red, is on the highest level in the fovea, no rods are present in the fovea. Rod density, displayed in blue, increases rapidly in the peripheral region. In the 'blind spot' neither rods nor cones are present [30, 78, 31]. Retrieved from Goldstein and Cacciamani [78].

Table 2.3 lists types of vision since the activity of the two receptor types depends on the light conditions. Only cones are active at luminance levels above  $10 \text{ cd m}^{-2}$  - the photopic vision (day vision). Moreover, there is a transition phase where cones and rods are active (dim vision), named mesopic vision [30, 76, 78, 31]. The mesopic area is highly relevant in the automotive context, as this framework includes many scenarios, such as parking lots or garages, illuminated roads at night, and dusk and dawn [80, 28]. At low luminance levels of less than  $0.001 \text{ cd m}^{-2}$ , only the rods are active, representing scotopic vision (night vision). Due to

the higher brightness sensitivity, the rods can perform a visual task even at low luminance in the human's field of view. Visual acuity strongly depends on the visual system's adaptation state [30, 76, 78, 31].

Table 2.3.: Interaction of the receptor types results in different types of vision and depends on the adaptation luminance [30, 31]. The overview is retrieved from Gross [31].

Scene	Vision	Receptor	Adaptation luminance in $\text{cd m}^{-2}$
night vision	scotopic	rods	< 0.001
dim vision	mesopic	rods and cones	between 0.001 and 10
day vision	photopic	cones	> 10

The activity of the cones and rods at different ambient brightnesses described previously and displayed in Table 2.3 enables the perception of visual stimuli in a wide range of varying luminance levels. The mechanism to adapt to a specific luminance area is called adaptation. Moreover, both receptor types influence the adaptation time differently. [30, 76, 78, 31, 79] Figure 2.6 illustrates the dark adaptation mechanism.

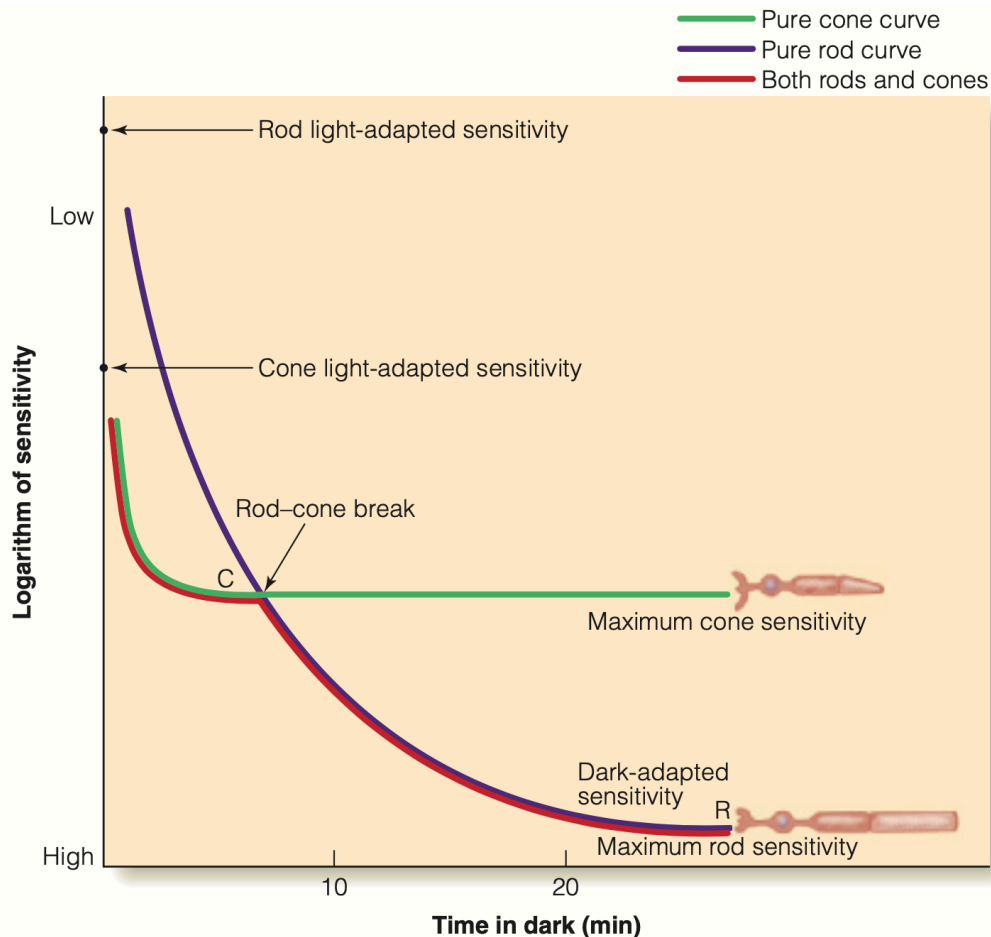


Figure 2.6.: Progress of dark adaptation: at the beginning of the dark adaptation, indicated in red, followed by cone adaptation, displayed in green. As soon as the cones have reached their maximum sensitivity, rod adaptation, shown in purple, determines the dark adaptation [30, 76, 77, 78, 31, 79]. Retrieved from Goldstein and Cacciamani [78].



---

Adaptation, which determines the visual system's performance in terms of visual acuity, color vision, and luminous sensitivity, occurs differently for light and dark adaptation. Thus, a bright adaptation from low to higher ambient luminance finishes within a minute [76]. Dark adaptation requires about 30 to 60 minutes in total. As shown in Figure 2.6, dark adaptation occurs in the first approx. eight minutes by the cones until they reach their sensitivity maximum. For maximal sensitivity in the dark, the dark adaptation continues by the rods for additional 30 to 60 minutes. The adaptation time depends on the luminance level before starting the dark adaptation mechanism. The transition is visible and marked with the rod-cone break/ kink in Figure 2.6. [30, 76, 77, 78, 31, 79]

This mechanism is crucial for participant testing since participants must complete tests under different ambient luminance levels to evaluate the influence of luminance on the tested parameter, like contrast threshold sensitivity or visual acuity. Therefore, the adaptation mechanism applies to the testing design in Chapter 5 to ensure correct perceptual conditions for evaluating light stimuli in different ambient luminance. In order to maintain constant test conditions, a sufficient adaptation time is necessary before the start of the test, depending on the adaptation luminance. The mesopic range is particularly complex in perception and dominant in the automotive context from dusk to nighttime traffic in the metropolitan area or parking lots.

Moreover, Chapter 5 determines the perception of contrast thresholds of either stimulus placed in the fovea or the peripheral field of view of the participants. Therefore, it enables determining a projector's illuminance on the projected surface from a user perspective thanks to psychophysical testing.

Therefore, a closer look at visual acuity behavior is necessary. So, the visual acuity differs across the retina and has its maximum in the fovea, which depends on the adaptation condition, ambient luminance, and the human's age. Visual acuity relates to pupil size - so the smaller the pupil's diameter, the better geometric images results. A generalized human being can achieve a visual acuity ( $VA$ ) of one, which would correlate to an observable size of 8.9 mm at a distance of 6.096 m and results in a size of 25  $\mu\text{m}$  on the retina, but it varies depending on the person. Chapter 3 derives the necessary fundamentals for the tests analytically to evaluate the visual acuity limitations for the testing procedure.

Exemplary, a change in vision from purely photopic vision with dominating cones at day vision to scotopic vision with only rods responsible for low luminance vision results in lower perceived resolution and resulting VA. The VA changes from 1 in the photopic ambient luminance of 1' perceivable detail size  $\alpha$  to a VA of 0.3 for dim vision conditions to 0.1 in the scotopic luminance levels with only 10' resolvable detail size. Equation 2.2 displays the theoretical relationship between the VA and the perceivable detail size. Figure 2.7 schematically displays that the VA and the resolvable resolution rely on various factors, such as acuity increasing with contrast and acuity reducing with higher stimulus dynamics. [30, 76, 78, 31, 79]

$$VA = 1/\alpha \quad (2.2)$$

The acuity of dynamic stimuli is named dynamic visual acuity (DVA). The DVA is the ability to perceive and resolve the stimulus's details with a relative motion difference between the stimulus and the observer. A possible DVA testing procedure is a moving Landolt ring at different speeds proceeding through a screen or VR headset, and the participant has to identify the opening direction of the Landolt ring. Another method to obtain DVA is by rotating/ moving the participant's head by herself/ himself or by an instructor while observing a static image. [81, 82, 83, 84, 85]

Additionally, ambient illuminance influences the VA. As mentioned, the retina resolves a brighter stimulus better (see Figure 2.7c). Additionally, a reduction in VA occurs with increasing age of the human eye (Figure 2.7d). Moreover, the VA is not constant for all eccentricities. The decrease in VA in the peripheral field of view relates primarily to the decreasing density of receptors (see Figure 2.5). [30, 76, 78, 31, 79]

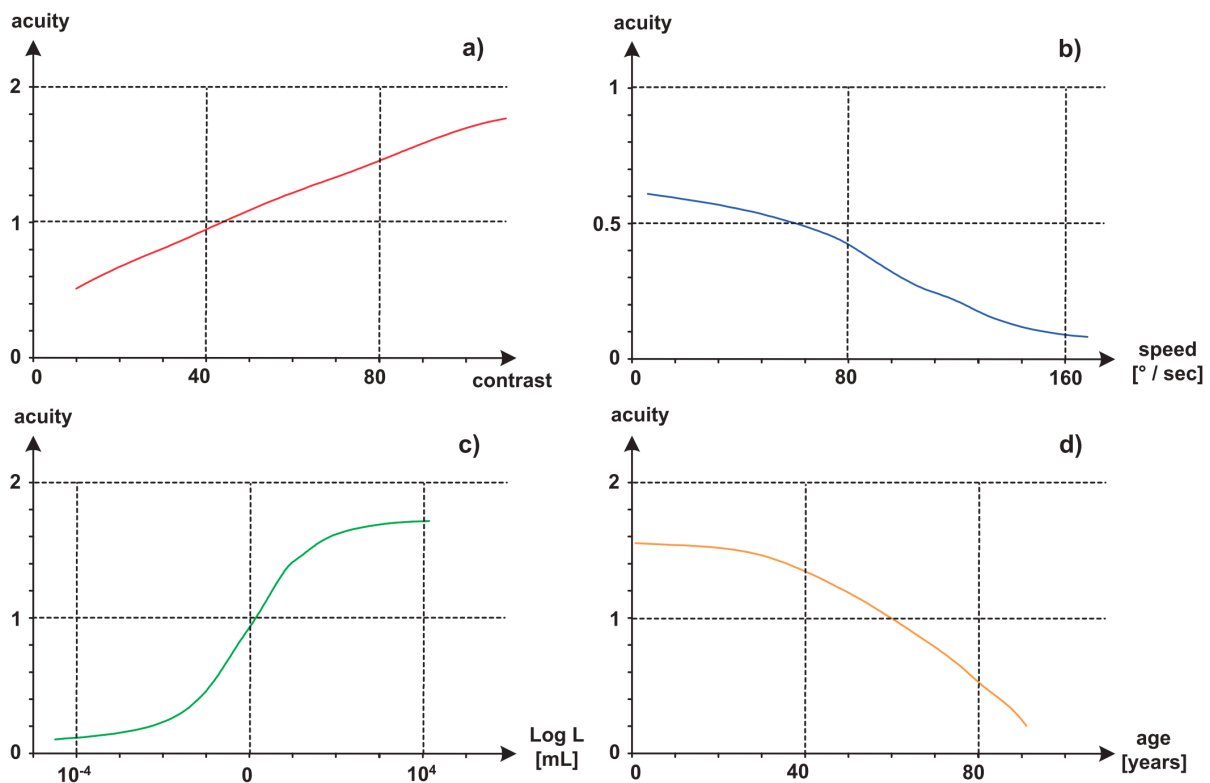


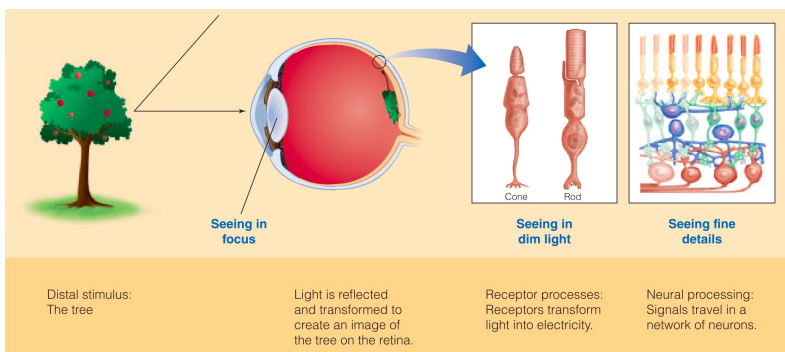
Figure 2.7.: Influence factors on the visual acuity, like a) the contrast dependency, b) the influence of the stimulus dynamics, c) the influence of ambient luminance, and d) age-dependency of the human visual system [31]. The schema is retrieved from Gross [31].

In conclusion, it is possible to differentiate lower contrast thresholds and resolve finer details when the adaptation luminance increases, so the VA increases. Therefore, Chapter 3 will focus on the resolvable details of near-field projections and define the user-orientated resolution for near-field projections. Especially the dependency of the stimulus dynamics and the ambient luminance levels are examined in Chapter 3 and the resulting analysis. Hence, the visual acuity and the resulting resolution on the retina are linked with perceiving a high-quality digital near-field projection and are evaluated later in this thesis.

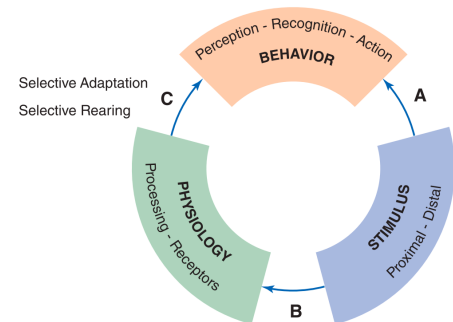
### 2.3.2. Perception and psychophysics

The visual process of perception divides mainly into three phases [78, 86, 87]: An example of a near-field projection displayed around the vehicle as the stimulus where the observer, first, **sees** the projected content, and the observer's retina receives the information about the scene, as displayed in Figure 2.8a with the tree as a stimulus example. Second, the retina converts the object's light into electrical impulses transmitted via a nerve connection to the brain's visual cortex. The light produces an image - **perception** takes place. Third, the brain compares the received image with already stored images - so **recognition** occurs. [78, 86, 87]

Figure 2.8 shows the three essential steps of the visual process in graphical form in Figure 2.8b and a schematic illustration in Figure 2.8a. The three-step model's advantage is its simple and intuitive comprehensibility (see Figure 2.8) [86, 87].



(a) An image of the tree (stimulus) focused on the retina on the back of the eye. The close-up of the retina receptors on the right shows the actuators (rods and cones and other contributors) of the receptor processing and the neural processing, which is necessary for the physiology and the behavior regarding the incoming stimulus (see Figure 2.8b) [78, 86, 87]. Retrieved from Goldstein and Cacciamani [78].



(b) Three stages of the perceptual vision process display their relation to each other. The three boxes represent the three main components of the perceptual process: Stimulus, Physiology, and Behavioral responses [78]. Retrieved from Goldstein and Cacciamani [78].

Figure 2.8.: According to Goldstein and Cacciamani, and Schmidt-Clausen and Freiding [78, 86], the process in the visual system for perception.

Moreover, Figure 2.8b shows the processes in more detail and describes perception with three stages but includes further details within the three stages. The blue box describes the stimulus, the green depicts physiological processes, and the orange includes perceptual responses [78]. According to Goldstein and Cacciamani, an available stimulus and its attention are necessary before the seeing process can start. However, converting the light stimulus into electrical signals and neuronal processing steps are necessary for perception. Recognition also means categorizing the perceived stimulus by comparing it with what is known. The actual goal of the described processing - an action - is the conclusion of the whole process. [78]

One outcome of psychophysical testing is that participants must interact with the perceived stimuli, e.g., log in a subjective rating after perceiving the stimuli.

When considering near-field projections, perception relates to a noticeable difference between a lit object and its background. However, since this difference depends on the background, the quotient of both represents the Weber contrast  $C_W$  [74], as displayed in Figure 2.9. Figure 2.9 displays an example of a possible test for contrast threshold determination on the left and the related psychometrical function to analyze the data of the constant stimuli method on the right [88, 89, 90, 74], where section 3.1.1 presents an application-based consideration of the theory.

Various quantitative methods that accurately measure correlations between the stimulus (*physics*) and subjective perception (*psycho-*) describe psychophysics. Nevertheless, various methods for performing psychophysical tests influence the resulting threshold depending on the applied method. However, the work focuses only on the constant stimuli method, displayed exemplarily in Figure 2.9 on the right. The stimulus intensities of the constant stimuli method are randomly presented one after the other from the predefined stimuli set. The method is very accurate but time-consuming. In other contributions, several researchers also summarized and analyzed other psychophysics methods and the necessary psychometric functions in detail. [88, 89, 90, 74, 91, 92, 93]

The x-axis of the example in Figure 2.9 on the right displays the various stimulus contrasts presented in random order and repeated multiple times, with visual examples of the lit object and its background. Black dots illustrate the proportion of correct answers for each contrast, which also delivers the corresponding percentage shares. The green curve best fits a psychometric function, and the arrow indicates the calculated contrast detection threshold ( $CT$ ) at a level of interest, e.g. of 75%. [74, 88, 89, 90, 91, 92, 93]



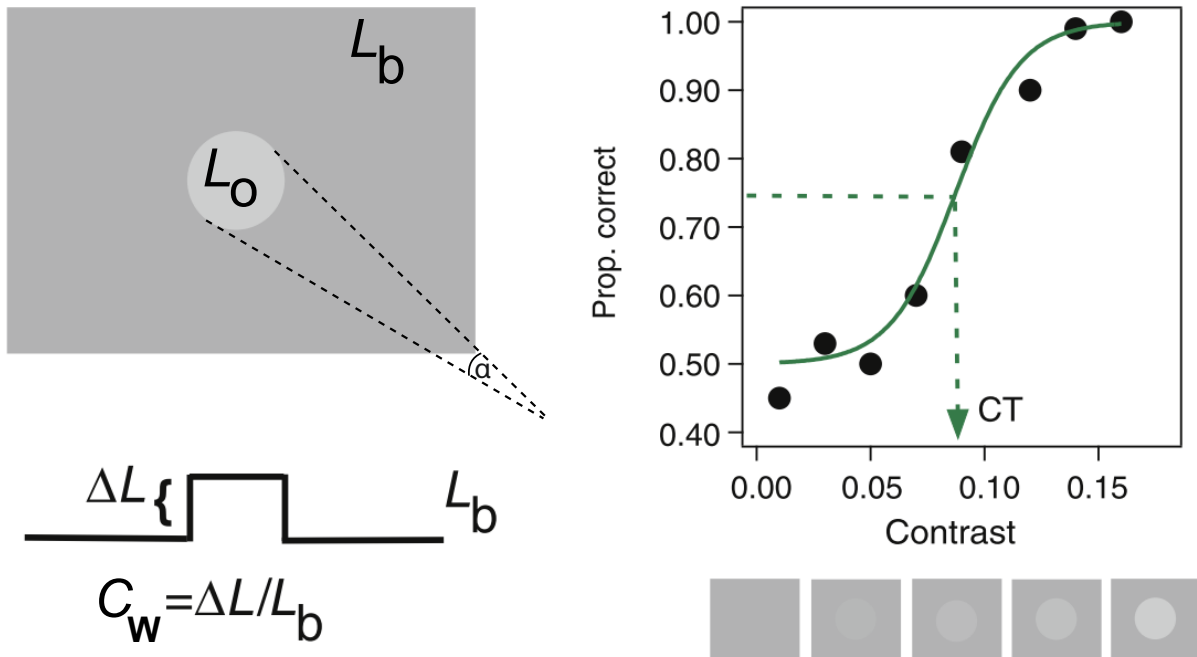


Figure 2.9.: On the left: circular test object with a size depending on the viewing angle  $\alpha$  on a uniform background and below the object's luminance progress and the resulting Weber contrast definition. On the right: plotted results of a standard two-interval-forced-choice (2IFC) experiment, which is part of the constant stimuli method. Retrieved and modified from Kingdom and Prins [74].

$L_o$  is the object luminance,  $L_b$  is the background luminance, and  $\Delta L = L_o - L_b$  describes the difference in luminance between object and background. Moreover,  $C_w$  is the Weber contrast in Figure 2.9, which is described in detail related to the participants testing in Chapter 3 and also in equation 3.7. [74, 94, 95] So, a definition of the psychometric function is possible [88, 89, 90, 92] - here, the logistic regression is presented extensively in sections 3.1.2 and 5.1.1 related to VA or contrast perception.

The psychophysical testing method determines the visual acuity perception based on the existing contrasts as a function of environmental parameters like viewing distance and ambient luminance. Additionally, the testing method defines contrast levels concerning the requirements as the position in the observer's field of view and environmental influences for subjective perceptual evaluation.

### 2.3.3. Subjective influence on perception

One possible influence factor for the perception of the RUs during dim or night vision is glare. CIE introduces the term "glare" in the international vocabulary of lighting [96]: As a visual condition that can awaken unpleasantness in the observer or result in a reduced visual function affected by an unwanted luminance distribution on the retina. Moreover, it is necessary to split the perception of glare into two categories, physiological and psychological glare: [30, 96, 94, 97]

- Physiological glare: Glare that results in a reduction of the visual function [30, 96, 94].
- Psychological glare: Glare that awakes unpleasantness in the observer without a noticeable reduction in visual function [96, 97].

---

This work focuses on the psychological glare since current projection technologies for near-field projections do not reach limits to imitate glare at the observer, as displayed in Table 2.2. Furthermore, it is crucial that other RUs, not the projection receiver, do not feel any discomfort by near-field projections and are not distracted from taking part in a traffic situation task.

Hence, measurable variables do not describe psychological glare, but evaluating the glared person's subjective opinion is possible. Different methods are available to determine how comfortable or uncomfortable the person considers the glare situation. One method uses category rating - the de-Boer scale, which relates to a Likert scale. The de-Boer scale contains nine levels relating to a selection between unbearable and unnoticeable glare. [97]

The Likert scale is the basis of the de-Boer scale. However, it is possible to modify the number of answers to improve efficiency and understandability without losing information with lower scale arguments [98, 99]. So, section 5.3.5 introduces a seven-argument Likert scale ranging from 1 (unnoticeable) to 7 (disturbing) to evaluate a possible glare or disturbance of a near-field projection in the peripheral field of view.

## 2.4. Research related to resolution requirements

As digital near-field projections around vehicles become more popular, tests are necessary to determine visual acuity requirements for near-field projections. Especially the resulting resolution that fits the user-orientated visual acuity aspects is an impact factor on the selection of the projector technology, as displayed in Tables 2.1 and 2.2. Therefore, an overview of investigations of visual acuity for viewer-related tests is given, using examinations for determining cinema-orientated resolution or visual acuity testing in general. However, the research tests examine general relationships and influencing factors that affect visual acuity. Additionally, already known limitations from the usage of projections of headlamps display the challenges of the automotive context.

### 2.4.1. Resolution requirements influenced by personal factors

When interacting with a near-field projection, several influencing factors affect the observer's perception, so there are two influence domains for the perception of near-field projections.

First, personal participant factors influence visual acuity, such as age, sign structure, or personal preferences [100, 101, 102, 103, 104, 105]. Bleecker et al. provide an analysis of age and sex impact on simple visual reaction times, where the results state that age influences the reaction times for participants older than 70 and that there is a sex difference [100]. Like Bleecker et al. results, McKendrick et al. provide evidence that participants have lower visual acuity and reduced contrast sensitivity with being older than 50 years. Furthermore, a comparison of foveal and para-foveal vision disclaims similar effects regarding aging, in which several factors, such as the eye's lens opacification, pupil size, and reduction of light transmittance, have an influence. [102] Gitting and Fozard examined distance acuity, which exhibits little change until age 60 when it declines, as displayed in Figure 2.10. Theoretically, uncorrected distance acuity declines linearly from age 30 to 80.

After 60 years, the improvement afforded by prescription lenses or other therapies decreases. The variability of presenting distance, uncorrected distance, and presenting near and uncorrected near acuities were constant across all ages in the Gittings and Fozard participant collective, where 577 men participated. However, with advancing age, there is a drop of 46 % in visual acuity between the youngest, about 45 years, and the oldest group above 80 (see Figure 2.10). Older persons in the testing are at a disadvantage regarding the amount of light reaching their retinas since the illumination of the target (10 to 15 foot-lamberts, which correspond to 34.26 to 51.39  $\text{cd m}^{-2}$ ) in this test was constant and low compared to environmental levels according to the authors, which may limit the results of the older participant group. [101]

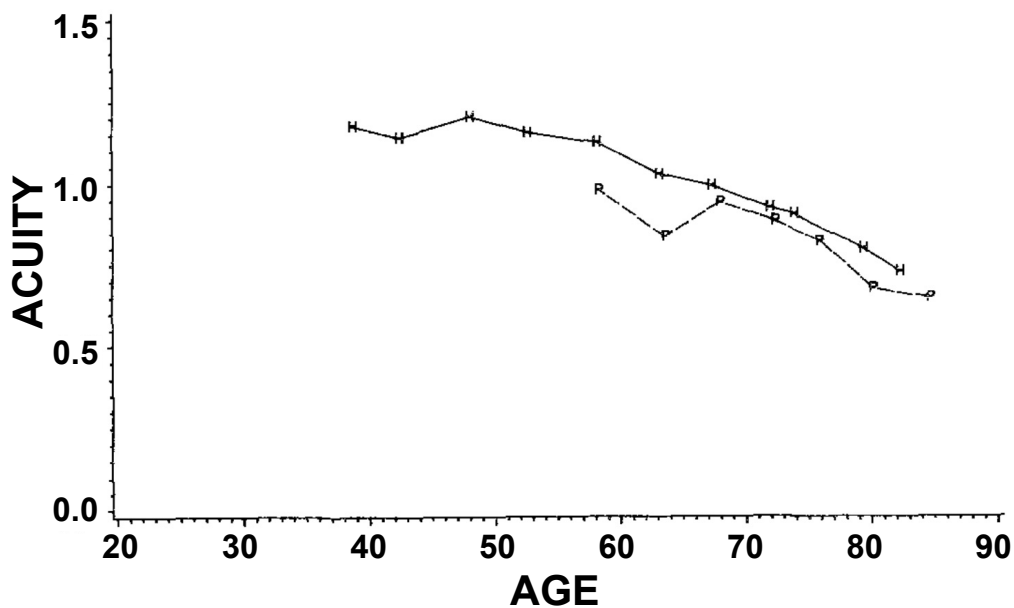


Figure 2.10.: Plots from Gittings and Fozard [101] represent visual acuity for different age groups of participants aged between 35 and 90 years old. The two plots compare subjects with healthy eyes, represented by an 'H', with subjects, represented by a 'P', with visual pathology diagnosis. The plots are retrieved from the original experiment report [101].

In total, most of the reviewed researchers display a critical age of about 50 years and older when the impact of aging is visible and may also be applicable in the testing for near-field projections.

The sign structure is highly complex; therefore, letters of different languages are the focus here. When considering projected illustrations like near-field projections, a text-based projection will vary in the used alphabet when comparing, e.g., Roman, Arabic, and Chinese letters. Wang et al. and Zhang et al. show an excerpt comparing the Roman and Chinese alphabets. They discovered a relationship between an increasing complexity of Chinese characters and the resulting increase in visual acuity requirements [104, 105]. Furthermore, Zhang et al. state that Chinese CC1 characters, with the lowest complexity of Chinese characters, require 37% higher visual acuity than English letters. Moreover, the acuity requirements steadily increased with the complexity of Chinese characters when focusing solely on the requirements for Chinese text-based illustrations. [105]

Besides, Wang et al. discovered a similar tendency that indicates Chinese characters demand higher visual acuity and larger critical character size than English letters [104].

The experiment of Emoto and Sugawara compares viewer behavior on a high definition (HD)-TV and an 8K TV system when watching the same content in an environmental illuminance of 30 lx - so the mesopic vision is dominant. It focuses primarily on the difference in viewing distance and the participant's subjective opinion. However, they also evaluate the subjective impressions of image quality, the degree of image detail, and participant behavior. The results showed that the subjective evaluation of image quality and image detail of the 8K resolution was not significantly different from the ratings of an HD-TV resolution. However, a high spatial resolution TV can generate greater viewer interest than a lower spatial resolution TV. [103]

Thus, personal factors such as age, or personal preferences influence visual acuity. The complexity and importance of this work are evident since the visual acuity influenced by age plays a significant role when driving a car because Sivak and Schoettle's investigation displays an increasing share of older drivers in eight investigated countries worldwide: Canada, Germany, Great Britain, Japan, Norway, Sweden, South

---

Korea, and the United States [6]. Henceforth, the aging population indicates the importance of focusing on older participants for visual tasks in the context of future mobility concepts in urban environments. Further, when the broad introduction of near-field projections is apparent, the influence of different cultures must be considered. The influence of not only the language and the resulting meaning plays a role, especially the type of letters, directly affecting visual acuity, leads to a remarkable influence factor for a correct conception of a near-field projector in order to be able to display all the necessary contents to the full extent. Furthermore, taste or personal preferences play a role in design-oriented content, as displayed in Figure 2.4a.

#### 2.4.2. Resolution requirements influenced by external factors

Besides the personal factors which influence the perception of the resolution aspects, there are also influence factors given by the environment and the external circumstances.

Second, the external factors impact human perception, such as the ambient luminance level, which needs the participant's adaptation as discussed in section 2.3.1, the projection surface characteristics, or the observation distance of the observer to the projection [67, 103, 106, 107, 108, 109, 110, 111, 112, 113]. In detail, the relationship between viewing distance, the resulting screen size, the projection dynamics, and the resulting perceptual influence on visual acuity has been under evaluation for several years for conventional displays or projection-based screens. So, previous research from the television or physiology sector indicates the preferred viewing distance and screen size when viewing an image or video. [103, 106, 107, 108, 109, 110, 111, 112]

The influence of subjective and objective perception, conditioned by the distance to the screen and the influenced factors of image size and corresponding resolution, is examined in television technology extensively.

Emoto and Sugawara investigated subjective evaluations of image quality, visible details, and personal interests of the participant examined under a screen illumination of 30 lx with a  $D65$  background, and the viewing distance was 1.35 m. The participants avoided the degradation of image quality by controlling their viewing distances. Furthermore, Emoto's and Sugawara's research shows that viewing distance decreases when TV images have a higher spatial resolution. The experiment's results verified the researchers' hypothesis that viewers adjust their viewing distance to a high spatial resolution when watching a TV. [103]

Similarly, Westerink's research investigated the preference by focusing on video sequences in a subjective experiment. At a constant distance, 20 subjects rated four various sizes of a video sequence in seven resolution qualities by evaluating with a rating scale the image quality. However, the display size influences the subjective rating in this experiment, where larger display sizes gained better rating scores than smaller ones. Nevertheless, the subjective rating saturates at a specific resolution level regardless of display size. [106]

The fundamental research of Heron et al. discovered a general influence of viewing distance for a visual acuity test with Bailey-Lovie acuity test charts, where three different participant collectives (18-31 years) had different maximal visual acuity levels depending on the viewing distance ranging between 7.55 to 0.19 m [107]. Furthermore, Heinrich et al. tested visual acuity under several ambient luminances to determine VA for scotopic ( $0.009 \text{ cd m}^{-2}$ ), mesopic ( $0.7 \text{ cd m}^{-2}$ ) and photopic ( $90 \text{ cd m}^{-2}$ ) vision for two participant groups of a younger group of 18–29 years old, and an older participant group ranging from 61 to 74 years [112]. Here, the visual acuity is described with logMAR, which is the tens logarithm of the gap width of the smallest still recognized gap of a Landolt ring, which is the VA, as described in equation 2.3[114].

$$\log MAR = \log(1/VA) \quad (2.3)$$

The motivation for such extensive research is based on the different luminance levels during driving, especially at night when the ambient luminance varies dynamically depending on the traffic situation. The researchers varied the presentation time of the stimuli in the Freiburg Acuity and Contrast Test. Figure 2.11 displays the summarized results of the investigation. [112]

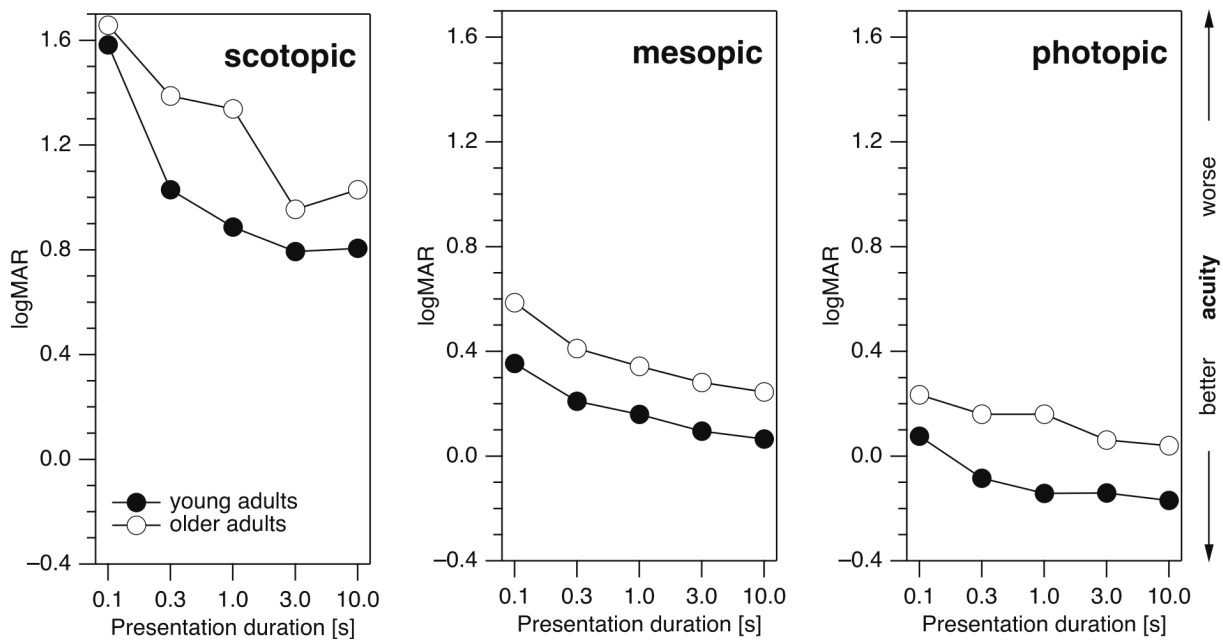


Figure 2.11.: Comparison of median logMAR values for visual acuity, where higher values result in lower visual acuity performance. The graphs display the groups of young (black dots) and older (circles) participants for scotopic, mesopic and photopic vision. Visual acuity is generally better for young participants (logMAR values are lower), the dependence on presentation duration was similar between the age groups. The graph is retrieved from Heinrich et al. [112]

As displayed in Figure 2.11, the VA of the younger and older participants improves with increasing ambient luminance from scotopic to mesopic or photopic vision. Additionally, Heinrich et al. state that the younger participant collective has better VA no matter what ambient luminance level compared with the older age group (see Figure 2.11) [112]. Additionally, Shlaer [110] evaluated the impact of the adaptation luminance, similar to Heinrich et al. [112]. The findings illustrate that visual acuity varies with different adaptation luminance due to the interaction of cones and rods on the retina (see section 2.3.1 for the detailed human eye mechanisms) [110, 111]. Furthermore, the tested target shape influences visual acuity and perception [110]. Therefore, it is necessary to evaluate if these effects also occur to apply near-field projections and thus more complex representations displayed and traffic situations in general.

Therefore, Jesty investigated the relationship by presenting static images in different sizes and random resolution levels to several observers to apply monochrome and color screens without a conventional acuity testing chart [108]. The investigation aimed to allow the participants to set their optimal viewing distance. The outcomes were that the resolution remains the same as the image size increases, and the distance to the monitor likewise increases [108]. Besides, Lund discovered in his experiments in television research a correlation between viewing distance and the resulting screen size preference [109]. Lund, similar to Jesty, let the participants set their optimal viewing distance for themselves in the various experiments for different settings (resolution qualities, displayed content, and various ambient luminance levels) and screen technologies [108, 109]. Both researchers, Jesty and Lund, modified the image size and the resolution in their investigations [108, 109].

Nevertheless, it is essential to mention that Lund mixes several influencing factors without considering the effect on the preference due to the usage of different screen technologies (conventional TV screen or projection screen) or various ambient lighting levels within the experiments, and in the end, concluding a general statement between all these variations of experiments [109]. In addition, Lund mentions that not solely the

resolution may influence the participants' preferences for colored video sequences [109]. Consequently, Lund's results need critical consideration since he mixes some methods and simultaneously changes several variables in his examinations to draw an universal conclusion. Additionally, Lund lists factors crucial for participant testing for the application, such as screen resolution, ambient lighting, video content, and personal factors like the participants' mindset [109]. However, Jesty's results display similar tendencies and effects [108].

Animated sequences or videos in screen development or designing a user-orientated near-field projection system are essential. Therefore, an indication of the dynamics when considering not just static visual acuity (SVA) but also dynamic visual acuity (DVA) is also considered in general examination [81, 82, 83]. There are several methods to test DVA of either moving objects in the screen (Figure 2.12 on the left) or a head-mounted device with specific speeds, fixating the participant's head and moving an object or either having a fixed object and moving the head of the participant with an oscillation (displayed in Figure 2.12 on the right). These measures are applied to identify the differences between DVA and SVA. [82, 83]

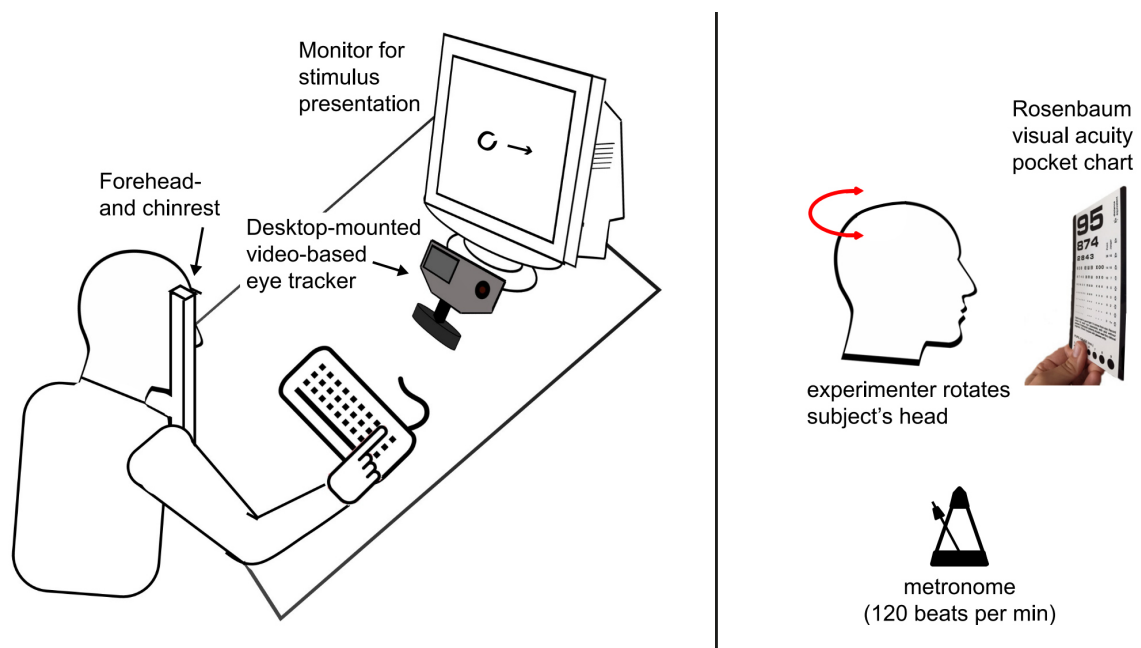


Figure 2.12.: Examples of testing methods for dynamic visual acuity (DVA) - on the left: Set-up for computerized dynamic-object DVA test including an eye tracking device, where the head of the person is fixated. On the right: Set-up for a clinical static-object DVA test, where the participant's head is oscillated. The illustration is extracted from Paladis et al. [83].

The perception of DVA is quite complex, as demonstrated by Long and Penn because it is impossible to predict DVA from an SVA value [81]. The importance of DVA becomes apparent when considering typical traffic scenarios where other RUs are constantly in motion, or the driver must perceive and resolve the oncoming vehicle and other RUs. Therefore, a basic investigation examines with Landolt C targets two presentation times of 250 ms and 400 ms for 35 and 160  $\text{cd m}^{-2}$  under three different target angular velocities of 60, 90, and 120 degrees per second for a horizontal speed. The background luminance was 32  $\text{cd m}^{-2}$ , corresponding to photopic vision. The test with 52 participants showed no relationship between DVA and contrast sensitivity, but an individual difference within the group and an influence of the target's moving speed. Specifically, a decrease in target luminance or presentation time decreased DVA. [81]

Additionally, Paladis et al. found that DVA at low speeds of about 50 degrees per second almost matched SVA conditions. However, eye movement and the resulting image on the retina generally affect visual acuity [83].



The person or the environment generally moves during the eye's perception. Therefore, it is independent of the environmental condition and thus valid for the entire use case in traffic, whether a driver or other RU.

The research on high-resolution headlights also describes the limitation of the quality of the projection optics in the automotive sector [67, 113].

Moisel chooses a theoretical approach to designing an optical system where he expresses the resolution in degrees, a typical representation in headlamp applications. Here he does not define the image's resolution as a limit but rather the resolution power of the projection optics, which he defines as  $0.5^\circ$  per pixel [67]. Such a derivation, he argues with the limitations of micro-optics, which should counteract chromatic aberrations, distortions, or inhomogeneities of the projection system. In addition, he also argues that the imaging unit alone can be considered to evaluate the projection system's capabilities in section 2.2. However, he does not reflect any user-oriented development and only considers the physical characteristics of a projection system. [67]

In contrast to Moisel [67], Pulliam considers a subjective rating on a 5-point Likert scale of possible projection symbols such as accident warnings and icy roads. The quality levels vary between  $0.012^\circ$ , corresponding to a maximum resolution of  $1080p$  of the system used at a projection distance of 2.75 m, and  $0.778^\circ$ . He found that an average resolution of  $0.195^\circ$  per pixel was preferred and that from a resolution of  $0.389^\circ$  per pixel, the images were no longer recognizable from the displayed projection. [113]

Therefore, Pulliam disagrees with Moisel's [67] limit of  $0.5^\circ$  per pixel and motivates extensive research in this area [113]. Examples of the resolutions are shown in Figure 2.13 from the testing by Pulliam.

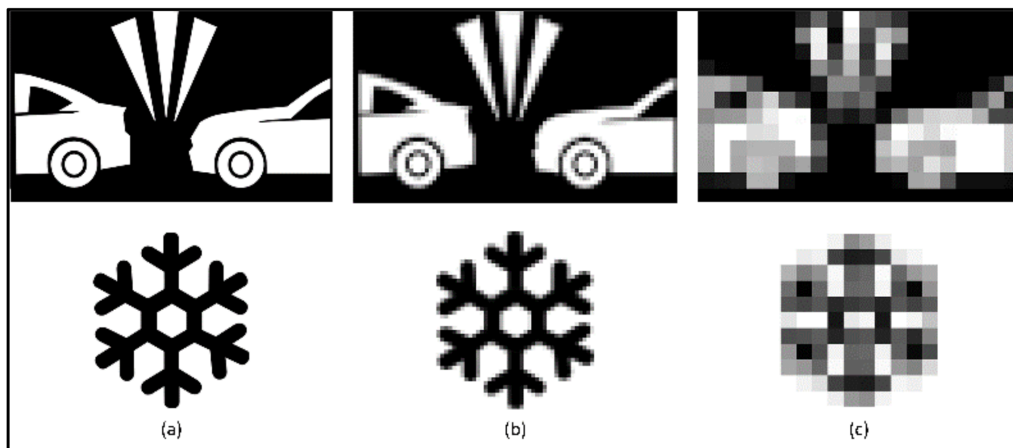


Figure 2.13.: Comparison of different resolution qualities of the tested symbols of collision warning and the icy road warning in qualities of a)  $0.012^\circ$ , b)  $0.097^\circ$ , and c)  $0.389^\circ$  per pixel. The illustration is retrieved from Pulliam's contribution [113].

Thus, these test results show what resolution is considered for a 'more consistent user experience' for high-resolution headlamp applications (less than  $0.1^\circ$  per pixel = 10 pixel per degree) [113]. However, whether these requirements are valid on near-field projections or other resolution requirements arises when discussing high-quality projections rather than the displayed content's recognizability is considered in this work.

Considering all the literature review for resolution aspects, only the self-conducted and published tests include a psychophysical approach to determine user-orientated resolution aspects in the automotive sector, especially for near-field projections [115].

Further, as indicated by the state of the art of research for visual acuity no matter if static or dynamic, the influence of ambient lighting, viewing distance, and projection content, which has different requirements regarding the perceptual processes displayed in section 2.3.2, and projection size are described in Chapter 3 and analyzed in Chapter 4. Additionally, the investigation focuses on perception-based evaluation of the

resolution for a constant contrast display of the tested projection content. Therefore, the next Chapter will review the fundamentals of contrast perception and the resulting conclusions for the participant testing based on the state of the research.

## 2.5. Research related to contrast perception

In addition to the requirements for visual acuity in the previous section, contrast perception plays a significant role in spatial vision, as mentioned by McKendrick et al. [102]. There are already some tests on contrast perception for headlamp applications and, since the last few years, increasingly on applications for near-field projections, which also consider conventional projectors such as slide or microlens array projectors in addition to digital projections. Nevertheless, these studies are fundamental for designing contrast perception tests and covering the state of the art in research. It is also necessary to understand human perception in different situations and elaborate on various research investigations that display state of the art and its impact on perception. Furthermore, an overview summarizes the automotive field's contrast and brightness perception examinations. Finally, it is possible to derive the main conditions and conclusions for the design of the thesis's tests in the following chapters.

### 2.5.1. Fundamentals of contrast perception

One of Blackwell's first tests of contrast threshold, conducted in 1946, was the 50 % probability of detecting a visual target on a homogeneous background under static viewing conditions in a laboratory environment [116]. Adrian's model describes visual performance over a difference threshold  $\Delta L$  between background luminance  $L_b$  and object luminance  $L_o$ . It is necessary to determine a minimum difference threshold necessary for detection: the smaller the difference threshold  $\Delta L$ , the greater the contrast detection capability (Figure 2.9). Adrian's experiments examine a particular viewing angle  $\alpha$  that spans the observed object, such as the diameter of a circular test target (see Figure 2.9), at an object luminance  $L_o$  and an environment luminance  $L_b$ . [94, 117]

The difference threshold  $\Delta L$  depends on the visual angle  $\alpha$  (see Figure 2.9) of the object. It consists of two regions described by the following relations, shown graphically in Figure 2.14 and equation 2.4 [94, 117]. The viewing angle is critical to the application area in which contrast perception is studied. On the one hand, Ricco's law states that the threshold  $\Delta L$  depends nonlinearly on the size of the visual object  $\alpha$  up to a certain object size. On the other hand, for large visual angles  $\alpha$ , the difference threshold  $\Delta L$  is independent of the visual angle and is determined only by background luminance. According to Weber's law,  $\log \Delta L$  is constant (see Figure 2.14). [94, 117]

However, Adrian describes the difference threshold  $\Delta L$  by the following relationship, derived from previously obtained data [94, 95]:

$$\Delta L = k \cdot \left( \frac{\sqrt{\Phi}}{\alpha} + \sqrt{L} \right)^2 \quad (2.4)$$

The difference threshold  $\Delta L$  contains the luminous flux  $\Phi$  (Ricco's law) and the luminance function  $L$  (Weber's law) in equation 2.4. Furthermore, equation 2.4 includes viewing angle  $\alpha$  in angular minutes, and the factor  $k$  as the detection probability factor, where the values  $k = 1$  correspond to 50 % detection probability and  $k = 3.1$  relates to 100 % detection probability. The correction factor is necessary because Adrian calculates the detection probability using data from Blackwell and Berek to feed the model. [94, 95, 116, 117]

The graph in Figure 2.14 shows that Weber's law starts at an angle of about  $200'$  ( $=3^\circ 20'$ ), and therefore it is crucial to consider this value for the participant tests described in Chapters 5 and 6 so that a psychophysical consideration of contrast perception is valid.



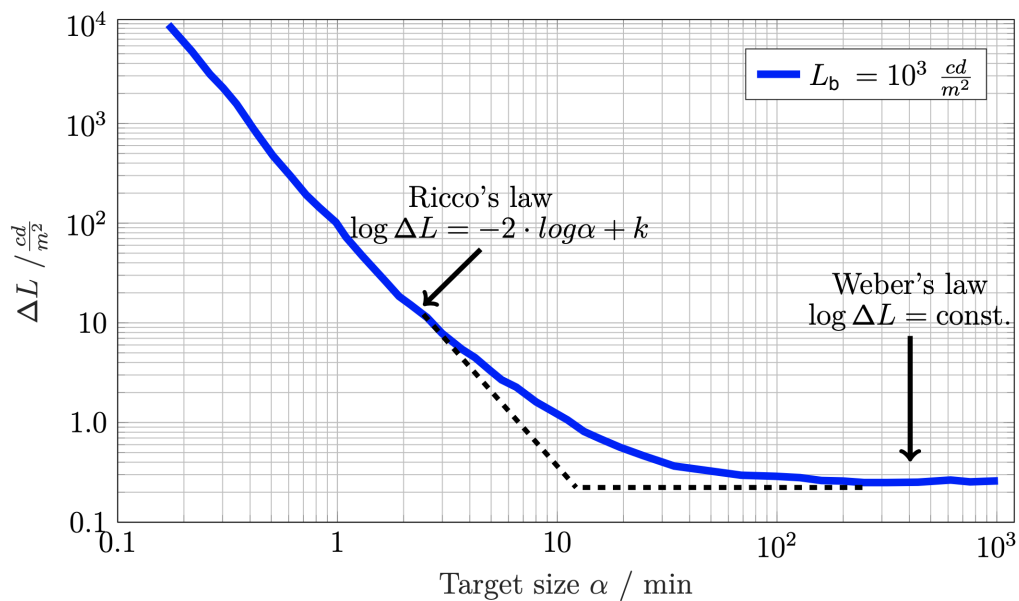


Figure 2.14.: Illustration of the luminance dependency related to the object size in angular minutes. In detail, luminance threshold  $\Delta L$  as a function of the observation angle  $\alpha$  at a background luminance  $L_b = 1000 \text{ cd m}^{-2}$ , which is in the photopic vision. For small angles of observation, Ricco's law is valid, and for large angles, Weber's law [94]. The illustration is retrieved from Schneider's thesis [118].

The model describes the visibility of small target objects, valid for several applications, such as driving a car at night. Furthermore, the model calculates the target contrast by considering the object's size, whether the contrast is positive or negative (polarity) [94]. However, only the positive contrast is considered further when using near-field projections. Further, the model includes the adaptation luminance, the age of the participant, the target presentation time, and the possible influence of glare, which affects the contrast threshold. When physiological glare is present, objective visual performance is reduced by the glare luminance present, as discussed in the section 2.3.3. The glare source reduces the contrast of the visual object, and the differential threshold required for perception and detection needs greater values for the object's luminance. In addition, glare increases with age due to the eye's aging process. [30, 94, 95, 96] Contrast perception depends on the luminance of the environment or background  $L_b$ , as shown in Figure 2.9, top left, which the participant or human generally perceives. The main limitation of Adrian's model is that it is just examined under lab conditions and not in realistic examination settings, e.g., traffic situations [94].

Adrian's model has been used in several investigations of headlamp detection tasks to determine an appropriate headlamp distribution based on contrast detection and perception [16, 94, 95, 118, 119]. However, the headlamp application differs from the used object size for a near-field projection, as near-field projection sizes are over 200' and thus follow Weber's law, which allows a consideration of the Weber contrast.

In addition to general contrast perception, the position where an object must appear and thus be perceived also plays a role in the application case of the vehicle. Thus, it is crucial to consider contrast perception in the peripheral field of the observer. Figure 2.5 shows that cone density outside the fovea decreases dramatically, and the rods have a higher distribution in the peripheral field of view. Thus, focusing on, e.g., mesopic vision, which occurs in many road traffic situations, objects such as near-field projections, can be detected outside the fovea. Additionally, depending on the driving situation, the stimulus can be focused more precisely with the fovea.

Fleck investigated contrast perception, which shows contrast thresholds as a function of stimulus eccentricity

in Figure 2.15 [120, 121]. The investigation splits into two phases: In the first step, he analyzed single-target detection, i.e., the perception of the presence of a target on a homogeneous background. In a second step, he investigated single-target discrimination for the same test condition.

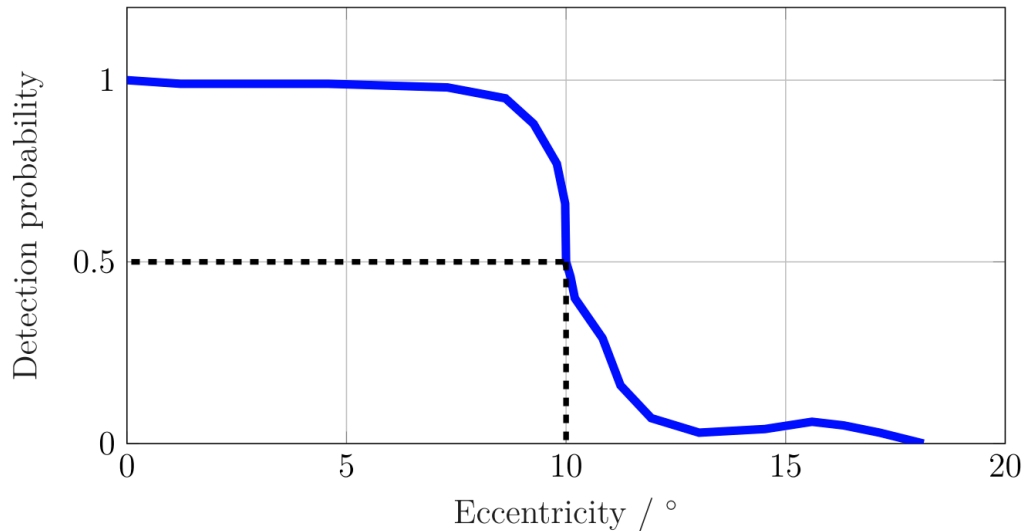


Figure 2.15.: Detection probability of a test stimulus as a function of eccentricity. The test target is the letter 'O' with a size of 18' x 36' [120, 121]. The illustration is retrieved from Schneider [118].

The subject fixated a marker in the middle row of a screen at a distance of 0.41 m under adaptation luminance of  $20 \text{ cd m}^{-2}$  (photopic vision), and the targets appeared every 6 s for 300 ms at a foveal fixation point or peripherally up to  $30^\circ$ . Target onset positions were  $2^\circ$  apart. Furthermore, the targets were the letters 'O' and 'D' (angular size 18' x 36') or a rectangle (sized 27' x 48'). [120, 121]

Because Fleck used the constant stimulus method, the participant responded if a stimulus was visible or not in the detection task with a simple keyboard. Furthermore, decreasing peripheral detection performance with increasing viewing angle strongly depends on the degree of adaptation as shown in Figure 2.15 [120, 121]. There are two limitations to Fleck's investigation: the focus on laboratory circumstances in photopic vision and the small object sizes of the tested stimuli, which do not apply to near-field projections. Therefore, specific consideration and investigation are needed if the displayed relationships are also valid for near-field projections.

Schneider explicitly investigated the mesopic range for contrast perception in a laboratory environment while focusing on either  $0.1$  or  $1 \text{ cd m}^{-2}$  as the adaptation luminance of the background (see Figure 2.16). She tested eccentricities of 0, 2.65, 5, 10, and 20 degrees in the peripheral field of view with two test targets - a circle and a deer pattern. Results of the examination include that with increasing background luminance, there is better detection of low contrasts, which is valid for foveal and peripheral stimuli (see Figure 2.16). Therefore, the green dashed line of the deer pattern is lower for higher background luminance, as displayed in Figure 2.16. For a complex test target such as a deer symbol, maximum contrast is apparent at  $10^\circ$  in Figure 2.16, but the circle increases monotonically with increasing eccentricity. [118]

The difference in the task is a possible indication of the cognitive workload, which measures an individual's mental effort to complete one or more cognitively demanding tasks [122]. There are several types of cognitive workloads and what causes them, for example, the task's complexity, presentation style, and the user's ability to understand the material entirely [122, 123].

The perceptual process and the distribution of the cones and rods can significantly describe the results [78, 31, 30, 118, 120, 121].

Furthermore, Schneider also conducted a field test, which summarized that the participants needed higher contrasts than in the laboratory test [118]. In addition, Schneider [118] elaborates on possible influences on the model set up by Adrian [94], such as static or dynamic viewing of the stimuli, level of attention, adaptation, target location in the peripheral vision, and parameters specific to the vehicle application.

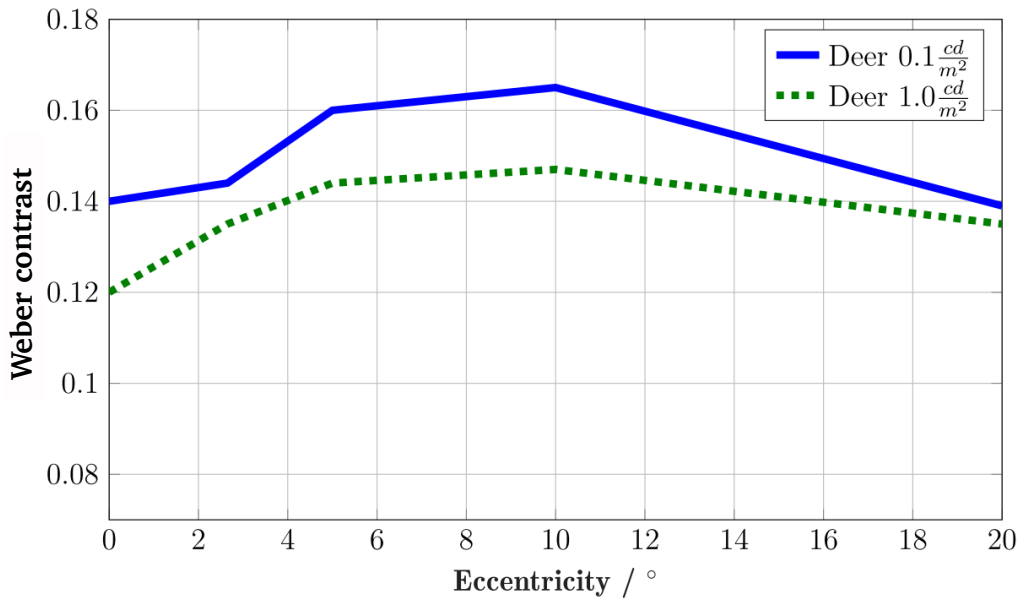


Figure 2.16.: Distribution of the contrast detection at the probability of (99 %) at two background luminance levels ( $0.1$  and  $1 \text{ cd m}^{-2}$ ) depending on the eccentricities in the field of view for the target shape of a deer with a target size of  $1^\circ$ , retrieved from Schneider’s contribution [118].

Thus, investigations related to near-field projection need consideration of the perception and the influencing factors in more detail in the next section.

### 2.5.2. Evaluation of the state of the art in near-field projections

As the application of near-field projection around vehicles becomes increasingly popular, different research institutions or projector manufacturers have conducted several investigations on contrast perception. The tests differ in the type of considerations, either theoretical derivations, carried-out subjective or field examinations. Aspects include the essential benefit of near-field projections, contrast or brightness perception, factors of perception influence, like ambient brightness, type of projection display (static and dynamic), and the projection background characteristics. Additionally, researchers examine also the technical design of near-field projectors. As mentioned in the section 2.2, no consideration is given to headlight high-resolution projections in this state-of-the-art comparison, as other research institutions have already presented this in detail [13, 14, 37, 38, 15, 39, 40, 51, 16, 66, 67, 68, 17, 18, 69, 70].

In addition, this work neglects investigations conducted in virtual reality, as these tests have different conditions related, e.g., to luminance perception compared to tests conducted in real life, and these are not comparable with the conducted tests from Chapters 3 and 5 [55, 56, 59, 24, 124].

Many investigations focus primarily on safety-relevant urban traffic situations, such as the investigation by Shibata et al. [27], which investigates the influence of a direction indicator projected onto the road during a turn situation. The ambient luminance varied between 800, and 10 lx, and two test images were projected: rectangle and herringbone pattern. The scenario was changed by having the subjects walk once along the path

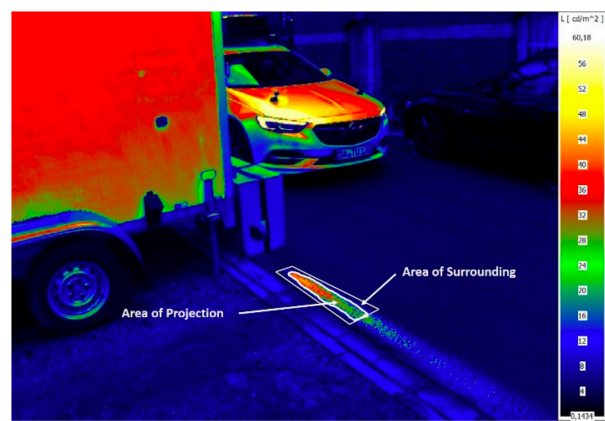
by the projection, facing a cell phone and another time facing the road. Besides the physical values of Weber contrast, the subjective perception of the brightness of the ground projection was evaluated with a 7-level Likert scale. In addition, the test design tracks the reaction time for the projection's detection. [27] Shibata et al. concluded that higher contrast is necessary to detect an object at lower ambient illumination levels. In the present case, the projected pattern did not affect the subjects' perception of brightness - a Weber contrast of 0.4 results in detection in the scenario facing the asphalt [27]. Considering the ambient illuminance influence, it is clear that the influence is current since a Weber contrast of 0.22 is necessary for 800 lx compared to 2.74 at an ambient luminance of 10 lx for similar detection rates. When the gaze was directed at the cell phone, the difficulty of the subjects increased significantly for the subjective evaluation of the project's detection, which relates to the concentration required to focus on the cell phone and the eyes' adaptation to the brighter display. [27] In addition, these factors also indicate a higher cognitive workload [122, 123].

The following test by Shibata et al. in 2021 [26] investigates how easily pedestrians can detect a projection of a reversing vehicle compared to conventional reversing lights. In addition to a button press upon detection, subjective evaluation rates the clarity of the projected pattern. As shown in the previous investigation [27], higher detection contrasts are necessary for low ambient illumination levels [26]. Furthermore, Shibata et al. examine four different ambient luminance levels which cover applications of dark intersections at night (10 lx) to a particular degree at dusk and dawn (1000 lx). In addition, Shibata et al. find an influence of the experience level of projections since, e.g., naive participants need a higher Weber contrast for detection compared to experienced participants. Dynamic representations (flashing arrow, sequentially arrow) have a higher detection rate than static projected illustrations and are the most understandable regarding clarity of intention. In case of distraction, the participants need a higher detection contrast if looking at a cell phone. Additionally, for every ambient luminance level, luminous intensity is defined to achieve the detection rates of the testing results for a projection, which is displayed 3 m apart from the vehicle and is projected from a height of 0.9 m, e.g., 4297 cd for a static illustration for 200 lx. [26]

Singer et al. studied the behavior in a critical situation with autonomous vehicles. The dynamic field test simulated a hidden pedestrian scenario. The participant's starting point was next to a trailer that completely blocked the view of the left side of the road where a vehicle was approaching. A warning with a projected bar indicates to the unaware participants an approaching vehicle, displayed in Figure 2.17a.



(a) Display of the testing procedure for one exemplary participant who experiences a projected bar on the street surface, retrieved from Singer et al. [7].



(b) Luminance measurement of the participant testing by Singer et al. [7] with the marked area of the perceived projection.

Figure 2.17.: Picture of actual participant testing and luminance measurement of the tested scenario, retrieved from Singer et al. [7].

---

Each test person performed 15 crossings, 14 without any projections on the ground for familiarization purposes. Only in the last round does the experimenter manually activate the projection system (Figure 2.17). Due to local conditions, the vehicle always approached at a speed of approx.  $10 \text{ km h}^{-1}$ . The bar varied between a static and a flashing presentation randomly per participant under realistic conditions in a parking lot. Due to various times of day and changing weather conditions, luminance recordings were necessary after each completed test run to track the changes, displayed for one participant in Figure 2.17b. So, it was possible to determine the contrast between each perceived projection and road surface per participant. In conclusion, a contrast below 0.4 did not detect the static projection. Controversially, the participants' detection contrast levels below 0.4 are detectable for dynamically displayed projections, which correlates with the findings by Shibata et al. [27].

Baumann et al. investigate the intuitiveness of symbols and their message for different age groups of pedestrians. For this purpose, a static test setup is used in a lab environment, which unfortunately does not have asphalt as a projection surface. [60] Furthermore, a projection distance of 10 m is chosen [60], which does not apply to near-field projections according to Schlöder's definition (below 5 m) [19]. As a result, a Weber contrast of 11.5 is obtained, with an ambient luminance of  $0.8 \text{ cd m}^{-2}$ , which corresponds to the mesopic range, and a symbol luminance of  $10 \text{ cd m}^{-2}$ . The results show three symbol representations for the message 'STOP' with higher detection probabilities of 80 % for children (5 to 8 years old) and six representations for detection thresholds higher than 80 % for adults (18 to 63 years old). The comparison between children and adults shows that the dynamic type of projection does not influence the detection probability for children, unlike the adults, who have higher detection rates for both dynamic and static projections. [60]

From a different perspective, Namyslo et al. look at a safety-relevant scenario, the turning of a vehicle, in a dynamic investigation from a cyclist's point of view [25]. In addition to the investigations for pedestrians already mentioned [60, 26, 27, 7], reducing accidents with cyclists has potential by applying projections in urban traffic [25]. The investigation evaluated an ambient illuminance of 200 lx, with a Weber contrast selected to be about 1. The subjective survey results show that the participants feel safer in the tested scenario, understand the driver's intention better, and are not averse to seeing projected turn signals. A projection turn signal and its possible characteristics at 200 lx ambient illuminance result in a luminous intensity of 12 000 cd at a projector's mounting height of 0.7 m for a projection displayed 3.4 m apart from the vehicle. [25]

Maier and Schlöder also conducted a subjective examination using a projection module that projects amber chevrons or a turning cyclist symbol [22]. The light levels of the projected symbols were measured from the perspective of bicyclists, pedestrians, or an oncoming vehicle on different surfaces. The central aspect of the testing focuses on the subjective perception from a cyclist's point of view, such as the brightness of the projection surface, the influence of a wet road surface, the roughness of the projection surface, a dynamic display type of the projection, and a colored display of the projection. A final evaluation of the authors concludes that the background's color and roughness significantly influence the projection's perception. Brighter projection surfaces have higher visibility ratings and wet projection surface further reduces perceived visibility. In addition, subjective perception shows that colored projections do not improve the visibility of near-field projections. However, the authors state that the dynamic display could compensate for an unfavorable projection surface. [22]

In addition, Thomas also presented the influence of the projection surface in his theoretical consideration/interpretation. In this case, the visibility of an automotive-ready DMD projector is limited depending on the time of day, the ambient brightness, or the sun's position [42].



## 2.6. Summary of the literature review

This chapter provides an overview of the literature review and identifies aspects that require further investigation. Therefore, Table 2.4 and 2.5 summarize the research for resolution aspects and contrast perception-related investigations in the automotive sector by focusing on near-field projections. Looking at both tables, the characteristics marked with a checkmark vary within the testing for the named research, such as different resolution levels or various target luminances, external factors such as several viewing distances, or personal factors like various age groups within the participant collective. Furthermore, items in brackets illustrate a variability of the item or variable, which the reviewed literature does not clearly state. Not-marked sections display non-available information for this specific parameter.

First, Table 2.4 states that except for Lund’s study [109], no systematic research of different projection contents under a constant ambient setting is evident since Lund lists several studies under various external factors [109]. Furthermore, no studies of Table 2.4 have changed the projection size for different resolution levels but mostly link the size of the image or the testing screen to the resolution itself; then, the test participants set the viewing distance according to their subjective preference. Moreover, there is mainly theoretical evaluation of moving content, for example, a variation of DVA tests [81, 83]. Finally, besides Pulliam [113], Stuckert and Khanh [115], and to some extent, Lund [109], no researcher deals with projections and thus reflective systems, but mostly direct-imaging screens or printed test charts for defining VA. Hence, focusing on the resolution-specific research allows us to deduce the gap in research from the missing or not extensively considered user-orientated data in the boxes of Table 2.4.

Table 2.4.: Literature review related to resolution aspects, including test parameters and possible impact aspects such as external and personal factors. Table 2.3 indicates different levels of vision.

		Emoto and Sugawara [103]	Westerink and Roufs [106]	Heron et al. [107]	Heinrich et al. [112]	Jesty [108]	Lund [109]	Long and Penn [81]	Pulliam [113]	Stuckert and Khanh [115]
<b>Test parameters</b>	Target luminance				(✓)		(✓)	✓		
	Resolution	✓	✓			✓	✓		✓	✓
	Content						(✓)			✓
	Size	✓	✓	✓	(✓)	✓	✓			
	Dynamics		✓					✓		
<b>External factors</b>	Vision	mesopic			scotopic, mesopic, photopic		(scotopic), mesopic	photopic		mesopic
	Viewing distance	✓		✓		✓	✓			✓
	Viewing setup	TV	TV	Chart	Screen	TV	Various screens	TV	Street	Street
<b>Personal factors</b>	Peripheral viewing									
	Age			✓	✓					

Second, Table 2.5 lists the investigations for contrast perception, which mainly deal with analyses from the automotive industry or explicitly the application of near-field projections except for Fleck’s research [120, 121], which is theoretical and serves as primary literature for examinations on peripheral viewing.

Therefore, it is clear that no one explicitly modifies the test target’s brightness or luminance except for Shibata’s studies [26, 27]. Further, except for Schneider [118], who has other circumstances due to Ricco’s law (see Figure 2.14), none changes the object size of the perceived stimuli, which are perceived to be of different sizes by either the object size itself or the viewing distance for the observer.

Table 2.5.: Summary of the literature review related to contrast perception, including test parameters and possible impact aspects such as external and personal factors. Table 2.3 indicates different levels of vision.

		Fleck [120, 121]	Schneider [118]	Shibata et al. [26, 27]	Singer et al. [7]	Baumann et al. [60]	Namyslo et al. [25]	Maier and Schlöder [22]
<b>Test parameters</b>	Target luminance	✓		✓				
	Resolution							
	Content	(✓)	✓	✓		✓		✓
	Size		✓					
	Dynamics			✓	✓	✓		✓
<b>External factors</b>	Vision	photopic	mesopic	mesopic	mesopic, (photopic)	mesopic	mesopic	mesopic
	Viewing distance							
	Viewing setup	Screen	Screen, street	Street	Street	Carpet	Street	Multiple surfaces
<b>Personal factors</b>	Peripheral viewing	✓	✓					
	Age		✓			✓		

Most of the literature calls for investigating near-field projections in day-like scenarios with higher ambient luminance levels incorporated and conducted in the investigations of Chapters 5 and 6 [22, 42, 25, 26, 27, 7], which is illustrated by the listing of vision variable in Table 2.5 since most research groups focus on mesopic vision conditions. Finally, only examinations with small test targets have been conducted in the peripheral field [120, 121, 118]. Therefore, it is necessary to investigate the conditions of peripheral contrast perception for near-field projections in more detail.

In summary, the literature research shows that besides static or dynamic visual tasks (e.g., visual acuity, contrast perception), influences like viewing distance or stimulus size are decisive for the results and the testing design. Furthermore, for both aspects (resolution and contrast perception), the influence of projection content is considered in more detail, as the cognitive load influences the visual process [78, 86, 122, 123].

The influencing parameters focus not only on the technological domain but also on the perceptual domain for an user-oriented definition of near-field projections. So, these findings provide a basis for the later design of the experimental setup and the necessary methods. In addition, the results of this thesis are compared to those of, e.g., Shibata et al. [26, 27] or others of Tables 2.4 and 2.5, and psychophysical tests will complete the other subjectively evaluated investigations with physical values for resolution aspects and contrast perception. Finally, an evaluation of technologies for near-field projections is possible with the extensive literature review to link the technological domain to the psychophysical (user-orientated) results like the resolution aspects for the microdisplay or the luminance of near-field projectors for safety-relevant situations.

## 2.7. Identified research questions

Finally, the values of Table 2.2 show an excerpt of the current technological development. However, the question arises, are these projector characteristics listed in Table 2.2 as examples sufficient for the three application areas of near-field projections (welcome and goodbye, safety-relevant, and projections for communication)? As mentioned in the literature, some application areas are already implemented with the mentioned technologies, especially welcome and goodbye projections [42, 20, 23, 21]. Nevertheless, it is questionable whether the framework conditions for near-field projections are realistically assumed since Thomas specifies ambient conditions of, for example, 10.8 lx as ambient illuminance during twilight [42]. However, parking garages

---

already have higher illuminance levels [80].

Therefore, it is crucial to question the projector components and the user's perspectives on who will see and perceive a near-field projection in the urban environment. It is essential to determine whether the three applications (Figure 2.4) will have different requirements and, thus, different prioritized implementations or potentials in technologies for the projector. A literature analysis regarding near-field projection systems' state of the art in Table 2.2 should serve as a basis. Further, the literature review of resolution aspects and the contrast perception of Section 2.6 highlights which aspects need detailed evaluation in this thesis through psychological testing for user-orientated development of near-field projectors. Thus, the following research questions arise:

- What are the user requirements as the minimum resolution for digital near-field projections? Is there a universal resolution quality, or will application-specific differences exist?
- Which of the specified technologies in Table 2.2 is sufficient for safety-relevant projections at the current maturity level?
- What technology would provide an universal solution for near-field projection and its lighting characteristics?
- What influence do street surface characteristics have on perception regarding the resolution and visibility of near-field projections?
- What are the visibility requirements for near-field projections in daytime ambient luminance scenarios, and which technology is suitable for enabling these scenarios? Does the projection content play a role in this consideration?
- What limitations can perception-related analyses derive for near-field projections in urban road traffic? Is it possible to reach the physical limits of projection technology, or does this define future development?

With this in mind, the thesis will condense an uniform fundamental work on the definition and configuration of near-field projections in order to focus on user-oriented projector design and, finally, to ensure a comparison between the technology and perception domains.



---

## 3. Experimental set-up and technical aspects for the definition of resolution requirements of near-field projections

---

In this chapter, an experiment defines limitations relating to the human visual system for the resolution requirements of near-field projections under different ambient luminance levels and various viewing distances. Additionally, the experimental setup and the used equipment have physical limitations. Therefore, an extensive characterization of the test environment is necessary to guarantee reproducible field tests, including deriving a minimal perceived detail on the projected asphalt in the testing environment. All tests mentioned in Chapter 3 and Chapter 5 apply the methods of constant stimuli, which is a standard method to measure physical values in psychology by applying the psychophysical approaches [74, 75], e.g., in this work, the resolution or contrast of near-field projections. Furthermore, this chapter describes the examined test parameters for different projection contents (symbol- and text-based) and types of illustration (static or animated). In the end, a questionnaire analysis depicts general information about the participants in the field studies.

### 3.1. Characterization of the projection surface

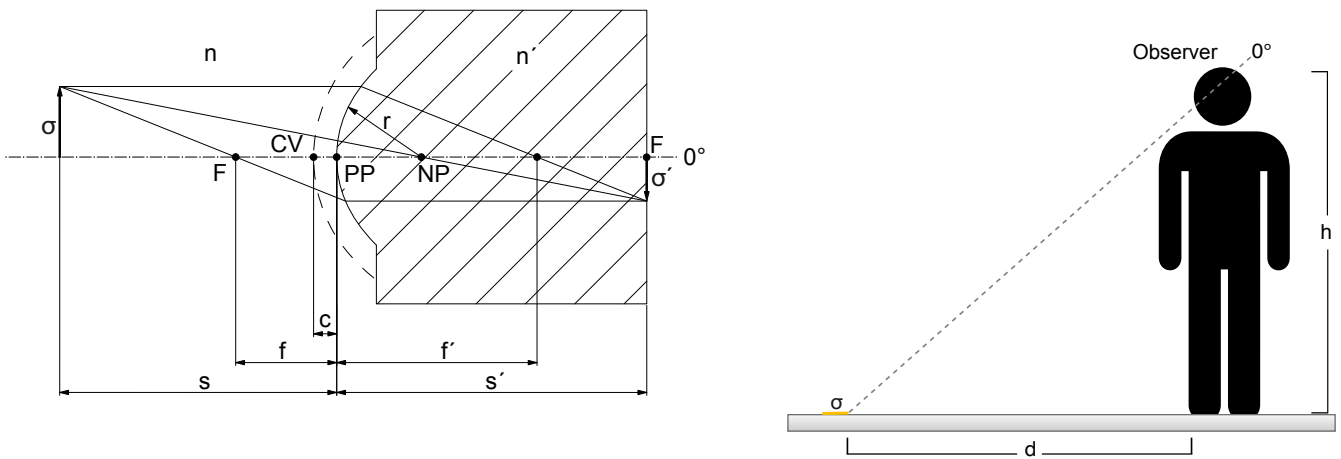
The test environment is examined in detail to design a comparable test and set the conditions for the resolution requirements, which are present with the fine-grained asphalt used. In order to define the resolution of the projection surface, a pre-test is carried out under different ambient luminance levels, which includes a modified visual acuity (VA) test for the participants. Hence, the following pre-test guarantees the usage of the testing environment to validate the resolution requirements for near-field projections around the vehicle based on the test of VA, which includes the ability to resolve and recognize subtle structural elements. VA definition does not include the resolution of details for the objects. Instead, it describes a separation of two neighboring lines or edges, e.g., the size of the gap of a Landolt ring or the gap between two neighboring lines (see Figure 3.1) [76, 30].



Figure 3.1.: Illustration of different test patterns for visual acuity testing listed from left to right, such as a letter chart, a Landolt ring and a Snellen E or a line pattern [76, 30].

A crucial point of performing a simplified VA test is reinforced by the fact that VA will differ when focusing on line patterns instead of a letter optotype. Thus, line patterns measure resolution or detection, whereas letter charts demand pattern recognition. Therefore, the letter chart VA method demands higher cognitive resources than the line pattern VA option because line pairs are more uncomplicated to detect than letters [30].

Before designing the testing parameters for an acuity test, it is essential to derive the framework conditions in the human visual system. For this purpose, a simplified model of an eye is considered as a simple optical model, which is displayed in Figure 3.2a [76]. Therefore, Figure 3.2a shows the following parameters, which help to calculate a human's maximum possible perceptible resolution. The distance between the centers of two adjacent cones in the highest cone density area (fovea) is approximately 2 to 2.5  $\mu\text{m}$  if the subject looks directly at the area to be evaluated [76, 30], as in Figure 3.2b. Thus, the distance between the cones is the image size on the retina  $\sigma'$ . Furthermore, the focal length of the eye is necessary to describe an optical system. The specifications vary from 17.06 mm [76] to 16.8 mm [30] for the eye's focal length  $f$ .



(a) Representation of the eye as a simple optical system based on Hauske [76] and the corresponding parameters are listed: The plotted points are the principal point  $PP$ , the nodal point  $NP$ , the anterior focal point  $F$ , the posterior focal point  $F'$ , and the corneal vertex  $CV$ . The refractive indices are  $n_{\text{air}} = 1$  and  $n'_{\text{water}} = 1.34$ . The geometric parameters are  $f = 16.8 \text{ mm}$  [30] -  $17.06 \text{ mm}$  [76],  $f' = 22.5 \text{ mm}$  [30] -  $22.785 \text{ mm}$  [76],  $r = 5.73 \text{ mm}$ , and  $c = 1.5 \text{ mm}$ . The anterior corneal surface of the actual eye is shown in dashed lines (radius  $7.8 \text{ mm}$ ) [76, 30].

(b) Illustration of an observer (height of the person  $h$ ) at a viewing distance  $d$  with a direct viewing position to the resolvable detail  $\sigma$  on the projection surface. The direct viewing position at  $0^\circ$  indicates the foveal vision. The simplified optical model of the sketch in Figure 3.2a is assumed as the observer's eye in the viewing angle of  $0^\circ$ .

Figure 3.2.: Schematic of the simple optical structure of a human eye (Figure 3.2a) and the constellation of an observer who is looking with a foveal vision on the illustrated small detail (Figure 3.2b).

Consequently, Hauske derived by using Newtonian imaging equations the following simplified relations in equation 3.1 [76].

$$\frac{\sigma'}{\sigma} = \frac{f}{f - s} \quad (3.1)$$

To determine the distance to the object  $s$  in the given situation, when a person looks directly at the surface, he/ she has to look from a certain distance  $d$  with a specific person's height  $h$  (see Figure 3.2b). Equation 3.2

summarizes the described geometric relation for the object distance  $s$ .

$$s = \sqrt{d^2 + h^2} \quad (3.2)$$

Further, equation 3.2 extends the equation 3.1 of Hauske [76] to the present application. Thus, the modified equation 3.3 describes the resolvable detail size  $\sigma$  on an observed surface with the consideration of the person's height  $h$ , viewing distance  $d$ , the eye's focal length  $f$ , and the image size on the human's retina  $\sigma'$ , in this case, the distance between two neighboring cones ( $=25 \mu\text{m}$ ).

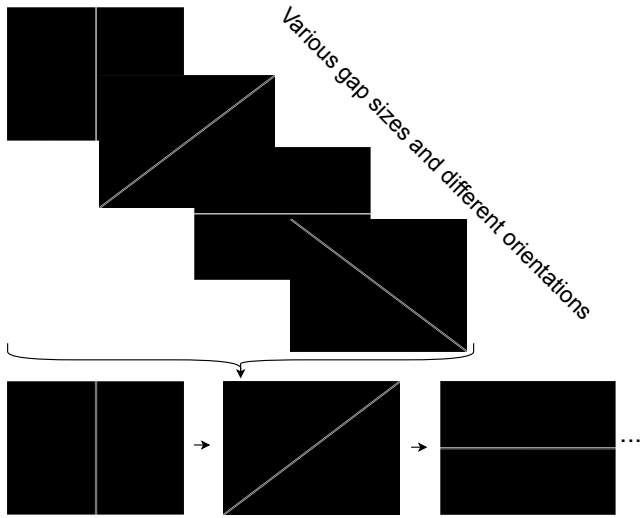
$$\sigma = \frac{\sigma'}{f} \cdot |f - \sqrt{d^2 + h^2}| \quad (3.3)$$

Equation 3.3 handles the following values: 1.68 m for the eye height of an average person in Germany, the viewing distance of 1 m, the focal length of the human eye 16.8 mm [30], and a distance between two cones of  $2.5 \mu\text{m}$  [30], resulting in an object size of  $\sigma=0.294 \text{ mm}$ . This object size is the smallest object a person can perceive in this theoretical consideration with the given setting in Figure 3.1 and the assumption of perfect foveal vision. Therefore, no objects below the size of 0.294 mm shall be tested because these details are not resolvable for a human without considering the used projection surface, which will test the influence of the fine-grained asphalt in the pre-test. This is in line with Bremer's evaluation that an object size of less than 3 mm is sufficient for design-oriented representations [126].

Considering all previous aspects, the concept for the pre-test follows the mentioned methods of a line pattern consisting of two lines with various gap sizes between them. The participants must distinguish if the projected content displays one or two lines next to each other on the ground. The used pattern is based on the line pattern shown in Figure 3.1, one of the possible VA test patterns [76, 30]. To avoid a learning effect and to increase the subjects' concentration during the test, the projected lines rotate  $\pm 45$  and  $\pm 90$  degrees on the projection surface, displayed schematically in Figure 3.3a. Additionally, Figure 3.3b shows a picture of the used setup with a vehicle and the mounted LCD laser projector [127] with roof construction.

In practice, values of 1 angular minute ( $1' = 1 \text{ arcmin} = 1/60^\circ$ ) relate to the smallest angle  $\alpha$  resolved between two neighboring objects like two bars (see Figure 3.1, 3.3a and 3.3b). The resolution of two neighboring objects corresponds to the limitation of the optical system given by the diffraction phenomena with a small pupil, which affects the size of the cones on the retina. Equation 3.4 describes the numerical value for VA. A value of 1.0 for VA is considered normal for an ambient illuminance level of 200 to 300 lx [76, 30]. Visual acuity also reaches a maximum value of 2 under the assumption of high ambient luminances and high contrast, which relates to viewing angles of  $0.5'$  [30]. Finally, this maximal level of  $VA = 2$  is achieved with the value of  $\sigma=0.294 \text{ mm}$  for the object size, which was theoretically determined before with equation 3.3.

$$VA = 1/\alpha \quad (3.4)$$



(a) Variation of the used line pairs with various gap sizes and orientations, including a rotation of  $\pm 45$  and  $\pm 90$  degrees. Consequently, the randomized image sequence is displayed exemplarily below.



(b) Picture of the used setup, which includes a vehicle with an LCD laser projector [127] mounted via a roof construction with a projection of a line pair rotated  $45^\circ$ . The displayed testing environment shows an ambient illuminance of 196 lux to 235 lux depending on the viewing distance to the projection.

Figure 3.3.: Executed procedure in the pre-test to define the size between two depicted lines related to the visual acuity testing. Figure 3.3a depicts the testing algorithm. Figure 3.3b displays a picture of the setup, including the projection area marked with a dashed line and a projection of a line pair.

Further, the limitations for the design of the test patterns relate to equation 3.5 and the corresponding theoretical limitation of the eye structure. Therefore, the thickness of the lines is 2.93 mm on the projection's surface so that the participants can see the projection with a VA of less than 1 (see Table 3.1). The visible structure  $\sigma$  is described by equation 3.5,  $d$  indicates the viewing distance, and  $\alpha$  describes the viewing angle in degrees when looking at the visible element. The variation of the used gap sizes is illustrated in Table 3.1 to display the used stimuli, assuming an average height of a person 1.72 m in Germany [125] and an eye height of  $h = 1.68$  m.

$$\sigma = \tan(\alpha) \cdot \sqrt{h^2 + d^2} \quad (3.5)$$

The mentioned stimuli in Table 3.1 is also valid for the line pairs, which are rotated by  $\pm 45$  and  $\pm 90$  degrees. To indicate the relation to the theoretical values of  $1'$ , which is the differentiability threshold [76, 30], therefore, Table 3.1 illustrate the results as the multiple of one angular minute. Accordingly, the factor of 60 applies to equation 3.6, which is the rearranged variant of equation 3.5.

$$\alpha = \arctan\left(\frac{\sigma}{\sqrt{h^2 + d^2}}\right) \cdot 60 \quad (3.6)$$

All used gap sizes besides the tiniest gap at 3 m viewing distance are above  $1'$ . Nevertheless, none of the tested gap sizes is below  $0.5'$ , the smallest detail a person can perceive theoretically. Consequently, in this case, the participants can detect all tested gap sizes between the line pair with a  $VA > 1$  except the smallest gap at a 3 m distance.

Table 3.1.: List of the used gap sizes on the projection surface in mm and as multiple of 1' depending on the participant's viewing distance of either 1 m or 3 m to the projection area.

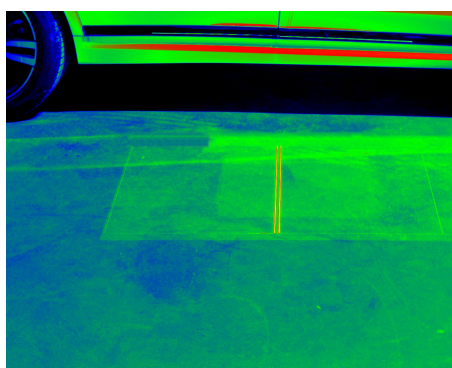
Gap size in mm	Gap size for 1 m as multiple of 1'	Gap size for 3 m as multiple of 1'
0.75	1.32	0.75
1.27	2.23	1.27
1.73	3.04	1.73
2.28	4.01	2.28
2.93	5.15	2.93
3.64	6.40	3.64
4.27	7.51	4.27
5.35	9.41	5.35

With these conditions, it is necessary to define the use cases and their ambient illuminances/ luminance since the ambient lighting conditions influence human visual performance significantly [76, 30].

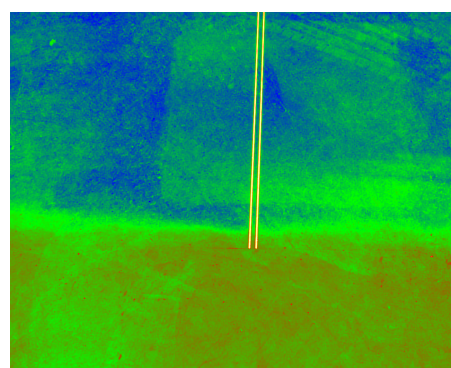
### 3.1.1. Selection of the experiment scenarios

It is necessary to evaluate which scenarios suit the pre-test to evaluate the test environment in general, including minor details that are resolvable on the fine-grained asphalt as the projection surface (see Figure 3.3b). Furthermore, considering the statement of Hauske and Valberg that a VA of 1.0 is usually at 200-300 lx [76, 30], it is essential to know which mechanisms influence VA and to what extent.

The retina includes cones and rods, photoreceptors relevant to visual performance, and influence vision under different ambient environments. Hence, the cones are responsible for daylight vision - photopic vision -, and the rods are relevant during nighttime for vision - scotopic vision. Additionally, there is a vision range between photopic and mesopic vision, where cones and rods are both active - mesopic vision [30]. Therefore, the background luminances  $L_{\text{Background}}$  for the viewing distance of 1 m and 3 m under different ambient illuminance levels are measured with a luminance camera (see Figure 3.4).



(a) Luminance measurement for the parking garage scenario (PGS) with the viewing distance of 3 m.



(b) Luminance measurement for the dusk/dawn scenario (DDS) with the viewing distance of 1 m

Figure 3.4.: Pictures of the luminance measurements for the PGS and DDS in either 1 m or 3 m viewing distance to the projection area. All measurements were taken with the luminance camera *LMK5 - 1color*. The pictures show an example of a gap size of 5.35 mm for 2.93 mm thick lines.

The importance and relevance of the use cases derive the corresponding illuminance for the pre-test, which includes the factor when the near-field projections will be most likely used and seen by the car owner or other RUs.

There are two scenarios: First, a parking garage scenario (PGS) with an illumination level (15 to 19lx) similar to that of the standard for parking lots with high traffic volume [80] (luminance level of approx.  $1 \text{ cd m}^{-2}$ ). Secondly, a dusk/ dawn scenario (DDS) has an illuminance level (197 to 235 lx) related to a sunrise or sunset (luminance level of about  $4 \text{ cd m}^{-2}$ ). The DDS represents the daily use of a vehicle by its user, who goes to work and returns home at dusk and dawn. Both scenarios are crucial for near-field projections around the car since the participants' perception is influenced by the ambient luminance, such as the visual acuity, and the resulting resolution requirements.

The luminance measurements and, in the end, the resulting contrast are performed from a first-person perspective, where the luminance camera is tilted to the projection area from the height of the average German person (1.72 m) [125], which corresponds to an eye height of approx. 1.68 m. The resulting viewing angles to the projection are  $59.24^\circ$  at a 1 m viewing distance (displayed in Figure 3.4b) and  $29.25^\circ$  for a 3 m for viewing distance (illustrated in Figure 3.4a). Further, the detailed list of the measured object luminances  $L_{\text{Object}}$ , which is the projection of the line pair with a gap size of 5.35 mm, and the background luminances  $L_{\text{Background}}$  is indicated in Table 3.2 for used viewing distances in the pre-test. The selected pattern for the measurements of 2.93 mm thick lines with a 5.35 mm gap size refers to the limitations of the luminance camera *LMK5 – 1color* and, thus, conditional analysis [128].

Table 3.2.: Measured luminance levels for viewing distance of either 1 m or 3 m to the projection in the PGS or DDS. The measurements relate to a 2.93 mm thick lines with a 5.35 mm gap size.

	Luminance of PGS in $\text{cd m}^{-2}$	Luminance of DDS in $\text{cd m}^{-2}$
$L_{\text{Object, 1 m}}$	10.46	41.39
$L_{\text{Background, 1 m}}$	0.47	2.67
$L_{\text{Object, 3 m}}$	10.2	43.51
$L_{\text{Background, 3 m}}$	0.52	3.38

Additionally, Valberg defines a maximal acuity above  $2 \text{ cd m}^{-2}$  [30], which is present in comparing the two scenarios of PGS and DDS. Further, it is crucial to ensure a constant Weber contrast  $C_{\text{Weber}}$  so that the perceived contrast  $C_{\text{Weber}}$  will not influence the participants, which is shown by equation 3.7, where  $L_{\text{Object}}$  describes the luminance of the projection and  $L_{\text{Background}}$  is the luminance level of the background around the projection, which is the street's surface without any projected content [74].

$$C_{\text{Weber}} = \frac{L_{\text{Object}} - L_{\text{Background}}}{L_{\text{Background}}} \quad (3.7)$$

Contrast measurements ensure that the variation in observation distance does not affect the participants' perception. However, excessive variation in contrast levels may affect the subjects and their VA. Thus, Table 3.3 displays the resulting Weber contrast  $C_{\text{Weber}}$  of the pre-test, calculated by applying equation 3.7 to the measured values of Table 3.2.



Table 3.3.: List of resulting Weber contrasts  $C_{\text{Weber}}$  in the pre-test depending on the viewing distance (1 m or 3 m) and the scenario (PGS or DDS).

Scenario	$C_{\text{Weber}}$ for 1 m viewing distance	$C_{\text{Weber}}$ for 3 m viewing distance
PGS	21.19	18.79
DDS	14.42	11.87

Consequently, the contrast levels are slightly decreasing with increasing viewing distance. However, the difference of the contrasts for each scenario is not significant for the perception, which is displayed in Table 3.3. Thus, the pre-test results are not influenced by the perceived contrast when varying the viewing distance to the projection area but by changing the scenario for ambient lighting.

### 3.1.2. Determination of the resolution on the projection surface

Finally, a conducted pre-test derives the resolution of the projection surface. For this purpose, eight participants ( $N = 8$ ) with an average age of 41 years ( $M = 41.13$ ;  $SD = 13.03$ ) participate in the test, of which two are women (27 to 29 years old), and six are men (30 to 60 years old). The participants were asked to wear the visual acuity aid they needed to be part of the study. Thus, the test corresponds to the everyday conditions of the participants, so a visual aid use of 62.5% was found in the subjects' collective.

Consequently, every participant had about 10 min to adapt to the ambient illumination in every scenario before the testing started or between switching the scenarios, which ensures the activation of rods in their sensitivity [76, 30]. So the illustrated projections do not discomfort the subject, which is guaranteed by the nearly constant Weber contrast per scenario (see Table 3.3). The participants used a modified keyboard, with only the keys N and Y accessible. The keyboard is connected to a computer via a USB cord to ensure no latencies. Matlab R2018b with the graphical toolbox Cogent 2000 version 1.33 represents the visual stimuli and the implementation of data handling [129]. All instructions and the questionnaire used the German language. Stuckert and Khanh used this approach and methodology before evaluating the studies for the resolution requirements of near-field projections [115].

The study design follows the constant stimuli method [74, 75] with the variation of the same stimulus as displayed in Figure 3.3a, where a mixed between-within-design, with ambient lighting being the between-subjects factor and the viewing distance being the within-subject factor. In addition, the procedure is based on the schematic sequences mentioned by Schiller [130], which are modified in certain elements and displayed in Figure 3.5.

First, the participants read an instruction sheet to adapt to the ambient illuminance level and to get over an adaptation time. Then, before the test started, a welcome screen and examples of the minimal and maximal gap sizes were displayed to the participants. The examples ensured that every participant understood that the gap size could vary. However, they were kept from knowing if two lines would always be displayed or just one. While focusing on the projection area, the participants had to press 'Y' if they saw two lines next to each other or 'N' if they just saw one line. Second, the participants got familiar with the test setup with a test run, as shown schematically in Figure 3.5. Third, eight different gap sizes (see Table 3.1) are projected three times randomly (Figure 3.3a), resulting in 24 total representations per sequence. This low number of representations is selected due to the participation of each test participant in both scenarios at once and to guarantee a short overall testing time of fewer than 45 minutes. The test time of 45 minutes for two distances and two illumination levels guarantees that the subjects do not fatigue.

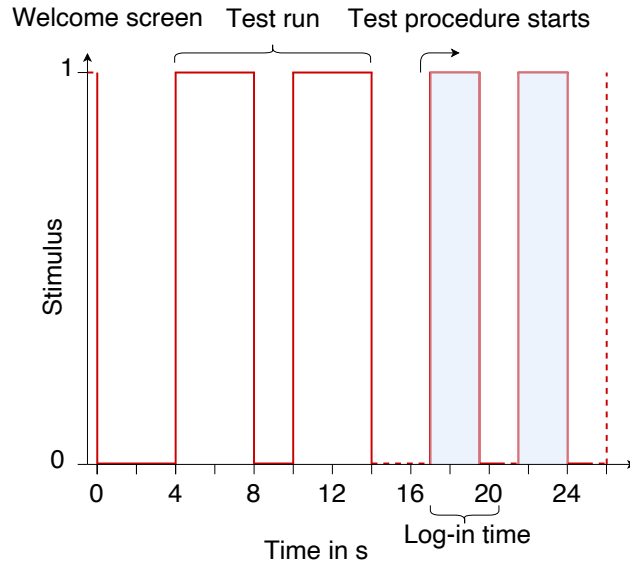


Figure 3.5.: Schematic visualization of the pre-test derived from Schiller [130] contains sequences with a welcoming screen, the test run phase, and the testing procedure. The stimulus illustrates with a '1' a projection of the line pattern appearing on the projection area and a '0' no projection. In addition, shading displays the log-in time in the graph.

Further, the participants had 2.5 seconds to decide whether they perceived one or two lines displayed on the projection surface. The display time of every projection was 2.5 s (Figure 3.5). The experiment followed a forced choice method of constant stimuli [74, 75] with a random delay between every sequence from 0.5 s to 1 s to prevent learning effects. After the delay, visual feedback illustrates the successful logging of the answer. The order of tested distances was randomly chosen per participant between 1 m and 3 m. Fourth and last, a questionnaire asked for general personal information. Stuckert and Khanh used the mentioned method in defining resolution aspects for near-field projections [115].

The logistic function interprets and evaluates the pre-test's response data to the associated gap sizes. In this case, the function in the simplified form derived by Linschoten and Harvey is used and further simplified by Stuckert and Khanh [115, 88, 89, 90]. Here, equation 3.8 describes the detail size per threshold level  $\sigma_{\text{quality}}$  using of logistic regression. Implementing the  $\alpha_{\text{quality}}$  defines the stimulus (e.g., the gap size between the two lines) at a 50% probability within the given stimuli range. Further, the steepness of the fitting function is described by  $\beta_{\text{quality}}$  and the threshold  $th_{\text{quality}}$  is a specific percentage to evaluate this probability level.

$$\sigma_{\text{quality}} = \alpha_{\text{quality}} \cdot \left( \frac{1}{th_{\text{quality}}} - 1 \right)^{\left( \frac{1}{-\beta_{\text{quality}}} \right)} \quad (3.8)$$

The mentioned equation 3.8 is used to evaluate the recorded data during the pre-study, which results in the graphs (PGS on the left and DDS on the right) displayed in Figure 3.6. The y-axis displays the probability of detection, which relates to the threshold level in equation 3.8. On the x-axis, the gap size is in mm. Further, the labeling is handled equally in both graphs. The solid line indicates the logistic regression fit for 1 m, and the dashed line displays the logistic regression fit for 3 m. Additionally, the crosses mark the data for every gap size and the resulting detection probability with blue crosses for 1 m and black circles for 3 m. Every data in Figure 3.6 consists of 192 data points (= 3 repetitions · 8 gap sizes · 8 participants), and concluding the probability of the evaluated gap sizes are calculated.



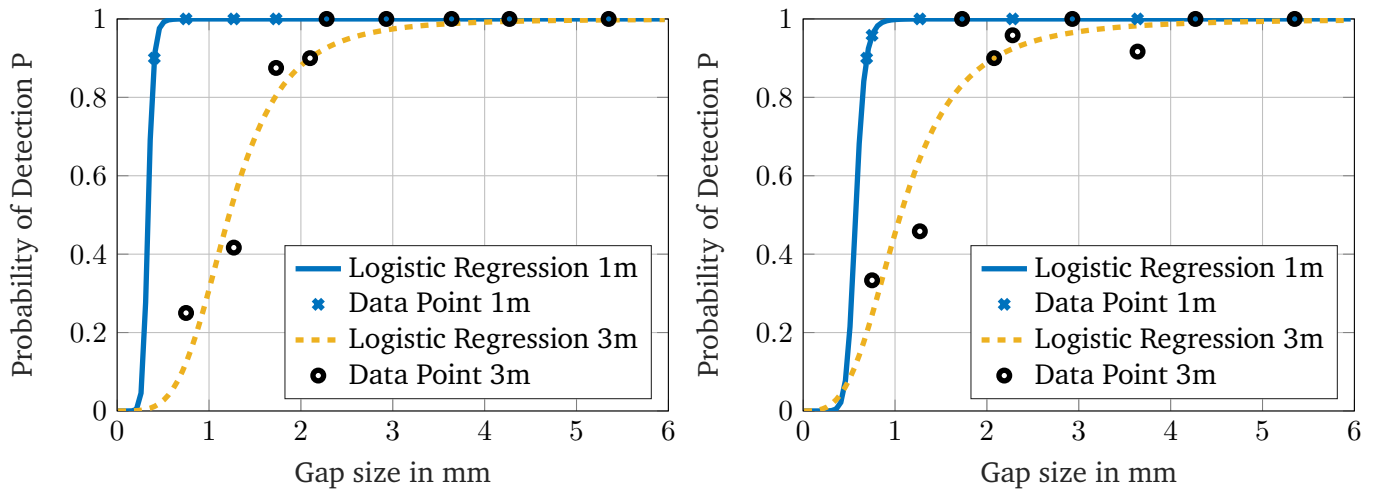


Figure 3.6.: Analysis of the perceived gap size in mm between two lines projected on the street’s surface at 1 m and 3 m away from the test participant. Both graphs include the probability for every gap size under viewing distances and the logistic regression fitted to the probability data (as indicated in equation 3.8). The graph on the left displays the gap size in the PGS testing environment, and the right graph shows the gap size for the DDS scenario.

The graphs in Figure 3.8 display the complete data and fitted functions for the pre-test. For further evaluation, the threshold ( $th_{quality} = 0.9$ ) is set to 90% to estimate a minimal resolvable detail on the projection surface, which is valid for 90% of the cases of the participants. Therefore, Table 3.4 lists the 90% thresholds for the PGS and DDS in either mm or as multiple of one angular minute. Although the participants’ average age is 41.13 years, the participant collective indicates a visual acuity below 0.71 for PGS and DDS in a viewing distance of 1 m (see Table 3.4). Therefore, the participants can detect and distinguish details more minor 1' on the projected street’s surface, which results in objects of 0.41 mm at 1 m in PGS and 0.67 mm in DDS. However, the perceived detail size is still more extensive than the theoretical size of the smallest perceivable detail of 0.294 mm, which is the limitation of the human visual system. So, the participants do not have the maximal  $VA = 2$ , which states that the theory also approves the used realistic setting in the pre-test. The 90%-threshold results in smaller perceived gap sizes than available gap sizes in the testing set of line pairs (see Table 3.1).

Looking at the results of the pre-test at 3 m viewing distance, the visual acuity is above 2' for both scenarios (see Table 3.4). For both scenarios, the gap size is about 2 mm. However, the results from the 3-meter distance are not the focus of the review due to the shallower angle and rotation of the graphs in the subject test. Mainly when the opening of the lines rotates by 90 degrees compared to Figure 3.4a, the gap width has been detected less at the 3 m viewing distance due to the shallow angle =  $29.25^\circ$  like the variation in Figure 3.4a. The study’s results at one meter with a viewing angle of  $59.24^\circ$  are more similar to a standard vision test at ideally  $90^\circ$ . Therefore, the preliminary test results show a clear tendency that the viewed projection background is suitable for further psychological studies to evaluate resolution requirements and can additionally display objects or the gap between a line pair under one angular minute and above the theoretical limitation of 0.5'.

Evaluating the influence of the ambient illuminance levels of PGS and DDS, there is no clear tendency when looking at the results of the 1 m viewing distance results, and at the 3 m-results. This behavior relates to the diffuse reflectance characteristics of the tested asphalt in this testing, which is examined in detail in Section 5.1.1.

Table 3.4.: Perceived detail size on the ground for a 90 % threshold level evaluated by the participants for the line pair projected under different adaptation luminance levels (PGS and DDS) defined in mm and as a multiple of one angular minute by applying equation 3.6.

90 % threshold level	Viewing distance 1 m	Viewing distance 3 m
PGS in mm	0.41	2.09
DDS in mm	0.67	2.08
PGS as multiple of 1'	0.71	2.09
DDS as multiple of 1'	1.16	2.07

Furthermore, the setup used for the main study is described in detail, and necessary characterizations, which are essential for a study to define resolution requirements, are listed. Additionally, a deduction of test parameters and the displayed projection content shows the aims of further studies.

### 3.2. Experimental setup

A detailed experiment characterization is conducted to ensure an equal test environment for all participants. First of all, the adaptation luminance in the testing room is characterized by possible viewing distances of the participants of 1 m, 3 m, and 5 m away from the projection area to provide a homogeneous ambient lighting condition within the test and the ambient lighting scenario. The selected viewing distances relate to different use cases. For example, the viewing distances of 3 m and 5 m refer to possible distances in urban environments for highly automated vehicle communication in safety-relevant situations with vulnerable road users such as cyclists or pedestrians [131, 132]. Moreover, the 1 m viewing distance is possible when entering or exiting the vehicle or experiencing the vehicle in a showroom [131, 132]. The experimental setup is displayed in the visualization in Figure 3.7.

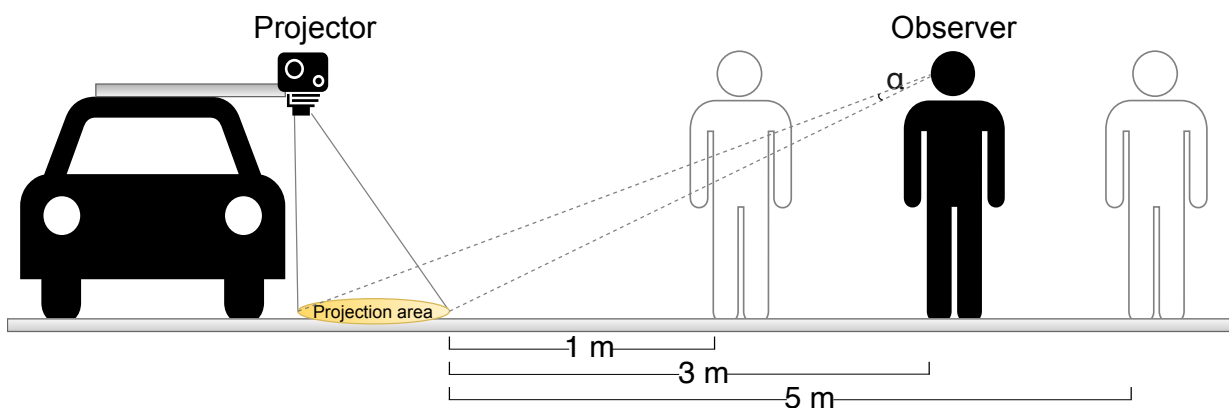


Figure 3.7.: Schematic illustration of the experimental setup for further tests for the definition of resolution requirements, where an LCD laser projector [127] is mounted on a vehicle. The visualization displays the three possible viewing distances of 1 m, 3 m, or 5 m. In addition, the viewing angle  $\alpha$  indicates the observer's viewing angle to the projection area for the 3 m observation distance. The setup is identical to the structure used by Stuckert and Khanh [115].

Therefore, the scenario with 191 to 263 lx ambient illuminance refers to DDS in this and the next section

of the work. The DDS scenario varies slightly in every study regarding the vehicle's position or the possible viewing distances to the vehicle. Another ambient illuminance scenario is the PGS with about 20 to 25 lx. Further, it is crucial to ensure a constant Weber contrast so that the perceived Weber contrast  $C_{\text{Weber}}$  will not influence the participant's perception no matter the projection content, as mentioned in equation 3.7 and Section 3.1.1.

All mentioned contrasts indicate the first-person perspective by measuring with a luminance camera at three viewing distances with a measuring height of 1.68 m. Furthermore, the viewing angles range between  $59.24^\circ$  at 1 m to  $18.57^\circ$  at 5 m viewing distance, assuming an average German person [125], displayed in the illustration in Figure 3.7, exemplary for the observer at 3 m.

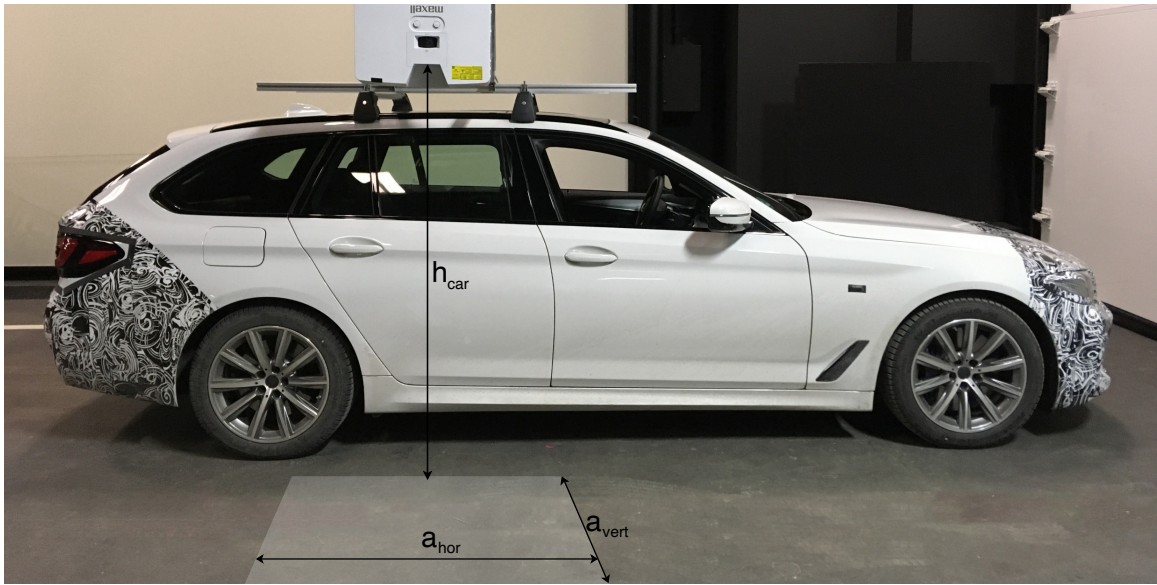


Figure 3.8.: Picture of the used setup with a test-vehicle, where the projector [127] is mounted with construction to the roof rails. Furthermore, the vehicle's height ( $h_{\text{car}} = 1.66$  m) is indicated, as well as the schematic illustration of the projection area with the horizontal ( $a_{\text{hor}} = 1.20$  m) and vertical length ( $a_{\text{vert}} = 0.67$  m) of the projection.

Consequently, the contrasts are valid for the smooth and fine-grained asphalt surface with a luminance coefficient of 0.03 for the experimental setting in PGS and DDS (Figure 3.8). Additionally, the angle-dependent reflection behavior  $S$  is classified according to the CIE standard [133], which refers to a diffusely scattering surface ( $S < 0.4$ ) for the PGS ( $S = 0.09$ ) and DDS ( $S = 0.09$ ), identically used by Stuckert and Khanh [115]. In addition, a questionnaire included the question for rating an eventually perceived glare during the testing to collect the subjective data of the participants to validate the selected contrasts.

The projection size is selected as maximal as possible with the projector at  $h_{\text{car}} = 1.66$  m (see Figure 3.8). So a width of the image of  $a_{\text{hor}} = 1.20$  m and a height of  $a_{\text{vert}} = 0.67$  m) with a resulting area of  $0.8$  m<sup>2</sup> is present. The projector has a resolution of 1920 pixels by 1200 pixels [127]. Thus, equation 3.9 describes the size of one single pixel  $\eta_{\text{hor, vert}}$ , which the used setup can project. So, the length or width  $a_{\text{hor, vert}}$  is divided by the resolution of the projector  $res_{\text{hor, vert}}$ . A respective number for the size per pixel results in  $0.63$  mm/ $px$  for the horizontal  $\eta_{\text{hor}}$  and  $0.56$  mm/ $px$  for the vertical  $\eta_{\text{vert}}$ . These are the system limitations for the smallest size, which can be projected on the surface for the selected and characterized setup in the further tests displayed in Figure 3.8.

$$\eta_{\text{hor, vert}} = \left( \frac{res_{\text{hor, vert}}}{a_{\text{hor, vert}}} \right) \quad (3.9)$$

Comparing the physical limitations of the setup with the previously conducted test in Section 3.1.2, it is evident that the study verifies its physical limitations (Figure 3.8). In addition, each subject is guaranteed to perceive and process these pixels at the critical distance of 1 m presented in the study (see Table 3.4 top section).

Therefore, this thesis aims to evaluate a selection of different projection contents that relate to different use cases and may result in perceptual requirements when evaluating resolution aspects for near-field projections. Consequently, first, the theory needs validation, which Valberg [30] mentions if various projection contents for near-field projections show similar relationships compared to textual acuity tests, which demand higher visual acuity than sign-based tests regarding the higher cognitive load of the participant. Second, if the variation in projection sizes influences the perception of visual acuity as displayed in Figure 3.11, which Jetsy and Lund observe with other given setup parameters for the application in the television industry [108, 109].

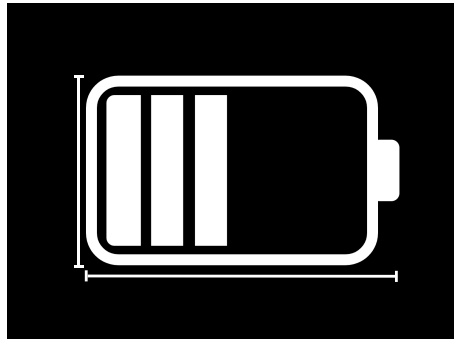
### 3.3. Test parameters

This section describes the test parameters necessary for the different studies for the perceived resolution. For this purpose, on the one hand, the framework conditions, such as viewing distances and the set ambient illuminations, are described for each study. On the other hand, this section likewise describes the projection content in more detail, which differs between the studies. The difference in the graphics is not only due to the size but also to the content itself, which ranges from symbol- or text-based to design-oriented graphics. In addition, an extensive focus is set on the perceived resolution influenced by animated sequences and the influence of the font in text-based illustrations. Finally, an overview of the different subject collectives in all studies conducted is listed and compared.

#### 3.3.1. Static projection content

Various aspects are essential when designing graphics for the testing symbol-/ text-based or design-orientated illustrations, which generate the results in the psychophysical tests. Good legibility is the main requirement for texts. For example, DIN 1450 [1] specifies the number of criteria for text-based illustrations, including font type, stroke width, or character spacing. However, the requirements for the nominal sizes of a font vary depending on the type of text and the intention of the communicated information. In addition, the viewing angle, which relates to the viewing distance, influences the perception and the clarity of reading a font. Therefore, good legibility is necessary. However, the symbol-based pattern or the smallest letters of the text-based projection fulfill ISO 3864 [134] and guarantee the text's legibility from a 5 m viewing distance. Therefore, the used projection sizes of the symbol (68.5 cm wide and 40.5 cm high) or text (93 cm wide and 37.5 cm high) are selected in the PGS, and DDS tests (displayed in Figure 3.9) and are also part of the research by Stuckert and Khanh [115].

The selected sizes ensure no influence by the contrast since even the smallest dimension of 37.5 cm ( $=4.06^\circ = 243'$ ) of the text result in an object size higher than the transition to Weber's law of  $3^\circ 20'$  at a viewing distance of 5 m (see Figure 2.14).



(a) The graphic illustrates a loading battery symbol (68.5 cm wide and 40.5 cm high).



(b) Depiction of the text 'Welcome to Munich' used the front style Helvetica (93 cm wide and 37.5 cm high).

Figure 3.9.: Symbol- and text-based projection content for the PGS and DDS tests with the indication of the dimensions.

All the tested patterns are evaluated regarding the importance for a broad group of participants by multiple surveys [135, 136]. Therefore, Figure 3.9a displays the test pattern as a battery symbol, one of the essential projections based on the surveys [135, 136]. The use case relates to a scenario where the customer sees a battery status of an electrified vehicle projected next to the car.

The test persons' evaluation of the resolution quality shall not only be based on single, prominent areas within the displayed test pattern. Therefore, participants are encouraged to view and rate the graphic according to their preferences in their daily life. The PGS and DDS use the battery test pattern, named a symbol-based projection.

However, the plain Helvetica font is ultimately used for the subject study to ensure legibility with the 'Welcome to Munich' text-based pattern (see Figure 3.9b). This font style is familiar to most people in road traffic due to the usage of traffic signs [138]. The use case of a welcoming scenario is also crucial in the surveys [135, 136].

Additionally, symbols with more extensive filled areas in low-light conditions are easier to distinguish [139]. It is advantageous if the symbol has corners and edges. On the one hand, these are clear fixation points [140]. On the other hand, sharpness or blurriness can be detected, particularly in these areas [141], which leaves the subjects an indication for a generalized evaluation of quality, such as resolution requirements. All aspects considered, another symbol-based projection pattern results - the weather symbol (see Figure 3.10a), which shall indicate to the car user what possible weather forecast is in the location of the drive's destination. The weather symbol features corners and edges, which helps to evaluate if more versatile projection graphics has similar requirements to the loading battery symbol. In addition, the weather symbol (Figure 3.10a) is designed symmetrically along a vertical axis.

Furthermore, the perception when reading a text strongly depends on the font. Finally, given the various font types, the question arises as to whether an italic font has similar resolution requirements as a plain one. Therefore, text-based projection content displays the wording 'Welcome back' in either Helvetica font (Figure 3.10b) or Courgette font (Figure 3.10c), which is an italic font type [137]. Hence, a test examines the difficulty of evaluating the quality/ resolution needs of two different fonts, shown in the examples in Figure 3.10, named the font relation (FR) test.





(a) The graphic illustrates a weather symbol displayed in three sizes: 15.5 cm wide x 10.5 cm high; 48 cm wide x 33 cm high; 92 cm wide x 63.5 cm high.

(b) Depiction of the text 'Welcome back' used the front style Helvetica displayed in three sizes: 27.5 cm wide x 13 cm high; 55 cm wide x 25.5 cm high; 91.5 cm wide x 42 cm high.

(c) Depiction of the text 'Welcome to Munich' used the front style Courgette displayed in three sizes: 25.5 cm wide x 13 cm high; 49.5 cm wide x 25.5 cm high; 82.5 cm wide x 42 cm high.

Figure 3.10.: Symbol- and text-based projection content for the SP and FR tests.

The patterns in Figure 3.10 examine the relationship between the projection size and the impact on the resolution requirements. To this end, the displayed graphic varies between different quality/ resolution levels and sizes during the study. Therefore, the symbol or text is displayed randomized between three different sizes, which are the following: weather symbol with sizes of 15.5 cm wide and 10.5 cm high, 48 cm wide and 33 cm high, or 92 cm wide and 63.5 cm high (Figure 3.10a ), for the plain text (27.5 cm wide x 13 cm high; 55 cm wide x 25.5 cm high; 91.5 cm wide x 42 cm high)(Figure 3.10b), and the italic text (Figure 3.10c) varying from 25.5 cm wide and 13 cm high to 49.5 cm wide and 25.5 cm high or 82.5 cm wide and 42 cm high. Moreover, Figure 3.11 displays the variation of the sizes present during the testing for the participant from a first-person perspective of an average German person [125].



Figure 3.11.: Display of the text-based testing pattern for the SP and FR tests. From left to right: the smallest size of the plain text-based illustration from 3 m viewing distance and further the different sizes from small (27.5 cm wide x 13 cm high), middle (55 cm wide x 25.5 cm high), and big (91.5 cm wide x 42 cm high) patterns from 1 m distance. The images are taken from the perspective of the viewer.

Therefore, the abbreviation of the tests for considering the perception of size compared to the resolution requirements is size perception (SP). Figure 3.11 displays an exemplary depiction of the SR testing of the plain text for a 1 m viewing distance. Further, Figure 3.11 displays on the left how a small-sized plain text projected on the ground looks like from 3 m away. However, not all projection content or tests have the same

observation distance variety; therefore, Table 3.5 summarizes which observation distances were considered by the participants per test, where also the dynamic projection (DP) test is listed.

Table 3.5.: Summary of the variation of viewing distances and the resulting viewing angles assuming a person's height of 1.72 m [125] for all conducted studies in Chapter 3 and 4.

Parameters	PGS	DDS	SP	FR	DP
Viewing distance in m	1; 3; 5	1; 3; 5	1; 3	1	1; 3
Viewing angle in °	59.24; 29.25; 18.57	59.24; 29.25; 18.57	59.24; 29.25	59.24	59.24; 29.25

The examined participants took place in the tests of SP and FR under DDS ambient lighting levels, which had an illuminance distribution between 197 lx to 250 lx.

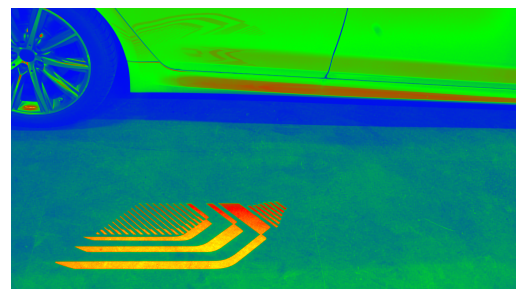
An extension in the SP and FR tests to the PGS and DDS investigations includes a fixation marker to reduce or limit the possible head movement of the subject in the SP and FR testing. Thus, the participants look at a fixation cross at the bottom of the test graph throughout the study. The fixation avoids frequent eye movements, especially when viewing high-resolution images [142]. In addition, saccades interrupt stimulus reception as a neuronal reorganization occurs during this time [143]. Thus, with the gaze on a fixation cross, there is a steady stimulus perception guaranteed for the entire presentation time of the test pattern. Nevertheless, the test graphics' fixation point differs from the typical application for near-field projections. Therefore this will underline the theoretical approach of the SP and FR testing with the realistic viewing behavior of PGS and DDS tests. Further animated sequences will extend the realistic scenarios in the following section.

### 3.3.2. Dynamic projection content

With the examination of static visualizations, which focus on static visual acuity, it is also necessary to focus on developed functionalities, which are dynamic. The surveys underline this focus, where especially design-orientated projection contents were rated with high importance [135, 136]. For this reason, it results in a dynamic graphic design that imitates a so-called light carpet, see Figure 3.12. BMW already has light carpets that display dynamic content [144], so the design-oriented test pattern relates to it. The test pattern shown in Figure 3.12 has a frame rate of 25 *fps* with a size of 82.3 cm width and 30.7 cm height.



(a) Design-orientated projection content was used for the DS test. The displayed picture illustrates one exemplary shaping: moving within a duration of 8 s. The pattern's size within the presentation is about 82.3 cm wide x 30.7 cm high.



(b) Depiction of the text design-orientated pattern next to the vehicle in a luminance measurement picture with the same dimensions as mentioned in Figure 3.12a.

Figure 3.12.: Design-orientated projection content was used for the DS test.

The animation speed of the test graphic (Figures 3.12a and 3.12b) relates to the example [144]. It, therefore, includes animation speeds varying from 0.25 to 1 Hz. The tested pattern is smaller than the design pattern of the BMW i7 [144] because that the whole animated sequence shall be in the participant's field of view in a 1 m viewing distance, as depicted in Figure 3.12b. The DP test has similar test conditions as the DDS, SP, and FR tests with an ambient illuminance in the test room of 224 to 252 lx.

### 3.3.3. Research participant collectives

In the end, all investigations have one in common, the test patterns, no matter if the static or dynamic mode is helping to understand what resolution requirements are present in the current collectives of participants and how the static or dynamic visual acuity is applied in the field of near-field projections compared to the fundamental or theoretical research that is present in the literature [76, 30, 31]. Hence, it is crucial to understand the common aspects and differences for the participant's collectives in the tests to determine the quality/ resolution aspects for near-field projections.

Finally, we will take a look at the subject collectives. The respective studies will be compared with personal data to show how the subject groups differ. Therefore, the following parameters are listed in Table 3.6: Number of subjects  $N$ , age of the subjects, and the standard deviation of the age in the collective, including the age range in the participant collective, the number of female or male, and the proportion of visual aid use.

Table 3.6.: List of the subject collectives' characteristics for all participants of the tests for defining the resolution requirements of near-field projections. The characteristics consist of the number of subjects  $N$ , the age of the subjects, including the standard deviation of the age in every collective, the age range in every test, the number of females or males, and the proportion of visual aid usage.

Parameters	PGS	DDS	SP	FR	DP
Participants' number $N$	25	70	52	16	44
Average age in years	35.68	34.86	37.79	39.44	36.07
Standard deviation in years	11.82	10.75	10.87	10.67	9.91
Age range in years	20 to 58	21 to 59	20 to 59	24 to 56	24 to 59
Number of female / male	9 / 16	19 / 51	7 / 45	2 / 14	11 / 33
Visual aid usage in %	56	48	48	50	52

Regarding the average age, it is clear that especially study FR and SP have older subjects than the others in Table 3.6. The remaining studies have an average age of around 36 years (see Table 3.6). Similarly, study FR (2 women) and SP (7 women) have the lowest proportion of women in the sample (equivalent to 13% women per study). The remaining studies have a higher proportion of women with PGS (36%), DDS (27%), and DP (25%). All studies have a similar age range between 20-59 years (detailed in Table 3.6). Finally, all studies have approximately 50% visual aid use except for the PGS study, where 56% of subjects use a visual aid.

## 3.4. Summary of the experimental setup

Finally, this section summarizes the differences and commonalities of the various tests used to define resolution aspects. Here, the studies differ in ambient illumination or effective luminance and the resulting perceived Weber contrast (see Table 3.7). PGS and DDS tests evaluate the influence of ambient circumstances. In addition, the differences in the test graphics highlight certain aspects: do the resolution requirements differ



between different graphics (battery charging and weather symbol) and between different texts (Welcome to Munich or Welcome back) (DDS vs. SP), where a desired reduction of the binding word is applied, or fonts (Helvetica and Courgette) (SP vs. FR), which represent italic fonts that are also present in daily life. In addition, a comparison of study DDS and SP checks if a fixation mark influences the resolution requirements. Furthermore, in the SP and FR tests, the influence of the projection size on the resolution requirements is described. Finally, DP tests the influence of a dynamic design-oriented graphic, representing the influence of animation speed on the perception of digital content compared to some extent with the symbol-based content of the tests DDS and SP.

Table 3.7.: Summary of the variation of the executed tests involving the characteristics for the ambient illuminance levels, ambient luminances on the street's surface, and the perceived Weber contrast of the projected content on the street.

Parameters	PGS	DDS	SP	FR	DP
Ambient illuminance in lx	20-25	191-263	197-252	197-252	224-252
Ambient luminance in $\text{cd m}^{-2}$	0.59-1.39	4.17-6.41	6-9.18	6-8.3	6.74-8.01
Weber contrast $C_{\text{Weber}}$	16.66-17.81	23.16-49.82	10.93-23.75	10.83-20.13	9.26-11.45

In the following chapter, a separate analysis of the studies checks for each test, indicating the resolution aspects of each study under the given conditions or test contents. In addition, the correlation between the studies is shown thanks to a statistical evaluation. Finally, the respective comparisons take into account the influence of the variations. The variations are composed as follows for each test per participant:

- **PGS:** 10 qualities  $\times$  3 repetitions  $\times$  3 viewing distances  $\times$  1 projection size  $\times$  2 projection contents = 180 data points
- **DDS:** 10 qualities  $\times$  3 repetitions  $\times$  3 viewing distances  $\times$  1 projection size  $\times$  2 projection contents = 180 data points
- **SP:** 6 qualities  $\times$  3 repetitions  $\times$  2 viewing distances  $\times$  3 projection sizes  $\times$  2 projection contents = 216 data points
- **FR:** 6 qualities  $\times$  3 repetitions  $\times$  1 viewing distance  $\times$  3 projection sizes  $\times$  2 projection contents = 108 data points
- **DP:** 8 qualities  $\times$  3 repetitions  $\times$  2 viewing distances  $\times$  1 projection size  $\times$  1 projection content = 48 data points



---

## 4. Experiment results and derived resolution requirements of near-field projections

---

This chapter defines the results for near-field projections of the tests mentioned in Chapter 3. An extensive analysis evaluates the influence factors such as ambient lighting scenarios, viewing distances of the observer to the projection, and the projection size of different projection contents, which are either symbol- or text-based. Additionally, design-orientated projections extend the content variation, focusing on animated sequences compared to static illustrations to derive a dynamic visual acuity (DVA) relationship for applying near-field projections. Finally, in addition to a statistical evaluation of the dependencies between the influence factors, a definition of the perceived resolution of the tested participants is applied with the help of the logistic regression on the collected testing data [88, 90]. Additionally, this chapter describes the methods to analyze and evaluate the test data in detail. Additionally, a brief questionnaire review defines the high-quality aspects, projection content, and perception of the animation speed for near-field projections in the Appendix A.4. The questionnaire review enables a general perspective on near-field projections and, further, an outlook for animated sequences, which are a target point in the future of near-field projections.

Ultimately, the perceived resolution and the concluding relationships are summarized, emphasizing which influence factors are crucial for near-field projections and setting the first definition of resolution aspects for near-field projections in the automotive sector.

### 4.1. Influence factors on resolution aspects for near-field projections

After the exemplary analysis of the questionnaire aspects of the DP test, several influence factors on the resolution aspects for near-field projections discover dependencies and relationships for designing a digital near-field projection system. Therefore, ambient lighting, viewing distance, projection content, and size, as well as projection's animation speed, ensure an analysis to define dominant influence factors, which are, on the one hand, tested on statistical dependencies and, on the other hand, compare the physical values for the resolution aspects described in pixel per degree (*ppd*).

Further, logistic regression defines the methods used to analyze and evaluate the collected data in this chapter. The data analysis of all tests mentioned in section 3.4 applied a logistic regression defined by Linschoten et al. [88] and Harvey [90]. In addition, Stuckert and Khanh [115] explained a detailed derivation of the logistic regression to apply to near-field projections for generating resolution aspects. A simplified logistic regression function results with the assumption of no random or wrong answers related to the study design of constant stimuli for the perceived projection quality on the street's surface [115]. The simplified function (equation 4.1) evaluates the collected data by fitting the presented stimuli and the corresponding responses from the forced choice method. The shown stimuli illustrate the different resolution levels projected on the street's surface and correlate to the  $\sigma_{\text{quality}}$  data for equation 4.1 below.

$$RES = \frac{1}{\arctan\left(\frac{25.4 \text{ mm}}{\sigma_{\text{quality}}} \cdot \sqrt{h^2 + d^2}\right)} \quad (4.1)$$

Henceforth, to provide a technology-independent solution for the perceived resolution aspects, considering the participants' average height depending on the test specifies a resolution. Thereupon, the average height of the subjects  $h$  of each study, the viewing distance  $d$  for either 1 m, 3 m, or 5 m (dependent on the summary in section 3.4 per test), and the calculated resolution for the threshold level in dots per inch ( $dpi$ ) of the logistic regression  $\sigma_{\text{quality}}$  characterize the perceived resolution  $RES$  on the ground in  $ppd$  for every study. All resolution aspects relate to a 90 % threshold level excluded from the continuous logistic regression to gain the related perceived resolution on the ground. The selected threshold quality ensures a high-quality resolution requirement, considering the worst-case scenario since the performed studies had a fine-grained asphalt surface (see section 3.2). The resolution values  $RES$  correspond to the subjects' responses to the perceived projections with different resolution levels, independently specified using the Matlab curve fitting toolbox for every observed parameter in every test for the applied testing condition. Besides, a statistical analysis applied a chi-square test to assess a 5 % significance level by comparing the critical values of the chi-square distribution [145]. The chi-square test indicates and evaluates possible dependencies for the perceived resolution aspects by considering factors such as ambient lighting, viewing distance, projection content, projection size, and animation speed if the participants view an animated representation in the test. To some extent, Stuckert and Khanh [115] also used the same method by applying a logistic psychophysical function like equation 4.1 and a statistical analysis to define the resolution aspects, which this thesis will extend further for other dependencies and other projection content in the following sections.

#### 4.1.1. Ambient lighting

This section considers the symbol-based projection content (loading battery in Figure 3.9a), displayed in Figure 4.1, by comparing the tests' results in PGS and DDS. In addition, appendix B includes the graphs (Figure B.1) for text-based content evaluation.

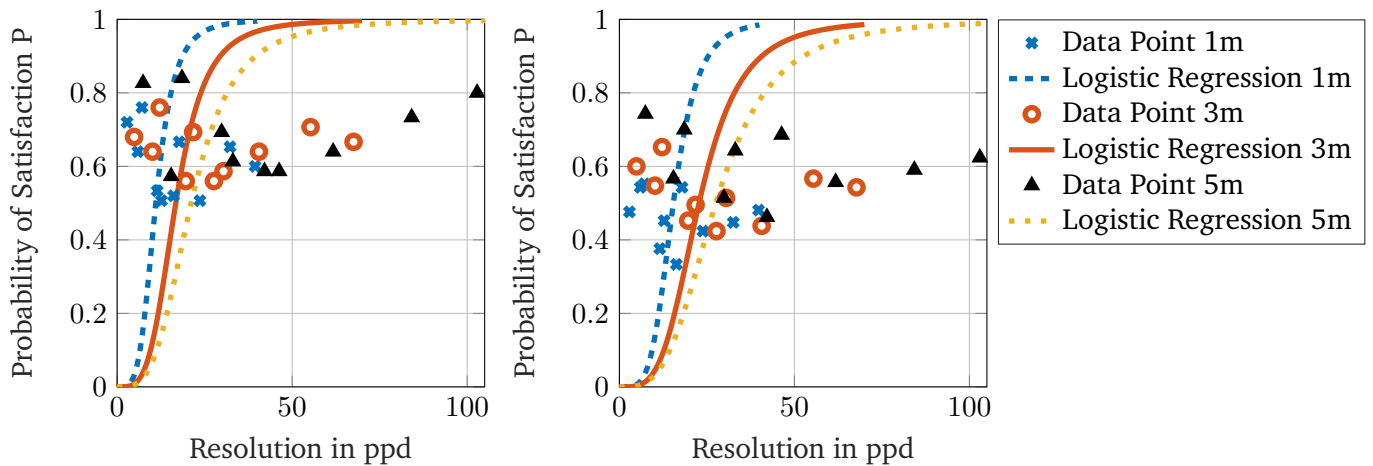


Figure 4.1.: Results of the analyzed data applying the logistic regression equation 4.1 to identify the 90 % threshold for the resolution in  $ppd$ , including the probability of satisfaction in the PGS and DDS. On the left: A detailed illustration of the logistic regression of the symbol-based projection in the PGS, including the raw data marked with crosses for 1 m data, circles for 3 m data, and triangles for 5 m data. On the right: The detailed logistic regression of the symbol-based projection in the DDS includes the raw data, marked with crosses for 1 m data, with circles for 3 m data, and triangles for 5 m data. The legend on the right relates to both graphs' colors and symbols.

On the one hand, Figure 4.1 displays the probability of satisfaction per given resolution quality on the

y-axis. On the other hand, the resolution qualities in *ppd*, displayed on the x-axis, depend on the average height  $h$  of each participant's collective, which is 1.77 m in the PGS and 1.79 m in the DDS. Therefore, the data points in Figure 4.1 represent the probability per resolution for 1 m with blue crosses, 3 m with red circles, and 5 m with black triangles. Moreover, equation 4.1 fits the testing data to generate a continuous function in a dashed blue line for 1 m data, a solid red line for 3 m data, and a yellow dotted line for the 5 m data to evaluate the threshold level. Further, the continuous logistic regression (Figure 4.1) allows identifying a 90 % threshold level to achieve a perceived resolution  $RES$  on the projection surface, illustrated in Table 4.1 for the symbol-based projection under the three viewing distances and two ambient lighting levels of PGS and DDS. For the displayed combinations, the confidence intervals are included in brackets to display the lower bound (left number) and the upper bound (right number) of the perceived resolution in pixels per degree. For example, the resolution for the PGS increases with viewing distance from 18.7 *ppd* to 39.62 *ppd*. Similarly, the results of the DDS follow the trend of increasing resolution with increasing viewing distance from 25.41 *ppd* to 52.62 *ppd* (Table 4.1).

Table 4.1.: Results for the perceived resolution on the projection surface for a 90 % threshold level fitted by the logistic function for the symbol-based projection content under different adaptation luminance levels defined in pixels per degree (*ppd*). The numbers in brackets indicate the confidence intervals of 95 %, with the lower bound as the left number and the higher bound as the right number for the three distances and two ambient lighting levels tested in the PGS and DDS.

Resolution in <i>ppd</i>	1 m	3 m	5 m
Symbol PGS	18.70 (18.12; 19.84)	29.45 (28.71; 30.86)	39.62 (38.35; 42.12)
Symbol DDS	25.41 (24.78; 26.34)	40.71 (39.53; 42.46)	52.62 (51.34; 54.50)

The chi-square analysis (displayed in full extent in the appendix in Table B.1) states that for every tested viewing distance, the symbol- or text-based projection are significantly different ( $p < .05$ ) regarding the two ambient lighting levels of PGS and DDS with a small effect ( $V \leq 0.3$ ) [146]. Indeed, as already stated in the literature, ambient luminance influences the visual system's perception of stimuli [76, 30, 110]. Thus, as stated by the data in Figures 4.1 and B.1, the phenomenon is present in the perception of near-field projections since Valberg mentions a maximal acuity above  $2 \text{ cd m}^{-2}$  [30], which is present in the DDS (above  $4 \text{ cd m}^{-2}$ ). Therefore, the resolution aspects in the PGS are 33 % to 38 % lower compared to the DDS values (Table 4.1). The ambient illuminance of the PGS with approximately  $1 \text{ cd m}^{-2}$  is below the maximal acuity and in the mesopic range. The interaction of rods and cones in the mesopic range of adaptation luminance causes an increasing acuity at increasing luminance levels [76], leading to the significant effect of the PGS and DDS. Therefore, all further studies focusing on the ambient luminance over  $2 \text{ cd m}^{-2}$  guarantee that even while viewing with the maximal visual acuity, the defined resolution aspects are valid for high-quality near-field projections.

The considered use case with an ambient luminance of  $2 \text{ cd m}^{-2}$  thus corresponds to a maximum visual acuity, as mentioned by Valberg [30], and is, therefore, mainly relevant for design-oriented use cases. Nevertheless, the PGS scenario primarily represents the use case for safety-relevant projections and the necessary perceived resolution since initial investigations on contrast perception have already been carried out for these ambient conditions, shown in Table 2.5. Therefore, it is crucial to present the results of this chapter for both scenarios in terms of technology in Table 2.2. Table 4.1 shows the lower resolution requirements for the darker scenario PGS, supported by statistical tests. For example, extracting the required resolution for a viewing distance of 3 m displays that the raw image data requires approximately a resolution. 446 x 268 pixels for *DDS* and 389 x 235 pixels for *PGS* at the microdisplay level. Thus, the DMD and LCoS from Table 2.2 meet the resolution

---

requirements for both ambient luminance scenarios (PGS and DDS) for applying symbol-based projections, which extends the presented area of application by Thomas of just ambient luminance levels for application during night [42]. Still, the  $\mu$ LED microdisplay needs to increase the resolution by a factor of 3.57 for the PGS scenario and a factor of 4.67 to accomplish the resolution requirements for symbol-based near-field projections (see Table 2.2). Further, Chapter 6 examines whether the projection technologies of Table 2.2 also meet the brightness and contrast requirements of the test participants.

### 4.1.2. Viewing distance

The previous section describes, to some extent, the viewing distance as an influencing factor (listed in Table 3.5). However, this section also considers the impact of the SP test besides the PGS and DDS tests. Therefore, the detailed statistical analysis is in the appendix with the following Tables B.1 and B.2. On the one hand, the comparisons of the different viewing distances show that in the PGS ( $N = 25$ ), all compared relationships show no significance ( $p > 0.05$ ) besides the comparison of 1 m with 5 m for the symbol-based projection content ( $\chi^2(9) = 18.48, p < 0.05, V = 0.14$ ), which is significant with a small effect.

On the other hand, as stated, ambient luminance influences visual acuity (Table 4.1). Thus, all analyzed relationships regarding viewing distance are significant ( $p < 0.05$ ) with a small effect ( $V \leq 0.3$ ) in the DDS ( $N = 70$ ) no matter what projection content. However, none of the comparisons regarding the viewing distance relationship is significant for the SP ( $N = 52$ ) test (Table B.2), which might also correlate to the older participants in the SP test compared to the DDS test (Table 3.6) and the resulting lower VA compared to the literature [147] displayed in Figure A.11. Nevertheless, this finding leads to the consideration of the mentioned phenomena by Amrhein et al. [148], since statistical testing, in this case, the chi-squared test may indicate wrong significance, e.g., due to a low number of participants  $N$ . Especially looking at Figure 4.1 and others in appendix B.1, the physical values of the resolution aspects defined by the logistic regression (equation 4.1) do differ and, ultimately, are the focus of this thesis. Moreover, several other researchers discovered similar trends in related experiments for conventional or projection-based displays resulting in a correlation between viewing distance and the resulting screen size [108, 109, 149, 107, 110].

### 4.1.3. Projection content

Moreover, a chi-squared test also checks the dependencies for the projection content, which involves the tests of PGS, DDS, SP, and FR. Finally, these tests compare the symbol-based with a text-based projection (PGS, DDS (Figure 3.9)), and SP test (Figure 3.10a and Figure 3.10b) and various font styles of the SP and FR tests (Figure 3.10b and 3.10c) for viewing distances of 1 m, 3 m, or 5 m. For example, looking at the comparison of the symbol- and text-based projection in the PGS, none of the comparisons were significant ( $p > 0.05$ ) for all viewing distances (Table B.1). Therefore, this finding procures that at luminance levels of approx.  $1 \text{ cd m}^{-2}$  (PGS), a projection system design will be content independent whether the projection is a symbol- or text-based content for projecting regarding the perceived resolution aspects.

However, in the DDS, the viewing distance of 3 m ( $\chi^2(8) = 23.23, p < 0.05, V = 0.11$ ) and 5 m ( $\chi^2(8) = 23.96, p < 0.05, V = 0.10$ ) indicate a significant difference between the answer distribution of symbol- and text-based projections. This difference is comparable to a visual acuity test that Valberg [30] mentioned in that text-based visual test charts have higher cognitive demands on the subject, which is again reflected mainly in the perceived resolution (Table 4.3). Additionally, the DDS testing contains an ambient luminance level where a maximal VA is current [30, 76]. Further, the statistical analysis for comparing the projection content of SP and FR tests does not indicate any dependencies regarding the projection content ( $p > 0.05$ ) displayed in detail in Table B.3 in the appendix.

However, the physical values in Table 4.3 indicate an overlap of the perceived resolution between symbol-

---

and text-based projection content in the PGS test considering the confidence intervals. Additionally, partially there are overlaps between the DDS and SP tests or within the SP tests for the projection content, which also indicates no influence of the fixation mark current in the SP testing and no impact of a binding word such as 'to' compared to the two texts of DDS 'Welcome to Munich' and SP 'Welcome back'. Nevertheless, depending on the viewing distance, it is visible that the textual content has higher or equal resolution requirements, e.g., SP big 3 m symbol vs. text with a difference in resolution or DDS 5 m symbol vs. text with similar resolution requirements.

Thus, a universal projector design for design-driven- and safety-relevant use cases can accomplish near-field projections, mainly if ambient illuminance conditions of the DDS scenario derive a system, e.g., for safety-relevant use cases. In that case, the focus is on the representation of communication using symbol-based near-field projections to reach every RU no matter the cultural or linguistic background worldwide [55, 150, 151, 152]. Additionally, symbol-based near-field projections are language-independent and do not have translation difficulties or different visual acuity requirements depending on the design of the characters. Nevertheless, prior to general use in traffic, it is essential to familiarize urban road users with the symbols used. Wang et al. and Zhang et al. describe the characters' differences, where they found a higher complexity of Chinese characters than English characters [104, 105].

Additionally, the more complex font style of the italic text style has higher perceived resolution requirements than the regular text, especially in the smallest projected size with 35 % (comparison of text FR small and text SP small in Table 4.3). Table 4.3 specifies a detailed overview of all size-dependent comparisons, including the resolution requirements in *ppd*.

#### 4.1.4. Projection size

Another aspect of the perceived resolution requirements is the influence of projection size, especially those not covered by the DIN 1450 and ISO 3864 [1, 134] related to the symbol and text sizes and font style used for traffic signs. Moreover, several experiments discovered an influence between viewing distance and the resulting screen size by varying the image size or the resolution in a lab environment [103, 108, 109]. Therefore, the sizes of the symbol and text projections, called middle or small in the SP and FR tests, depending on the viewing distance, are below the requirements of DIN 1450 and ISO 3864 [1, 134], which need examination under the consideration size-dependency for near-field projections. All sizes are displayed in their resulting horizontal or vertical angular size in Table A.1 for an average participant height in the SP test of 1.8 m.

Therefore, a statistical analysis in Table B.2 displays the comparisons of different sizes at 1 m and 3 m viewing distances. Figures B.2, B.3, and B.4 display the fitted data of the size-dependent SP and FR tests which derive the 90 % thresholds for the resolution aspects depending on the projection size. The chi-squared analysis displays that for the symbol-based projections, the comparison between the small- vs. middle-sized and the small- vs. big-sized projection for both viewing distances (1 m and 3 m) is significant with a small effect (see Table B.2). However, the relation between the middle- vs. big-sized projection shows no significance for both viewing distances for the symbol-based projection (Table B.2). However, the text-based projection shows other relationships regarding size dependency. Then, the small- vs. middle-sized projection comparison displays no significant difference ( $p > 0.05$ ) for both viewing distances. The middle- vs. big-sized at 3 m viewing distance shows no significant difference from the symbol-based projection. Nevertheless, there is a significance for this comparison for the viewing distance of 1 m ( $\chi^2(5) = 12.60$ ,  $p < 0.05$ ,  $V = 0.11$ ). Further, a significant dependency is given in the match of small- vs. big-sized projections for both viewing distances for the text-based content (Table B.2), similar to the symbol-based near-field projections of the SP test.

By taking a closer look at the physical values, no matter what content (symbol or text) and no matter what viewing distance (1 m or 3 m), the middle- and big-sized projections overlap with the confidence intervals



except the big symbol-based projection at 3 m viewing distance. Furthermore, the same effect and overlap are in the FR test under the limitation of the 1 m observation. In conclusion, the overlap of the physical values in Table 4.3 leads to the outcome that symbol- or text-based projections have similar resolution requirements above a size of 48 cm in width and 25 cm in height. So there is a saturation of size-dependency above the mentioned size, which Lund [109] and Barten [149] also discovered for their lab experiments.

Regardless, texts not compliant with DIN 1450 and ISO 3864 [1, 134] are not used for safety-relevant scenarios and, therefore, must not contain italics and too-small text sizes as mentioned by the norms. Thus, systems with flexible resolution demands (see Table 2.2) and the resulting requirements for safety-critical projections lead to lower resolution aspects, as displayed exemplarily for symbol-based projection content in Table 4.1. Still, near-field projectors need consideration for a design-oriented application. In that case, the requirements for the projection must consider how fine the desired details must be, like viewing the small text with the italic font at a 1 m viewing distance with 43 *ppd* compared to the SP text in similar size with 32.49 *ppd*, which results in 33% higher resolution requirements. Thus, the responsible for specifying the near-field projection function must be aware that designing systems with high resolution will result in no support for a high resolution caused by the projection surface, such as gravel or rough asphalt, which affects the quality of the projection, as mentioned earlier by Virsek [21]. This influence reduces the use cases for high-resolution projectors to projection surfaces that are smooth to display fine details, such as a showroom parquet or smooth concrete in a parking garage.

#### 4.1.5. Animation speed

In the end, an analysis of the influence of the animation speed on the resolution requirements evaluates if there is a similar trend for near-field projections of a decreasing VA for an animated sequence which is one kind of dynamic VA (DVA) [31] compared to static illustrations such as pictures (SVA). Consequently, Figure 4.2 depicts the results of the DP test for the 1 m and 3 m viewing distances.

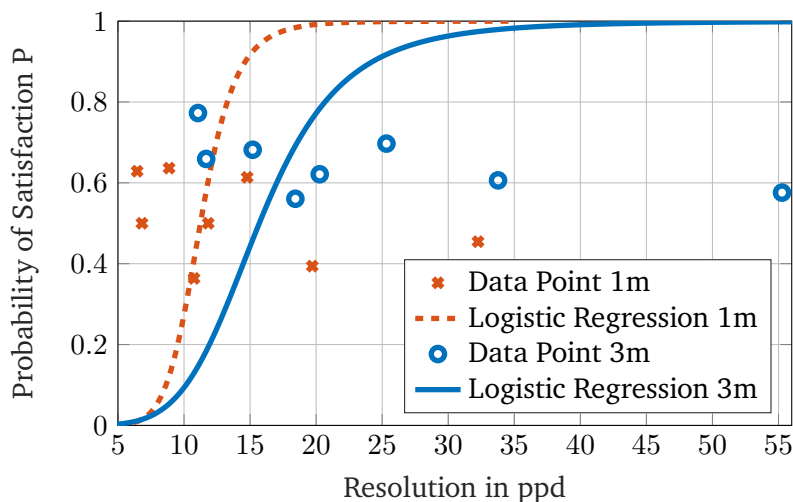


Figure 4.2.: Results of the analyzed data applying the logistic regression equation 4.1 to identify the 90% threshold for the resolution in *ppi*, including the probability of satisfaction in the DP test. The logistic regression of the design-based animated projection in the DP includes the raw data marked with crosses for 1 m data and circles for 3 m data.

There are two ways to evaluate and define DVA: first, the object is moving, such as an animated sequence, and the participant has a fixed gaze, or second, the gaze of the participant is moving, such as when an



instructor stimulates or rotates the participant’s head while the displayed pattern is static [81, 84, 83, 153, 82]. In the case of the DP test, the participants evaluated an animated sequence with an animation speed range of 0.25 to 1 Hz. The participants were also not explicitly told to focus their gaze at one point to generate as natural results as possible since both conditions appear in daily life when they spontaneously see an animated near-field projection on the street in a traffic situation. Figure 3.12 shows the evaluated test pattern, including the relative size of the vehicle.

By reviewing the distributions with the application of a chi-squared test to the data of 1 m and 3 m, a significant dependency results with a small effect:  $\chi^2(7) = 45.44$ ,  $p < 0.05$ ,  $V = 0.19$ . Additionally, the displayed Figure 4.2 represents the difference between the two viewing distances due to the different gradients of the two fitted logistic regressions. Table 4.2 then shows the results for the 90 % thresholds of the DDS symbol-based and DP design-based animated projections, where the static projection (Symbol DDS) has higher resolution requirements than the dynamic projection (Animation DP) at the same threshold level. In fact, the animation has about 42 % lower requirements at 1 m and about 40 % at 3 m compared to the DDS symbol-based projection.

Table 4.2.: Resolution on the projection surface for a 90 % threshold level fitted by the logistic function for the symbol-and design-based projection content under different viewing distances defined in pixels per degree (*ppd*). The numbers in brackets indicate the confidence intervals of 95 %, with the lower bound as the left number and the higher bound as the number on the right for the DDS and DP tests.

Resolution in <i>ppd</i>	1 m	3 m
Symbol DDS	25.41 (24.78; 26.34)	40.71 (39.53; 42.46)
Animation DP	14.64 (14.36; 15.14)	24.28 (23.75; 25.18)

Consequently, the named results indicate a trend where the DVA applies in the sector of near-field projections and approves the theory [31, 81, 84, 83]. As shown in Table 4.2, animated sequences and, thus, DVA requires a lower resolution at the same quality level (90 % threshold). Therefore, the technologies used for the near-field projection (DLP and LCoS in Table 2.2) meet the resolution requirements. Still, the  $\mu$ LED microdisplay has potential since the resolution can be limited to 283 x 171 pixels on the microdisplay plane of the shown design-orientated illustration in Figure 3.12, which is only 1.89 times that of the  $\mu$ LED imager compared to 4.67 times higher pixel demand of the symbol-based test pattern. As in Fig. 2.1, a possible solution of the projector’s design for an automotive application without illumination optics and the larger pixels of the  $\mu$ LED microdisplay (e.g., approx. 50  $\mu$ m [52, 47]) simplify the fabrication of the imaging optics. Mainly because for DMD systems, Moisel [67] already mentions imaging optics as a limiting factor for the imaging quality with the limitations of 0.5° per pixel, not the microdisplay’s characteristics itself.

## 4.2. Summary of the resolution requirements for near-field projections

The previous Section 4.1 focuses on the dependencies for the possible influence factors ambient lighting, viewing distance from the participant to the projection, projection content and size, and animation speed involving statistical analysis. However, due to the low number of participants for statistical analysis and the contrary interpretation of the chi-squared test, the physical values in Table 4.3 have moved into the spotlight.

If the focus is on the physical values alone, possible groupings arise. In the PGS, the projection contents can be grouped up to the 5 m viewing distance since the resolution requirements are similar, among other things, due to the overlapping of the confidence intervals.

Looking at the studies above  $2 \text{ cd m}^{-2}$ , we see that symbol and text projections are similar in their resolution requirements in the DDS test except for 1 m text, which has higher resolution requirements  $31.72 \text{ ppd}$  compared to symbol 1 m DDS with  $25.41 \text{ ppd}$ . Considering the application for safety-relevant situations of near-field projections, the 1 m viewing distance is not a point of interest, as this is a critical viewing distance that is too short for a reaction of a cyclist or pedestrian to interact with a vehicle [154].

Table 4.3.: The participants evaluated the resolution requirements on the projection surface for a 90 % threshold level fitted by the logistic regression for the symbol-, text- and design-based projection content under different adaptation luminance levels and various viewing distances defined in pixels per degree (*ppd*). The numbers in brackets indicate the confidence intervals of 95 %, with the lower bound as the left number and the higher bound as the number on the right of the perceived resolution on the street under the consideration of the characteristics displayed in Table 3.7.

Resolution in <i>ppd</i>	1 m	3 m	5 m
Symbol PGS	18.70 (18.12; 19.84)	29.45 (28.71; 30.86)	39.62 (38.35; 42.12)
Text PGS	20.89 (20.11; 22.45)	31.70 (30.64; 33.93)	47.46 (46.07; 50.31)
Symbol DDS	25.41 (24.78; 26.34)	40.71 (39.53; 42.46)	52.62 (51.34; 54.50)
Symbol SP big	26.54 (25.96; 27.61)	48.17 (47.11; 50.15)	-
Symbol SP middle	24.18 (23.94; 24.66)	37.04 (36.13; 39.17)	-
Symbol SP small	31.78 (31.16; 32.92)	40.67 (39.88; 42.10)	-
Text DDS	31.72 (30.92; 32.88)	39.92 (39.05; 41.22)	51.40 (50.14; 53.30)
Text SP big	26.21 (25.70; 27.13)	43.52 (42.64; 45.11)	-
Text SP middle	28.74 (28.07; 29.98)	40.70 (39.88; 42.32)	-
Text SP small	32.49 (31.89; 33.56)	53.58 (52.17; 56.16)	-
Text FR big	28.34 (27.74; 30.33)	-	-
Text FR middle	27.92 (27.61; 28.97)	-	-
Text FR small	43.00 (40.59; 50.11)	-	-
Animation DP	14.64 (14.36; 15.14)	24.28 (23.75; 25.18)	-

Furthermore, the mid and big projection sizes in the FR test have overlapping physical values and coincide with the resolution aspects of the DDS test (Table 4.3). However, the DDS test uses a different content (symbol or text) than the FR test. This phenomenon results in a projection system that can design projection content independently, regardless of the projection size of these two variations and the tested projection content. Nevertheless, there are outliers, such as, for example, the symbol SP big at three meters viewing distance, with higher resolution aspects ( $48.17 \text{ ppd}$ ) than the middle-sized projection ( $37.04 \text{ ppd}$ ) or the DDS symbol ( $40.71 \text{ ppd}$ ). These outliers, among others, concerning in limitations for projection technologies and the design of these involving the selection of the content since, for example, italic fonts ( $43 \text{ ppd}$ ) have higher requirements in very small projection sizes than fonts oriented according to the DIN 1450 standard ( $32.49 \text{ ppd}$  text SP small) [1]. Therefore, the design of especially safety-relevant projections shall be based on the daily traffic's known symbols or font style to encourage recognizability [1, 134].

Additionally, the projection size influences the perceived resolution of the content, regardless of whether text or symbol, of the small projection size (small in Table 4.3), shown in terms of a specific size in degrees in Table A.1 in the appendix. A possible influence on the small projection sizes may be the actual VA of the subjects of the test SP since this is partly below the VA data of the more detailed literature of Owsley et al. [147], shown in the appendix in comparison to the literature (Figure A.11). Avoiding small-sized projection content reduces the resolution of the projection system, as shown in the Table 4.3 for the results of small-sized

---

projections. It guarantees that the projection surface, which might also be a rough street surface, does not influence the degree of details of the projection content [21].

Moreover, the animated sequence (DP test) has lower resolution requirements than a symbol-based projection, such as in DDS and SP (see in Table 4.3). Thus, using animated projections enables designing of high-quality content with low-resolution projection systems. Besides, the realistic method of the DP test encourages this finding, which covers a wide frequency range of possible animation speeds (0.25 to 1 Hz) without limiting the subjects to a fixed gaze. The theory also discovers the trend when comparing SVA with DVA, which requires a lower VA for dynamic VA testing than SVA testing [31, 81, 84, 83]. Table 4.3 contains the detailed resolutions, including confidence intervals, which require for all tests lower resolution requirements like the one angular minute named in the literature [76, 30], since none of the results has higher resolution requirements than 60 *ppd* which would refer to one pixel per one angular minute.

### 4.3. Discussion and guidance for the resolution requirements of near-field projections

Consequently, resolution aspects at a 3 m viewing distance that may be relevant for a safety-critical projection require about 30 *ppd* for an ambient luminance of approx.  $1 \text{ cd m}^{-2}$  and 40 *ppd* for ambient luminance above  $2 \text{ cd m}^{-2}$  without explicitly considering the projection content. At a viewing distance of 5 m, 50 *ppd* is sufficient for both ambient luminance levels. Still, an animated graphic requires about 25 *ppd* in the brighter scenario, requiring almost half the resolution compared to symbol- or text-based static content. Nevertheless, all performed tests regarding the resolution requirements are performed for high contrast values above 9 for the Weber contrast, as displayed in Table 3.7.

So, the application of near-field projection correlates to the theory which applies that the viewing distance influences the perception [103, 107, 108, 109] and the dynamics of the representation concerning DVA [81, 82, 83].

The state of the art of near-field projectors needs consideration if the visibility conditions listed in Chapter 6 are possible to reach since safety-critical projections require higher visibility, which results in higher luminance levels on the road or higher projector illuminance levels, as in a design-oriented display in a welcome or goodbye scenario. However, it is essential to find a compromise between the test subjects' demand for higher resolution, typical in the consumer electronics that accompany us every day, and good visibility, which can reduce the number of accidents in critical traffic situations. The application's requirements define the projection system since the application might simplify the selection of the projection system and its characteristics. Further, adaptation to near-field projection may occur after an introductory phase as it becomes an everyday feature [29]. Nevertheless, intuitive communication for projection must be predominant to increase safety [55, 150, 151, 152].

In the future, as projection systems evolve and might become brighter, brighter ambient conditions will no longer be a problem - not even for safety-relevant projections as indicated by the current state of the art [22, 25, 26, 42, 27]. This thesis guides to pre-estimate the required resolution depending on the projection content and purpose by suggesting resolution requirements depending on the use case, such as welcome and goodbye, safety-relevant projections, and vehicle's intention communication as displayed in the examples of Figure 2.4.

A synergy of a low-resolution projector for safety-related content and a high-resolution projection system for design would satisfy an all-encompassing projection system configuration. Such a system offers flexibility in terms of use case coverage. However, the scale of the use cases or the goals of the OEM may vary and, thus, the requirements for the projection systems. Over-performing the system, e.g., in terms of resolution, if only safety-critical projections are desired from further viewing distances such as 3 or 5 m, avoids too high resolution. Especially since the 1 m consideration in the various tests of Table 4.3 shows the resolution aspects

---

as a possible costs reducer, including, e.g., the complexity of the projector and the quality of the projection optics if considering systems with lower optics accuracy of  $0.5^\circ$  per pixel. Therefore, Table 2.2's state of the art must consider the effect on the technology selection with the resolution aspects and the visibility conditions in Chapter 6.

---

## 5. Experiment for the definition of contrast perception

---

This chapter focuses on the characterization of the test environment for testing the detection and perception of threshold contrasts and brightness of the projection system. Therefore, the used projection system is extensively examined to understand the system's limitations and, thus, the resulting limitations for the tests. In addition, an extensive review of the luminance coefficient and reflection behavior of several projection surfaces was undertaken to understand how the experiment's setting influences the results and which projection surface is suitable for the participant tests. Further, the tests include not only various ambient luminance levels, which influence the participants' adaptation and contrast perception but also the viewing distance to the projection and how the participant views the projection. The projection is either located in the direct viewing, so the participant perceives it in the foveal vision, or the projection is located somewhere in the participant's peripheral field of view. In the end, the results of the used projection system will derive contrasts for perceiving different projection contents and thus result in a variation of an automotive projector suitable for safety-relevant projection applications in urban traffic. Similar to Chapter 3, all tests apply the methods of constant stimuli [74, 75]. Furthermore, this chapter describes the examined test parameters for various adaptation levels (mesopic and photopic), different projection contents (symbol- and text-based), and types of illustration modes (static or dynamic).

### 5.1. Characterization of the test setup

Before the characterization and description of the setup can take place, the projector used is examined in more detail. Hence, the examinations include the burn-in time of the projector (Figure C.1), so there is a guarantee that the test participants can perceive a signal in a constant luminance/ illuminance on the projection surface. Thus, the stimuli shown are also reproducible for the constant stimuli tests. In addition, appendix C shows the burn-in behavior, representing measurements up to 60 min after switching on the projector, with a balanced range of illuminance reaching after 7 min (Fig. C.1). For this purpose, the projector was entirely set to white so that the surface is illuminated, as already shown in Figure 3.8, and the center of the image is the measuring point for the displayed behavior in Figure C.1. Finally, the burn-in time indicates the preparation time necessary before every test or measurement. Consequently, the projector is balanced after 7 min.

Further, 45 measurement points evaluate the projector's homogeneity, which results in a surface plot for a white (Fig. C.2) and a black projection (Fig. C.3). The black projection (Figure C.3) is measured individually to see how much stray light the projector generates through the LCD micro display (3 LCD laser projectors [127]) onto the road. The LCD projector is a subtractive projection system and cannot project a 'true' black color due to leakage [34, 33, 14]. The projector has only inhomogeneities at the edges of the projection surface. Therefore, a variation of about 8% appears in the all-white projection for the 21 measurement points in the middle of the projection ranging from 5042 lx to 5459 lx when neglecting the data points at the edges of the projection area (Figure C.2). Nevertheless, it is crucial to understand how the properties influence the projector's luminance on the projection surface since the illuminance is independent of the characteristics of the projection surface. A measurement of the reflection behavior and a pre-test evaluate the perception of similar projection illuminances on various surfaces.

### 5.1.1. Luminance coefficient and reflection of different projection surfaces

The influence of the projection surface is already mentioned by different researchers or projector manufacturers and evaluated for different materials to some extent for near-field projections [21, 42, 22]. First, however, the setup environment for the perception tests in this and the following chapter needs an extensive evaluation of the projection surface's characteristics and how it influences the participants' perception.

Based on the test target used to detect and determine visibility level at night, a 20 cm x 20 cm squared target is the projection content to evaluate the luminance coefficient of various projection surfaces [155, 95, 156, 119]. Further, based on the approach of de Boer et al. [157], measurements define an angle-dependent characterization of the luminance coefficient in the ambient lighting scenarios of the parking garage *PGS* and dusk and dawn *DDS* both in the mesopic vision, which is described and used before in Section 3 [30, 31]. The extensive measurement method examines whether the surface materials have angle-dependent reflection behavior and whether this behavior depends on the ambient conditions between the PGS (approx.  $1 \text{ cd m}^{-2}$ ) and DDS (about  $4 \text{ cd m}^{-2}$ ). Finally, the measured surface materials are characterized based on the classification types [133], e.g., whether they are diffuse scattering or reflective surface materials.

Therefore, the method of de Boer [157] was modified to some extent, which is displayed in Figure 5.1a, where luminance  $L_{\text{target}}$  is measured in  $0^\circ$  and  $63.5^\circ$  in a measuring distance  $d$  as well the illuminance  $E_{\text{target}}$  is measured in the middle of the 20 cm x 20 cm test target with a lux-meter on the ground. Henceforth, the luminance coefficient  $q$  results from the division of luminance with the illuminance in equation 5.1 [157].

$$q = \frac{L}{E} \quad (5.1)$$

The projection distance from the projector to the surface is 2.02 m. Picture 5.1b displays the measurement setup at  $\gamma = 63.5^\circ$  in the DDS. So, the reflectance coefficient is defined in the DDS and the PGS with equation 5.1 for five different surfaces: asphalt, rubber, white panel, brown leather, and white leather (Figure C.4).

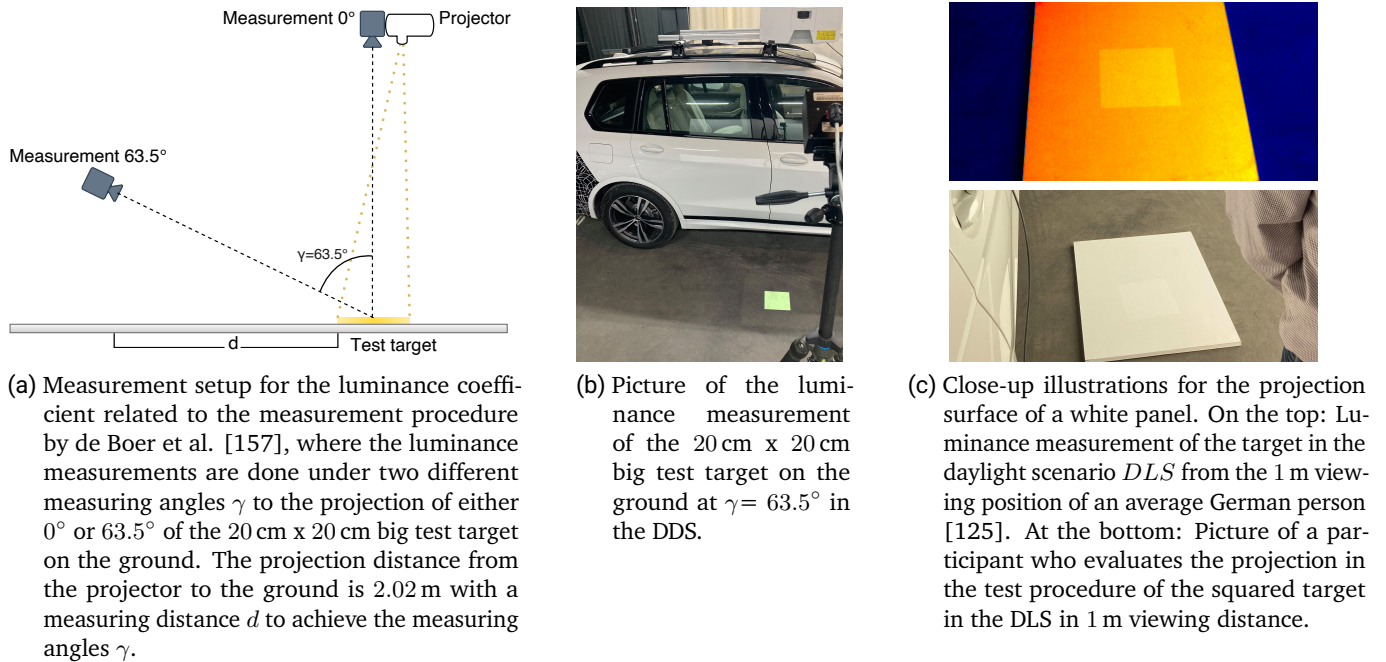


Figure 5.1.: Detailed illustrations for the luminance coefficient measurements.



Further, the CIE [133] classifies the surfaces with a reflection  $S$ , which is described by equation 5.2, where  $S < 0.4$  defines a diffusely scattering surface material (C1-class) and  $S \geq 0.4$  reflective materials (C2-class).

$$S = \frac{q_{63.5^\circ, \text{scenario}}}{q_{0^\circ, \text{scenario}}} \cdot \cos^3(63.5^\circ) \quad (5.2)$$

In the end, Table 5.1 displays the results of the measured and calculated reflection classifications for all materials. The characterized materials are not viewing angle-dependent nor ambient lighting level-dependent (Tables C.1 and C.2). All are classified as diffusely scattering (Table 5.1). De Boer et al. [157] and Jackson [42] also measured other materials, which include not only C1- but also C2-class materials.

Table 5.1.: Overview of the reflection  $S$  classification according to the CIE [133] for the five measured surface materials of asphalt, white panel, rubber, white leather and brown leather for the PGS and DDS. All materials are diffusely scattering  $S < 0.4$ .

$S$ for each scenario	Asphalt	White panel	Rubber	White leather	Brown leather
PGS	0.09	0.08	0.07	0.09	0.09
DDS	0.09	0.08	0.07	0.09	0.09

Second, with the knowledge of the classification of Table 5.1, a perception pre-test of the squared test target projection examines the dependencies of the viewing distance and the various surface materials in the daylight scenario (DLS with a luminance level of approx.  $235 \text{ cd m}^{-2}$ ) to obtain the detection rate of the test target on the projected surface. Therefore, the setup is similar to the setup used in Section 3 (Figure 3.7). Besides, the light setup in the testing room enables a simulation of daylight-like scenarios with luminance levels about  $235 \text{ cd m}^{-2}$  to achieve homogeneous illumination in the projection area. As mentioned before, also the methods for the perception tests in this chapter use the constant stimuli approach to define detection thresholds for the target's luminance or contrast (equation 3.7) [74, 75]. Moreover, the test design consists of eight different illuminance intensities of the projection, which were selected in advance using a small number of participants, viewed under two viewing distances (1 m and 5 m) for the five possible materials of asphalt, white panel, rubber, white and brown leather (Figure C.4). Every illuminance intensity was repeated three times. The resulting 24 stimuli (8 illuminance intensities x 3 repetitions) are displayed in a randomized order similar to the method in Chapter 3 and the application in other studies [130, 115, 119, 118, 120, 121]. The representation time for every stimulus is 350 ms, which also Schiller uses for his stimuli detection testing [130]. Due to the lower viewing angle of the participants at 5 m:  $18.57^\circ$  compared to the 1 m:  $59.24^\circ$  the same illuminance intensities result in different Weber contrasts depicted per ambient lighting scenario in Table C.3, which were determined using a luminance camera (TechnoTeam LMK-5 Color [128]). Finally, every participant evaluated 120 stimuli (= 8 illuminance intensities x 3 repetitions x 5 surfaces x 1 ambient lighting level) per viewing distance.

Before the participants conducted the test, they read an instruction sheet to, on the one hand, ensure the participant's eyes adapted to the DLS's ambient luminance, and, on the other hand, the instruction defined an explicit definition of what is meant by detection when completing this test. Therefore, the main task in this test for the participant is that the button 'Y' has to be pressed when the participants detect a light stimulus of the target on the various surfaces. For programming and performing the test uses the Psychophysics Toolbox Version 3 [158]. Figure 5.1c displays a picture of the actual test and the corresponding luminance measurement with a luminance camera exemplarily [128].

After all, the pre-test for the perception of the various projection surfaces consists of seven participants ( $N = 7$ ) - four women and three men - with a mean age of 33.51 years ( $SD = 13.25$  years) ranging from 25 to 57 years. The requirement during testing for all participants is to wear visual aids if they are necessary and

prescribed. Due to the low number of participants ( $N = 7$ ) no statistical analysis is performed. Therefore this test's purpose is to discover tendencies of the influence of the surface's characteristics on the contrast perception and its threshold levels. A modified version of the logistic regression function fits the detection's answers for the corresponding projector's illuminance, where the probability of randomly positive results is zero ( $\gamma = 0$ ) [88, 89, 90]:

$$P_{\text{detection}}(C_{W, \text{stimulus}}) = \frac{1}{1 + \left(\frac{C_{W, \text{stimulus}}}{\alpha_{\text{stimulus}}}\right)^{-\beta_{\text{stimulus}}}} \quad (5.3)$$

The detection probability  $P_{\text{detection}}(C_{W, \text{stimulus}})$  describes the threshold which is defined by the Weber contrast  $C_{W, \text{stimulus}}$  stimuli of the presented data set. The two other constants in equation 5.3 describe a stimulus of a 50% probability with  $\alpha_{\text{stimulus}}$  and  $\beta_{\text{stimulus}}$  describes the steepness of the fitting curve [88]. The MATLAB curve fitting tool supports the analysis of the contrast thresholds in this work. Figure 5.2 displays the experimental data of the perceived Weber contrasts  $C_{W, \text{stimulus}}$  with the resulting logistic regression, including the corresponding probability of detection for the five different projection surfaces in the pre-test.

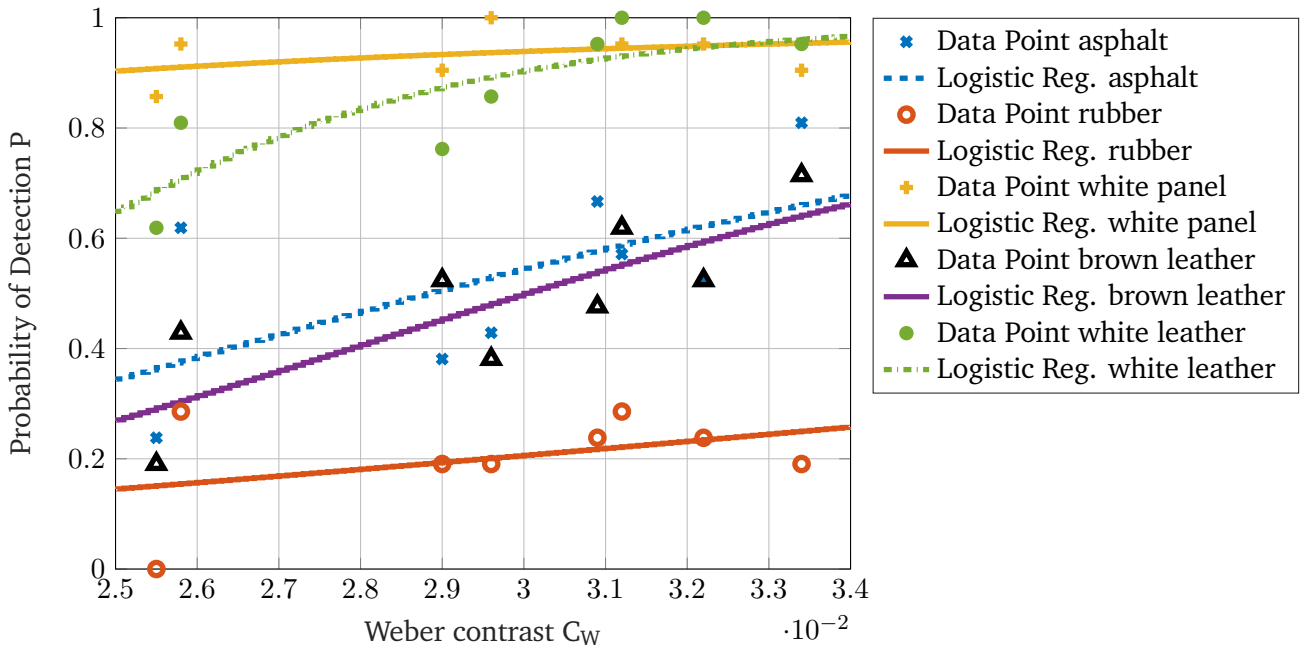


Figure 5.2.: Analysis of the detection contrast of the test target for the five different projection surfaces at a 1 m viewing distance. The graph includes the detection probability for every contrast level for every projection material and the logistic regression fitted to the probability data as indicated in equation 5.3. The tested projection materials are asphalt, rubber, a white panel 5.1c, and brown and white leather with seven participants ( $N = 7$ ). The low Weber contrast values on the x-axis are represented with a factor of  $10^{-2}$  for better readability.

Figure 5.2 illustrates the different fitted logistic regression curves, illustrating the detection trend for every projection surface. Moreover, a ranking of the resulting trends can be determined since the trends do not intersect, which is as follows from high to low probability of detection: white panel, white leather, asphalt, brown leather, and rubber. Similar to Chapter 3 and 4, a threshold level of 90% is the value of interest. Moreover, Table 5.2 lists all threshold levels for the 1 m viewing distance, which displays a similar ranking of



the Weber contrast thresholds similar to the fitted trends, where the white panel has the lowest threshold for the Weber contrast followed by the white leather, asphalt, and brown leather and at the end the rubber surface material. Additionally, the appendix displays the data of the 5 m viewing distance for the pre-test in Figure C.5 followed by the Weber contrast threshold Table C.4.

Table 5.2.: Detection contrasts extracted from Figure 5.2 for a 90 %-threshold level of the fitted data for a 1 m viewing distance of the five projection surfaces: asphalt, rubber, white panel, and brown and white leather.

Surface material	Weber contrast for a 90 %-threshold
Asphalt	0.05
Rubber	0.14
White panel	0.02
Brown leather	0.05
White leather	0.03

The results correlate with the data of Maier and Schlöder [22] where white surface materials have better subjective visibility compared to darker surfaces which are similar to the threshold levels of Tables 5.2 and C.4 and the depiction of the materials in Figure C.4. Also, an investigation of the roughness of the surface material is examined by Maier and Schlöder, where direct viewing of rough and smooth surfaces show significant differences [22] similar to the rubber surface, which is a rough surface compared to the other materials in the pre-test (see Figure C.4). Further, they state that the conditions of the surfaces play a significant role, as the dry asphalt is perceived better in direct viewing on the near-field projection as well as peripheral viewing than the wet asphalt [22], but this was not part of the conducted pre-study of this work. In addition, also Jackson [42] presents that the surface reflection influences the resulting luminance on the surface. Nevertheless, the reflection (Table 5.1) of the tested materials is not significantly different to result in such differences of the perceived contrast thresholds (Tables 5.2 and C.4). Therefore, it might not be a suitable parameter for predicting contrast perception. Finally, the surface's characteristics influence the participant's perception of near-field projections as indicated or suspected by [21, 42, 22] and confirmed by the pre-test.

Thus, in the following tests, the focus is set on asphalt as a projection surface because, on the one hand, this surface appears daily for the application of near-field projections, such as a parking garage or a street in the city. However, on the other hand, the asphalt allows contrast ranges for the 3LCD laser projector [127] in daylight scenarios (DLS with a luminance level of approx.  $235 \text{ cd m}^{-2}$ ) and also in darker scenarios such as the PGS (approx.  $1 \text{ cd m}^{-2}$ ) or DDS (approx.  $4 \text{ cd m}^{-2}$ ), which fulfills the desire of several researchers to consider DLS in order to define the brightness limits based on tests and not only theoretical derivations [19, 21, 42, 22, 25, 27, 26, 7, 159]. This desire thus leads to the definition of the contrast and perception testing scenarios in the following sections.

## 5.2. Experimental setup

The test setup for the perception and contrast studies is similar to the tests for the resolution requirements in Chapter 3. Thus, among other things, the schematic representation is similar to Figure 3.7. However, in the following tests, only the viewing distances of 1 m and 5 m are considered (instructions in Appendix C.4). In order to guarantee the participants a stable test environment and thus also to make the stimulus perception of the various luminance levels of the projector precisely, the contrasts are measured per ambient brightness and distance from the viewpoint of an average German person [125], so the contrast behaves differently per

projection content and distance. The chosen viewing distances of 1 m and 5 m relate to use cases - 1 m to derive the projection's perception in a welcome or goodbye scenario or to inform the car user of the vehicle's information, such as the loading status. The 5 m viewing distance determines safety-relevant projections in road traffic and the necessary visibility thresholds in the studies for contrast perception. The safety-relevant perception of the contrasts will be tendencies for both vulnerable RUs: pedestrians and cyclists. However, in this case, the car is not viewed from the side of the vehicle as in Figures 3.7 and 3.8, but the participant looks past the vehicle, as shown in Figure 5.3. Furthermore, the projector's projection area and height from the road surface are the same as in Chapter 3 (Section 3.2). However, the projection contents are rotated by  $90^\circ$  to illustrate the projections recognizable in the participant's new position. Nevertheless, the viewing angles are identical with  $59.24^\circ$  at 1 m and  $18.57^\circ$  at 5 m viewing distance to the projection.

Finally, the perception tests focus on two test scenarios: first, the PGS, which, similar to Chapter 3.2, has an ambient illumination of 22.17 to 34.1 lx (Figure 5.3a), which corresponds to a mesopic range of vision ( $L_{\text{Background}} \approx 0.56 \text{ cd m}^{-2}$ ) and is already being considered to some extent by some research institutions [19, 22, 118, 25, 27, 26, 7, 159, 160]. Second, a daylight-like scenario (DLS) has an ambient illumination distribution between 2137 to 9124 lx, which depends on the viewing distance since the daylight light source is stationary and illuminates the testing environment from the side to guarantee the participant a photopic range of vision in Figure 5.3b ( $L_{\text{Background}} \approx 235 \text{ cd m}^{-2}$ ). Figure C.6 displays the burn-in behavior of the daylight light source, which is in a stable state after 3 min. However, some researchers or projector manufacturers claim the DLS is a challenging scenario [42, 22, 25, 27, 26], therefore a high-power consumer electronics projector (3LCD laser projector [127]) performs all tests.



(a) Picture of the experimental setup in the PGS ( $L_{\text{Background}} \approx 0.56 \text{ cd m}^{-2}$ ). The picture displays the car with the roof-mounted projector, which displays the projection area of the near-field projection (horizontal ( $a_{\text{hor}} = 1.20 \text{ m}$ ) and vertical length ( $a_{\text{vert}} = 0.67 \text{ m}$ ) of the projection).



(b) Picture of the experimental setup in the DLS ( $L_{\text{Background}} \approx 235 \text{ cd m}^{-2}$ ) with the ambient light source for the daylight-like ambient illuminance indicated on the right border of the picture.

Figure 5.3.: Illustrations of different ambient scenarios for testing the contrast perception.

Testing, especially in the DLS (see Fig. 5.3b), makes it possible to determine initial trends for future applications in order to provide a data basis for the near-field projectors and substantiate the theoretical design of the projectors with data of perception tests, and design them in a user-oriented manner to increase the road

---

safety of RUs such as pedestrians and cyclists in future road traffic. Furthermore, the laser projector [127] in the PGS enables an examination of the glare limit. Finally, these are the goals of the test's design to elaborate on contrast threshold in the direct and peripheral view for various projection contents and ambient luminance levels, and the feeling of glare. Additionally, a prediction based on the participant test's data determines the projector's illuminance depending on the ambient luminance levels.

### 5.3. Test parameters

The test parameters of the detailed examination extend investigations and derivations of various institutes and manufacturers who have tested various projection surfaces with different colors, roughness, projection surface conditions as dry and wet, or colorful projections either static or in a dynamic/ flashing mode without applying or verifying these parameters with detailed psychophysical tests to determine the detection contrast or threshold levels in mesopic (PGS) or photopic (DLS) scenarios [19, 22, 25, 42, 7, 27, 26, 159, 160, 94, 60]. Thus, the goal of the test results is not to be based on subjectively perceived brightness evaluation, theoretical formula derivation, or experience-/ expert-based statements. These tests serve as a foundation for further research that applies to near-field projections around the vehicle. Therefore, the following test parameters vary:

- projection content (symbol- or text-based)
- perception of the stimuli (foveal or peripheral)
- display mode (static or dynamic)
- subjective evaluation of different Weber contrast levels regarding glare or disturbance

All the test parameters consider ambient luminance level dependency, observation distance dependency, or dependency on the stimuli's position in the peripheral field of view.

#### 5.3.1. Selection of projection content

The selection of the projection content enables an application- and perception-related presentation of the test results. The application-related background is selected to make the projection content relevant for use cases from 1m to 5m viewing distance. Either symbol- or text-based projections are projected in the close surroundings of the vehicle, as shown in Figure 5.4 . The projection contents are only examples of welcome or information messages from the vehicle. However, the study's results also deliver the first indications for safety-relevant projections. The content shown in Figure 5.4 does not cover a safety-relevant application, which would need a significantly different setting for the experimental setup. Therefore, in addition to the application-related evaluation, the studies define the perception-related evaluation. Schmidt-Clausen [86] and the CIE (Commission Internationale de l'Éclairage) [87] explain the visual process of perception: Seeing, perceiving, and recognizing. In the first step of 'seeing,' the eye perceives a light stimulus of an object, here the near-field projection, which creates an image of the object on the retina. The perceived image (symbol- or text-based projections) generates stimuli on the retina, which are converted into electrical signals in the second step 'perceiving.' The signals reach the brain via the optic nerve, and by comparing them with already existing stored images, a 'recognizing' is completed and ready to react to the perceived stimulus. Further, 'detection' describes the mere perception of the presence of an object. 'Recognition' distinguishes the observed objects between the color or the type of the object [161]. Visual perception is essential in road traffic since objects must be recognized early to prevent accidents and ensure enough time to react to a safety-relevant situation. Highly automated vehicles will communicate visually with near-field projection with other RUs. In this context,

the perception of near-field projections is essential [162], especially when observing abstract symbols in the peripheral field of view, as they will appear in realistic situations in urban environments for vulnerable RUs which perform surely another task than focusing on a near-field projection. Shibata investigated the scenario where the participants had to look on a phone. At the same time, near-field projections appears around them [27].



Figure 5.4.: Symbol- and text-based projection content for the perception testing, including a photo of the setup including a text-based projection.

Therefore, to establish a possibility of also viewing the projection in the participant's peripheral field of view, the setup was changed compared to chapter 3 as already indicated in Figure 5.3. So, the projections result in different symbol- and text-based content geometries compared to the tests in chapter 3. So, the projection area is reduced to establish homogeneous projections in the perceptual test by reducing the projection area displayed in Figure 5.4 for the symbol- and text-based projection. Table 5.3 displays the horizontal and vertical angular sizes of the projection content displayed in Figures 5.4a and 5.4b. The size of the symbol- and text-based projection (Table 5.3) is still in Weber's range of the projection size (exceeding 100 ') in all possible directions to neglect the effect of object size on the contrast perception [94, 163]. Additionally, the projection content's size guarantees to be located in the homogeneous region of the projection area as stated in section 5.1.

Table 5.3.: Calculated viewing angles in horizontal and vertical direction from the distances 1 m and 5 m for the symbol- and text-based projections. An exemplary eye height of 168 cm was used for the calculation, which relates to an average German person [125].

Content	Viewing distance 1 m		Viewing distance 5 m	
	$\alpha_{\text{horizontal}}$ in '	$\alpha_{\text{vertical}}$ in '	$\alpha_{\text{horizontal}}$ in '	$\alpha_{\text{vertical}}$ in '
Symbol	1081.2	248.12	403.61	169.87
Text	1081.2	371.38	403.61	253.22



All possible Weber contrasts used in the studies are measured in the PGS and DLS to validate the theory. Figure 5.5 shows on the left that the contrast curves are nearly linear over an extensive range, especially at a distance of 5 m for the PGS. Further, the contrasts at a viewing distance of 5 m are lower than viewing at a distance of 1 m for the same projector intensities. So, the Weber contrast has a distance dependence for the PGS. For example, the symbol-based projection shows a maximum contrast of 60.24 at a distance of 1 m and a maximum contrast of 57.99 at a distance of 5 m and the maximum contrast is 73.06 at a 1 m distance and 53.59 at a distance of 5 m for the text-based projection. Figure 5.5 shows the contrast curves for the DLS on the right, which are not as linear as in the PGS. Nevertheless, the contrast curves show also a viewing distance dependency, where the contrasts of 1 m are higher compared to the 5 m viewing distance. The contrast levels themselves are lower in the DLS compared to the PGS since the maximum contrast of 0.25 at a distance of 1 m and a maximum contrast of 0.17 at a distance of 5 m for symbol-based projection and the maximum contrast is 0.40 at a 1 m distance and 0.21 at a distance of 5 m for the text-based projection.

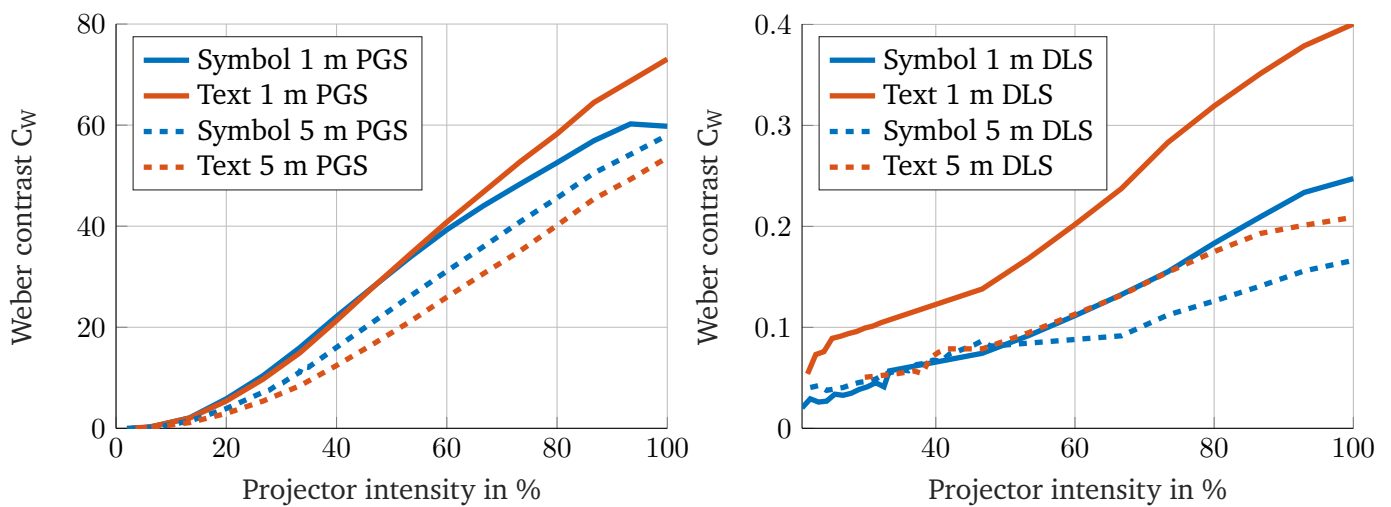


Figure 5.5.: Overview of the contrast curves for the presented stimuli (symbol and text) at distances of 1 m and 5 m depending on the projector's intensity for the two ambient luminance scenarios of PGS on the left and DLS on the right.

This extensive characterization of the projection size and the use of Weber contrast for the symbol- and text-based projections ensure a detailed analysis of the testing results in the next chapter. However, the different testing scenarios are stated before the analysis to create an overview of the tests' aims.

### 5.3.2. Contrast perception with direct viewing direction

This test determines the threshold contrast required for foveal viewing of near-field projections. The experiment includes both PGS and DLS ambient illuminance levels, where the different projections (symbol- or text-based) are viewed under different viewing distances. The subject stands at 1 m or 5 m from the projection area behind the vehicle centered on the middle of the projection area — the visual angle  $\alpha$  of the projections changes at different viewing distances, as shown in Table 5.3. Figure 5.6 displays on the left the vehicle's position and the participant's  $P$  location during testing. The test uses realistic ambient lighting scenarios to simulate a near-field projection confrontation in an urban environment at night-time in an urban area (PGS) or during a daytime-like environment, which occurs during the day (DLS). The PGS defines a mesopic setting described in detail in section 5.2, corresponding to the DIN norm for illumination levels in a parking garage [80].

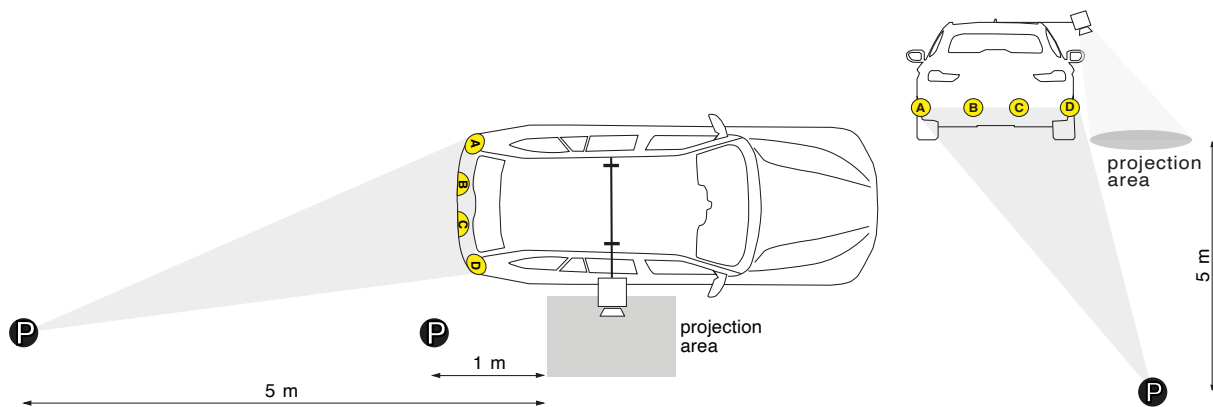
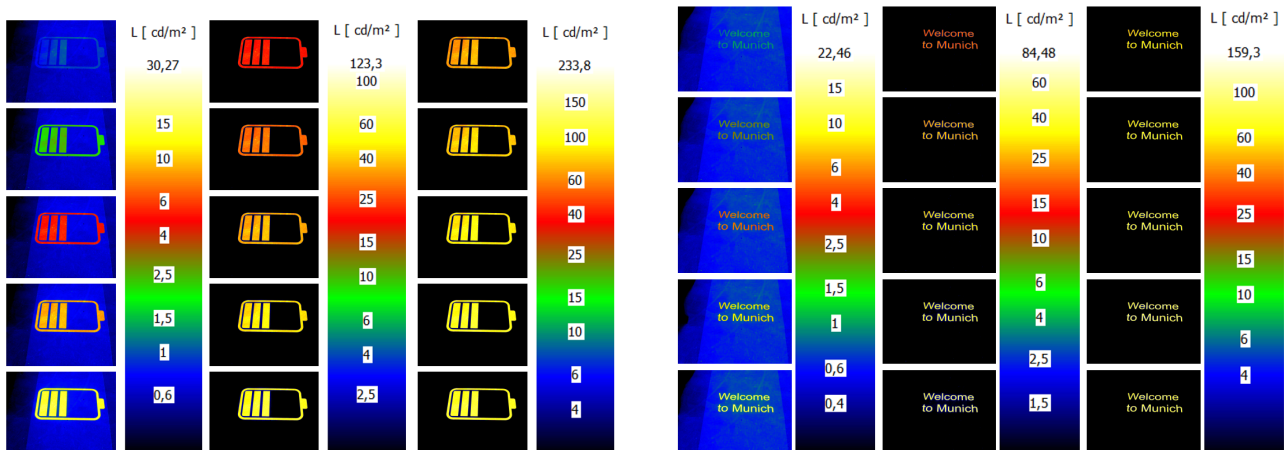


Figure 5.6.: The setup evaluates the contrast perception in the direct and peripheral field of view and the subjective evaluation of different contrast levels. Participant  $P$  is located centralized to the projection area in 1 m or 5 m away from it. The general setting is displayed on the left. On the right: the schematic view from the participant's perspective. Four fixation marks indicate the different fixation points on the vehicle from  $A$  to  $D$ , which correspond to 5, 10, 20, or 30-degree locations to the left of the participant's eccentricity, since the projection is located at 0 degrees to the participant. The contours of the vehicle imitate the G31 [32].

Figure 5.7 lists a range of displayed projection intensities for both projections contents (symbol- and text-based) in the PGS to illustrate the luminance measurements for determination of the Weber contrasts for the graphs in Figure 5.5. In order to determine the influence of daylight and the required Weber contrast, the DLS simulates a day with about 9700 lx. The various projections were measured using the LMK 5 Color [128] for different scenarios and viewing distances. Finally, the Weber contrasts were determined via the LMK Labsoft software using the 'contrast object' evaluation method [164]. Figures 5.7a and 5.7b show exemplary luminance measurements for the symbol- and text-based projections ranging from 6.6 % to 100 %.



(a) Shown grayscale for symbol-based projection in %, from top to bottom, from right column to left column: 6.67, 13.33, 20, 26.67, 33.33, 40, 46.67, 53.33, 60, 66.67, 73.33, 80, 81.57, 92.94, 100

(b) Shown grayscale for text-based projection in %, from top to bottom, from right column to left column: 6.67, 13.33, 20, 26.67, 33.33, 40, 46.67, 53.33, 60, 66.67, 73.33, 80, 81.57, 92.94, 100

Figure 5.7.: Luminance images of the symbol- and text-based projection content for determining the contrast thresholds at a distance of 1 m in the PGS.

---

Appendix C.5 includes all luminance measures in detail, including the grayscale levels with the corresponding contrasts and illuminances for the different projection content related to the viewing distances and ambient illumination levels.

The different stimuli are presented per subject depending on the ambient illumination level and viewing distance in eight different grayscale levels, thus resulting in different stimuli brightnesses per projection content. The grayscale levels were determined using preliminary tests and are in the range of the potential detection threshold, which is determined using the hexadecimal or RGB color system. For example, in the RGB color system, 100 % corresponds to  $R = 255$ ,  $G = 255$ , and  $B = 255$ , which is the measurement placed in the last row and the most right column in Figures 5.7a and 5.7b. Preliminary tests have shown that text-based projections require higher gray levels for detection than symbol-based projections, which relates to the process of perceiving texts, which must not only be detected but also recognized [86, 87, 161]. Furthermore, showing the presented detection objects several times is recommended to balance personal deviations.

Here, perception consisted of detecting the light stimulus of the projection. The constant stimuli method presents subthreshold and suprathreshold stimuli to the participant in a randomized order to avoid learning effects [74, 75]. There are only two possible responses - if the stimulus is detected: 'Yes' corresponds to the key 'Y' on the keyboard, and if the participant does not perceive any stimulus: 'No,' which is the key 'N' on the keyboard. The keyboard logs the answers to the stimuli with the lowest latency possible for the corresponding reaction times to a computer via a USB connection. In detail, the participant logs within 1500 ms a spontaneous answer with a keyboard press if she/ he detects the presented projection (stimulus), which appears for a 350 ms stimulus period. A randomized waiting time (between 1000 and 2000 ms) between two stimuli is applied to reduce learning effects. The reaction times are recorded between the projected image's appearance and the participant's button press by presenting the stimulus multiple times at different intensities in one round., with a probability of detecting the stimulus results at every intensity level per greyscale or Weber contrast.

Moreover, the overall study time was at most 45 minutes, including the adaptation time to ensure concentrated participants for the whole testing procedure. In addition, a psychometric function generates a fitted sigmoid function from the yes- and no-responses of the participants at different intensity levels to determine the threshold contrast levels at specific percentages [88, 89, 90]. Finally, the participant sees 192 stimuli (8 grayscale levels x 3 repetitions x 2 viewing distances x 2 projection contents x 2 ambient illuminance levels).

### 5.3.3. Contrast perception of dynamic near-field projection

Some research institutions and studies report an influence of projection dynamics on contrast perception [22, 26, 7, 60]. Therefore, this test will also evaluate the viewing of dynamic near-field projections, using the same setup (Figure 5.6) as in the foveal viewing test and additionally experiencing a dynamic projection with the same grayscale levels, perceived contrasts (Tables C.5 and C.7) as in the direct viewing of the projection area. Here, only the battery symbol is selected, which appears for 350 ms at a frequency of 3 Hz for two seconds, which is the frequency of a flashing emergency stop signal [165]. In this case, the displayed projection symbolizes a critical vehicle's battery level to the participant or car owner. However, the difference to the results before is also applicable to the safety-related projections, as the detection thresholds for near-field projections are valid between static and dynamic projections.

Furthermore, the constant stimuli method is applied here to draw comparisons to the foveal observation testing. Thus, the results and interpretations of the other research groups with a larger scale psychophysical testing should confirm the trends and might present the relationships for the influence of the dynamics on near-field projections next to the vehicle. So, every participant experienced 48 stimuli (8 grayscale levels x 3 repetitions x 1 viewing distance x 2 ambient illuminance levels) at a viewing distance of 1 m.



---

#### 5.3.4. Contrast perception in the peripheral field of view

An additional test differs from the previous direct viewing testing because it appears next to the vehicle without looking directly at the projection. However, the subject must look at fixation marks on the vehicle in different eccentricities in the participant's field of view, as displayed in Figure 5.6. Here, the goal is to record the detection frequencies per brightness level of the stimuli perceived in the peripheral field.

The entire study procedure splits into two environmental lighting conditions: first, trials are conducted in a mesopic environment (PGS) and then in a photopic environment (DLS) to keep the adaptation times and, thus, the trial time short and the participants concentrated during the testing procedure. Four fixation marks indicate the different fixation points on the vehicle from *A* to *D*, which correspond to 5, 10, 20, or 30-degree locations to the left of the participant's eccentricity since the projection is located at 0 degrees to the participant. Every participant fixates randomly from *A* to *D* or *D* to *A* to have no learning effects (Figure 5.6). Before the start of the experiment, the participant will receive an initial questionnaire to provide personal data, which will be answered in the mesopic environment so the participant's eyes can adapt to the current level of ambient lighting. After the participant evaluated all stimuli in the mesopic environment, the setting of the environment was changed to the photopic environment to repeat the procedure.

During the test, participants perceive near-field projections in their peripheral vision. During every trial, the subjects direct their gaze to the respective fixation mark during the entire test (5, 10, 20, or 30°) while observing the projection from 5 m. Figure 5.6 displays the setting on the right where projections appear next to the vehicle on the passenger side. The subject averts his/ her gaze toward the driver's side as the observation distance is 5 m away from the vehicle. The task is to indicate whether a near-field projection was detected or not. Detection is the first perception or noticing of a light impression [86, 87, 161]. What matters is not what content is visible, but whether something has been noticed. Here only the symbol is chosen as projection content to reduce the cognitive processes of just detection and not recognition [86, 87, 161]. The size of the evaluated projections was always in the Weber range (above 100') [94, 163] (see Table 5.3). The quality of the projection is neglected in the perception tests. After an acoustic signal, the participant can log in the perceived reaction of the near-field projection to the system via a keyboard. Here, only a 'Y' is the key to press when a near-field projection is detected next to the vehicle; if no projection is detected, so no keyboard press is needed. The participants have 1.5 seconds to enter the response. In the end, every participant perceives during the whole testing procedure 192 stimuli in total (8 grayscale levels x 3 repetitions x 1 viewing distance x 2 ambient illuminance levels x 4 eccentricities).

#### 5.3.5. Subjective evaluation of contrasts

In addition to the psychophysical examination and the derivation of contrast thresholds, the participants evaluated near-field projections in peripheral vision in a subtest. The task for the participants is to subjectively evaluate with a Likert-based scale to determine a perceived glare or disturbance derived from the methodology of de Boer and Schreuder [97]. Figure C.8 displays the instruction of the testing procedure. The seven-argument Likert scale, which is an optimum number of alternatives according to Lozano et al. [98], labels the items from 1 (unnoticeable) to 7 (disturbing).

Before the start of the experiment, a test run displays an example of near-field projections and the procedure for one of the four different eccentricity levels similar to the contrast perception in the peripheral field of view testing (Figure 5.6 on the right). During one trial, four brightness levels of a near-field projection are presented with three repetitions in random order, like the other tests following the constant stimuli methods but with higher Weber contrast levels  $C_W$  between 31.1 to 58. The participant enters the response via a numerical keyboard entry; a list of the numerical numbers and the corresponding meanings is apparent during the whole test procedure for the participant next to the keyboard, with '1' being unnoticeable and '7' disturbing. During every trial, every participant looked at different fixation marks for each run, corresponding to 5, 10, 20, and

30° marked in the test with *A*, *B*, *C* and *D* in Figure 5.6 in the participant's field of view from a 5 m viewing distance. During the experiment, the participant sees a near-field projection in the peripheral field while focusing on the fixation marks. After every display of the projection, an acoustic signal indicates the log-in time for the personal evaluation so that the participant does not have to change his fixed view. The test is performed only in the PGS because the used projector [127] does not reach a possible glare/ disturbance threshold in a day-like scenario (DLS) limited by the maximum brightness of the projector.

To evaluate the perceived disturbance, the participant has to imagine the following scenario: She/ he is standing at a crosswalk and wants to cross the street. In his/ her peripheral field of view, a vehicle projects a near-field projection next to the vehicle. Therefore, she/ he has to evaluate the near-field projection in the following situation, considering the following aspect: 'Does the near-field projection arise bother/ disturbance while crossing the street and noticing such a near-field projection?'. Finally, every participant evaluates 48 stimuli subjectively (4 grayscale levels x 3 repetitions x 1 viewing distance x 1 ambient illuminance level x 4 eccentricities). Table 5.4 lists the stimuli variations and the related ranges of the stimuli concerning other relevant test parameters such as display time or projection content.

Table 5.4.: Summary of the used parameters in the subjective evaluation of perceived contrasts in the peripheral field of view like projection content, grayscale levels, Weber contrast range in the mesopic environment at a viewing distance of 5 m, the examined eccentricities and the display time of the near-field projection during testing.

Content	Grayscales in %	Weber contrast mesopic at 5 m	Eccentricities in °	Display time in ms
Symbol	60 - 100	31.10 - 57.99	5; 10; 20; 30	350

The subjective evaluation of contrast threshold levels allows the classification of the maximal contrast levels in the mesopic scenario (PGS), which will set the maximal brightness for the projector. Moreover, the maximal brightness is essential to successfully introduce near-field projections for highly automated vehicles or other vehicles since the newly implemented projections shall improve traffic safety and not disturb, distract, or glare other RUs in traffic situations.

### 5.3.6. Research participant collectives

Table 5.5 summarizes the participants' collectives information to give an overview and to compare the various tests since, e.g., the visual apparatus is influenced by age, and this factor might have an impact on the test results, which some research institutions have already defined but not in the context of near-field projections [147, 94, 100, 166]. Thus, the listing and comparison between studies are shown in Table 5.5 with parameters like the participants' number *N*, the participants' age, the age's standard deviation per collective, including the age range in the participant collective, the number of female or male, and the percentage of visual aid use.

Excluding the testing of the influence of dynamic projections, the other three tests have the same participant collective (mean age between 38.96 and 38.36), except that in the peripheral observation, five outliers led to the violation of the requirement of subthreshold or suprathreshold stimuli in the constant stimuli method [74, 75]. Some participants did not detect any stimulus or saw all stimuli and consequently were outliers. Moreover, the age distributions are similar for the direct, peripheral viewing, and subjective contrast evaluation. However, the influence of the outliers on peripheral viewing is evident in Table 5.5, e.g., the difference of age is 0.5 years lower for peripheral viewing ( $SD = 11.98$  years) than for direct viewing ( $SD = 12.5$  years). The participants in the perception test for dynamic near-field projections were about five years younger (mean age 33.21,  $SD = 9.56$ ), aged between 15 and 55, compared to the other tests ranging between 20 and 64. Along

with the younger age distribution of the participant collective for the influence of dynamics also, the usage of visual aid is 44.44 %, which is about 10 % lower compared to the other tests in Table 5.5. A value for the static representation of the near-field projection was identified with the same participants' collective separately in the same test to guarantee comparability and valid resulting relationships between static and dynamic display.

Table 5.5.: List of the participants collectives' characteristics for all participants of the contrast perception tests. The parameters are the participants's number  $N$ , the participants' age, the age's standard deviation in every collective, the age range, the number of females or males, and the visual aid usage in %.

Parameters	Foveal viewing	Foveal viewing influence of dynamics	Peripheral viewing	Disturbing contrast
Participants' number $N$	47	27	42	47
Average age in years	38.96	33.21	38.36	38.96
Standard deviation in years	12.5	9.56	11.98	12.5
Age range in years	20 to 64	15 to 55	20 to 64	20 to 64
Number of female / male	7 / 40	5 / 22	7 / 35	7 / 40
Visual aid usage in %	57.45	44.44	54.76	57.45

Moreover, the percentage of female participants is between 14.89 % and 18.52 %, which results in no further consideration of the gender-specific threshold levels. Nevertheless, all tests have in common that every collective has a visual aid usage between 44 to 58 %.

## 5.4. Summary of the experimental setup

Finally, this paragraph summarizes the differences and variations of the various tests used to evaluate contrast perception and the resulting brightness requirements for near-field projections in Table 5.6.

In Table 5.6, the tests differ in ambient light levels of either mesopic (approx.  $0.6 \text{ cd m}^{-2}$ ) or photopic ambient luminance (approx.  $210 \text{ cd m}^{-2}$ ) and the resulting perceived Weber contrasts for 1 m and 5 m viewing distance. Besides the viewing distance, the projection content varies to evaluate the perception process with psychophysical data [74, 78, 86, 87, 161]. In addition, the influence of the dynamics on the projection's perception is tested to evaluate and compare the previous findings [7, 27, 26, 60]. Further, the peripheral tests (contrast perception and subjective evaluation) evaluate contrast in the combination of the location's variation of the near-field projection depending on various eccentricities at an observation distance of 5 m. Besides the detection contrast thresholds in the participant's peripheral field of view, a rating determines possible disturbance or glare. These ratings create another limitation for near-field projections in future urban traffic not to disturb RUs from their intended traffic task. The mentioned methodology for the tests supports the development of near-field projections around the vehicle to reduce safety-critical traffic situations in urban areas where vehicle confrontation with other RUs will be present.

Table 5.6.: Overview of the variation of the executed tests of direct or peripheral viewing and the dynamics' influence involving the characteristics for the projection content, viewing distance, eccentricities in the peripheral view, projections' display time, and dynamics. The used grayscale levels of the projection and the perceived Weber contrasts for 1 m and 5 m viewing distance are also listed.

Parameter	Direct	Direct	Dynamics	Peripheral
Projection content	symbol	text	symbol	symbol
Viewing distance in m	1; 5	1; 5	1	5
Eccentricities in °	0	0	0	5; 10; 20; 30
Display time in ms	350	350	350; 2000	350
Dynamics in Hz	-	-	3 for 2 s	-
Grayscale mesopic in %	1.96 - 5.88	2.75 - 6.67	1.96 - 4.7	-
Weber contrast mesopic at 1 m	0.03 - 0.23	0.04 - 0.40	0.0039 - 0.1236	-
Grayscale mesopic in %	2.75 - 6.67	3.53 - 7.45	-	2.75 - 8.24
Weber contrast mesopic at 5 m	0.0029 - 0.2445	0.0606 - 0.3105	-	0.0029 - 0.4127
Grayscale photopic in %	20.78 - 29.02	21.57 - 29.80	20.39 - 23.14	-
Weber contrast photopic at 1 m	0.0202 - 0.0386	0.0539 - 0.0993	0.0218 - 0.0251	-
Grayscale photopic in %	21.96 - 30.20	29.80 - 38.04	-	26.67 - 44.31
Weber contrast photopic at 5 m	0.0404 - 0.0466	0.0506 - 0.0543	-	0.0404 - 0.0778



---

## 6. Contrast and illuminance requirements for near-field projections

---

This chapter deals with the evaluations of the tests described in Chapter 5 on the visibility and perception of near-field projections. The investigations involve the variation of two different viewing variants: on the one hand, the direct viewing of the participant on the projection surface on which the test target appears (symbol- or text-based presentation) and, on the other hand, the viewing of the target, which in this case is only a symbol, in the peripheral field of the test participant. All viewed projections have a target size to fulfill Weber's law for a constant contrast perception [94, 95]. In addition, external factors like the influence of the ambient lighting, the viewing distance, the projection content, the type of presentation (variation in the presentation dynamics), and the characteristics of the projection background are considered, which can influence the perception of near-field projections. The peripheral field of view investigations focuses on contrast perception and a subjective evaluation of Weber contrast levels for a symbol-based projection. As in Chapters 4 and 5, the analysis of the perception thresholds uses a logistic regression [88, 89], whereby a Likert scale analysis applies for the subjective evaluation of the possible disturbance by near-field projections in the peripheral visual field [97, 77].

Further, the results are compared with state-of-the-art of Chapter 2 to validate the psychophysical testing results for possible influences on contrast perception and the related Weber contrast thresholds for the given test conditions. Additionally, chi-squared testing underlines the significance of various influencing factors. In the end, the data from the psychophysical tests fuses into an interpretation of the projector characteristics to enable a user-oriented design of perceiving near-field projectors in the automotive field.

Finally, important influencing factors for the perception of near-field projections are derived, extending the existing results and increasing the importance of developing user-orientated near-field projections.

### 6.1. Influence factors on detection contrast with direct viewing direction

Following the detailed analyses of the external factors influencing the resolution aspects of the near-field projections in Chapter 4, the influences of the external factors on the perceptual thresholds for contrast are now investigated. This section focuses primarily on the direct viewing of the projection and the resulting foveal contrast thresholds of the participants for near-field projections. To ensure valid contrast perception, all tests of Chapter 5 ensured the necessary adaptation time, as described in section 2.3.1. In terms of external influences, the main focus is on factors like ambient lighting, which influences the type of vision (Table 2.3), viewing distance, and projection content, which can influence detection thresholds through the perceptual processes involved [78, 86], the animation speed of the projection, and the projection background with its properties such as color, roughness, or reflection behavior.

The data from the psychophysical tests of the investigated scenarios and the related participant collective of Table 5.5 in section 5.6 are evaluated using the logistic regression already determined in section 5.1.1 with the equation 5.3 for the contrast thresholds obtained for the pre-test of perceptual influence of varying projection surfaces. All detection thresholds in this chapter refer to a 90 % threshold level obtained from the resulting continuous logistic regression fits representing the perceived contrast values of the projection on the

ground under the respective conditions, e.g., external influences. The chosen 90 %-threshold covers all three possible use cases of near-field projections displayed in Figure 2.4, ranging from design-oriented (Figure 2.4a) to safety-relevant projections (Figure 2.4b), to achieve an essential requirement for visibility regardless of the application. Analogous to Chapter 4, chi-squared tests classify the distribution of responses of the different subtests for statistical significance (5 % significance level).

### 6.1.1. Ambient lighting

This section considers the symbol-based projection of Figure 5.4a, analyzed in Figure 6.1, by comparing the tests' results for the mesopic ( $L_{\text{Background}} \approx 0.6 \text{ cd m}^{-2}$ ) and photopic vision ( $L_{\text{Background}} \approx 235 \text{ cd m}^{-2}$ ). Further, the solid lines in Figure 6.1 refer to the fitted test's data of the mesopic vision, and the dashed lines refer to the photopic vision. Additionally, the legend of Figure 6.1 lists detailed information on the data point markers. The participants viewed the projection from an observation distance of either 1 m or 5 m.

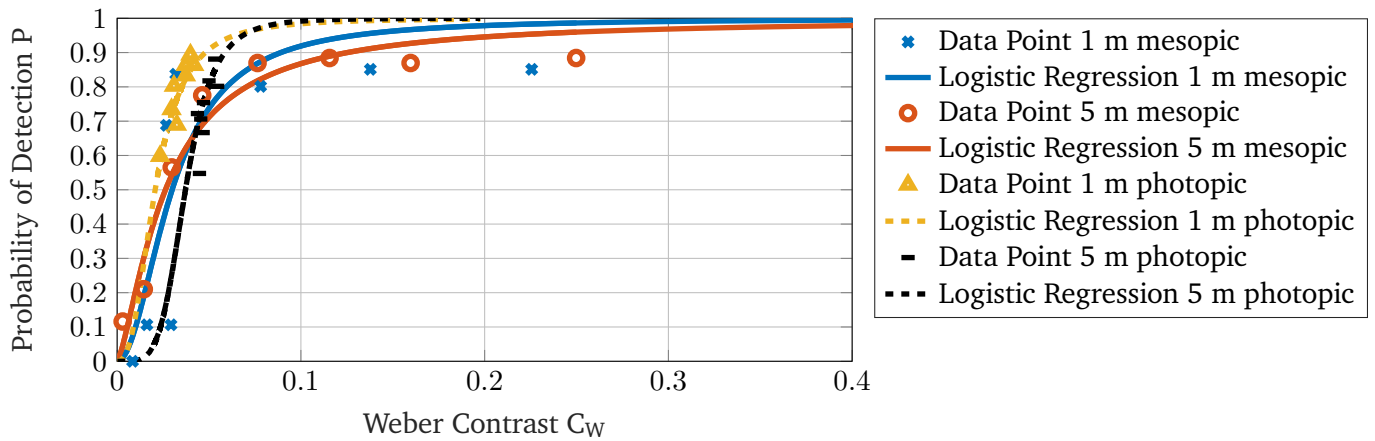


Figure 6.1.: Logistic regression fitted for the Weber contrasts including data points of the detection probability per Weber contrast value for the mesopic and photopic environmental settings. The solid lines relate to the mesopic fitted data for both viewing distances of 1 m and 5 m, and the dashed lines relate to the photopic data fit for directly viewing a symbol-based projection.

Table 6.1 lists the 90 % threshold levels for the detection contrasts of Figure 6.1, including the associated 95 % confidence intervals. Additionally, Table 6.1 considers, besides the symbol, the text-based projection content concerning both adaptation luminance levels (mesopic and photopic).

Table 6.1.: Results for the perceived Weber contrast on the projection surface for a 90 % threshold of the logistic function for the symbol- and text-based projection for two adaptation luminances ( $L_{\text{Background}} \approx 0.6 \text{ cd m}^{-2}$ ,  $L_{\text{Background}} \approx 235 \text{ cd m}^{-2}$ ). The numbers in the bracket indicate the confidence intervals of 95 %, with the lower bound (left number) and the higher bound (right number) for two viewing distances and two adaptation scenarios.

Scenario	Viewing distance in m	Symbol	Text
mesopic	1	0.0891 (0.0809; 0.1047)	0.1539 (0.1446; 0.1713)
	5	0.1253 (0.1138; 0.1460)	0.1855 (0.1752; 0.2042)
photopic	1	0.0480 (0.0444; 0.0574)	0.1244 (0.1195; 0.1337)
	5	0.0586 (0.0548; 0.0698)	0.0618 (0.0601; 0.0668)



Furthermore, the ambient luminance levels used for every participant in the testing applied the identical illuminant to ensure no influence by the visual spectrum of the distributed light on the test results to avoid any impact on the human perception due to the interaction of the visual system (see section 2.3.1 and Figure 2.5).

The values in Table 6.1 show that photopic detection contrasts are lower than for mesopic contrasts, e.g., 0.0480 for 1 m symbol photopic and 0.0891 for 1 m symbol mesopic. Figure 6.1 visualizes this behavior because the photopic viewing conditions (dashed curves) saturate with lower contrast values on the x-axis and have a steeper gradient to reach the 90% thresholds earlier (lower contrast levels) for a symbol-based projection. This relationship is independent of the projection content, as Table 6.1 lists the text-based projection content values. However, the value of 5 m for the text-based content in the photopic vision has to be viewed with caution since it is three times lower than the mesopic vision (see Table 6.1), although this chapter reviews several dependencies in detail. Furthermore, there is no overlap between the perceived contrast thresholds for the mesopic and photopic regions when looking at the confidence intervals. Table 6.2 supports the observation of the physical values of the contrast thresholds, as the chi-square tests regarding the influence of ambient luminance always show significance ( $p < 0.05$ ) with a small to medium effect [146], which leads to a significant difference for the two adaptation luminance levels. So, the perception of the projections' Weber contrast differs between mesopic and photopic vision no matter the displayed projection content.

Table 6.2.: Chi-square analysis defines the statistical effects of the ambient luminance influence responsible for a mesopic and photopic vision for 1 m and 5 m viewing distance for a symbol- and text-based projection.

Viewing distance in m	Compared items	Symbol	Text
1	mesopic x photopic	$\chi^2(7) = 145.22, p < 0.05,$ $V = 0.32$	$\chi^2(7) = 38.67, p < 0.05,$ $V = 0.17$
5	mesopic x photopic	$\chi^2(7) = 61.41, p < 0.05,$ $V = 0.21$	$\chi^2(7) = 30.51, p < 0.05,$ $V = 0.14$

A comparison of the review in Table 2.5, Schneider [118] and Shibata et al. [27, 26] also finds the same effect as the results mentioned in this section: lower detection contrasts are required at higher ambient luminance levels. However, the Weber contrasts of Shibata et al. for a symbol-based turning indicator projection are significantly higher at approx. 0.4 relates to a more complex study design where the participants also moved during the testing procedure [27]. The factor is about four times higher due to the more complex study design. The lower Weber contrasts for detection in photopic compared to mesopic vision refer to the density and distribution of the relevant receptors, e.g. cones and rods, on the retina as shown in Figure 2.5 [78, 31, 30, 118, 120, 121]. The dominant cones for photopic vision have their maximal density in the fovea, which refers to the direct viewing and are more sensible to the incident light entering the eye [30, 78, 31].

Nevertheless, Schneider has similar Weber contrast tendencies for foveal viewing of a deer symbol of about 0.12 at  $1 \text{ cd m}^{-2}$  ambient luminance displayed in Figure 2.16, which correlates with the symbol-based contrast thresholds in Table 6.1, especially for the mesopic vision in this thesis. In addition, the effect highlighted by Shibata et al. [26] may play a role in the results of this section, too, that naive participants require higher Weber contrast thresholds than experienced participants who are already familiar with the experimental setting and the perceived projections for already 30 minutes as mentioned in chapter 5 for every testing procedure.

However, if an universal projection system is desired, in that case, the design of the projector should be based on the requirements of the ambient condition with higher threshold contrasts - the mesopic region - which would allow the projections to benefit from higher Weber contrasts in the photopic vision. Further,

---

the projections for a symbol could thus have about twice the contrast in the mesopic region. However, the difference is insignificant for a text since, for example, the mesopic and photopic regions differ by only about 20 % for a viewing distance of 1 m. Nevertheless, section 6.1.6 will derive the illuminance necessary for the projector to achieve the perception-based requirements.

In addition, appendix D.2 includes further graphs related to the influence of ambient lighting on the contrast perception of the investigated participants.

### 6.1.2. Viewing distance

An essential factor for designing a perception-based projection system is the viewer's distance to the projection itself, which can vary depending on the traffic situation. Therefore, the results from Table 6.1 also evaluate the influence of the viewing distance. The statistical tests from Table D.1 show that the other chi-squared tests are insignificant apart from the symbol-based projection content with the mesopic adaptation luminance level. Taking into account the viewing distance for the symbol in mesopic vision, it shows a significance with a small effect ( $\chi^2(7) = 47.44, p < 0.05, V = 0.19$ ). Table 6.1 shows the corresponding physical values for 1 m and 5 m viewing distances, which differ by 9 %, taking into account the confidence intervals. In the photopic scenario for the symbol and the mesopic vision of the text, a summary related to the viewing distance dependency is possible as the respective value ranges overlap for considering the confidence intervals.

However, photopic observation of the text-based projection is considered with caution, as the contrast at a 5 m viewing distance is two times lower compared to a viewing distance of 1 m. The asphalt used in this section is also under investigation in the pre-test, and all results of section 5.1.1 display an increase in the physical values of the Weber contrast with increasing viewing distance. Nevertheless, a generalized statement based on the results of Table 6.1 encourages neglecting the viewing distance dependence due to the physical values with overlapping confidence intervals with small differences below 10 %. Additionally, Table D.1 lists the statistical analyses, which are all insignificant ( $p < 0.05$ ). Furthermore, the results extend the literature review of Table 2.5 with the concluded findings since no research investigated the influence of the viewing distance yet. Further, the projector's design pays no attention to the viewing distance to derive illumination requirements in section 6.1.6.

### 6.1.3. Projection content

Moreover, after analyzing the influence of ambient lighting and the viewing distance on the perception of near-field projections, it is also crucial to validate if there is an impact on the selection of the projection content. This section compares the symbol- and text-based content of Figures 5.4a and 5.4b. No matter that Shibata et al. have not measured any influence of the test pattern on the perceived contrast, which was a variation of a symbol-based projection in the examination of Shibata et al. [26]. Furthermore, also Maier and Schlöder [22] investigated the subjective influence of simple chevrons compared with a cyclist symbol for near-field projections and found a significance with a small effect for direct viewing of the projections. Similarly, the chi-square test results of Table D.1 display just a significant difference with a small effect for the mesopic vision and 1 m viewing distance for the projection content comparison. The other three comparisons are insignificant (see Table D.1).

However, the physical values in Table 6.1 differ between a symbol- and a text-based projection. In this section, the focus is on the physical values since the confidence intervals if comparing symbol- with text-based projection content do not interfere with each other in Table 6.1 no matter which combination by ignoring as mentioned before the 5 m text in the photopic ambient setting. Figure 6.2 displays the continuous logistic regression related to Table 6.1 for the symbol- and text-based projection in the mesopic vision and illustrates the urge of higher Weber contrasts to reach a certain detection probability of the text-based projection since

the graph on the right no matter what viewing distance do saturate at higher Weber contrast values which are on the x-axis.

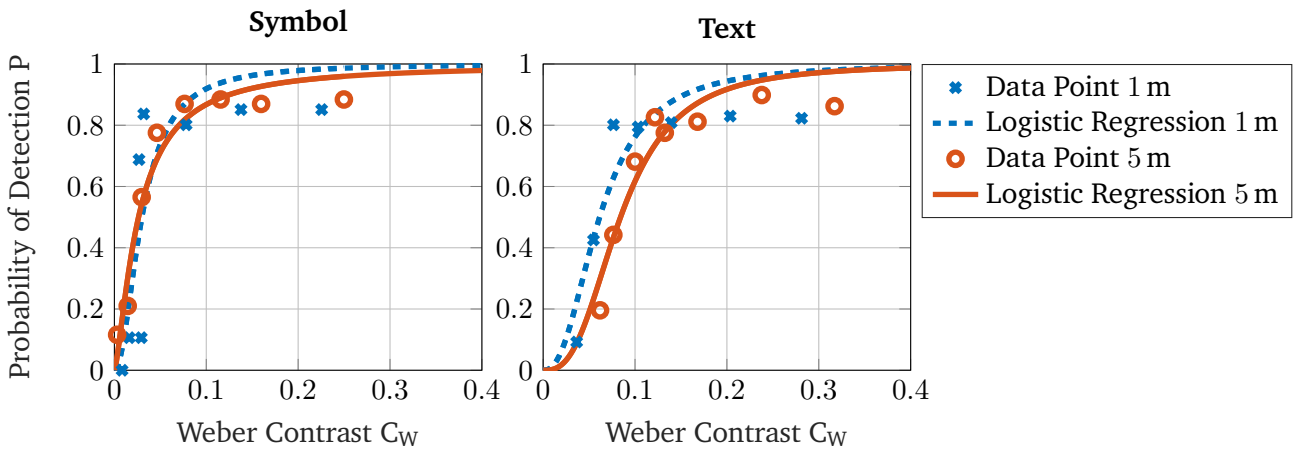


Figure 6.2.: Logistic regression fitted for the Weber contrasts with the corresponding data points of the detection probability per Weber contrast level in the mesopic vision range of approx.  $0.6 \text{ cd m}^{-2}$  of a symbol- (on the left) and text-based projection (on the right). The x-axis displays the individually measured Weber contrasts per tested projection luminance level for direct viewing of the projection. The graphs include the variation of 1 m and 5 m viewing distances.

Furthermore, Schlürscheid et al. [167] examined with the same group of participants of this thesis that for near-field projections, the Weber contrast for symbol-based projections is approximately 25 % lower compared to a text-based near-field projection independent of the observation distance for the mesopic vision. Further, they also investigated the reaction times which saturate between 600 to 650 ms for both projection contents. The reaction times saturate before reaching the 90 % contrast threshold level, which suggests that an arbitrary contrast increase does not reduce the observer’s reaction time. [167] The effect of higher contrast for text-based projections might relate to the perception mechanisms mentioned by Schmidt-Clausen and Freiding [86] and Goldstein and Cacciamani [78], where text-based content needs not just detection but also a recognition of the written text which implies a higher cognitive load due to higher task’s complexity and, thus, results in increasing Weber contrast thresholds for the given task to interact [122, 123].

Furthermore, Schlürscheid et al. support the results by providing the visibility level to support more evidence for the urgency of symbol-based over text-based projection for better visibility. An evaluation of possible age influence on the reaction time and the perceived detection contrast for direct viewing was not discovered in the analysis of Schlürscheid et al. [167].

Therefore, higher Weber contrast levels are necessary for detecting text-based projections for similar reaction times, which require higher illuminance of the projector, and these requirements shall be involved in designing an efficient projection system. Section 6.1.6 focuses on elaborating an user-orientated design of a future near-field projection system with the assumption of direct viewing. This thesis will extend the investigation also in viewing the projection in the peripheral field of view in section 6.2. Additional graphs are displayed in the appendix D.2 to support the analysis.

Nevertheless, it becomes evident with the support of Schlürscheid et al. [167] that symbol-based projections need prioritization for urban traffic mainly due to the lower contrasts for similar reaction times, which might occur with additional ambient lighting sources like advertisement screens or street lighting and to guarantee a higher understandability such as for kinds which are less familiar with reading as mentioned by Baumann et al. [60]. Therefore, the projector’s illumination design incorporates all the current data of the testing, no

matter the content, to achieve user-orientated requirements.

#### 6.1.4. Animation speed

Few research facilities already consider simple projection content's dynamic influence concerning subjective evaluation or detection contrasts [7, 22, 26]. Therefore, this thesis investigates a symbol-based projection - the loading battery of Figure 5.4a and the possible influence of dynamics on the participant's perception. Table 5.5 displays information about the participant collective. Additionally, the various projected contrast stimuli and the related greyscale input data are analyzed in Appendix D.2 for ambient lighting levels of mesopic and photopic vision. The projection surface impacts the contrast behavior as discussed in section 5.1.1 and, therefore, the measured stimuli differ from the progress of the related greyscale input data. The data of Figure D.5 and Figure D.6 provide the 90 % threshold levels for the perceived Weber contrast of the participants and the necessary greyscale input data of the projector to display these contrasts for a direct viewing distance of 1 m, which Table 6.3 lists:

Table 6.3.: Values of the continuous logistic regression fit determine the 90 % detection contrast for the symbol-based projection with the representations of dynamic with 3 Hz for a duration of 2 s, static representation for 350 ms, and static for 2000 ms under mesopic and photopic vision at a viewing distance of 1 m.

90 % threshold level	dynamic 3 Hz for 2 s	static 350 ms	static 2000 ms
Weber contrast mesopic	0.0245	0.0293	0.0339
Grayscale mesopic in %	2.76	2.93	3.12
Weber contrast photopic	0.0237	0.0243	0.0256
Grayscale photopic in %	21.52	22.42	23.64

Independent of mesopic or photopic adaptation luminance, the Weber contrast shows the lowest contrast value for a detection probability of 90 % belonging to the dynamic stimulus presentation mode. If comparing the values of Table 6.3, the Weber contrasts of a dynamic representation are up to 38 % lower compared to the static 2000 ms display mode in the mesopic vision and about 8 % for the photopic vision. The difference in greyscale levels is reasonably low since the values differ with a maximum of 0.36 % in the mesopic ambient setting and up to 2.12 % in the photopic environment.

The results of this thesis confirm the research of the given literature review since Shibata et al. [26] experienced lower detection probability for the dynamic representation of symbols compared to the static representation. Furthermore, Singer et al. state that in their study, dynamic representations were also detected with contrasts below 0.4 when the projection was in dynamic mode compared to a static representation where contrast higher 0.4 is necessary [7]. Moreover, also Maier and Schlöder [22] investigated the influence of a dynamic representation of the projection, too, for a subjective evaluation and discovered mainly in the peripheral field of view a significant influence of the dynamics, which refers to the effect that human perception in the periphery is significantly more sensitive to motion than in the fovea [168].

The results show that the dynamics influence the perception with a better detection probability of dynamic projections than static ones. Considering the impact of this effect, the ambient luminance plays a significant role since the effect is higher in the mesopic setting on the Weber contrast thresholds with 38 % than 8 % in the photopic environment.

The positive impact of dynamic representations on the detection rate encourages using dynamic projections in the urban environment to reduce accidents with vulnerable RUs, as mentioned in the motivation. Nevertheless, the implementation of dynamic projections is a design freedom of the application, and therefore to guarantee

detectability in the worst-case scenario, further implementations will consider static near-field projections. With this in mind, the design of the near-field projection system will benefit from dynamic representations regarding the increase of detection probability, and the impact on the system's power consumption will be marginal since the input image differs maximum of 2.12 %.

### 6.1.5. Projection surface

As examined in section 5.1.1, Figure 5.2 illustrates the different fitted logistic regressions of various projection surfaces like white panel, white leather, asphalt, brown leather, and rubber. Moreover, Table 5.2 lists all 90 % threshold levels for the 1 m viewing distance.

The outcomes in section 5.1.1 correlate with the results of Maier and Schlöder [22], where brighter surface materials have better subjective visibility than darker surfaces. Further, the surface conditions are essential, too, as dry asphalt is perceived subjectively better than wet asphalt [22]. Moreover, Singer et al. also had a variation of the surface conditions from wet to dry surface during the testing, which influenced the perceived Weber contrast levels [7].

Interacting with the impact of the street characteristics on the near-field projections forces the projection systems' design to include sensors to detect the surface conditions and enable interaction of the projection. This specific elaboration is separate from this thesis since the main focus is first on the fundamental visual requirements for the near-field projector. However, the next step is implementing power consumption efficient mechanisms in automotive near-field projectors, as provided in the previous sections.

### 6.1.6. Definition of projector illuminance for foveal detection

From the sections of Chapter 6.1, in addition to the perception-related contrast thresholds with the same subject data, the brightness requirements for the projector also result since the participant data of the testing stores the associated illuminance levels. Table 6.4 thus presents, in addition to the perception-related contrasts mentioned before, the user-oriented design of the projection's illuminance, which reaches the illuminance level on the projection surface for direct viewing. So, Table 6.4 lists the data for direct viewing the projection from 1 m and 5 m under mesopic and photopic environmental conditions for the symbol- or text-based projection content. The physical values of the projection's illuminance do not overlap for the symbol- or text-based projection no matter what ambient luminance level is apparent considering the confidence intervals in Table 6.4. The illuminance values are higher for the observation distance of 5 m for both projection contents.

Table 6.4.: Results for projector's illuminance levels of the psychophysical testing on the projection surface for a 90 % threshold of the logistic function for the symbol-based projection for two adaptation luminances ( $L_{\text{Background}} \approx 0.6 \text{ cd m}^{-2}$ ,  $L_{\text{Background}} \approx 235 \text{ cd m}^{-2}$ ). The numbers in the bracket indicate the confidence intervals of 95 %, with the lower bound (left number) and the higher bound (right number) for two viewing distances and two adaptation scenarios.

Scenario	Viewing distance in m	Illuminance of symbol in lx	Illuminance of text in lx
mesopic	1	24.11 (24.09; 24.16)	26.62 (24.53; 24.80)
	5	26.22 (26.10; 26.43)	29.49 (29.10; 30.18)
photopic	1	9685 (9662; 9744)	9434 (9419; 9458)
	5	9776 (9745; 9839)	9823 (9760; 9981)

Nevertheless, a uniform projection system is needed to enable a broad application in the automotive sector. Therefore, the further design of the projection systems does not differentiate if the projection content is a

symbol- or text-based and from which observation distance the projection is viewed. With these assumptions for an universal solution of a projection system, it is possible to predict the projection brightness for an ambient brightness and evolve a mathematical approach of the projection brightness as a function of the ambient brightness based on psychophysical data. Consequently, Figure 6.3 shows the derived relationship between the projection's illuminance and the ambient illuminance, which relates to the following equation 6.1, where  $y_{\text{object}}$  is the illuminance level of the projected object on the street and  $x_{\text{ambient}}$  relates to the ambient illuminance level.

$$y_{\text{object}} = 1.41 \cdot x_{\text{ambient}} + 3.11 \text{ lx} \quad (6.1)$$

Furthermore, the multiple dashed lines in Figure 6.3 the spread of the relationship with the related standard deviation since the used data does not differentiate between projection content and viewing distance. However, it is crucial to mention that the limitation of the model of Figure 6.3 and equation 6.1 relate to the restriction of just two interpolation points for the ambient illuminance due to the variation of the executed testing, which the boxplot-alike illustration in Figure 6.3 displays for the mesopic data in red and photopic data in yellow. However, according to the Weber-Fechner law of perception [74], the relationship in the equation 6.1 and 6.4 should be logarithmic, which requires a third examination of an ambient illuminance between the mesopic and photopic data tested.

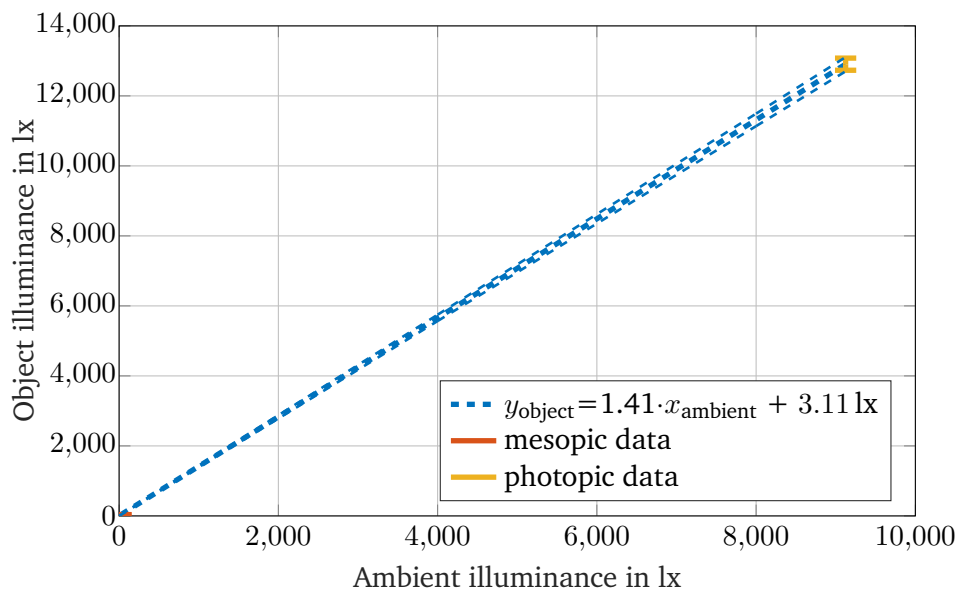


Figure 6.3.: Graphic illustration of the relationship of ambient illuminance and the projection's object illuminance, including the mesopic and photopic data, to result in the relationship of equation 6.2 for direct projection viewing. The ambient illuminance is on the x-axis, and the projection's object illuminance is on the y-axis. The spread of the dashed linear approximation displays the standard deviation of the test data, which is content independent of designing a universal projector.

With this in mind, the developed relationship enables rating the current state of the art of near-field projectors on the market listed in Table 2.2 and evaluating their current maximum application range for direct viewing regarding the ambient illuminance.



For the rating of the state-of-the-art near-field projectors, a simplified relationship of the illuminance and the luminous flux is provided by Hauske in equation 6.2 [76]:

$$E_{\text{object}} = \frac{\Phi_{\text{projector}}}{A_{\text{projection}}} \quad (6.2)$$

Equation 6.2 sets the illuminance of the projected object on the surface  $E_{\text{object}}$  with the luminous flux of the projector  $\Phi_{\text{projector}}$  and the projection size on the surface  $A_{\text{projection}}$ . The size of the projection is assumed similar to the symbol-based projection  $A_{\text{projection}} = 0.62 \text{ m} \cdot 0.41 \text{ m}$  displayed in Figure 5.4a. With this relation, it is possible to calculate the possible object illuminances the near-field projectors of Table 2.2 can achieve. Consequently, Table 6.5 lists the calculated illuminances for each technology.

Table 6.5.: The table includes the extracted luminous flux of Table 2.2 and the calculated object illuminance by the equation 6.2 with the assumed projection size analog to the symbol-based projection of  $A_{\text{projection}} = 0.62 \text{ m} \cdot 0.41 \text{ m}$ . Additionally, the inverse relationship of equation 6.3 concludes the maximal ambient illuminance for the illuminated projection to be detectable.

	DMD	LCoS	$\mu$ LED
Luminous flux in lm	120 [42]	27 [21]	800 [51]
Object illuminance in lx	472.07	106.22	3147.13
Maximal ambient illuminance lx	332.59	73.12	2229.80

To evaluate the the ambient illuminance the projection technologies can reach Table 6.6 lists possible ambient illuminance levels. With the values determined via equation 6.2, projected object illuminances of 472 lx for the DMD, 106 lx for the LCoS, and 3147 lx for a  $\mu$ LED projector result. To compare the achieved object illuminance levels and to put these values in relation, it is necessary to adjust the reciprocal of equation 6.2 to determine the maximum possible ambient illuminances:

$$x_{\text{ambient}} = \frac{y_{\text{object}} - 3.11 \text{ lx}}{1.41} \quad (6.3)$$

So equation 6.3 derives the maximal ambient illuminance levels of Table 6.5 to compare these with the ambient illuminance levels of various light scenarios during the day of the literature in Table 6.6.

Table 6.6.: Ambient illuminance levels, according to Kloppenburg [169], are ordered from high to low ambient illuminance levels.

Situation	Ambient illuminance in lx
Midday summer sun	90000
Cloudy sky	19000
Beginning dawn	750
Parking lot outside [80]	20
Street lighting P4 class [28]	5



---

Consequently, the comparison concludes that an LCoS system is suitable for the various scenarios in the city's illuminated streets, a DMD system provides visible projections until dawn, and a  $\mu$ LED system as a projection system for near-field projections is also visible after dawn.

Any ambient brightness corresponds to a visible projection illuminance according to the psychological testing data if it is above the blue trend line in Figure 6.3. So if the illuminance of the projected object is below the value after the relationship of equation 6.2, it is questionable if the projection is even detectable since the projection will not be visible for a detection probability of 90 % for direct viewing according to the psychophysical testing of Chapter 5. Of course, suppose lower detection probabilities are sufficient for the application. In that case, the values must not follow the relationship of equation 6.2 and can be below the blue trend line in Figure 6.3. However, the meaningfulness of non-detectable projection projections is very low. Hence, there is a recommendation to incorporate an illuminance sensor signal which delivers the ambient luminance levels to the projection unit to save energy by not projecting invisible information.

In addition to direct viewing, observing near-field projections in the peripheral field of view is also essential for vulnerable RUs, as this confrontation is a common situation in urban road traffic. The RUs will not always look directly at a near-field projection of an oncoming vehicle when safety-relevant situations occur. The following sections analyze the peripheral observation of near-field projections.

## 6.2. Contrast perception in peripheral field of view

When considering safety-relevant situations for a cyclist or pedestrian, it is noticeable that near-field projections from the RU's perspective cannot be placed exclusively in the direct field of view but will also appear in the peripheral visual field. The pictures of the participant test by Namyslo et al. [25] for the cyclist display a turning situation in Figures 1.3b and 1.3c. Singer et al. [7] illustrate in Figure 2.17a a pedestrian crossing the road, supporting the phenomenon of no guarantee to place near-field projection in the foveal viewing of the RUs. Furthermore, the leading cause of accidents involving pedestrians occurs while crossing the road [3, 4], e.g., due to concealed view of the pedestrian to the vehicle, as exemplified by Singer et al. in Figure 2.17a. The scenario displayed in Figure 2.17a emphasizes the importance that near-field projections must also be visible in the peripheral field of view to be suitable for daily usage in traffic and have a necessary illuminance that is detectable according to the ambient influence factors. Because most dangerous situations in road traffic often arise from suddenly appearing objects, perception under different environmental conditions, whether mesopic or photopic, is essential for near-field projections in urban road traffic. Suppose near-field projections are detectable in the peripheral visual field to catch the attention. In that case, they can be foveally targeted by a head or eye movement to allow recognition of the communicated message according to the perceptual process [78, 86, 168].

The evaluation of the experiments on the peripheral perception of near-field projections from Chapter 5, therefore, serves to determine detection contrasts as a function of the eccentricity in the peripheral visual field and the associated illuminance levels of the projection on the ground.

### 6.2.1. Detection contrast

Chapter 6.1 discusses possible influence factors, especially on the perception of detection contrast thresholds for direct viewing of near-field projections. However, since near-field projections will also appear in the peripheral field of view, evaluating the influence of the projection's location and the resulting contrast thresholds is crucial. Therefore, logistic regressions are applied to the data of peripheral testing listed with the details in Table 5.6 and result in the continuous logistic regression trends depending on the eccentricity of the projection's position in the peripheral field of view. Table 6.7 lists the extracted 90 % threshold level of Figure 6.4 for the mesopic

and photopic adaptation luminance level for the tested locations in the peripheral field of view of 5, 10, 20, and 30 degrees at a 5 m viewing distance.

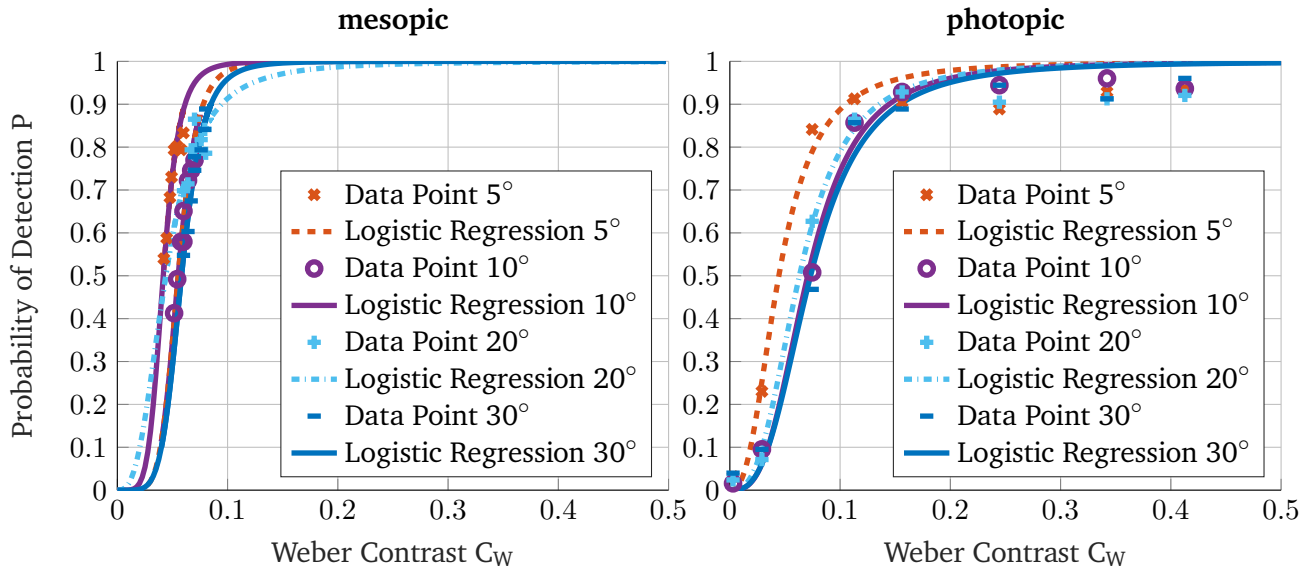


Figure 6.4.: Logistic regression for the detection probability per Weber contrast value for the mesopic and photopic environmental settings. The analyzed projection content is only a symbol-based illustration. The x-axis displays the projection’s Weber contrast level for the peripheral viewing of the projection, where the eccentricities varied for a viewing of the projection 5, 10, 20, and 30 degrees away from the direct viewing in both environmental settings.

Additionally, Table 6.7 includes the results of direct viewing (0°) of section 6.1 with the related confidence intervals for the mesopic and photopic ambient luminance to display an overall overview for the dependency of the near-field projection’s location.

Table 6.7.: 90% Weber contrast threshold levels determined for the mesopic and photopic vision for the symbol and text-based projection. The Weber contrasts per eccentricity of either 0, 5, 10, 20, or 30 degrees are displayed with the 95% confidence intervals (lower and upper bound in the brackets).

Eccentricity in degree	mesopic	photopic
0	0.0967 (0.0890; 0.1113)	0.0562 (0.0529; 0.0685)
5	0.1052 (0.1020; 0.1119)	0.0614 (0.0593; 0.0662)
10	0.1444 (0.1381; 0.1573)	0.0780 (0.0751; 0.0837)
20	0.1356 (0.1305; 0.1465)	0.0946 (0.0895; 0.1525)
30	0.1542 (0.1470; 0.1692)	0.0848 (0.0820; 0.0919)

Table 6.8 lists the performed chi-squared tests where all of the tests for photopic vision are insignificant ( $p > 0.05$ ), for the mesopic vision, the chi-square tests involving direct viewing (0°) and 5° eccentricity are significant with a small effect size. The statistical tests considering 10 with 20 or 30 degrees comparisons show no significance (see Table 6.8). Nevertheless, by considering the physical values of Table 6.7 with the related confidence intervals show a relationship for both ambient scenarios (mesopic and photopic), the values of the eccentricities of 0° and 5° remain at the same level as well as the values of 10, 20 and 30 degrees. This behavior is also visualized in Figure 6.5 for the mesopic and photopic contrast threshold levels depending on

the eccentricity of the near-field projection located in the peripheral visual field, where a saturation appears after the eccentricity of 10°. Consequently, the values of the contrasts for 0° and 5° projection's location can adapt to the values of the 10, 20, or 30 degrees which refers to a shift of approx. 0.05 Weber contrast for the mesopic and photopic vision. So no matter where the projection is located in the peripheral visual field, the RUs can detect it.

Table 6.8.: Chi-square analysis defines the statistical effects of various eccentricities of the projection located in the peripheral field of view at a viewing distance of 5 m for mesopic and photopic testing environments. The Table also includes the related effect size (Cramer's V).

	Compared items	mesopic	photopic
Eccentricity	0° x 5°	$\chi^2(7) = 14.38, p < 0.05,$ V = 0.09	$\chi^2(7) = 1.61, p > 0.05,$ V = 0.03
	0° x 10°	$\chi^2(7) = 20.15, p < 0.05,$ V = 0.12	$\chi^2(7) = 2.17, p > 0.05,$ V = 0.04
	0° x 20°	$\chi^2(7) = 21.85, p < 0.05,$ V = 0.13	$\chi^2(7) = 3.51, p > 0.05,$ V = 0.05
	0° x 30°	$\chi^2(7) = 14.75, p < 0.05,$ V = 0.10	$\chi^2(7) = 1.91, p > 0.05,$ V = 0.04
	5° x 10°	$\chi^2(7) = 17.95, p < 0.05,$ V = 0.11	$\chi^2(7) = 1.11, p > 0.05,$ V = 0.03
	5° x 20°	$\chi^2(7) = 14.25, p < 0.05,$ V = 0.09	$\chi^2(7) = 5.23, p > 0.05,$ V = 0.06
	5° x 30°	$\chi^2(7) = 17.27, p < 0.05,$ V = 0.11	$\chi^2(7) = 0.71, p > 0.05,$ V = 0.02
	10° x 20°	$\chi^2(7) = 2.17, p > 0.05,$ V = 0.04	$\chi^2(7) = 8.88, p > 0.05,$ V = 0.08
	10° x 30°	$\chi^2(7) = 1.55, p > 0.05,$ V = 0.03	$\chi^2(7) = 1.23, p > 0.05,$ V = 0.03
	20° x 30°	$\chi^2(7) = 4.59, p > 0.05,$ V = 0.06	$\chi^2(7) = 5.46, p > 0.05,$ V = 0.06

Alike Chapter 6.1.1, the influence of ambient illuminance is also apparent in Figure 6.5 and Table 6.7 where photopic detection contrasts have lower threshold values than in the mesopic vision with the similar detection rate of 90 %.

Schneider [118] selected a detection rate of 99 % in the mesopic range for a small object of just 1° target size. She evaluated a similar trend as displayed in Figure 2.16 to the results in Figure 6.5. In Schneider's results, the symbol-based detection target of a deer illustration saturated already in about 5° for both mesopic luminance levels of Figure 2.16 [118], which relates to the smaller target size (1°) than the used size of the symbol-based projection content of Figure 5.4a with the size of  $403.61' = 6.67^\circ$  (see Table 5.3). The projection's size of  $6.67^\circ$  interacts still with the dominant receptors in the fovea if placed in the 5°-eccentricity as displayed in Figure 2.5. Additionally, Koenderink et al. [170] discover a similar trend of the independence of the test target's size. With increasing target size, the smaller the change appears in contrast sensitivity in the peripheral visual field [170]. With a projection's location of 10 degrees or higher eccentricities, the rods dominate the contrast perception.

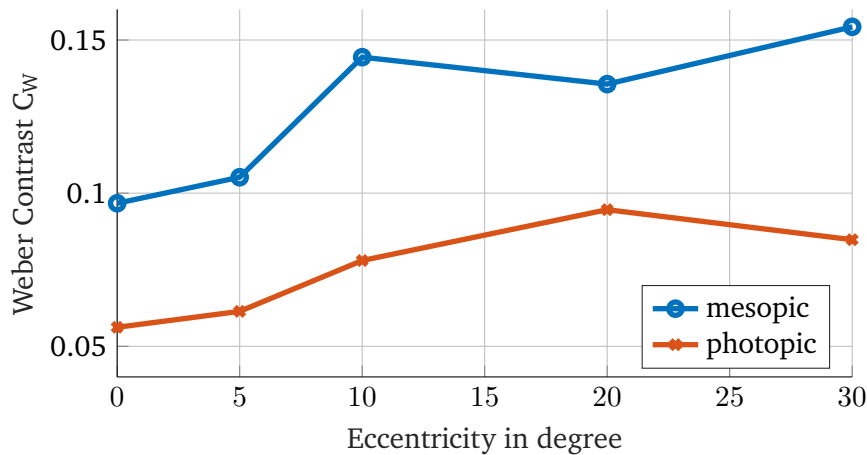


Figure 6.5.: The relationship of the perceived Weber contrasts threshold values (y-axis) for a symbol-based projection plotted for different eccentricity levels of 0, 5, 10, 20, and 30 degrees (x-axis) for the mesopic (blue graph) and photopic environmental settings (red graph).

Furthermore, Maier and Schlöder [22] investigated a subjective evaluation of symbol-based near-field projection of directly viewing and perceiving the projection in the peripheral field of view. The exact location of the projection is not mentioned. However, they discovered a decrease in subjective visibility for peripheral vision since they used a constant contrast value through the testing procedure [22].

Additionally, Fleck [120, 121] examined detection probability for small target with a fixed contrast value in his testing for photopic vision and discovered that the detection probability decreases rapidly after about  $8^\circ$ , which refers to the distribution of the cones dominant in the photopic vision for the visual perception as displayed in Figure 2.5. Therefore, there is a similar tendency in the results of Figure 6.5 where the contrast thresholds increase above an eccentricity of 10 degrees and the maximum Weber contrast value of  $20^\circ$  refers to the blind spot of the visual system displayed in Figure 2.5 where no receptors are present, but due to the target size of  $6.67^\circ$  a perception is still possible in the peripheral vision of the tested near-field projection.

Table 6.7 and Figure 6.5 summarize the distribution of Weber contrast thresholds depending on the projection's location by perceiving near-field projection with peripheral vision for several eccentricity levels. However, besides detecting the near-field projection in urban traffic scenarios by a RU, it is also crucial to understand what contrasts for projections, especially in the peripheral visual field, are disturbing. Disturbance by a projection, or even perceived glare from a projection by any RU, can interfere with a driver's driving task or distraction from the road situation of a cyclist or pedestrian. Hence, the subjective feeling of glare or disturbance is essential for designing an user-orientated projection system since these values limit the maximum illumination for the projected object on the ground.

### 6.2.2. Disturbing contrast

In addition to attracting attention with near-field projections in the peripheral field of view, it is also crucial not to create any additional distraction that could put the RU in a dangerous driving situation, for example. The question, therefore, arises as to when a RU feels disturbed by a near-field projection, which is investigated in this section using a subjective evaluation of different contrast levels of near-field projections. Table 5.4 lists the contrasts for the symbol-based projection and the other necessary test parameters. Finally, Figure 6.6 shows the evaluated subjective ratings of the subjects for the Likert scale-based survey, plotted against the angles of the projection position in the peripheral visual field. Figure 6.6 indicates the four contrast levels tested with their values in the legend.

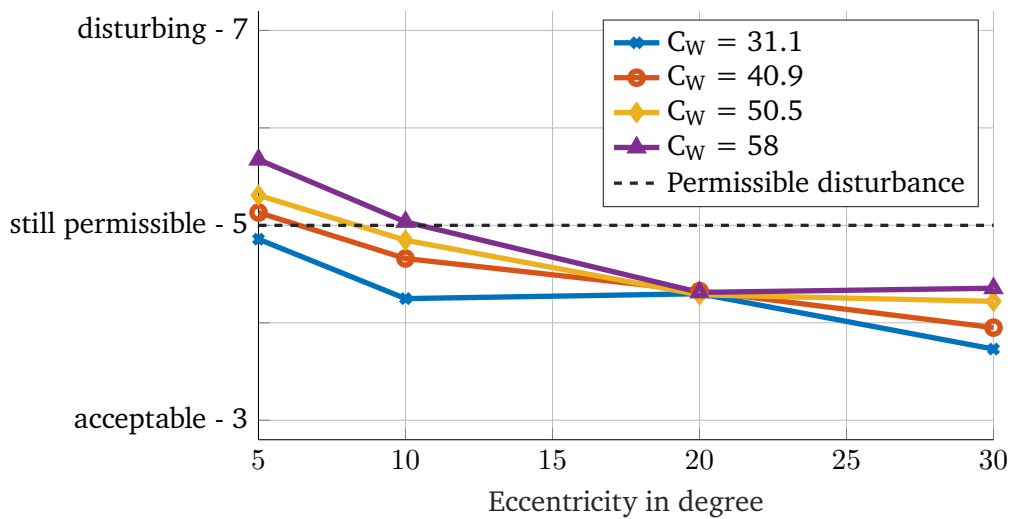


Figure 6.6.: The relationship of the Likert scale evaluation (y-axis) of various Weber contrasts levels for a symbol-based projection indicated in the legend in the peripheral field of view plotted for different eccentricity levels of 5, 10, 20, and 30 degrees (x-axis) for the mesopic vision. The displayed values of the subjective evaluation are mean values of the Likert scale analysis - the values of the Likert scale range from 1 (discreet) to 7 (disturbing).

Each participant evaluated the question 'Does the near-field projection arise bother/ disturbance while crossing the street and noticing such a near-field projection?' for each eccentricity level, and Figure 6.6 displays the average rating according to the Likert scale. The rating 5, declared 'still acceptable,' is highlighted. The subjective rating above permissible disturbance level 5 is critical due to the disturbance awareness. However, just two eccentricity levels surpass this limit with contrast levels  $C_W$  above 40 for near-field projections placed at  $5^\circ$  in the peripheral field of view and Weber contrasts above  $C_W = 58$  for the peripheral location of  $10^\circ$ .

Accordingly, no matter what location in the peripheral visual field, the Weber contrast of 31.1 always does not cause any disturbance. The Weber contrast of 31.1 relates to a projection illuminance of 1703 lx, which is the maximal nondisturbing illuminance for the projected object on the surface and therefore limits the optical parameters of the projection system independent on the applied technology. Nevertheless, this investigation displays the extensive range of applicable Weber contrasts, specifically in the mesopic vision from a peripheral detection of 0.1052 for a projection located  $5^\circ$  away from direct viewing to a contrast value of 31.1 which does not awake disturbance for the participants no matter what location in the periphery. Accordingly, this investigation displays a wide range of applicable contrast values and illuminance levels for near-field projections to avoid disturbance of other RUs.

Due to the significant influence of ambient lighting on contrast perception, the Weber contrast value of 31.1 cannot be applied in photopic vision. However, besides the contrast threshold values, next, the specifications to implement on the projection system are discussed for the illumination levels of the projection in the peripheral field of view.

### 6.2.3. Projector illuminance in the peripheral field of view

Analogous to Chapter 6.1.6, an illuminance for the projection and, thus, a minimum brightness for the projection is defined to guarantee detection in the peripheral field. Although the testing procedure considered only symbol-based projections in the peripheral field, defining a minimum projection illuminance for the peripheral field considers all tested eccentricities, as in urban traffic, it is impossible to define where a RU

who is also in motion will perceive the near-field projection. Finally, a consideration of the illuminance levels depending on the location in the peripheral field is shown in Figure 6.7, which has identical progress as Figure 6.5 for the perceived Weber contrast eccentricities but showing the illuminance of the projected object on the y-axis instead.

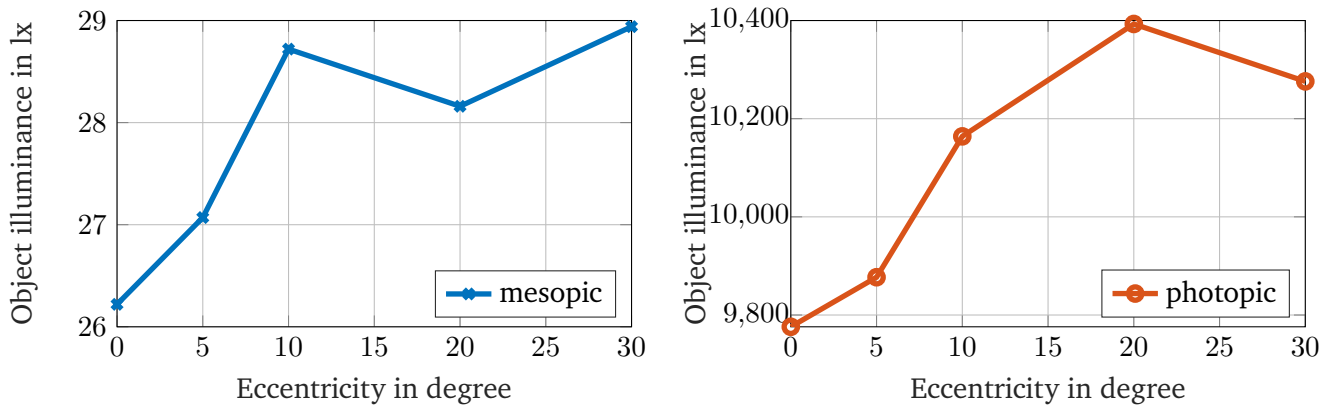


Figure 6.7.: The relationship of the projection’s object illuminance (y-axis) for direct viewing and also in the peripheral field of view plotted for different eccentricity levels such as 5, 10, 20, and 30 degrees (x-axis) for the mesopic vision on the left and the photopic vision on the right.

With this in mind, a derivation of a trend line analogous to the procedure in section 6.1.6 results in Figure 6.8 by considering the psychophysical data of Figure 6.5 involving the upper and lower limit derived by the standard deviation of the model and the belonging data.

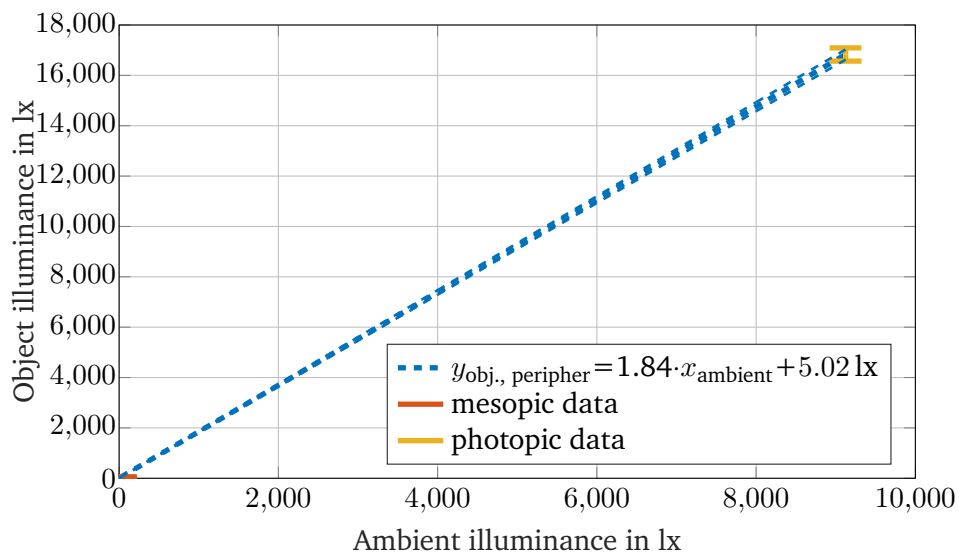


Figure 6.8.: Graphic illustration of the relationship of ambient illuminance and the projection’s object illuminance, including the mesopic data for a symbol-based projection, to result in the relationship of equation 6.4 for viewing the projection located in the peripheral field of view. The ambient illuminance is on the x-axis, and the projection’s object illuminance is on the y-axis. The spread of the dashed linear approximation displays the standard deviation of the test data, which is content independent of designing an universal projector.

So, the following equation represents the relationship for peripheral viewing regardless of position in the peripheral field in the range of the ambient illuminance for mesopic and photopic scenarios and the derived projection's illuminance in equation 6.4:

$$y_{\text{object, peripher}} = 1.84 \cdot x_{\text{ambient}} + 5.02 \text{ lx} \quad (6.4)$$

Therefore, considering the inverse of equation 6.4, it is possible to define the ambient illuminance levels for peripheral viewing and the resulting limitation for each technology of the current state of the art as displayed in Table 2.2 by considering the values of the object illuminance of Table 6.5, which Table 6.9 displays.

Table 6.9.: The table includes the extracted luminous flux of Table 2.2 and the calculated object illuminance by the equation 6.4 with the assumed projection size analog to the symbol-based projection of  $A_{\text{projection}} = 0.62 \text{ m} \cdot 0.41 \text{ m}$ . Additionally, the inverse relationship of equation 6.4 concludes the maximal ambient illuminance for the illuminated projection to be detectable by peripheral vision.

	DMD	LCoS	$\mu$ LED
Maximal ambient illuminance lx	253.83	54.99	1707.67

Consequently, the results of Table 6.9 indicate a usage limitation depending on the ambient scenario regarding the peripheral vision. LCoS systems are still reasonable to project information during the night with lit street lighting up to 55 lx, the range of detection is limited for the DMD projection system until 254 lx which enables almost a peripheral visibility in a showroom which has an ambient illuminance of minimum 300 lx [171]. However, the limitation on the  $\mu$ LED technology is reasonably low since a projection with this technology will still be detectable after dawn in the peripheral field of view with a maximum ambient illuminance of 1708 lx.

### 6.3. Summary of the contrast and illuminance requirements for near-field projections

In addition to a detailed analysis of the influences on the visibility of near-field projections, such as ambient lighting, viewing distance, the selected projection content, an animation of the displayed content, and the projection surface characteristics, this Chapter 6 also includes the position of the projection in the viewer's field of view in mesopic and photopic environments. For all tested near-field projections, a white projection was used to neglect the color influence, which Maier and Schlöder identified to decrease the visibility of the projection [22]. Generally, a contrast threshold of 90 % considers applying all three use cases identified in the literature review to display a uniform solution of a near-field projector's design.

Finally, the analysis identifies an influence of the environmental conditions, e.g., ambient illuminance, for considering near-field projections, which have already been examined by other research institutions [7, 27, 26]. Another environmental influence, the projection surface characteristics, also significantly influence the detection rate and thus the detection contrast, which Maier and Schlöder also identified [22]. Section 5.1.1 illustrates the investigation of this thesis in detail. The viewing distance, however, does not play a role up to the considered viewing distance of 5 m. However, there are significant influences on the recognizability of projection content, which require lower contrasts for symbol-based than text-based projections for identical reaction times as discovered by [167]. Finally, a detection contrast for projections located in the periphery is



---

defined as a function of the position of the projection in the peripheral field to consider more realistic scenarios that occur in road traffic since no RU can always look directly at the near-field projection.

With the help of these psychophysical tests, it is also possible to derive the influence of the tested parameters on the properties of the projector. A first approximation derives the relationships between the ambient illuminance, e.g., the existing lighting scenario, and the required projection brightness. Equation 6.1 shows the relationship for the direct viewing and equation 6.4 for the peripheral viewing of the projection. The importance of equation 6.4 results from the peripheral consideration since, in urban scenarios, design-oriented and safety-relevant projections also appear in the RU's peripheral visual field for a detection probability of 90 %. So the attention is awakened by detectable near-field projections in the periphery to recognize and perceive them foveally afterward.

Moreover, equations 6.1 and 6.4 define a technology-independent solution to predict when a projection will not be visible for direct or peripheral viewing, which motivates an adaptive projection system in future vehicles where the projection can be adjusted with dimming to the environmental factors or even not be lit since the near-field projection is not detectable with a specific probability. Table 6.9, therefore, shows the ambient illuminance levels determined in state of the art for each technology (see Table 2.2) for the peripheral consideration. According to Table 6.9,  $\mu$ LED projection technology shows a high potential for application scenarios that can be visible after dawn; a DMD projector would have limited visibility before the beginning of dawn, and an LCoS projector is only suitable for illuminated roads at night. Due to the limited application to illuminated streets at night, it is evident that an intensive development process is still necessary for an LCoS projection system to raise the technology properties to the level of DMD or  $\mu$ LED (see Tables 6.5 and 6.9).

Nevertheless, all three projection technologies suit safety-critical projections in the USA [3], where most accidents involving pedestrians occur in the dark (74.48 %). However, in Germany's statistics, where 23.6 % of accidents occur at night,  $\mu$ LED projections show high potential to make projections visible well beyond the dusk and dawn threshold. At the same time, DMD technology must improve the brightness by three times to be visible in dusk and dawn.

In addition, a subjective evaluation derives a disturbing contrast that other RUs might perceive as disturbing for a near-field projection. This results in brightness for the projection on the ground of 1703 lx for the mesopic vision, which implies a luminous projector flux of 433 lm using equation 6.2. Table 6.9 enables the comparison of the projector's flux limitation for other technologies of the literature review. Therefore, it is noticeable that the  $\mu$ LED projection should be dimmed depending on the background condition, which significantly influences the projections' detectability (see section 5.1.1). The luminous flux limitation does not concern a DMD projector with 120 lm or an LCoS projector with 27 lm.



---

## 7. Summary and outlook

---

This chapter critically reviews the investigations, including the results, gives suggestions for extension, and presents ideas for further investigations. The present work deals with the fundamental user-orientated design of near-field projections based on psychophysical testing and resulting aspects. On the one hand, the requirements define the perception of the displayed resolution on the road next to the vehicle. On the other hand, the perceptual testing on the contrast detection of near-field projections at different ambient brightness levels from the mesopic to the photopic range derives further aspects for the detectability and illuminance of near-field projections. Therefore, fundamental user-oriented requirements of resolution and visibility to introduce and design near-field projections increase road safety with this novel signal lighting application.

Based on the state of the art and research, which technologies are suitable for near-field projections and which photometric properties they already enclose are first derived. Initial investigations on evaluating near-field projections have already shown no fundamental consideration of near-field projections involving the impact factors that influence the perception of the projection's observer. Therefore, the analysis of state of the art and research concludes further research questions, which are answered with the support of the tests conducted.

- What are the user requirements as the minimum resolution for digital near-field projections? Is there a universal resolution quality, or will application-specific differences exist?
- Which of the specified technologies in Table 2.2 is sufficient for safety-relevant projections at the current maturity level?
- Which technology would be a universal solution for near-field projections and their lighting characteristics?
- What influence do street surface characteristics have on perception regarding the resolution and visibility of near-field projections?
- What are the visibility requirements for near-field projections in daytime ambient luminance scenarios, and which technology is suitable for enabling these scenarios? Does the projection content play a role in this consideration?
- What limitations can perception-related analyses derive for near-field projections in urban road traffic? Is it possible to reach the physical limits of projection technology, or does this define future development?

A series of tests answer the research questions on the resolution related to the visual acuity and brightness perception, which relates to the contrast perception of near-field projections conducted under different illumination situations, such as the mesopic and photopic viewing ranges. Both of the mentioned aspects are defined in the literature as spatial vision [102].

When looking at the user-oriented requirements for the minimum resolution of digital near-field projections, the results show that the ambient lighting influences the perceived resolution and the resulting visual acuity,

---

as shown in Table 4.3. All displayed projections had a perceived projection size big enough to comply with Weber's law [94, 95] to neglect any influence of the perceived Weber contrast while examining the resolution requirements. Considering the viewing distances of 3 and 5 m relevant for safety-critical situations, a resolution of 30 *ppd* at 3 m can be defined for a scenario of about  $1 \text{ cd m}^{-2}$  (PGS) without dependence on the projection content, and a resolution of 40 *ppd* for a brighter scenario of about  $4 \text{ cd m}^{-2}$  (DDS). The resolution aspect requirements at 1 m are irrelevant for safety-critical projections. However, these requirements are relevant for design-oriented use cases. Hence, compliance with DIN 1450 [1] also allows guidelines for reducing the resolution requirements since fonts that are too small and complex, such as italics, have higher requirements for resolution, and the related visual acuity, can be neglected. So, Table 4.3 shows that at a viewing distance of 1 m, the resolution requirements for the text small in the FR test are 33 % higher than for the text small in the SP testing, which used a DIN 1450 compliant font [1].

The current technology in Table 2.2, with the mentioned user-oriented requirements of the psychophysical tests, displays that LCoS and DMD projection systems can meet the resolution requirements in both scenarios (PGS and DDS). However, the  $\mu$ LED projector, for example, needs six times the current resolution for a static symbol- or text-based projection and still 2.5 times for animated projection content. Consequently, the  $\mu$ LED projector still has the development potential to accomplish the user-oriented resolution requirements.

In order to derive suitability for safety-relevant projections, the visibility of the projections for the viewer is also an essential aspect in addition to the requirements for the digital projections. Therefore, the performed tests investigate the technologies' suitability for safety-relevant projections regarding contrast and brightness perception. The main task for these examinations is also to define a detection contrast threshold where the road users can see the projection in urban traffic and keep the level of disturbance as low as possible not to harm or irritate road users not addressed by the near-field projection.

Thus, the influence of the projection background, the ambient brightness, the viewing distance, the projection content, and the animation speed of the projection were examined. In conclusion, in the four tests, the projection background influences the detection probability of a chosen level of 90 % suitable for all three applications of near-field projections as welcome and goodbye scenario, safety-relevant projection, and vehicle intention communication. So far in the literature review, the extensive examination was conducted with elementary test targets relating to visual testing procedures as Landoldt C, cycles or dots [30, 76, 118, 120, 121, 7, 25, 27]. Thus, the detection contrast, described in more detail in section 5.1.1, underlines the studies of other research institutions and manufacturers that mention the ambient luminance as an influencing factor but have yet not explicitly investigate it for near-field projections besides a subjective survey or an analytical calculation [94, 95, 118, 27, 26, 42]. The ambient brightness and thus the adaptation luminance, whether in the mesopic or photopic range, influence the detection thresholds of the contrast perception thresholds where the threshold values are smaller for brighter ambient illuminance levels, which also the fundamental literature states [76, 30, 31, 78]. However, this work provides the contrast threshold values for application to near-field projections with the necessary framework conditions such as viewing distance and projection surface condition, e.g., for a symbol-based projection which needs more than doubled contrast threshold values for the mesopic adaptation ( $L_{\text{Background}} \approx 0.6 \text{ cd m}^{-2}$ ) with 0.1253 compared to a photopic adaptation level of  $L_{\text{Background}} \approx 235 \text{ cd m}^{-2}$  with a contrast threshold value of 0.0586. In addition, the variation of viewing distance is investigated, which shows no effect on the detection contrasts and thus allows a viewing-independent projector design (see section 6.1.2).

When considering the two other factors, such as the influence of the projection content and the animation speed of the projection, which can be design parameters of the content, e.g., the displayed warning signals of safety-relevant projections, these factors allow better detectability or visibility with the concluded results of Chapter 5. Thus intuitiveness can increase, on the one hand. A potential reduction of energy consumption, on the other hand, if the projected content of near-field projections follows the possible design patterns: Despite

---

identical saturation for reaction times, symbol-based projections are detected with 25 % lower detection contrast thresholds compared to text-based projections, allowing for energy savings as lower contrasts are associated with lower luminous flux values and thus a dimmed light source of the projection system. Alternatively, such a system can achieve even better visibility for projections by designing a system according to the requirements of text-based projections and still applying symbol-based content since it is internationally understandable.

Moreover, the conducted tests only apply to languages with a similar alphabet, like English, due to various specific requirements connected to other alphabets as the visual acuity requirements [104, 105]. Furthermore, the possibility to increase the visibility by displaying the projections with animation, as described in section 6.1.4, shows improved visibility of 38 % in the mesopic vision and by a factor of 38 % in the photopic vision with a projection flashing at 3 Hz for 2 s according to United Nations Regulation No. 48 [165] compared to a projection displayed statically for only 2 s. In addition to the direct consideration of the projection, which does not apply to all use cases and conflict situations in urban road traffic, a view of the projections in the peripheral field of view defines the detection contrasts in the periphery and the contrasts which arouse subjective disturbance by other RUs. The trend of the perceived detection contrasts as a function of the location of the near-field projection in the peripheral field of view of section 6.2 shows a similar trend to Schneider [118], who, however, had investigated smaller target sizes ( $1^\circ$ ), which explains the differences with the documented data with object sizes of  $6.67^\circ$ , as the influence of the target size is discussed by Koenderink et al. [170]. The contrast perceived in the periphery defines the contrast which awakes the road user's attention and thus is the minimal contrast for safety-relevant projections. The contrasts, subjectively perceived as disturbing, therefore allow setting a limit for the maximum contrast and the resulting maximum illuminance of the projection of 1703 lx, corresponding to a luminous flux of the projector of 422 lm for an assumed area of the symbol of  $0.25 \text{ m}^2$ . The maximal parameters are essential to set a maximum for distraction and disturbance for the participating road users in urban traffic and reduce the risk of an information overflow in urban areas when several vehicles are equipped with near-field projections.

With the investigations carried out and considering the respective influencing factors, it is possible to create a user-oriented model that, depending on the ambient brightness, enables the necessary projection brightness and the related luminous flux for either direct or peripheral viewing of the projection, regardless of the projection content. With the help of these models, it is possible to define which projection technology can enable which ambient conditions according to the state of the art of Table 2.2, e.g., in meeting with country-specific accident data to reduce fatalities since most pedestrian accidents in the USA occur at night ( $\approx 75\%$ ) [3]. At the same time, in Germany, vulnerable RUs are primarily injured in bright ambient conditions, such as during the day ( $\approx 72\%$ ) [4]. Moreover, according to Table 6.9,  $\mu\text{LED}$  projection technology shows a high potential for application scenarios that can be visible after dawn and be suitable for the demanding high visibility application according to the German data of fatalities [4]. A DMD projector is limited to visibility before the beginning of dawn, and an LCoS projector is only suitable for illuminated roads at night, which makes both of the technologies suitable for countries where most of the fatalities occur during the night like it is exemplary in the USA [3] for applying safety-relevant near-field projections.

All the aspects listed allow the evaluation of the technologies of Table 2.2 in terms of their current suitability for safety-related projections based on a user-oriented model for projection illuminance and projector luminous flux and the required resolution. A DMD projector achieves the resolution requirements and existing visibility until dawn and dusk. Nevertheless, if it is possible to display projection content at a resolution of a  $\mu\text{LED}$  projector on the street - a  $\mu\text{LED}$  projector will be visible after dusk and dawn, enhancing the visibility for the use cases of safety-relevant projections for more situations into the day. Therefore, this thesis supports the choice of the projection system based on psychophysical data involving influence factors such as ambient illuminance level. As a result, the rate of deaths in road traffic accidents and vulnerable RUs might decrease

---

likelier by applying safety-relevant near-field projections as a new fundamental technology in urban traffic during the night and as much as possible during the day to no longer appear in the WHO's top ten causes of death [2].

Finally, the present thesis encourages future work in this field of research. Thus, with the models derived in Chapter 5, it is possible to determine the projection illuminance depending on the ambient illuminance level according to the type of observation. The determined requirements regarding the visible near-field projection need validation on a projector, e.g., DMD or  $\mu$ LED, depending on the investigated scenario in a dynamic test. The conducted testing can check the model's prediction to ensure that the limiting two selected ambient illuminance levels in the mesopic and photopic vision form a suitable model or that these need optimization. Further studies can deduce optimization factors since Shibata et al. and Singer et al. results show higher Weber contrast values of 0.4 with more complex test designs and naive participants [27, 26, 7]. The primary investigations have shown that static investigations are only a basis, especially for applying safety-relevant projections due to the complex situation with different moving traffic participants and different secondary tasks of pedestrians or cyclists, e.g., looking at a smartphone in urban traffic scenarios.

Therefore, the validation study should include a dynamic, realistic test setup with naive participants since the essential value ranges for resolution and visibility, including contrast or illuminance thresholds, have been defined in this work. A fundamental study focuses on the first realistic setting for near-field projections related to the perception of a fixed projection's contrast value with a cyclist in motion and a moving vehicle for a safety-relevant investigation by Namyslo et al. [25]. Here, in further investigations and research work, a system design that includes sensor-based and situation-adaptive feedback to the projection system needs attention to display the user-orientated contrast or illuminance perceptible to the viewer depending on the environmental conditions defined by the psychophysical testing, such as the influence by the ambient illuminance level or the characteristics of the road, which Figure 7.1 displays in a possible theoretical implementation in the vehicle's architecture.

Thus, Figure 7.1 considers the near-field projections as an adaptive assistance system. Therefore, it is necessary to respect the two most essential aspects of human perception, supported by various surveys [136], such as the resolution requirements for digital projections and contrast perception. The near-field projector will be a part of the adaptive assistance system because further components play a role besides the projector. Figure 7.1 displays the input variables of the different sensor data, including the necessary control units, which, besides processing the sensor data, also use prioritization and the necessary sensor fusion algorithms to display the correct projection to the viewer, depending on the scenario (main controller in Figure 7.1). Thus, the vehicle knows its environment established by the GPS data, can perceive the current scenarios, and recognizes critical situations such as bus stops related to the situative input data like camera images and GPS data. These are critical scenarios in the investigation by Singer et al. [7]. In addition, the vehicle uses the rain-light-sensor to detect the illuminance of the vehicle and can, therefore, react to local changes such as shadows cast.

Further, there is also the possibility of using camera images to obtain information about the environment, such as projection surface characteristics, but also to detect other RUs. The recognition allows the location of the projection's correct position in the vehicle's near-field, which the addressed RU should perceive. The processing of all data is thus handled centrally in the main controller (see Figure 7.1), which evaluates and fuses the various sensor data to guarantee the correct projection placement for the addressed RU using AI-based object detection algorithms. Finally, the main controller recognizes what type of scenario is present with the different sensor data because, depending on the viewing distance or ambient brightness, the visibility of the projection must be guaranteed and modified. The main controller processes all this sensor data, and if

more current data is required, the sensors are queried for current sensor data by the main controller. For example, in specific safety-related situations, the most critical RU is determined by the number of sensor data (GPS, ambient lighting, and camera data) to whom the near-field projection will be addressed. Due to the sensor data and AI-based algorithms, the vehicle then knows how the near-field projection has to be adjusted for the RU. With this in mind, this work defines the foundation for calculating the human-oriented resolution requirements and perceivable contrasts or illumination of the near-field projection for different detection thresholds, e.g., the 90 % threshold in this work.

By extending the developed model of sections 6.1.6 and 6.2.3, which is based on just two ambient lighting environments, there is a possibility to define the luminous flux of the near-field projector more precisely. In the end, the PWM value of the illumination source of the projector relates to specific luminous flux and contrast values, which are detectable by other RUs. All these steps, shown in Figure 7.1, enable near-field projections for an adaptive driver assistance system, which will provide a human-oriented projection in the near-field of the vehicle.

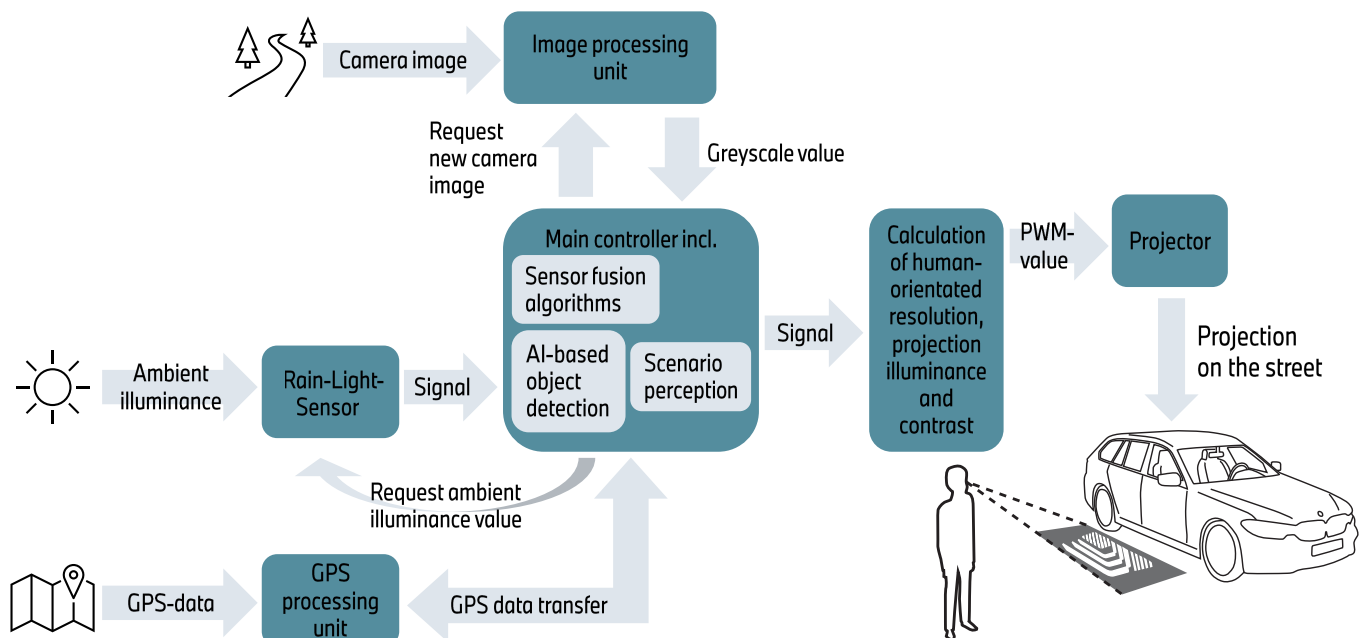


Figure 7.1.: Various data inputs, such as ambient illuminance by the rain-light sensor or location-specific data based on camera images or GPS data, are processed by several algorithms for applying adaptive near-field projection as a driver assistance system.

Furthermore, depending on the environmental parameters, the possibility of saving the projector's energy would be desirable, as the light source in the projector is dimmable, and energy-saving systems increase the range for electric-driven vehicles. Depending on the application but especially for design-driven projections such as welcome and goodbye scenarios, an adaptive system can save energy by not showing the projection when the vehicle's system know the built-in projector is not visible to the owner or RU since it is below the, e.g., 90 % detection threshold. This adaptive projection system needs explicit validation to enable the different sensor data of various sensors, such as light sensors, cameras, GPS, or others, to apply adaptive near-field



---

projections to the processes of sensor data processing. This workflow allows working with the defined model or with a modified variant of this model that can consider various location-related influences and the complexity of real urban traffic scenarios.

---

## Bibliography

---

- [1] DIN. *Lettering - Legibility (DIN 1450:2013-04)*. 2013. DOI: <https://dx.doi.org/10.31030/1938221>.
- [2] World Health Organization. *Global status report on road safety 2018*. Ed. by World Health Organization. Geneva, 2018, p. 403. ISBN: 9789241565684. URL: <https://apps.who.int/iris/rest/bitstreams/1164010/retrieve>.
- [3] National Safety Council (NSC). *Pedestrians*. 2023. URL: <https://injuryfacts.nsc.org/motor-vehicle/road-users/pedestrians/> (visited on 06/06/2023).
- [4] Statistisches Bundesamt (Destatis). *Verkehr - Verkehrsunfälle*. Tech. rep. 2022. URL: <https://www.destatis.de/DE/Themen/Gesellschaft-Umwelt/Verkehrsunfaelle/Publikationen/Downloads-Verkehrsunfaelle/verkehrsunfaelle-jahr-2080700217004.pdf>.
- [5] National Highway Traffic Safety Administration. *TRAFFIC SAFETY FACTS 2020*. Tech. rep. Washington, DC: National Highway Traffic Safety Administration, 2022, p. 222. URL: <https://crashstats.nhtsa.dot.gov/Api/Public/ViewPublication/813375>.
- [6] Michael Sivak and Brandon Schoettle. “Recent Changes in the Age Composition of Drivers in 15 Countries”. In: *Traffic Injury Prevention* 13.2 (2012), pp. 126–132. DOI: 10.1080/15389588.2011.638016. URL: <https://doi.org/10.1080/15389588.2011.638016>.
- [7] Timo Singer et al. “Behaviour of Automated Vehicles in Critical Situations with Pedestrians”. In: *VISION*. Paris: SIA VISION, 2021, pp. 174–178.
- [8] Mingshu Wang and Neil Debbage. “Urban morphology and traffic congestion: Longitudinal evidence from US cities”. In: *Computers, Environment and Urban Systems* 89 (2021), p. 101676. ISSN: 0198-9715. DOI: <https://doi.org/10.1016/j.compenvurbsys.2021.101676>. URL: <https://www.sciencedirect.com/science/article/pii/S0198971521000831>.
- [9] Feng Han, Rui Xie, and Mingyong Lai. “Traffic density, congestion externalities, and urbanization in China”. In: *Spatial Economic Analysis* 13.4 (2018), pp. 400–421. DOI: 10.1080/17421772.2018.1459045. URL: <https://doi.org/10.1080/17421772.2018.1459045>.
- [10] Yu Sang Chang et al. “Population Density or Populations Size. Which Factor Determines Urban Traffic Congestion?” In: *Sustainability* 13.8 (2021). ISSN: 2071-1050. DOI: 10.3390/su13084280. URL: <https://www.mdpi.com/2071-1050/13/8/4280>.
- [11] ITF. *Road Safety Annual Report 2022*. Tech. rep. Paris: OECD Publishing, 2022, p. 36. URL: <https://www.itf-oecd.org/sites/default/files/docs/irtad-road-safety-annual-report-2022.pdf>.
- [12] Zweirad-Industrie-Verband (ZIV). *Zahlen zum Fahrradmarkt 2021*. 2022. URL: <https://www.adfc.de/neuigkeit/zahlen-zum-fahrradmarkt-2021> (visited on 07/01/2023).
- [13] Gerolf Kloppenburg, Alexander Wolf, and Roland Lachmayer. “High-resolution vehicle headlamps: Technologies and scanning prototype”. In: *Advanced Optical Technologies* 5.2 (2016), pp. 147–155. ISSN: 21928584. DOI: 10.1515/aot-2016-0001.

- 
- [14] Marvin Knöchelmann et al. “High-resolution headlamps - Technology analysis and system design”. In: *Advanced Optical Technologies* 8.1 (2019), pp. 33–46. ISSN: 21928584. DOI: 10.1515/aot-2018-0060.
- [15] Carsten Gut. “Laserbasierte hochauflösende Pixellichtsysteme”. German. PhD thesis. Karlsruher Institut für Technologie (KIT), 2018, p. 240. DOI: 10.5445/KSP/1000073122.
- [16] Anil Erkan. “Optimierung von Frontscheinwerferlichtverteilungen anhand wahrnehmungsphysiologischer Kriterien”. PhD thesis. Darmstadt: Technische Universität Darmstadt, 2023, p. 153. DOI: <https://doi.org/10.26083/tuprints-00023805>. URL: <http://tuprints.ulb.tu-darmstadt.de/23805/>.
- [17] Marina Budanow. “Entwicklung eines lichtbasierten Fahrerassistenzsystems”. PhD thesis. Karlsruher Institut für Technologie (KIT), 2020, p. 314. ISBN: 9783731510185. DOI: 10.5445/KSP/1000105925.
- [18] F. Krieft et al. “Symbol Projections: Gain or Gadget?” In: *Proceedings of the 13th International Symposium on Automotive Lighting (ISAL) 2019*. Darmstadt: ISAL 2019, 2019, pp. 321–330.
- [19] Ulrike Schlöder. “Dynamic Ground Projections around the Car: The Headlamp as Integrator”. In: *14th International Symposium on Automotive Lighting*. Darmstadt: Darmstädter Lichttechnik Volume 19, 2022, pp. 538–547.
- [20] M Rosenauer et al. “Digital Projections: The next level of freedom and customization in vehicle design”. In: *Société des Ingénieurs de l’Automobile (SIA) VISION*. Paris: SIA VISION, 2022.
- [21] Marko Viršek. “Automotive car-body lighting digital projector based on LCoS technology”. In: *14th International Symposium on Automotive Lighting*. Darmstadt: Darmstädter Lichttechnik Volume 19, 2022, pp. 222–232.
- [22] Felix Maier and Ulrike Schlöder. *Dynamische Bodenprojektionen - Experimentelle Untersuchungen bzgl. photometrischer Anforderungen*. Tech. rep. Düsseldorf: VDI Verlag, 2022, pp. 167–186. DOI: <https://doi.org/10.51202/9783181024003>. URL: <https://elibrary.vdi-verlag.de/10.51202/9783181024003/optische-technologien-in-der-fahrzeugtechnik-2022?page=1>.
- [23] Brandon Seiser. *Dynamic Ground Projection using DLP® Technology for Automotive Exterior Lighting*. Tech. rep. Dallas: Texas Instruments, 2020. URL: [https://www.ti.com/lit/wp/slyy187/slyy187.pdf?ts=1657029920770&ref{\\\_}url=https{\%}253A{\%}252F{\%}252Fwww.google.com{\%}252F](https://www.ti.com/lit/wp/slyy187/slyy187.pdf?ts=1657029920770&ref{\_}url=https{\%}253A{\%}252F{\%}252Fwww.google.com{\%}252F).
- [24] K. Murata, T. Kitazawa, and H. Ishida. “Investigation of effectiveness and conflict of a road projection lamp for bicyclists, using a VR system”. In: *SIA VISION 2021*. Paris: SIA VISION, 2022, p. 7.
- [25] Stefan Namyslo, Marine Courcier, and Eric Moisy. “360° Near Field Projection - Enhanced safety or just a nice gadget?” In: *14th International Symposium on Automotive Lighting*. Darmstadt: Darmstädter Lichttechnik Volume 19, 2022, pp. 511–520.
- [26] Y. Shibata et al. “Detection rate of projected light signals by lighting condition and activation mode”. In: *SIA VISION 2021*. Paris: SIA VISION, 2021, pp. 53–58.
- [27] Y. Shibata et al. “Requirement Performance of Road Projection Lamp in Conjunction with Turn Signal Lamp”. In: *13th International Symposium on Automotive Lighting (ISAL)*. 2019, pp. 362–373.
- [28] DIN. *Road lighting - Part 2: Performance requirements; German version EN 13201-2:2015*. 2016. DOI: <https://dx.doi.org/10.31030/2275375>.

- 
- [29] Markus Rotmüller, Pernille Holm Rasmussen, and Signe Alexandra Vendelbo-Larsen. “Designing for Interactions with Automated Vehicles: Ethnography at the Boundary of Quantitative-Data-Driven Disciplines”. In: *Ethnographic Praxis in Industry Conference Proceedings* (2018), pp. 482–517. DOI: 10.1111/1559-8918.2018.01219.
- [30] Arne Valberg. *Light Vision Color*. Chichester: John Wiley & Sons, Ltd, 2005, pp. 76–79. ISBN: 0470012129.
- [31] Herbert Gross. “Handbook of Optical Systems”. In: *Handbook of Optical Systems*. 4th ed. Vol. 1. Weinheim: WILEY-VCH Verlag GmbH & Co. KGaA, 2005, pp. 36–86. ISBN: 978-3-527-40380-6. DOI: 10.1002/9783527699223.
- [32] BMW AG. *BMW 5er TOURING: MOTOREN & TECHNISCHE DATEN*. 2023. (Visited on 06/06/2023).
- [33] Fleming Chuang. *Projection displays - LCD/MEMS/LCoS based*. Ed. by Elsevier. Vol. 1-5. Elsevier Ltd., 2018, pp. 32–43. ISBN: 9780128149829. DOI: 10.1016/B978-0-12-803581-8.09627-2. URL: <http://dx.doi.org/10.1016/B978-0-12-803581-8.09627-2>.
- [34] Matthew S. Brennessholtz and Edward H. Stupp. *Projection displays*. Ed. by Anthony C. Lowe; and Michael A. Kriss. Second Edi. Chippenham: J. Wiley and Sons, 2008, p. 432. ISBN: 9780470518038.
- [35] David Armitage, Ian Underwood, and Shin-Tson Wu. “Projection Displays”. In: *Introduction to Microdisplays*. Ed. by Anthony C. Lowe. John Wiley & Sons, Ltd, 2006. Chap. 10, pp. 307–336. ISBN: 9780470057056. DOI: <https://doi.org/10.1002/9780470057056.ch10>. URL: <https://onlinelibrary.wiley.com/doi/abs/10.1002/9780470057056.ch10>.
- [36] Charles W. Mclaughlin. “Progress in projection and large-area displays”. In: *Proceedings of the IEEE* 90.4 (2002), pp. 521–532. ISSN: 00189219. DOI: 10.1109/JPROC.2002.1002524.
- [37] H.-D. Kim and J.-U. Kim. “High Resolution Pixel Lamp”. In: *ISAL 2019*. Darmstadt: ISAL 2019, 2019, pp. 689–698.
- [38] Yang Li, Qian Li, and Roland Lachmayer. “Analysis of high-resolution vehicle headlamp development”. In: *IFAL 2021*. Shanghai: IFAL, 2021, pp. 125–138.
- [39] S. Groetsch et al. “Mockup and Demonstrator of a High-Resolution Active Pixel-LED headlamp with 100k Pixel Performance”. In: *SIA VISION 2021*. Paris: SIA VISION, 2021, pp. 39–44.
- [40] Sadiq Rizvi et al. *Survey of on-road image projection with pixel light systems*. Tech. rep. Prague, Czech Republic, 2017. DOI: 10.1117/12.2292740.
- [41] Texas Instruments. *DLP3021-Q1 0.3-Inch WVGA Automotive DMD*. 2020. URL: <https://www.ti.com/document-viewer/DLP3021-Q1/datasheet/GUID-9AB2CFA6-11C1-4AF7-B674-925C6BD2E246{\#}TITLE-DLPS183DLPS0001089> (visited on 06/22/2023).
- [42] Jackson Thomas. *Dynamic Ground Projection Application Requirements*. Tech. rep. Dallas: Texas Instruments, 2020. URL: <https://www.ti.com/document-viewer/lit/html/DLPA116/>.
- [43] Wen-Shing Sun et al. “Compact LED projector design with high uniformity and efficiency”. In: *Applied Optics* 53.29 (2014), H227. ISSN: 0003-6935. DOI: 10.1364/ao.53.00h227.
- [44] Jake Pulliam and Shashank Dabral. “Innovative Application of Phase Light Modulation for Energy Efficient Projection in Automotive Use-Cases”. In: *14th International Symposium on Automotive Lighting*. Darmstadt: Darmstädter Lichttechnik Volume 19, 2022, pp. 709–718.
- [45] Sony. *Liquid Crystal Microdisplay*. 2023. URL: <https://www.sony-semicon.com/en/products/microdisplay/lcd.html> (visited on 06/22/2023).
- [46] A Lizana et al. “Influence of the incident angle in the performance of liquid crystal on silicon displays.” eng. In: *Optics express* 17.10 (2009), pp. 8491–8505. ISSN: 1094-4087 (Electronic). DOI: 10.1364/oe.17.008491.

- [47] Yuge Huang et al. “Prospects and challenges of mini-LED and micro-LED displays”. In: *Journal of the Society for Information Display* 27.7 (2019), pp. 387–401. ISSN: 19383657. DOI: 10.1002/jsid.760.
- [48] H. Hesse. “BMBF-Project VOLIFA 2020 - High resolution light distribution by using a LCD”. In: *ISAL 2015*. Darmstadt: ISAL 2015, 2015, pp. 495–502.
- [49] Yuge Huang et al. *Mini-LED, Micro-LED and OLED displays: present status and future perspectives*. 2020. DOI: 10.1038/s41377-020-0341-9.
- [50] Vincent W. Lee and Ioannis Kymissis. “A directly addressed monolithic LED array as a projection source”. In: *Journal of the Society for Information Display* 18.10 (2010), p. 808. ISSN: 10710922. DOI: 10.1889/jsid18.10.808.
- [51] M. Urlaub et al. “Micro-LED and Matrix-LED: A hybrid light-source architecture for high-resolution headlighting”. In: *SIA VISION 2021*. Paris: SIA VISION, 2021, pp. 76–81.
- [52] Vincent W. Lee, Nancy Twu, and Ioannis Kymissis. “Micro-LED Technologies and Applications”. In: *Frontline Technology* (2016), pp. 16–23. DOI: 10.1002/j.2637-496X.2016.tb00949.x. URL: <https://onlinelibrary.wiley.com/doi/epdf/10.1002/j.2637-496X.2016.tb00949.x>.
- [53] Grötsch Stefan et al. “HIGH RESOLUTION LED-HEADLAMP CONCEPT”. In: *14th International Symposium on Automotive Lighting*. Darmstadt, 2022, pp. 63–72.
- [54] Brunne David. “Digital lighting for headlamps to fulfill international regulations and ratings”. In: *14th International Symposium on Automotive Lighting*. Darmstadt, 2022, pp. 318–323.
- [55] Trung Thanh Nguyen et al. “Designing for Projection-based Communication between Autonomous Vehicles and Pedestrians”. In: *Proceedings of the 11th International Conference on Automotive User Interfaces and Interactive Vehicular*. AutomotiveUI ’19, 2019. ISBN: 9781450368841. DOI: 10.1145/3342197.3344543.
- [56] A. Dietrich et al. “Projection-based external human-machine interfaces – enabling interaction between automated vehicles and pedestrian”. In: *Proceedings of the Driving Simulation Conference Europe* (2018), pp. 43–50.
- [57] Claudia Ackermann et al. “An experimental study to investigate design and assessment criteria: What is important for communication between pedestrians and automated vehicles?” In: *Applied Ergonomics* (2019). ISSN: 18729126. DOI: 10.1016/j.apergo.2018.11.002.
- [58] Lex Fridman et al. “To Walk or Not to Walk: Crowdsourced Assessment of External Vehicle-to-Pedestrian Display”. In: *Transportation Research Board Annual Meeting* (2017). URL: <https://arxiv.org/abs/1707.02698>.
- [59] Timo Singer. “Untersuchungen von Lichtsignal-Konzepten für automatisierte Fahrzeuge in der virtuellen Realität”. PhD thesis. Darmstadt: Technische Universität Darmstadt, 2022, xvi, 189 Seiten. DOI: <https://doi.org/10.26083/tuprints-00022417>. URL: <http://tuprints.ulb.tu-darmstadt.de/22417/>.
- [60] M. Baumann et al. “Symbol Projection for Pedestrians”. In: *ISAL 2021*. Darmstadt: Darmstädter Lichttechnik Volume 19, 2022, pp. 555–566.
- [61] Mitsubishi Electric Corporation. *Mitsubishi Electric Introduces Road-illuminating Directional Indicators*. Tech. rep. Tokyo: Industrial Design Center, 2015. URL: [https://emea.mitsubishielectric.com/en/news-events/releases/2015/1023-a/pdf/151023-2970{\\\_}Road-illuminating{\\\_}Directional{\\\_}Indicators-G.pdf](https://emea.mitsubishielectric.com/en/news-events/releases/2015/1023-a/pdf/151023-2970{\_}Road-illuminating{\_}Directional{\_}Indicators-G.pdf).

- 
- [62] Andrea Leitner-Garnell. *PROJEKTIONEN AUF DER FAHRBAHN: JAGUAR LAND ROVER ENTWICKELT NEUE TECHNOLOGIEN FÜR MEHR VERTRAUEN IN AUTONOME FAHRZEUGE*. 2019. URL: <https://media.jaguarlandrover.com/de-de/news/2019/01/projektionen-auf-der-fahrbahn-jaguar-land-rover-entwickelt-neue-technologien-fuer-mehr> (visited on 06/23/2023).
- [63] Mercedes-Benz. *Der Mercedes-Benz F 015 Luxury in Motion*. 2015. URL: <https://www.mercedes-benz.com/de/innovation/autonomous/forschungsfahrzeug-f-015-luxury-in-motion/{\#}contact> (visited on 01/27/2020).
- [64] MINI. *DER MINI CONCEPT ACEMAN*. 2022. URL: [https://www.mini.de/de{\\\_}DE/home/explore/concept-cars/aceman-concept.html](https://www.mini.de/de{\_}DE/home/explore/concept-cars/aceman-concept.html) (visited on 08/17/2022).
- [65] AUDI AG. *Audi A6 e-tron concept: E-Volution mit klassischen Linien*. 2021. URL: <https://www.audi.com/de/innovation/e-mobility/Audi-A6-e-tron-concept.html> (visited on 05/25/2022).
- [66] A Wolf et al. “DMD Based Automotive Lighting Unit”. In: *DGaO Proceedings* (2016), pp. 5–6. DOI: <https://doi.org/10.15488/4004>.
- [67] Jörg Moisel. “REQUIREMENTS FOR FUTURE HIGH RESOLUTION ADB MODULES”. In: *11th International Symposium on Automotive Lighting*. Darmstadt, 2015, pp. 161–169.
- [68] Masashige Suwa, Masatoshi Nishimura, and Reiko Sakata. “LED Projection Module Enables a Vehicle to Communicate with Pedestrians and Other Vehicles”. In: *IEEE International Conference on Consumer Electronics (ICCE)*. Las Vegas, NV, USA: IEEE, 2017. ISBN: 9781509055449. DOI: 10.1109/ICCE.2017.7889220. URL: <https://ieeexplore.ieee.org/document/7889220>.
- [69] B. Reiss and S. Cladé. “Road Marking Solutions with Pixelized Light Source”. In: *Proceedings of the 13th International Symposium on Automotive Lighting (ISAL) 2019*. Darmstadt: ISAL 2019, 2019, pp. 343–352.
- [70] Patric Jahn, Iulia Cristea, and Cornelius Neumann. “High-Resolution Light-Based Driver-Assistance - Optimal Contrast for Symbols”. In: *12th International Symposium on Automotive Lightning (ISAL)*. 2017, pp. 43–52.
- [71] BMW. *BMW LED-Türprojektoren*. 2020. URL: <https://www.bmw.de/de/shop/lis/dp/physical-goods/639940> (visited on 02/05/2023).
- [72] Audi. *Digitale Matrix LED-Scheinwerfer: eine Million Pixel im Tanz*. 2019. URL: <https://www.audi.com/de/experience-audi/mobility-and-trends/e-mobility/matrix-led-headlights.html> (visited on 02/09/2020).
- [73] Timo Singer et al. “Displaying the Driving State of Automated Vehicles to Other Road Users: An International, Virtual Reality-Based Study as a First Step for the Harmonized Regulations of Novel Signaling Devices”. In: *IEEE Transactions on Intelligent Transportation Systems* 23.4 (2020), pp. 2904–2918. ISSN: 1524-9050. DOI: 10.1109/tits.2020.3032777.
- [74] Frederick A.A. Kingdom and Nicolaas Prins. “Varieties of Psychophysical Procedures”. In: *Psychophysics*. Elsevier, 2016, pp. 37–54. DOI: 10.1016/b978-0-12-407156-8.00003-7.
- [75] Neil A. Macmillan and C. Douglas Creelman. *Detection Theory - A User's Guide*. 2nd Editio. New York: Psychology Press, 2004, p. 512. ISBN: 9781410611147. DOI: <https://doi.org/10.4324/9781410611147>.
- [76] Gert Hauske. *Systemtheorie der visuellen Wahrnehmung*. Stuttgart: B.G. Teubner, 2003, p. 280. ISBN: 3-8322-1293-0.



- [77] M Royer et al. “Recommended methods for conducting human factors experiments on the subjective evaluation of colour rendition”. In: *Lighting Research & Technology* 54.3 (2022), pp. 199–236. DOI: 10.1177/14771535211019864. URL: <https://doi.org/10.1177/14771535211019864>.
- [78] E B Goldstein and L Cacciamani. *Sensation and Perception*. 11th ed. MindTap Course List Series. Boston: Cengage, 2021. ISBN: 9780357446478. URL: <https://books.google.de/books?id=Mz8BzgEACAAJ>.
- [79] Werner Herkner. “Wahrnehmung”. In: *Psychologie*. 1st ed. Vienna: Springer Verlag, 1986, pp. 1–79. ISBN: 978-3-7091-3424-5. DOI: 10.1007/978-3-7091-3424-5\_1. URL: [https://doi.org/10.1007/978-3-7091-3424-5{\\\_}1](https://doi.org/10.1007/978-3-7091-3424-5{\_}1).
- [80] Deutsches Institut für Normung. *DIN EN 12464-2:2014-05: Light and Lighting - Lighting of Work Places - Part 2: Outdoor Work Places*. Tech. rep. Berlin: Beuth-Verlag, 2014, p. 20.
- [81] Gerald M. Long and David L. Penn. “Dynamic visual acuity: Normative functions and practical implications”. In: *Bulletin of the Psychonomic Society* 25.4 (1987), pp. 253–256. ISSN: 00905054. DOI: 10.3758/BF03330347.
- [82] Jolien De Letter et al. “Exploratory Study on User’s Dynamic Visual Acuity and Quality Perception of Impaired Images”. In: (2020). arXiv: 2001.03542. URL: <http://arxiv.org/abs/2001.03542>.
- [83] Dimitrios J. Palidis et al. “Distinct eye movement patterns enhance dynamic visual acuity”. In: *PLoS ONE* 12.2 (2017). ISSN: 19326203. DOI: 10.1371/journal.pone.0172061.
- [84] Domenic Vital et al. “A new dynamic visual acuity test to assess peripheral vestibular function”. In: *Archives of Otolaryngology - Head and Neck Surgery* 136.7 (2010), pp. 686–691. ISSN: 08864470. DOI: 10.1001/archoto.2010.99.
- [85] Iuliia Rottc and Victor Musalimov. “Regularity of dynamic visual acuity change in the training results”. In: *58th IWK, Ilmenau Scientific Colloquium*, 58, 2014 (2014). URL: <http://uri.gbv.de/document/gvk:ppn:815855478>.
- [86] Hans-Joachim Schmidt-Clausen and Achim Freiding. *Sehvermögen von Kraftfahrzeugen und Lichtbedingungen im nächtlichen Verkehr. Berichte der Bundesanstalt für Straßenwesen : Mensch und Sicherheit*. 158th ed. Bremerhaven: Fachverlag NW in Carl Ed. Schünemann KG, 2004. ISBN: 9783865091024.
- [87] Commission Internationale de L’Eclairage. *CIE 100-1992 Fundamentals of the visual task of night driving*. 1992.
- [88] Miriam Linschoten et al. “Fast and accurate measurement of taste and smell thresholds using a maximum-likelihood adaptive staircase procedure”. In: *Perception & Psychophysics* 63.8 (2001), pp. 1330–1347.
- [89] A C Harvey. “Estimating Regression Models with Multiplicative Heteroscedasticity”. In: *Econometrica* 44.3 (1976), pp. 461–465. DOI: <https://doi.org/10.2307/1913974>. URL: <http://www.jstor.org/stable/1913974>.
- [90] Lewis O. Harvey. “Efficient estimation of sensory thresholds with ML-PEST”. In: *Spatial Vision* 11.1 (1997), pp. 121–128. DOI: 10.1163/156856897x00159.
- [91] Manuel Kühner et al. *Adaptive Verfahren in der Psychophysik Effiziente Bestimmung von Absolut- und Unterschiedsschwellen*. 2012.
- [92] Johannes (Hans) van Houwelingen and Saskia Le Cessie. “Logistic Regression, a Review”. In: *Statistica Neerlandica* 42.4 (1988), pp. 215–232. DOI: 10.1111/j.1467-9574.1988.tb01237.x. URL: <https://onlinelibrary.wiley.com/doi/abs/10.1111/j.1467-9574.1988.tb01237.x>.



- 
- [93] H. Levitt. “Transformed Up-Down Methods in Psychoacoustics”. In: *The Journal of the Acoustical Society of America* 49.2B (1971), pp. 467–477. ISSN: 0001-4966. DOI: 10.1121/1.1912375.
- [94] W. Adrian. “Visibility of targets: Model for calculation”. In: *Lightning Res. Technologie* 6.11 (1989), pp. 181–188. ISSN: 1098-6596. arXiv: arXiv:1011.1669v3.
- [95] Werner K Adrian and Ronald B Gibbons. “Visibility level und die Sichtbarkeit in der Straßenbeleuchtung”. In: *Licht* 10 (1993), pp. 734–739.
- [96] CIE. *International Lighting Vocabulary: Internationales Wörterbuch der Lichttechnik*. 2020, p. 252. URL: <https://www.beuth.de/de/norm/cie-s-017/333383905>.
- [97] J B de Boer and D A Schreuder. “Glare as a Criterion for Quality in Street Lighting”. In: *Transactions of the Illuminating Engineering Society* 32.2\_IEStrans (1967), pp. 117–135. DOI: 10.1177/147715356703200205. URL: <https://doi.org/10.1177/147715356703200205>.
- [98] Luiz M. Lozano, Eduardo García-Cueto, and José Muñiz. “Effect of the number of response categories on the reliability and validity of rating scales”. In: *Methodology* 4.2 (2008), pp. 73–79. ISSN: 16141881. DOI: 10.1027/1614-2241.4.2.73.
- [99] Leonard J. Simms et al. “Does the Number of Response Options Matter? Psychometric Perspectives Using Personality Questionnaire Data”. In: *Psychological Assessment* 31.4 (2019), pp. 557–566. ISSN: 1939134X. DOI: 10.1037/pas0000648.
- [100] Margit L Bleecker et al. “Simple visual reaction time: Sex and age differences”. In: *Developmental Neuropsychology* 3.2 (1987), pp. 165–172. DOI: 10.1080/87565648709540372. URL: <https://doi.org/10.1080/87565648709540372>.
- [101] Neil S. Gittings and James L. Fozard. “Age related changes in visual acuity”. In: *Experimental Gerontology* 21.4-5 (1986), pp. 423–433. ISSN: 0531-5565. DOI: 10.1016/0531-5565(86)90047-1.
- [102] Allison M. McKendrick, Yu Man Chan, and Bao N. Nguyen. “Spatial vision in older adults: perceptual changes and neural bases”. In: *Ophthalmic and Physiological Optics* 38.4 (2018), pp. 363–375. ISSN: 14751313. DOI: 10.1111/opo.12565.
- [103] Masaki Emoto and Masayuki Sugawara. “Viewers’ optimization of preferred viewing distance by spatial resolution of TV display”. In: *Displays* 45 (2016), pp. 1–5. ISSN: 01419382. DOI: 10.1016/j.displa.2016.07.003.
- [104] Chen-Xiao Wang, Na Lin, and Ying-Xuan Guo. “Visual requirement for Chinese reading with normal vision”. In: *Brain and Behavior* 9.4 (2019), e01216. DOI: <https://doi.org/10.1002/brb3.1216>. URL: <https://onlinelibrary.wiley.com/doi/abs/10.1002/brb3.1216>.
- [105] Jun-Yun Zhang et al. “Legibility variations of Chinese characters and implications for visual acuity measurement in Chinese reading population.” eng. In: *Investigative ophthalmology & visual science* 48.5 (2007), pp. 2383–2390. ISSN: 0146-0404 (Print). DOI: 10.1167/iovs.06-1195.
- [106] J.H.D.M. Westerink and J A J Roufs. “Subjective image quality as a function of viewing distance, resolution and picture size”. In: *SMPTE journal* 98.2 (1989), pp. 113–119. ISSN: 0036-1682.
- [107] G. Heron et al. “Relationship between visual acuity and observation distance”. In: *Ophthalmic and Physiological Optics* 15.1 (1995), pp. 23–30. ISSN: 0275-5408. DOI: 10.1016/0275-5408(95)92788-G.
- [108] L C Jesty. “The relation between picture size, viewing distance and picture quality”. In: *Proceedings of the IEE - Part B: Radio and Electronic Engineering* 105.23 (1958), 425–439(14). ISSN: 2050-2656. URL: <https://digital-library.theiet.org/content/journals/10.1049/pi-b-1.1958.0320>.

- 
- [109] Arnold M. Lund. “Influence of Video Image Size and Resolution on Viewing-Distance Preferences”. In: *SMPTE Journal* 102.5 (1993), pp. 406–415. ISSN: 00361682. DOI: 10.5594/J15915.
- [110] Simon Shlaer. “The Relation between Visual Acuity and Illumination”. In: *Journal of General Physiology* (1937).
- [111] H. Selig. “The Relation between Visual Acuity and Illumination”. In: *The Journal of General Physiology* (1927).
- [112] Sven P Heinrich et al. “The ”speed” of acuity in scotopic vs. photopic vision”. In: *Graefe’s Archive for Clinical and Experimental Ophthalmology* 258 (2020), pp. 2791–2798. DOI: 10.1007/s00417-020-04867-6/Published. URL: <https://doi.org/10.1007/s00417-020-04867-6>.
- [113] Jacob Pulliam. “Investigating Symbol Recognition Time as a Function of System Resolution”. In: *14th International Symposium on Automotive Lighting*. Darmstadt: Darmstädter Lichttechnik Volume 19, 2022, pp. 162–171.
- [114] W. Wesemann et al. *Neue DIN- und ISO-Normen zur Sehschärfestimmung*. Tech. rep. 2019.
- [115] Alexander Stuckert and Tran Quoc Khanh. “Resolution Aspects for Near-Field Projections”. In: *Applied Sciences* 13.2 (2023), pp. 1–14. ISSN: 20763417. DOI: 10.3390/app13021039.
- [116] HR Blackwell. “Contrast thresholds of the human eye.” eng. In: *Journal of the Optical Society of America* 36.11 (1946), pp. 624–643. ISSN: 0030-3941 (Print). DOI: 10.1364/josa.36.000624.
- [117] Werner K Adrian. “Die Unterschiedsempfindlichkeit des Auges und die Möglichkeit ihrer Berechnung”. In: *Lichttechnik* 1 (1969).
- [118] Katharina Schneider. “Object contrast determination based on peripheral vision under night-time driving conditions”. In: August (2017), p. 241. URL: <https://tuprints.ulb.tu-darmstadt.de/id/eprint/83003>.
- [119] Anil Erkan et al. “Influence of Headlight Level on Object Detection in Urban Traffic at Night”. In: *Applied Sciences* 13.4 (2023). ISSN: 2076-3417. DOI: 10.3390/app13042668. URL: <https://www.mdpi.com/2076-3417/13/4/2668>.
- [120] Hermann-Josef Fleck. “Zur peripheren Wahrnehmung von Sehzeichen”. In: *VDI Reihe* 17:34 (1985), p. 255.
- [121] Hermann-Josef Fleck. “Measurement and modeling of peripheral detection and discrimination thresholds”. In: *Biological Cybernetics* 61.6 (1989), pp. 437–446. DOI: 10.1007/BF02414905.
- [122] Ryan McKendrick and Amanda Harwood. “Cognitive Workload and Workload Transitions Elicit Curvilinear Hemodynamics During Spatial Working Memory”. In: *Frontiers in Human Neuroscience* 13 (2019). ISSN: 1662-5161. DOI: 10.3389/fnhum.2019.00405. URL: <https://www.frontiersin.org/articles/10.3389/fnhum.2019.00405>.
- [123] Vasileios Skaramagkas et al. “Review of Eye Tracking Metrics Involved in Emotional and Cognitive Processes”. In: *IEEE Reviews in Biomedical Engineering* 16 (2023), pp. 260–277. ISSN: 19411189. DOI: 10.1109/RBME.2021.3066072.
- [124] Alexandros Rouchitsas and Håkan Alm. “External Human–Machine Interfaces for Autonomous Vehicle-to-Pedestrian Communication: A Review of Empirical Work”. In: *Frontiers in Psychology* 10 (2019), p. 2757. DOI: <https://doi.org/10.3389/fpsyg.2019.02757>. URL: <https://www.frontiersin.org/articles/10.3389/fpsyg.2019.02757/full>.

- 
- [125] Statistisches Bundesamt (Destatis). *Mikrozensus - Fragen zur Gesundheit - Körpermaße der Bevölkerung, 2017*. Tech. rep. 2018, p. 17. URL: <https://www.destatis.de/DE/Themen/Gesellschaft-Umwelt/Gesundheit/Gesundheitszustand-Relevantes-Verhalten/Publikationen/Downloads-Gesundheitszustand/koerpermasse-5239003179004.html>.
- [126] Christopher Bremer. “TECHNOLOGISCHE UND PHYSIOLOGISCHE BEWERTUNG DYNAMISCHER PROJEKTIONS- SYSTEME IM AUTOMOBIL”. PhD. Karlsruher Instituts für Technologie (KIT), 2021, p. 293. DOI: <https://doi.org/10.5445/IR/1000149706>. URL: <https://publikationen.bibliothek.kit.edu/1000149706/149145196>.
- [127] MAXWELL. *MP-WU5603 Laser Projector*. 2022. URL: <https://maxellproav.com/product/mp-wu5603-laser-projector/> (visited on 08/08/2022).
- [128] TechnoTeam. *LMK Video Photometers*. 2014. URL: [https://www.technoteamvision.com/apool/tnt/content/e5183/e5432/e5733/e6644/LMK{\\\_}web{\\\_}eng.pdf](https://www.technoteamvision.com/apool/tnt/content/e5183/e5432/e5733/e6644/LMK{\_}web{\_}eng.pdf) (visited on 08/17/2020).
- [129] Cogent. *Cogent 2000*. 2020. URL: [http://www.vislab.ucl.ac.uk/cogent{\\\_}2000.php](http://www.vislab.ucl.ac.uk/cogent{\_}2000.php).
- [130] Christoph Schiller. “Untersuchungen über spektrale Kontrastempfindlichkeitsfunktionen des menschlichen Auges im mesopischen Bereich und ihre Einflussparameter”. Dissertation. Darmstadt: Technische Universität Darmstadt, 2015. URL: <http://tuprints.ulb.tu-darmstadt.de/4970/>.
- [131] Plastic Omnium. *PROJECTION SOLUTIONS*. 2023. URL: <https://www.plasticomnium.com/en/projection-solutions/> (visited on 03/20/2023).
- [132] Valeo. *360° LIGHT PROJECTION ON THE GROUND*. 2023. URL: <https://www.valeo.com/en/360-light-projection-on-the-ground/> (visited on 02/21/2023).
- [133] Commission Internationale de L’éclairage. *CIE 144:2001 - Road Surface and Road Marking Reflection Characteristics*. Tech. rep. Vienna: CIE, 2001, p. 40.
- [134] DIN. *Graphical symbols - Safety colours and safety signs - Part 1: Design principles for safety signs and safety markings (ISO 3864-1:2011)*. 2012. DOI: <https://dx.doi.org/10.31030/1888973>.
- [135] Alexander Stuckert, Timo Singer, and Tran Quoc Khanh. “Analysis and definition of resolution requirements for projections in the near field of a vehicle”. In: *14th International Symposium on Automotive Lighting*. Darmstadt: Darmstädter Lichttechnik Volume 19, 2022, pp. 521–530.
- [136] Alexander Stuckert, Tabea Schlürscheid, and Tran Quoc Khanh. “Review of user’s evaluation and the needs for road projections around a vehicle”. In: *VISION*. Paris: SIA VISION, 2022, pp. 80–87.
- [137] DIN. *Classification of types (DIN 16518:1998-09)*. 1998.
- [138] DIN. *Typefaces - Sans Serif - Part 1: General (DIN 1451-1:2018-12)*. 2018. DOI: <https://dx.doi.org/10.31030/3000206>.
- [139] O S Adams et al. “Relations among some Measures of Pattern Discriminability”. In: *Journal of Experimental Psychology* 48.2 (1954). DOI: [10.1037/h0060143](https://doi.org/10.1037/h0060143).
- [140] Lloyd Kaufman and Whitman Richards. “Spontaneous fixation tendencies for visual forms”. In: *Perception & Psychophysics* 5 (1969), pp. 85–88. DOI: <https://doi.org/10.3758/BF03210527>.
- [141] Chulhee Lee. “Objective video quality assessment”. In: *Optical Engineering* 45.1 (2006). DOI: [10.1117/1.2160515](https://doi.org/10.1117/1.2160515). URL: <https://doi.org/10.1117/1.2160515>.
- [142] T. Judd, F. Durand, and A. Torralba. “Fixations on low-resolution images”. In: *Journal of Vision* 11.4 (2011), pp. 14–14. ISSN: 1534-7362. DOI: [10.1167/11.4.14](https://doi.org/10.1167/11.4.14).

- 
- [143] Carmen Koch. "Rolle visueller Referenzen bei der Objektlokalisierung". PhD thesis. Ludwig Maximilians Universität München, 2005, p. 219. DOI: <https://doi.org/10.5282/edoc.4175>. URL: <https://edoc.ub.uni-muenchen.de/4175/>.
- [144] BMW Group. *The new i7: Der erste vollelektrische BMW i7*. 2022. URL: <https://www.bmw.de/de/neufahrzeuge/bmw-i/i7/2022/bmw-i7-limousine-highlights.html> (visited on 03/03/2023).
- [145] Andy Field, Jeremy Miles, and Zoë Field. *Discovering statistics using R*. Vol. 50. 04. 2012, pp. 818–830, 940. ISBN: 9781446200452. DOI: 10.5860/choice.50-2114.
- [146] Paul D. Ellis. *The Essential Guide to Effect Sizes: Statistical Power, Meta-Analysis, and the Interpretation of Research Results*. 1st ed. Hong Kong: Cambridge University Press, 2010, p. 173. ISBN: 9780521142465. DOI: <https://doi.org/10.1017/CB09780511761676>.
- [147] Cyxthia Owsley, Robert Sekuler, and in AL Birmingham Birmingham. "Contrast sensitivity throughout adulthood". In: *Vision Research* 23.7 (1983), pp. 689–699.
- [148] Valentin Amrhein, Sander Greenland, and Blake McShane. "Scientists rise up against statistical significance". In: *Nature* 567 (2019), pp. 305–307. DOI: [doi:https://doi.org/10.1038/d41586-019-00857-9](https://doi.org/10.1038/d41586-019-00857-9).
- [149] P G J Barten. "The effects of picture size and definition on perceived image quality". In: *IEEE Transactions on Electron Devices* 36.9 (1989), pp. 1865–1869. DOI: 10.1109/16.34260.
- [150] Amir Rasouli and John K. Tsotsos. "Autonomous Vehicles That Interact With Pedestrians: A Survey of Theory and Practice". In: *IEEE Transactions on Intelligent Transportation Systems* (2019). ISSN: 1524-9050. DOI: 10.1109/tits.2019.2901817.
- [151] Michael Clamann. "Evaluation of Vehicle-to-Pedestrian Communication Displays for Autonomous Vehicles". In: *Human Factors: The Journal of the Human Factors and Ergonomics Society* (2015). URL: [https://hal.pratt.duke.edu/sites/hal.pratt.duke.edu/files/u10/Clamann{\\\_}etal{\\\_}TRB2016.pdf](https://hal.pratt.duke.edu/sites/hal.pratt.duke.edu/files/u10/Clamann{\_}etal{\_}TRB2016.pdf).
- [152] Ina Othersen et al. "Designing for Automated Vehicle and Pedestrian Communication: Perspectives on eHMIs from Older and Younger Persons". In: *Human Factors and Ergonomics Society Europe Chapter 2018 Annual Conference* (2018). URL: <https://www.hfes-europe.org/wp-content/uploads/2018/10/0thersen2018.pdf>.
- [153] Cecilia Ramaioli et al. "Vestibulo-ocular responses and dynamic visual acuity during horizontal rotation and translation". In: *Frontiers in Neurology* 10.APR (2019), pp. 1–11. ISSN: 16642295. DOI: 10.3389/fneur.2019.00321.
- [154] Matthias Gaul. *Bicycle: It Depends on the Braking Power*. 2020. URL: <https://www.dekra-solutions.com/2020/12/bicycle-it-depends-on-the-braking-power/?lang=en>.
- [155] W. Adrian. "Visibility Levels Under Night-Time Driving Conditions". In: *Journal of the Illuminating Engineering Society* 16.2 (1987), pp. 3–12. ISSN: 00994480. DOI: 10.1080/00994480.1987.10748682.
- [156] B Buyukkinaci et al. "Determining minimum visibility levels in different road lighting scenarios". In: *Lighting Research & Technology* 50.7 (2018), pp. 1045–1056. DOI: 10.1177/1477153517709868. URL: <https://doi.org/10.1177/1477153517709868>.

- [157] Jan De Boer et al. *Überprüfung verschiedener lichttechnischer Kennziffern bezüglich ihrer Eignung zur Erfassung der Helligkeit von Straßendeckschichten und die Entwicklung einer transportablen Einrichtung für die Messung der Helligkeit vor Ort und im Labor*. Tech. rep. Stuttgart: Fraunhofer-Gesellschaft e.V., 2009, pp. 30–33. DOI: IBP-BerichtWB145/2009. URL: [https://www.asphalt.de/fileadmin/user\\_upload/downloads/forschungsberichte/aif15083bglichttechnischekennziffern.pdf](https://www.asphalt.de/fileadmin/user_upload/downloads/forschungsberichte/aif15083bglichttechnischekennziffern.pdf).
- [158] *Psychophysics Toolbox Version 3*. 2021. URL: <http://psychtoolbox.org/> (visited on 08/05/2021).
- [159] S. Azougui et al. “Contrast Requirements of Road Projections for Situational Awareness: Field test versus Virtual Reality testing”. In: *Société des Ingénierus de l'Automobile (SIA) VISION*. 2021, pp. 64–71.
- [160] Sadiq Rizvi et al. “Road safety enhancement: an investigation on the visibility of on-road image projections using DMD-based pixel light systems”. In: 60. February (2018). ISSN: 1996756X. DOI: 10.1117/12.2290456.
- [161] Marc Green et al. *Forensic Vision with Application to Highway Safety*. Lawyers & Judges Publishing Company, 2008, p. 496. ISBN: 9781933264547. URL: <https://books.google.de/books?id=1t7fAH0s7QYC>.
- [162] Michael Rosenauer, Jasmin Muster, and Georg Forster. “Lichtlösungen zur Akzeptanzsteigerung autonomer Fahrzeuge”. In: *ATZelextronik* 15.4 (2020), pp. 56–59. ISSN: 2192-8878. DOI: 10.1007/s35658-020-0175-5. URL: <https://doi.org/10.1007/s35658-020-0175-5>.
- [163] M. Berek. “Zur physiologischen Grundgesetz der Wahrnehmung von Lichtreizen”. In: *Zeitschrift für Instrumentenkunde* 13 (1943), pp. 297–309.
- [164] *LMK LabSoft - TechnoTeam Bildverarbeitung GmbH*. URL: <https://www.technoteam.de/e5183/e5432/e5436/e5483/indexger.html?preview=previewhttps://www.technoteam.de/productoverview/photometercolorimeter/software/lmklabsoft/indexeng.html> (visited on 08/05/2021).
- [165] UN/ECE GRE. *Regelung Nr. 48 der Wirtschaftskommission der Vereinten Nationen für Europa (UN/ECE) — Einheitliche Bedingungen für die Genehmigung von Fahrzeugen hinsichtlich des Anbaus der Beleuchtungs- und Lichtsignaleinrichtungen [2016/1723]*. 2016.
- [166] Christine E Wright and Nevilee Drasdo. “The influence of age on the spatial and temporal contrast sensitivity function”. In: *Documenta Ophthalmologica* 59.4 (1985), pp. 385–395. ISSN: 00124486. DOI: 10.1007/BF00159172.
- [167] Tabea Schlürscheid et al. “An analysis of visibility requirements and reaction times of near-field projections”. In: *Applied Sciences* x.x (2023), pp. 1–15.
- [168] D Finlay. “Motion perception in the peripheral visual field.” eng. In: *Perception* 11.4 (1982), pp. 457–462. ISSN: 0301-0066 (Print). DOI: 10.1068/p110457.
- [169] Gerolf Kloppenburg. “Scannende Laser-Projektionseinheit für die Fahrzeugfrontbeleuchtung”. PhD. Leibniz Universität Hannover, 2017, p. 162. DOI: <https://doi.org/10.15488/3488>.
- [170] J J Koenderink et al. “Perimetry of contrast detection thresholds of moving spatial sine wave patterns. III. The target extent as a sensitivity controlling parameter.” eng. In: *Journal of the Optical Society of America* 68.6 (1978), pp. 854–860. ISSN: 0030-3941 (Print). DOI: 10.1364/josa.68.000854.
- [171] DIN. *Light and lighting - Lighting of work places - Part 1: Indoor work places; German version EN 12464-1:2021*. 2021. DOI: <https://dx.doi.org/10.31030/3233193>.
- [172] Robert B Zajonc. “Attitudinal effects of mere exposure.” In: *Journal of Personality and Social Psychology* 9.2 (1968), pp. 1–27. ISSN: 1939-1315(Electronic),0022-3514(Print). DOI: 10.1037/h0025848.



- 
- [173] Romy Blüher and Sabine Pahl. “Der “Mere-Exposure”-Effekt und die Wahl von Produkten”. In: *Zeitschrift für Sozialpsychologie* 38.3 (2007), pp. 209–215. DOI: 10.1024/0044-3514.38.3.209. URL: <https://doi.org/10.1024/0044-3514.38.3.209>.
- [174] JASP Team. *JASP (Version 0.17)[Computer software]*. Amsterdam, 2023. URL: <https://jasp-stats.org/>.
- [175] Jakob Nielsen and Thomas K Landauer. “A Mathematical Model of the Finding of Usability Problems”. In: *Proceedings of the INTERACT '93 and CHI '93 Conference on Human Factors in Computing Systems*. CHI '93. New York, NY, USA: Association for Computing Machinery, 1993, pp. 206–213. ISBN: 0897915755. DOI: 10.1145/169059.169166. URL: <https://doi.org/10.1145/169059.169166>.
- [176] OCULUS Optikgeräte GmbH. *OCULUS Binoptometer® 4P OCULUS Benutzerhandbuch*. Wetzlar, 2023. URL: [https://www.oculus.de/fileadmin/downloads/sonstiges/binoptometer-4p-sw-updates/BH{\\\_}59860{\\\_}0516{\\\_}de.pdf](https://www.oculus.de/fileadmin/downloads/sonstiges/binoptometer-4p-sw-updates/BH{\_}59860{\_}0516{\_}de.pdf).

# A. Additional material for the resolution tests

## A.1. Materials for the PGS and DDS tests



### Instruktion Wertigkeit einer Umfeldprojektion

In dieser Studie geht es um die subjektive Wahrnehmung der Wertigkeit einer Bodenprojektionsdarstellung neben dem Fahrzeug.

Ihre Aufgabe innerhalb dieses Versuchs ist es, eine Bewertung von Bildern in verschiedenen Wertigkeitsstufen durchzuführen.

Die Studie wird unter Ihren persönlichen Normalbedingungen durchgeführt, dies bedeutet, falls Sie eine Sehhilfe benötigen, tragen Sie bitte die notwendige Sehhilfe während des gesamten Tests. Bevor Sie die verschiedenen Wertigkeitsstufen der Bilder bewerten dürfen, bekommen Sie Beispiele eines Bildes mit geringer und hoher Wertigkeit gezeigt, die nicht in der Bildfolge enthalten sind.

Nach der Betrachtung der Beispielsbilder, beginnt die Qualitätsbewertung der Bodenprojektion. Platzieren Sie sich hierfür an den markierten Stellen, welche sich in einem Abstand von 1m, 3m oder 5m von der Nahfeldprojektion befindet. Somit durchlaufen Sie je Test drei verschiedene Betrachtungsabstände. Ihr Blick sollte dabei frontal auf das Auto gerichtet sein.

Der Versuchsleiter präsentiert Ihnen jeweils zehn Bilder (einerseits eine Bildfolge aus Grafiken und andererseits aus Buchstaben) in verschiedenen Qualitätsstufen, die auf dem Boden projiziert werden und sich mehrfach wiederholen. Zwischen jeder Bildprojektion wird die Ausgabe des Projektors auf schwarz gestellt.

Sobald Ihnen der Versuchsleiter ein Zeichen gibt, wird die Bildfolge gestartet. Dabei bestätigen Sie spontan (ohne zu überlegen) mit der **Tastaturtaste Y**, dass die Bodenprojektion wertig wirkt, und mit der **Tastaturtaste N** legen Sie fest, dass die Qualität der Bodenprojektion unzureichend ist. Sie haben **zwei Sekunden** Zeit die Projektion zu bewerten.



Bitte wenden

**BMW  
GROUP**

**BMW  
GROUP**

(a) Page 1

(b) Page 2

Sobald Sie einen Durchlauf des Tests abgeschlossen haben, erscheint eine „Danke“-Grafik. Der Versuchsleiter gibt Ihnen Bescheid, wenn der nächste Testdurchlauf wieder zum Start bereit ist. Wiederholen Sie diesen Vorgang für jede der sechs Testmöglichkeiten (Grafik bei 1m, 3m oder 5m und Text bei 1m, 3m oder 5m).

Im Anschluss erhalten Sie einen Fragebogen. Ein allgemeiner Überblick über das Probandenkollektiv wird erstellt, dabei besteht der erste Teil des Fragebogens aus personenbezogenen Daten. Der zweite Teil dient der Bewertung der Bodenprojektion.


Alle von Ihnen preisgegebenen Daten werden im Nachgang vertraulich und anonymisiert für die weitere Auswertung und Analyse verwendet.

Vielen Dank für Ihre Teilnahme.



Figure A.1.: Illustration of the introduction text for the participants used in the PGS and DDS tests in German.



 **Fragebogen**  
**Personenbezogene Daten**

Vielen Dank für Ihre Teilnahme an dieser Studie. Ihre Daten werden vertraulich behandelt und anonymisiert für die weitere Auswertung verwendet.

**Persönliche Angaben**

1. Geschlecht?
  - Weiblich
  - Männlich
  - Divers
  
2. Alter?
  
3. Benötigen Sie eine Sehhilfe?
  - Nein
  - Ja, welche? (Brille, Kontaktlinse)


Falls ja, sind Sie kurz- oder weitsichtig?

  - kurzsichtig
  - weitsichtig
  
4. Wie groß sind Sie?

Bitte wenden für weitere Fragen ☺ 



(a) Page 1

 **Fragebogen**  
**Bewertung der Seitenscheibenprojektion**

Bitte Bewerten Sie diese Fragen anhand der von Ihnen am wertigsten wahrgenommenen Bodenprojektion.

Die Bodenprojektion wirkt innovativ.

Trifft überhaupt nicht zu Trifft voll und ganz zu

Ich werde mein zukünftiges Auto mit einer Projektion ausstatten (Ausstattungspreis ca. 500€).

Trifft überhaupt nicht zu Trifft voll und ganz zu

Welche Inhalte würden Sie sich von einer Bodenprojektion erhoffen?

- Welcome-/ Goodbye- Nachricht
- Design Darstellungen (statisch, dynamisch)
- Wetterangaben
- Informationen zur Route
- Fahrzeugladestatus (el. KFZ)
- Sonstiges:

Welche weiteren Aspekte sind für eine hochwertige Projektion notwendig?


- Helligkeit
- Farbtreue
- Auflösung
- Kontrast
- scharfe Darstellung
- Größe
- Farbe
- Sonstiges:

Ich habe mich von der Projektion während des Probandentests geblendet gefühlt.

Trifft überhaupt nicht zu Trifft voll und ganz zu

Haben Sie lichttechnische Vorkenntnisse?

Trifft überhaupt nicht zu Trifft voll und ganz zu

Vielen Dank für Ihre Teilnahme. 



(b) Page 2

Figure A.2.: Illustration of the questionnaire used in the PGS and DDS tests in German.

## A.2. Materials for the SP and FR tests

### Instruktionsbogen.



#### Einleitung:

In dieser Studie geht es um die **variable Größe einer Bodenprojektion** neben dem Fahrzeug und dessen Abhängigkeit von der subjektiv wahrgenommenen Abbildungsqualität.

Ihre Aufgabe innerhalb dieses Versuches ist es, eine **Bewertung** von **unterschiedlich großen** Bildern in **verschiedenen Qualitätsstufen** durchzuführen. Falls Sie eine Sehhilfe benötigen, tragen Sie diese bitte während des gesamten Tests.

Um den Kontext der projizierten Grafiken verständlicher zu machen, können Sie sich folgende Szenarien vorstellen: Kurz vor dem Einsteigen wird Ihnen beim Blick auf Ihr Fahrzeug zum einen ein Schriftzug mit einer **Welcome-Nachricht** gezeigt. Zum anderen sehen Sie ein Symbol, das für Ihr nächstes Zielort die **Wetterprognose** darstellt.

#### Ablauf des Versuches:

Der Versuchsleiter wird Sie in einem bestimmten Betrachtungsabstand positionieren. Bevor der Versuch beginnt, bekommen Sie zunächst Beispiele eines Bildes mit hoher und geringer Wertigkeit (Qualität) gezeigt, die nicht in der Bildfolge enthalten sind.

Nach der Betrachtung der Beispielbilder, beginnt der eigentliche Versuch. Sie sollten dabei Ihren gesamten Körper frontal zum Auto richten und den **Blick stets auf das rote Fixationskreuz** am unteren Rand der Projektion halten.

Vor Ihnen wird eine Serie von Bildern auf den Boden projiziert, die verschiedene Qualitätsstufen des Schriftzuges bzw. Symbols zeigt und sich mehrfach wiederholt. Sobald Sie ein Bild sehen, drücken Sie bitte **spontan** (sofort/ ohne zu überlegen) die **Taste Y** („Yes“), falls die Bodenprojektion für Sie wertig wirkt. Wenn die Qualität der Bodenprojektion für Sie unzureichend ist, drücken Sie bitte die **Taste N** („No“). Sie haben **zwei Sekunden** Zeit die Projektion zu bewerten.



Wertig Nicht wertig

Bitte wenden

BMW GROUP

### Instruktionsbogen.



Nach diesem ersten Durchgang platziert Sie der Versuchsleiter in einem **neuen Betrachtungsabstand**. In dieser Entfernung wird der gesamte Versuch nochmals wie oben beschrieben wiederholt.

#### Abschluss:

Am Ende erhalten Sie einen **Fragebogen**, mit dem Angaben zu Ihren persönlichen Daten und Ihre Bewertung der gezeigten Nahfeldprojektion erfasst werden.

Zuletzt wird mithilfe eines automatischen Sehprüfgerätes ein **Sehtest** durchgeführt. Beim Blick in das Gerät werden Ihnen **vier Zeilen mit je fünf Ringen** präsentiert, die in 8 verschiedene Richtungen geöffnet sein können.



oben, rechts oben, rechts, rechts unten, unten, links unten, links, links oben

Teilen Sie dem Versuchsleiter bitte von oben beginnend Zeile für Zeile die **Öffnung des Rings** mit.

Alle von Ihnen preisgegebenen Daten werden im Nachgang vertraulich und anonymisiert für die weitere Auswertung und Analyse verwendet.

**Vielen Dank** für Ihre Teilnahme!

Und jetzt: **Viel Spaß!**

BMW GROUP

(a) Page 1

(b) Page 2

Figure A.3.: Illustration of the introduction text for the participants used in the SP and FR tests in German.

**Fragebogen.**  
Persönliche Angaben.



1. Geschlecht  
 Weiblich  
 Männlich  
 Divers

2. Alter

3. Benötigen Sie eine Sehhilfe?  
 Nein  
 Ja, welche? (Brille, Kontaktlinsen)  
  
 Sind sie kurz- oder weitsichtig?  
 kurzsichtig  
 weitsichtig

4. Körpergröße

5. Sind Sie selbst Fahrer eines Kraftfahrzeuges?  
 Ja  
 Nein

6. Haben Sie lichttechnische Vorkenntnisse?  
 Trifft überhaupt nicht zu  Trifft nicht zu  Trifft eher nicht zu  Trifft eher zu  Trifft zu  Trifft voll und ganz zu

7. Wie schwer ist es Ihnen gefallen, den Blick **dauerhaft** auf dem roten Fixationskreuz zu halten? Bitte **Schwierigkeitsgrad** ankreuzen.  
 Überhaupt nicht schwer  Nicht schwer  Eher nicht schwer  Eher schwer  Schwer  Sehr schwer

Probanden-Nr.: \_\_\_  
 V<sub>cc</sub>: \_\_\_\_\_



Bitte wenden

(a) Page 1

**Fragebogen.**  
Bewertung der Nahfeldprojektion.



8. Ich lege mehr Wert auf die Abbildungsqualität der Projektion als auf die Größe.  
 Trifft überhaupt nicht zu  Trifft nicht zu  Trifft eher nicht zu  Trifft eher zu  Trifft zu  Trifft voll und ganz zu

9. Ich habe mich während des Probandentests geblendet gefühlt.  
 Trifft überhaupt nicht zu  Trifft nicht zu  Trifft eher nicht zu  Trifft eher zu  Trifft zu  Trifft voll und ganz zu

10. Die dargestellte **Größe** der Projektionsgrafiken empfand ich im **Verhältnis** zum Fahrzeug und der Entfernung als angemessen.

Entfernung	Grafik	Trifft nicht zu	Trifft eher nicht zu	Trifft eher zu	Trifft zu
1 m	Klein	<input type="checkbox"/>	<input type="checkbox"/>	<input type="checkbox"/>	<input type="checkbox"/>
	Mittel	<input type="checkbox"/>	<input type="checkbox"/>	<input type="checkbox"/>	<input type="checkbox"/>
	Groß	<input type="checkbox"/>	<input type="checkbox"/>	<input type="checkbox"/>	<input type="checkbox"/>
3 m	Klein	<input type="checkbox"/>	<input type="checkbox"/>	<input type="checkbox"/>	<input type="checkbox"/>
	Mittel	<input type="checkbox"/>	<input type="checkbox"/>	<input type="checkbox"/>	<input type="checkbox"/>
	Groß	<input type="checkbox"/>	<input type="checkbox"/>	<input type="checkbox"/>	<input type="checkbox"/>

11. Wie schwer ist Ihnen die Bewertung der Abbildungsqualität beim **Text** im Vergleich zum Symbol gefallen (unabhängig von der Entfernung)? Bitte **Schwierigkeitsgrad** ankreuzen.  
 Überhaupt nicht schwer  Nicht schwer  Eher nicht schwer  Eher schwer  Schwer  Sehr schwer

12. Kreuzen Sie bitte den entsprechenden **Schwierigkeitsgrad** der Qualitätsbewertung der Grafiken bei den jeweiligen Entfernungen an.

Entfernung	Grafik	Nicht schwer	Eher nicht schwer	Eher schwer	Schwer
1 m	Kleines Symbol	<input type="checkbox"/>	<input type="checkbox"/>	<input type="checkbox"/>	<input type="checkbox"/>
	Kleiner Schriftzug	<input type="checkbox"/>	<input type="checkbox"/>	<input type="checkbox"/>	<input type="checkbox"/>
3 m	Mittleres Symbol	<input type="checkbox"/>	<input type="checkbox"/>	<input type="checkbox"/>	<input type="checkbox"/>
	Großer Schriftzug	<input type="checkbox"/>	<input type="checkbox"/>	<input type="checkbox"/>	<input type="checkbox"/>



(b) Page 2

Figure A.4.: Illustration of the questionnaire used in the SP and FR tests in German.

Table A.1.: Projection sizes of the SP and FR tests displayed in the resulting viewing angle (vertical and horizontal) of the participants with an average German person's height [125] in degrees. The participant is either 1 m or 3 m apart from the projection area.

Viewing angle in °	SP symbol			SP text			FR text		
	small	middle	big	small	middle	big	small	middle	big
$\phi_{\text{vert}}$ , 1 m	2.52	7.46	13.23	3.10	5.88	9.27	3.10	5.88	9.27
$\phi_{\text{hor}}$ , 1 m	8.42	23.28	38.49	14.71	27.41	41.42	13.65	24.76	37.65
$\phi_{\text{vert}}$ , 3 m	0.83	2.49	4.46	1.03	1.96	3.10	1.03	1.96	3.10
$\phi_{\text{hor}}$ , 3 m	2.91	8.67	15.79	5.14	10.05	16.22	4.76	9.05	14.65

### A.3. Materials for the DP test



#### Instruktion Wertigkeit einer dynamischen Umfeldprojektion

In dieser Studie geht es um die subjektive Wahrnehmung der Wertigkeit einer Bodenprojektionsdarstellung neben dem Fahrzeug.

Ihre Aufgabe innerhalb dieses Versuchs ist es, eine Bewertung von Videosequenzen in verschiedenen Wertigkeitsstufen durchzuführen.

Die Studie wird unter Ihren persönlichen Normalbedingungen durchgeführt, dies bedeutet, falls Sie eine Sehhilfe benötigen, tragen Sie bitte die notwendige Sehhilfe während des gesamten Tests.

Bevor Sie die verschiedenen Wertigkeitsstufen der Bilder bewerten dürfen, bekommen Sie Beispiele einer Videosequenz mit geringer und hoher Wertigkeit gezeigt, die nicht in der Bildfolge enthalten sind.

Nach der Betrachtung der Beispielvideos, beginnt die Qualitätsbewertung der dynamischen Bodenprojektion. Platzieren Sie sich hierfür an den markierten Stellen, welche sich in einem Abstand von 1m oder 3m von der Projektionsfläche befinden. Somit durchlaufen Sie je Test zwei verschiedene Betrachtungsabstände. Ihr Blick sollte dabei frontal auf das Auto gerichtet sein.

Der Versuchsleiter präsentiert Ihnen jeweils acht Videosequenzen in verschiedenen Qualitätsstufen, die auf dem Boden projiziert werden und sich mehrfach wiederholen. Zwischen jeder Bildprojektion wird die Ausgabe des Projektors auf schwarz gestellt.

Sobald Ihnen der Versuchsleiter ein Zeichen gibt, wird der Test gestartet. Dabei bestätigen Sie, wenn Sie mit der Nachricht „**Bitte geben Sie ihre Antwort jetzt ab!**“ aufgefordert werden, spontan (ohne zu überlegen) mit der **Tastaturtaste Y**, dass die Bodenprojektion wertig wirkt, und mit der **Tastaturtaste N** legen Sie fest, dass die Bodenprojektion nicht wertig wirkt. Sie haben **zwei Sekunden** Zeit die Projektion zu bewerten.



Bitte wenden

**BMW  
GROUP**

**BMW  
GROUP**

(a) Page 1

(b) Page 2

Figure A.5.: Illustration of the introduction text for the participants used in the DP test in German.

Sobald Sie einen Durchlauf des Tests abgeschlossen haben, erscheint eine „Danke“-Nachricht. Der Versuchsleiter gibt Ihnen Bescheid, wenn der nächste Testdurchlauf wieder zum Start bereit ist. Wiederholen Sie diesen Vorgang für jede Betrachtungsentfernung.

Im Anschluss erhalten Sie einen Fragebogen. Ein allgemeiner Überblick über das Probandenkollektiv wird erstellt, dabei besteht der erste Teil des Fragebogens aus personenbezogenen Daten. Der zweite Teil dient der Bewertung der Bodenprojektion.

Alle von Ihnen preisgegebenen Daten werden im Nachgang vertraulich und anonymisiert für die weitere Auswertung und Analyse verwendet.

Vielen Dank für Ihre Teilnahme.





Fragebogen  
Personenbezogene Daten

Probandennummer: \_\_

Vielen Dank für Ihre Teilnahme an dieser Studie. Ihre Daten werden vertraulich behandelt und anonymisiert für die weitere Auswertung verwendet.

Persönliche Angaben

1. Geschlecht?

- Weiblich
- Männlich
- Divers

2. Alter?

3. Benötigen Sie eine Sehhilfe?

- Nein
- Ja, welche? (Brille, Kontaktlinse)

Falls ja, sind Sie kurz- oder weitsichtig?

- kurzsichtig
- weitsichtig

4. Wie groß sind Sie?

5. Haben Sie lichttechnische Vorkenntnisse?

- Trifft überhaupt nicht zu  Trifft nicht zu  Trifft eher nicht zu  Trifft eher zu  Trifft zu  Trifft voll und ganz zu

6. Ich habe mich von der Projektion während des Probandentests geblendet gefühlt.

- Trifft überhaupt nicht zu  Trifft nicht zu  Trifft eher nicht zu  Trifft eher zu  Trifft zu  Trifft voll und ganz zu

7. Die Animationsgeschwindigkeit der gezeigten Videosequenz empfand ich als störend.

- Trifft überhaupt nicht zu  Trifft nicht zu  Trifft eher nicht zu  Trifft eher zu  Trifft zu  Trifft voll und ganz zu

8. Die Bodenprojektion wirkt innovativ.

- Trifft überhaupt nicht zu  Trifft nicht zu  Trifft eher nicht zu  Trifft eher zu  Trifft zu  Trifft voll und ganz zu



(a) Page 1



Fragebogen  
Bewertung der Umfeldprojektion

9. Die Animationsgeschwindigkeit der gezeigten Videosequenz empfand ich als angenehm.

- Trifft überhaupt nicht zu  Trifft nicht zu  Trifft eher nicht zu  Trifft eher zu  Trifft zu  Trifft voll und ganz zu

9a. Die Animationsgeschwindigkeit der gezeigten Videosequenz empfand ich als langsam.

- Trifft überhaupt nicht zu  Trifft nicht zu  Trifft eher nicht zu  Trifft eher zu  Trifft zu  Trifft voll und ganz zu

9b. Die Animationsgeschwindigkeit der gezeigten Videosequenz empfand ich als schnell.

- Trifft überhaupt nicht zu  Trifft nicht zu  Trifft eher nicht zu  Trifft eher zu  Trifft zu  Trifft voll und ganz zu

10. Für wie wichtig erachten Sie folgende Inhalte einer Bodenprojektion? Setzen Sie ein Kreuz pro Faktor.

	Nicht wichtig	Eher nicht wichtig	Eher wichtig	Sehr wichtig
Welcome-/ Goodbye- Nachricht				
Wetterangaben				
Statische design Darstellungen (z.B. Bild)				
Dynamische design Darstellungen (z.B. Video)				
Personalisierter Inhalt (Lieblingsverein, Haustier etc.)				
Fahrzeugladestatus (el. KFZ)				
Interaktive Elemente (Spiele etc.)				

11. Für wie wichtig erachten Sie die folgenden Faktoren in Hinblick auf eine Bodenprojektion? Setzen Sie ein Kreuz pro Faktor.

	Nicht wichtig	Eher nicht wichtig	Eher wichtig	Sehr wichtig
Farbe				
Größe				
Bewegungsgeschwindigkeit				
Helligkeit				
Auflösung				
scharfe Darstellung				
sichtbar bei Tag				
sichtbar bei Dämmerung/Nacht				
Kontrast				

12. Ich würde mein zukünftiges Auto mit einer Projektionstechnik ausstatten (Ausstattungskosten: 500€).

- Trifft überhaupt nicht zu  Trifft nicht zu  Trifft eher nicht zu  Trifft eher zu  Trifft zu  Trifft voll und ganz zu

Vielen Dank für Ihre Teilnahme!

(b) Page 2

Figure A.6.: Illustration of the questionnaire used in the DP test in German.

## A.4. Questionnaire analysis

In order to understand which aspects require more detailed consideration, interviews were conducted with almost 200 participants, listed in Table 3.6, on various focus topics. Thus, the questionnaire analysis defines the necessary aspects and establishes the correlation or effect between the different subject collectives. In general, it is essential to understand which aspects are important for near-field projections. Therefore, in addition to the factors for high-quality projections, the projection content is evaluated using a questionnaire. These are the selected aspects of this review, and Appendix A lists the original questionnaires and test introductions. Furthermore, all questionnaires are formulated and asked in German, as this is the native language of the subjects who participated in Munich. Finally, the results of the questionnaires guarantee the customer opinion

through the aspects discussed here and other aspects considered in detail in published papers [135, 136].

The following analysis focuses on the questionnaires asked in the DP test after the testing since the participants were able to experience not only static projected content on the street’s surface but also animated sequences (described in detail in Section 3.3.2), which ensures the subjective feedback of the participants regarding projection content, aspects for high-quality projections and animation speed’s perception. Therefore, the timing of the questionnaire (before or after the representation of the projected content) does not play a significant role in the reviewed results [136]. Furthermore, depending on the relevant question of the questionnaire, an influence of aspects such as age or previous experience with lighting technology is evaluated by statistical testing. The experience of lighting technology, specifically if the participants are experts in developing lighting systems, can influence their subjective perception and the rating of the projection quality [172, 173].

#### A.4.1. Projection content for near-field projections

The questionnaire of the DP test, as in the other tests (Appendix A), is separated into three parts: the first segment consists of general personal information such as gender, age, and prior experience with lighting technology. The question about lighting experience used an even-numbered Likert rating scale [99, 98]. Second, the participant’s perception of animation speed for the experienced animated sequences of the design-orientated projection content. The third questionnaire’s segment evaluated the projection content and aspects for high-quality near-field projections.

With this in mind, two main influence factors can affect the questionnaire results related to the participants’ collective: First, the participant’s age and, second, the previous experience/ knowledge with lighting technology. The knowledge level refers to the rating’s six points from ‘1: Strongly Disagree’ to ‘6: Strongly Agree’ [99, 98] on the Likert scale. In conclusion, these knowledge levels refer to *expert* with the response options 5 and 6, *neutral* relates to response options 3 and 4, and *layperson* refers to response options 1 and 2. Figure A.7 illustrates the answers of 44 participants in the DP test for the question ‘Is the following content of a near-field projection important for you?’ in a boxplot chart.

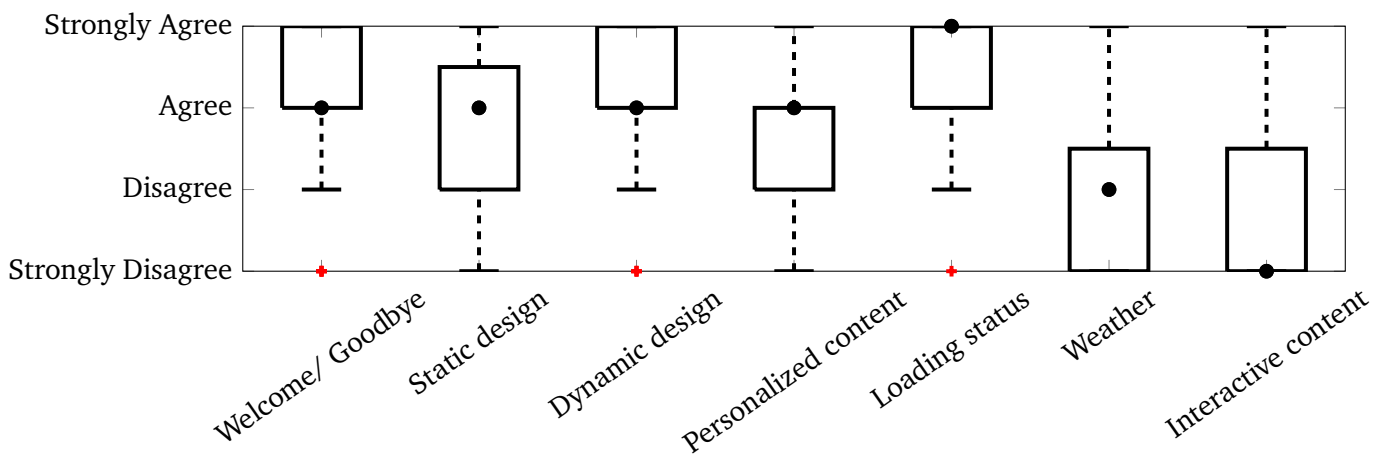


Figure A.7.: Illustration of the question in the DP test: ‘Is the following content of a near-field projection important for you?’ The following items are listed: Welcome/ Goodbye, Static design, Dynamic design, Personalized content, Loading status, Weather, and Interactive content. The illustration of the boxplots from a strong disagreement or strong agreement with the question indicates the answers of the 44 participants. A bullet point marks the median value, and the red crosses indicate the outliers of the boxplots. One cross for outliers can indicate multiple entries.

The value that lies precisely in the middle of a theoretical data distribution is called the median [145] and allows in this analysis of the questionnaires a simplified representation of the trends of the answer to the question in Figure A.7. For example, the projection contents of welcome/ goodbye message, static design, dynamic design, and personalized content have the same median, which refers to the trend, that the participants agree that these projection contents are essential for them to appear as a near-field projection. The exhaustive presentation of the boxplots, including the scattering and the outliers, is displayed in detail in Figure A.7. Further, the content loading status has a notable trend, which strongly agrees with the importance of projection content for near-field projections. Contradictorily, there are also contents such as weather information or interactive content, which is rated with a disagreement or strong disagreement by the participants and therefore is unsuitable for near-field projections according to the 44 participants in the DP test (Figure A.7). Moreover, the results of the DP test have similar tendencies related to the projection content [135, 136].

No focus is on the influence of gender due to the low number of females in most of the tests, which also limits the usage of statistical analysis methods. All statistical analysis uses the statistical program JASP [174]. Additionally, the influence factors of the questionnaire (age and knowledge) generate groups of more than nine participants, which assures that an estimated standard deviation of 5% is current in the participant collective, according to Nielsen and Landauer [175]. Nevertheless, the depicted contents for near-field projections (Figure A.7) are analyzed with a MANOVA considering the influence of age and knowledge of the participants. The age groups are 20-29, 30-39, and 40 and older to have groups of more than nine participants [175]. The knowledge levels refer to expert, neutral, and layperson, defined above as related to the Likert scale rating. A MANOVA was used to compare the projection contents under the observation of the factors, which were not significant, Wilks'  $\Lambda = 0.737$ ,  $F = 0.779$ ,  $p = .687$  for age, and Wilks'  $\Lambda = 0.791$ ,  $F = 0.587$ ,  $p = .866$  for knowledge (Table A.2). Nevertheless, it does not lead to a generalized statement [148] that age or previous knowledge/ experience cannot influence the results. No significance was found in this participant's collective, which may correlate to the low number of participants  $N = 44$ .

Table A.2.: MANOVA with the Wilks test for the near-field projection contents displayed in Figure A.7 under the consideration of influence factors such as age and previous knowledge for the DP test.

Cases	df	Approx. F	Wilks' $\Lambda$	Num df	Den df	p
Age	2	0.779	0.737	14	66.000	0.687
Knowledge	2	0.587	0.791	14	66.000	0.866
Residuals	39					

#### A.4.2. Aspects for high quality near-field projections

The participants fill out the questionnaire after the DP test; thus, the subjects know the mentioned aspects for a high-quality projection due to the relation of the seen projections of the testing. For example, the questionnaire lists the following aspects: brightness, daytime visibility, night/ dusk visibility, contrast, resolution, sharpness, size, animation speed, and color for evaluation as essential aspects for near-field projections. Figure A.8 displays the evaluated results in a boxplot graph with rating ranges from strong disagreement to strong agreement for the possible high-quality aspects of near-field projections. On the one hand, the features of brightness, nighttime/ dusk and dawn visibility, resolution, and sharpness strongly agree to be necessary for near-field projections. Further, daytime visibility, contrast, and size are also positively rated (median equal or above 'Agree') for their importance for near-field projections.

On the other hand, all these factors have slight deviations ranging with their whiskers from strong agreement



to disagreement, besides the nighttime/ dusk and dawn visibility, which highlights its importance by just ranging in the agreement sector (displayed in Figure A.8). Additionally, these named factors so far (brightness, daytime visibility, night/ dusk visibility, contrast, resolution, sharpness, and size) are specific factors, which are evaluated in this work further with physical values, such as Weber contrasts, resolution and projection's target luminance, and were defined in section 3 before. Besides, animation speed and color deviate stronger than the other aspects and cover the whole range of possible ratings, which displays a divergent opinion for these two aspects (Figure A.8). However, the aspect of animation speed is evaluated extensively with a subjective opinion in a questionnaire by the participants in the next section.

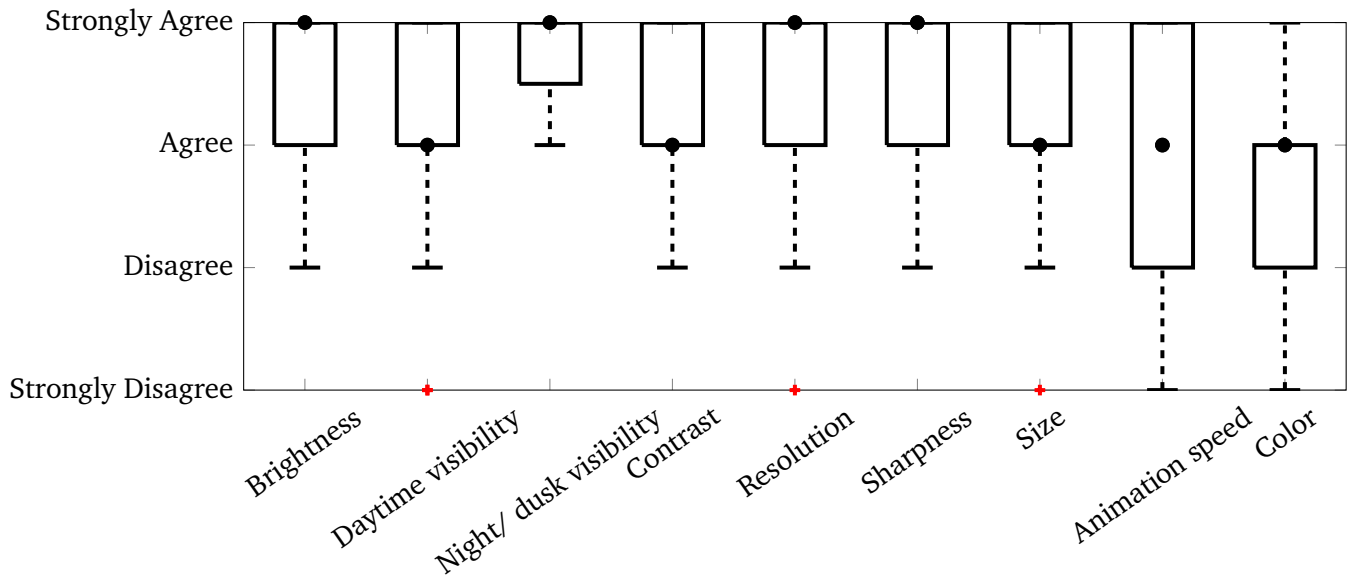


Figure A.8.: Illustration of the question in the DP test: 'Are the following aspects for high-quality near-field projection important for you?' The following items are listed: Brightness, daytime visibility, night/ dusk visibility, contrast, resolution, sharpness, size, animation speed, and color. The illustration of the boxplots from a strong disagreement or strong agreement with the question indicates the answers of the 44 participants. A bullet point marks the median value, and the red crosses indicate the outliers of the boxplots. One cross for outliers can indicate multiple entries.

Moreover, a MANOVA compares the aspects of Figure A.8 under the observation of the age factor, including the same three age groups as mentioned in section A.4.1, which was not significant, Wilks'  $\Lambda = 0.497$ ,  $F = 1.486$ ,  $p = .125$ . Nevertheless, all aspects mentioned for high-quality near-field projections are crucial since they are always displayed or mentioned in articles or illustrations for projection technology in the automotive sector [131, 132, 144, 42].

Table A.3.: MANOVA with the Wilks test for aspects of high-quality for near-field projections displayed in Figure A.8 under the consideration of age as an influencing factor for the DP test.

Cases	df	Approx. F	Wilks' $\Lambda$	Num df	Den df	p
Age	2	1.486	0.497	18	64.000	0.125
Residuals	40					

### A.4.3. Perception of the animation speed of the dynamic near-field projections

In addition to the general information in the near-field projection context, an evaluation of the participants' perception of the experienced design-orientated animated sequence is essential. For example, the perception of the animation speed is essential for understanding if the selected animation speed may cause a disturbing or pleasant feeling in the participant, which can influence the participant's evaluation of the task of defining a high-quality illustration of the near-field projection. Additionally, the subjective evaluation of the speed perception via questionnaires supports the DVA facet of near-field projections.

Therefore, the participants filled out a questionnaire after experiencing the animated design-orientated projection content (described in section 3.3.2), which had a defined range of the animation speed of 0.25 to 1 Hz that is also applied to some extent in the semi-dynamic light carpet of the BMW i7 [144]. The asked aspects include the subjective perception of the experienced animated sequence in four conditions, whether the animation speed appears pleasant, slow, fast, or disturbing. The resulting boxplots are displayed in Figure A.9.

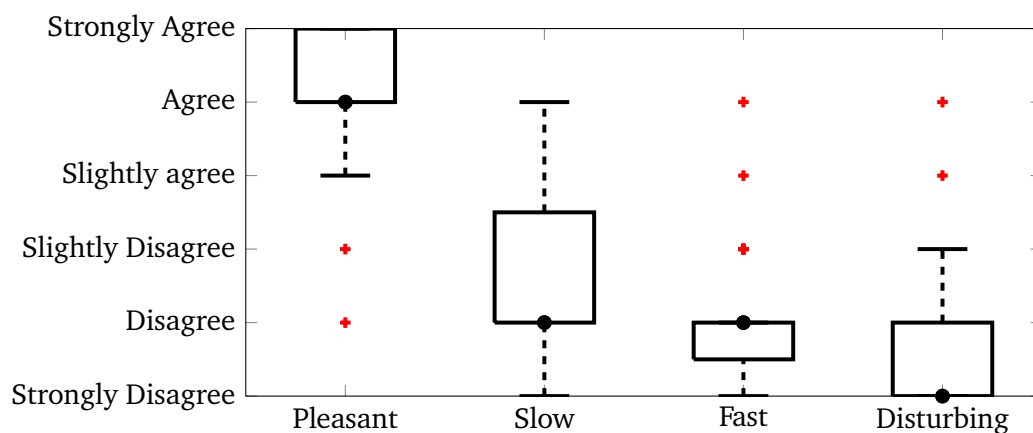


Figure A.9.: Illustration of the question in the DP test: 'I perceive the animation speed of the shown projection sequence as ...'. The following features regarding the animation speed are: Pleasant, slow, fast, and disturbing. The illustration of the boxplots ranges from a strong disagreement or strong agreement with a six-grade Likert scale with the answers of 44 participants. A bullet point marks the median value, and the red crosses indicate the outliers of the boxplots. One cross for outliers can indicate multiple entries.

The Likert scale has a six-grade scale, which Lozano et al. and Simms et al. verify, to evaluate the perception of the selected animation speeds from 0.25 to 1 Hz. According to the 44 participants, the speed is agreed as pleasant, with some outliers. However, the main boxplot and its whisker are above slight agreement (Figure A.9). Further, the participants evaluate the animation speed as not too slow even tho the boxplot has a significant deviation ranging from strong disagreement to an agreement (Figure A.9). Additionally, the selected range of 0.25 to 1 Hz is perceived as not fast due to the disagreement in Figure A.9. The boxplot is also very small, indicating a clear opinion of the 44 participants (with some outliers). Finally, the animation speed does not disturb the participants (Figure A.9), which completes the overall positive opinion that the selected speed range of 0.25 to 1 Hz is suitable for design-orientated near-field projections. Besides, the favorable opinion of the participants allows the interpretation of the evaluation of resolution aspects in this chapter since the participants felt pleasant and not disturbed by the animation sequence they experienced in the DP test. Furthermore, a MANOVA indicates that the possible influence factors of age and previous knowledge were not significant for the aspect of speed perception, Wilks'  $\Lambda = 0.828$ ,  $F = 0.940$ ,  $p = .489$  for age, and Wilks'  $\Lambda = 0.866$ ,  $F = 0.707$ ,  $p = .684$  for knowledge (Table A.4).

However, looking into detail, the MANOVA on the aspect that the animation speed feels pleasant, indicates an age significance  $F(2, 41) = 3.294, p = .047$ .

Table A.4.: MANOVA with the Wilks test for the perception of the animation speed of the projected content, which refers to Figure A.7, under the consideration of influence factors such as age and previous knowledge for the DP test.

Cases	df	Approx. F	Wilks' $\Lambda$	Num df	Den df	p
Age	2	0.940	0.828	8	76.000	0.489
Knowledge	2	0.707	0.866	8	76.000	0.684
Residuals	41					

Figure A.10 represents the boxplot involving the three different age groups. The 30-39-year-old participants have a slightly divergent answer distribution compared to the other two age groups listed in Appendix A. Nevertheless, the small number of participants leads to either a tendency or to the point of wrong significance related to the aspects mentioned by Amrhein et al. [148].

#### A.4.4. Additional material for the questionnaire analysis

Table A.5.: ANOVA regarding the animation speed perception if the displayed design-orientated animation in the DP test gave a pleasant feeling to the participants while observing the animation.

Cases	Sum of Squares	df	Mean Square	F	p
Age	4.695	2	2.347	3.294	0.047
Residuals	29.214	41	0.713		

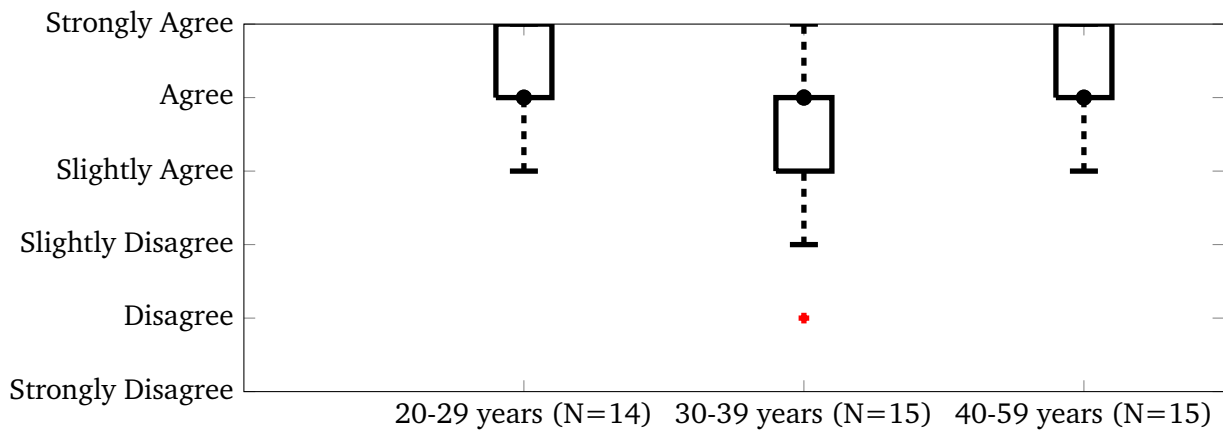


Figure A.10.: Illustration of the question in the DP test: 'I perceive the animation speed of the shown projection sequence as pleasant.' The illustration of the boxplots ranges from a strong disagreement or strong agreement with a six-grade Likert scale with the answers of 44 participants in three age groups of 20-29 years, 30-39 years, and older than 40 years. A bullet point marks the median value, and the red crosses indicate the outliers of the boxplots. One cross for outliers can indicate multiple entries.

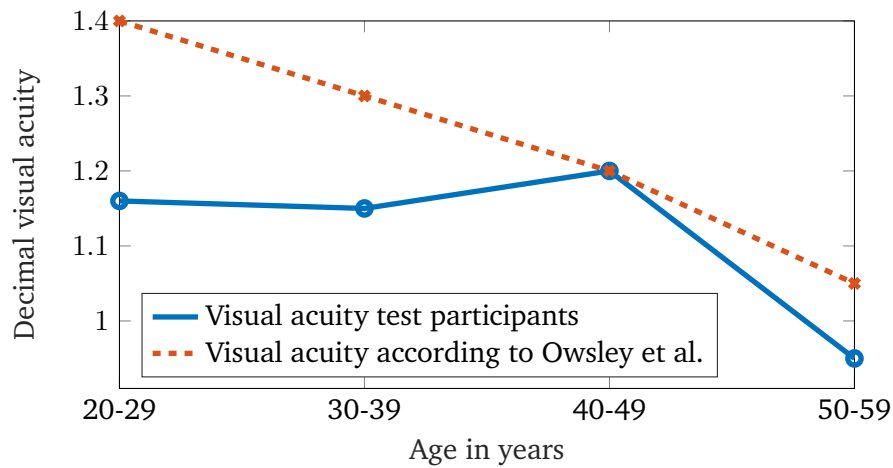


Figure A.11.: Visual acuity of the SP test participants (blue line) compared to the literature by Owsley et al. [147] (dashed red line), divided into four age groups between 20 and 59 years. The usage of a binoptometer determines the visual acuity of the study participants [176]. The method of Palidis et al. [83] calculated the participants' exact decimal visual acuity. Further, the graph shows the progression of the visual acuity of the test participants for the four age groups. Values from the literature of Owsley et al. are used for comparison [147], which are rounded for every respective age group.

## B. Additional analysis for resolution aspects of near-field projections

### B.1. Logistic regression analysis for resolution aspects

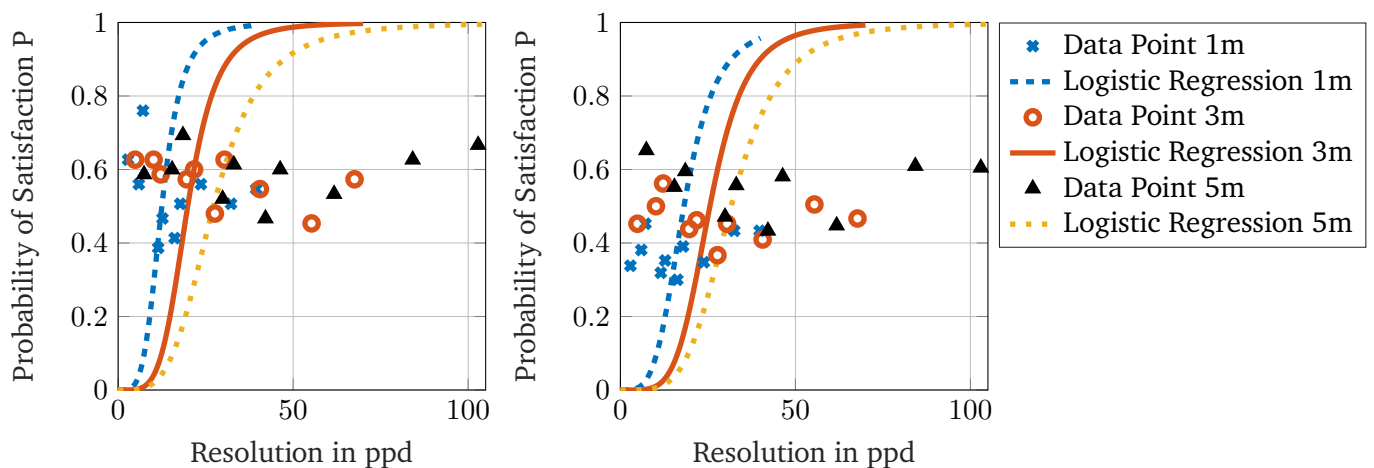


Figure B.1.: Results of the analyzed data applying the logistic regression equation 4.1 to identify the 90% threshold for the resolution in ppd, including the probability of satisfaction in the PGS and DDS. On the left: A detailed illustration of the logistic regression of the text-based projection in the PGS, including the raw data marked with crosses for 1 m data, circles for 3 m data, and triangles for 5 m data. On the right: The detailed logistic regression of the text-based projection in the DDS includes the raw data, marked with crosses for 1 m data, with circles for 3 m data, and triangles for 5 m data.

The legend on the right relates to both graphs' colors and symbols.

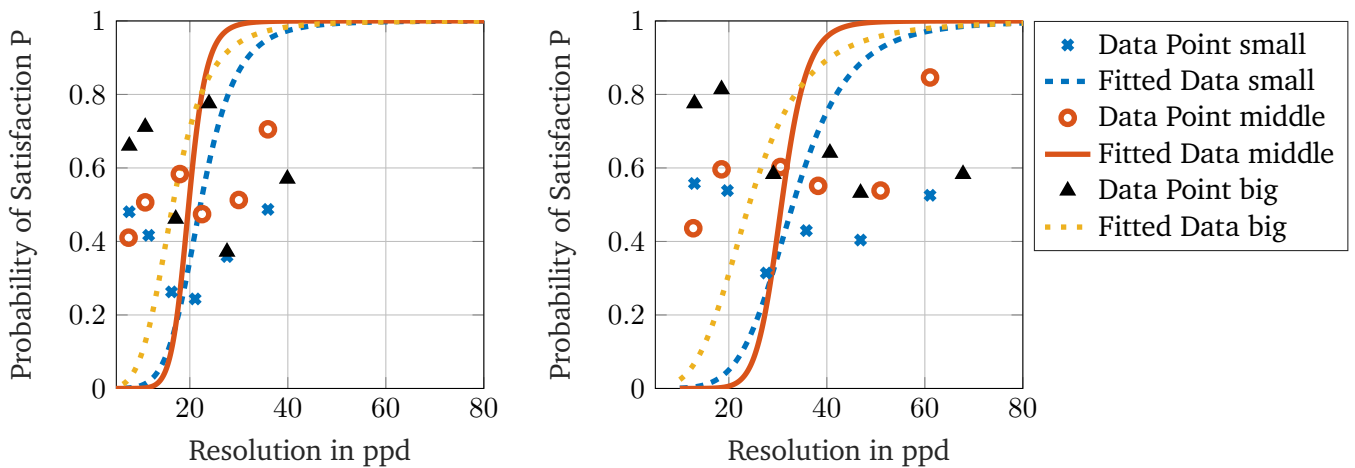


Figure B.2.: Results of the analyzed data applying the logistic regressing equation 4.1 to identify the 90 % threshold for the resolution in *ppd*, including the probability of satisfaction in the SP test. On the left: A detailed illustration of the logistic regression of the regular symbol-based projection in the SP at 1 m viewing distance, including the raw data marked with crosses for small-sized projection, circles for middle-sized projections and triangles for the big-sized projections. On the right: regression of the regular symbol-based projection in the SP at 3 m viewing distance, including the raw data marked with crosses for small-sized projections, circles for middle-sized projections, and triangles for the big-sized projections. The legend on the right relates to both graphs' colors and symbols.

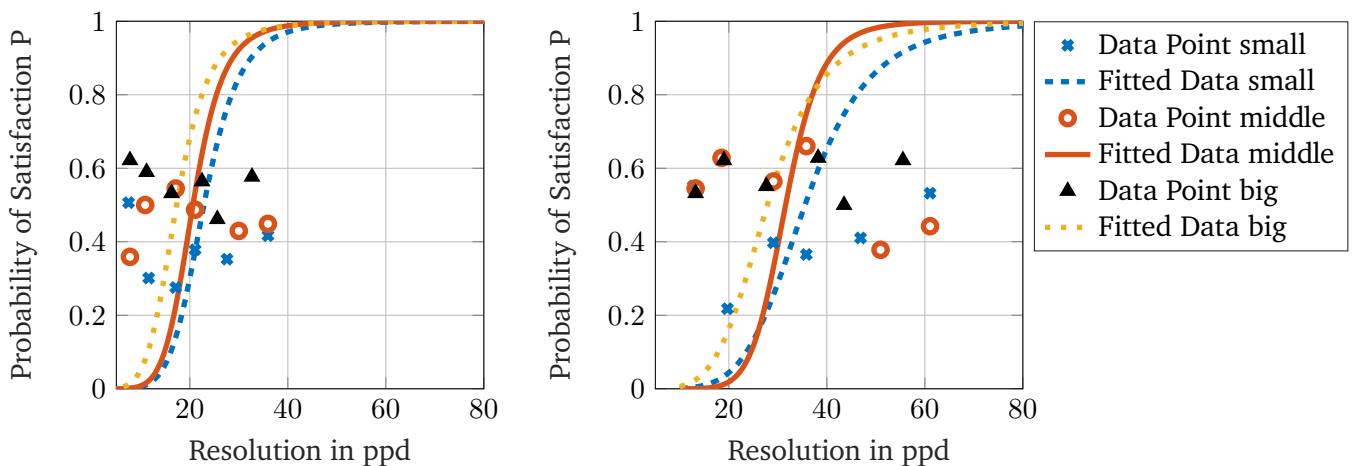


Figure B.3.: Results of the analyzed data applying the logistic regressing equation 4.1 to identify the 90 % threshold for the resolution in *ppd*, including the probability of satisfaction in the SP test. On the left: A detailed illustration of the logistic regression of the regular text-based projection in the SP at 1 m viewing distance, including the raw data marked with crosses for small-sized projection, circles for middle-sized projections and triangles for the big-sized projections. On the right: regression of the regular text-based projection in the SP at 3 m viewing distance, including the raw data marked with crosses for small-sized projections, circles for middle-sized projections, and triangles for the big-sized projections. The legend on the right relates to both graphs' colors and symbols.

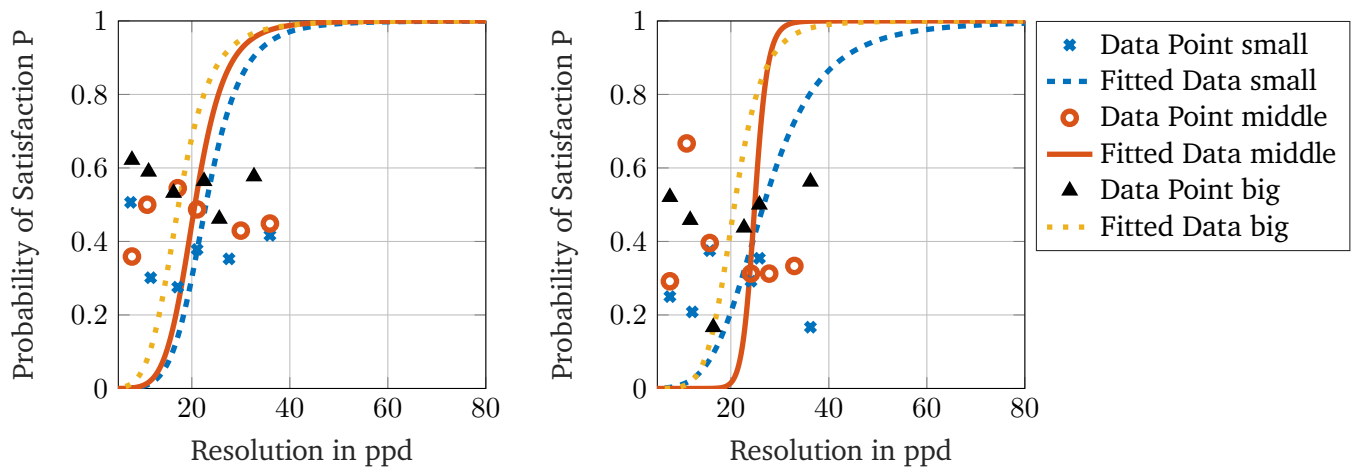


Figure B.4.: Results of the analyzed data applying the logistic regression equation 4.1 to identify the 90 % threshold for the resolution in *ppd*, including the probability of satisfaction in the SP and FR tests. On the left: A detailed illustration of the logistic regression of the regular text-based projection in the SP at 1 m viewing distance, including the raw data marked with crosses for small-sized projections, circles for middle-sized projections, and triangles for the big-sized projections. On the right: The detailed logistic regression of the italic text-based projection in the FR at 1 m viewing distance, including the raw data marked with crosses for small-sized projections, circles for middle-sized projections, and triangles for the big-sized projections. The legend on the right relates to both graphs' colors and symbols.



## B.2. Statistical analysis for dependencies of resolution aspects

Table B.1.: Chi-square analysis defines the statistical effects of viewing distance, ambient lighting, and projection content for PGS and DDS tests. The Table also includes the related effect size (Cramer's V).

	Compared items	Text	Symbol
Distance PGS	1 m x 3 m	$\chi^2(9) = 2.53, p > 0.05,$ $V = 0.06$	$\chi^2(9) = 4.29, p > 0.05,$ $V = 0.07$
	1 m x 5 m	$\chi^2(8) = 15.09, p > 0.05,$ $V = 0.13$	$\chi^2(9) = 18.48, p < 0.05,$ $V = 0.14$
	3 m x 5 m	$\chi^2(9) = 11.89, p > 0.05,$ $V = 0.11$	$\chi^2(9) = 9.71, p > 0.05,$ $V = 0.10$
Distance DDS	1 m x 3 m	$\chi^2(8) = 16.72, p < 0.05,$ $V = 0.10$	$\chi^2(9) = 16.96, p < 0.05,$ $V = 0.09$
	1 m x 5 m	$\chi^2(8) = 72.43, p < 0.05,$ $V = 0.19$	$\chi^2(9) = 68.47, p < 0.05,$ $V = 0.17$
	3 m x 5 m	$\chi^2(8) = 32.74, p < 0.05,$ $V = 0.12$	$\chi^2(8) = 22.39, p < 0.05,$ $V = 0.10$
Ambient lighting	1 m PGS x 1 m DDS	$\chi^2(8) = 30.39, p < 0.05,$ $V = 0.17$	$\chi^2(9) = 29.70, p < 0.05,$ $V = 0.14$
	3 m PGS x 3 m DDS	$\chi^2(9) = 24.19, p < 0.05,$ $V = 0.13$	$\chi^2(8) = 20.72, p < 0.05,$ $V = 0.11$
	5 m PGS x 5 m DDS	$\chi^2(8) = 17.01, p < 0.05,$ $V = 0.10$	$\chi^2(9) = 21.79, p < 0.05,$ $V = 0.11$
		<b>PGS</b>	<b>DDS</b>
Projection content	Text 1 m x Symbol 1 m	$\chi^2(9) = 5.73, p > 0.05,$ $V = 0.08$	$\chi^2(9) = 15.65, p > 0.05,$ $V = 0.09$
	Text 3 m x Symbol 3 m	$\chi^2(9) = 10.49, p > 0.05,$ $V = 0.11$	$\chi^2(8) = 23.23, p < 0.05,$ $V = 0.11$
	Text 5 m x Symbol 5 m	$\chi^2(9) = 11.53, p > 0.05,$ $V = 0.11$	$\chi^2(8) = 23.96, p < 0.05,$ $V = 0.10$

Table B.2.: Chi-square analysis defines the statistical effects of viewing distance, projection size, and projection content for the SP test. The Table also includes the related effect size (Cramer's V).

	Compared items	Text	Symbol
Sizes 1 m	small x middle	$\chi^2(5) = 6.51, p > 0.05,$ $V = 0.09$	$\chi^2(5) = 20.54, p < 0.05,$ $V = 0.16$
	small x big	$\chi^2(5) = 31.56, p < 0.05,$ $V = 0.19$	$\chi^2(5) = 48.05, p < 0.05,$ $V = 0.23$
	middle x big	$\chi^2(5) = 12.60, p < 0.05,$ $V = 0.11$	$\chi^2(5) = 10.59, p > 0.05,$ $V = 0.10$
Sizes 3 m	small x middle	$\chi^2(5) = 9.28, p > 0.05,$ $V = 0.10$	$\chi^2(5) = 13.69, p < 0.05,$ $V = 0.12$
	small x big	$\chi^2(5) = 19.95, p < 0.05,$ $V = 0.15$	$\chi^2(5) = 33.03, p < 0.05,$ $V = 0.18$
	middle x big	$\chi^2(5) = 3.67, p > 0.05,$ $V = 0.06$	$\chi^2(5) = 8.80, p > 0.05,$ $V = 0.09$
Distance (1 m x 3 m)	small	$\chi^2(5) = 9.12, p > 0.05,$ $V = 0.11$	$\chi^2(5) = 13.66, p < 0.05,$ $V = 0.13$
	middle	$\chi^2(5) = 8.81, p > 0.05,$ $V = 0.09$	$\chi^2(5) = 10.17, p > 0.05,$ $V = 0.09$
	big	$\chi^2(5) = 1.08, p > 0.05,$ $V = 0.03$	$\chi^2(5) = 5.01, p > 0.05,$ $V = 0.07$

Table B.3.: Chi-square analysis defines the statistical effects of the projection content of either the comparison of the symbol- and text-based projection and the two various fonts (regular and italic) for the SP and FR tests. The Table also includes the related effect size (Cramer's V).

	Compared items	1 m	3 m
Content	Symbol x Text (small)	$\chi^2(5) = 6.34, p > 0.05,$ $V = 0.09$	$\chi^2(5) = 2.22, p > 0.05,$ $V = 0.05$
	Symbol x Text (middle)	$\chi^2(5) = 8.25, p > 0.05,$ $V = 0.09$	$\chi^2(5) = 5.44, p > 0.05,$ $V = 0.07$
	Symbol x Text (big)	$\chi^2(5) = 2.35, p > 0.05,$ $V = 0.05$	$\chi^2(5) = 9.71, p > 0.05,$ $V = 0.10$
Font	regular x italic (small)	$\chi^2(5) = 6.25, p > 0.05,$ $V = 0.13$	
	regular x italic (middle)	$\chi^2(5) = 9.51, p > 0.05,$ $V = 0.09$	
	regular x italic (big)	$\chi^2(5) = 9.36, p > 0.05,$ $V = 0.13$	



---

## C. Additional material for the contrast and perception tests

---

### C.1. Measurements for characterizing the test setup

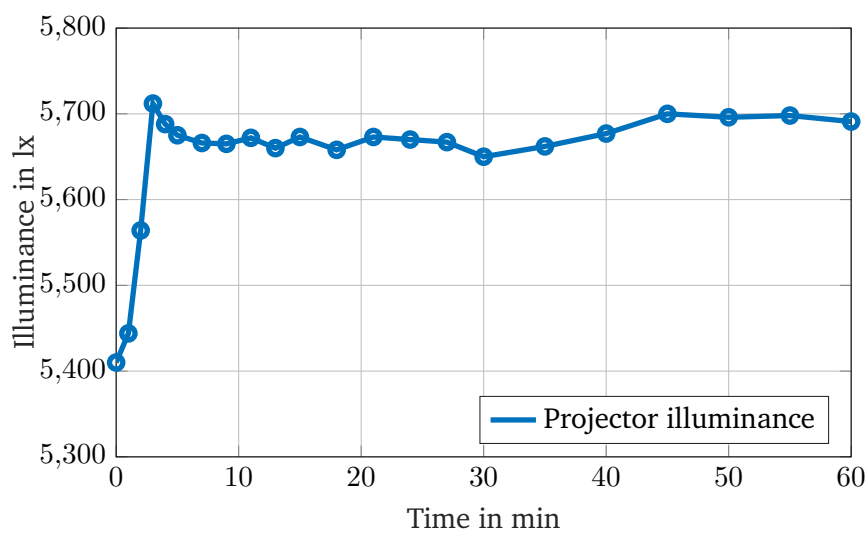


Figure C.1.: Burn-in time of the used projector [127] to guarantee a constant illumination and luminance of the displayed projections on the ground. The data is measured in darkness without other light sources lit.

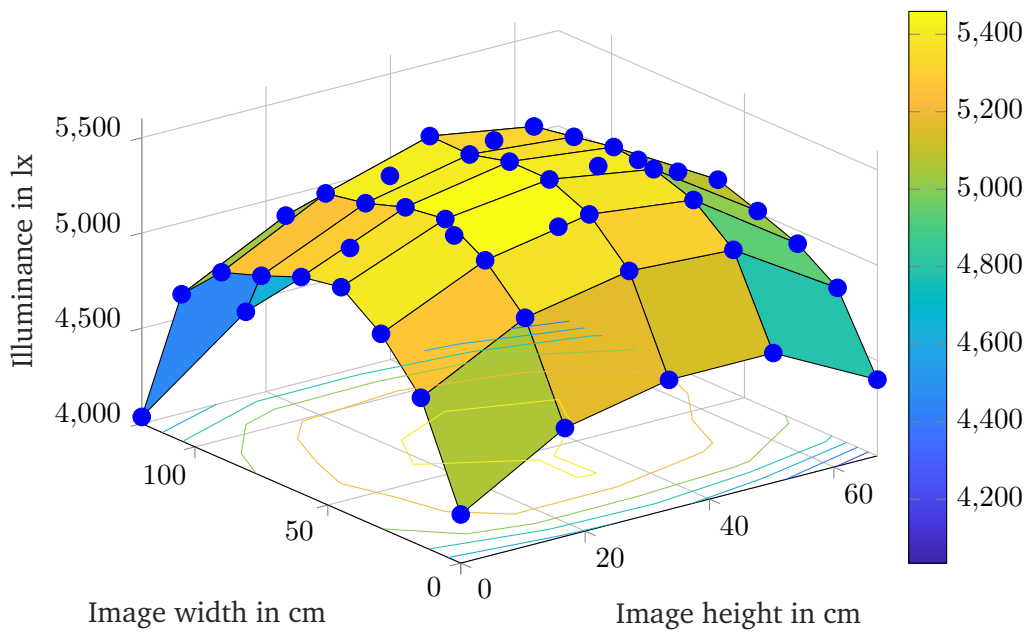


Figure C.2.: Illuminance surface plot of the projection on the ground of the maximal lit surface (1.2 m wide and 0.67 m height), which is illustrated schematically in Figure 3.8. In this case, the lit surface is projecting an all-white picture of the used LCD laser projector [127]. The blue dots mark the measured illuminance data points.

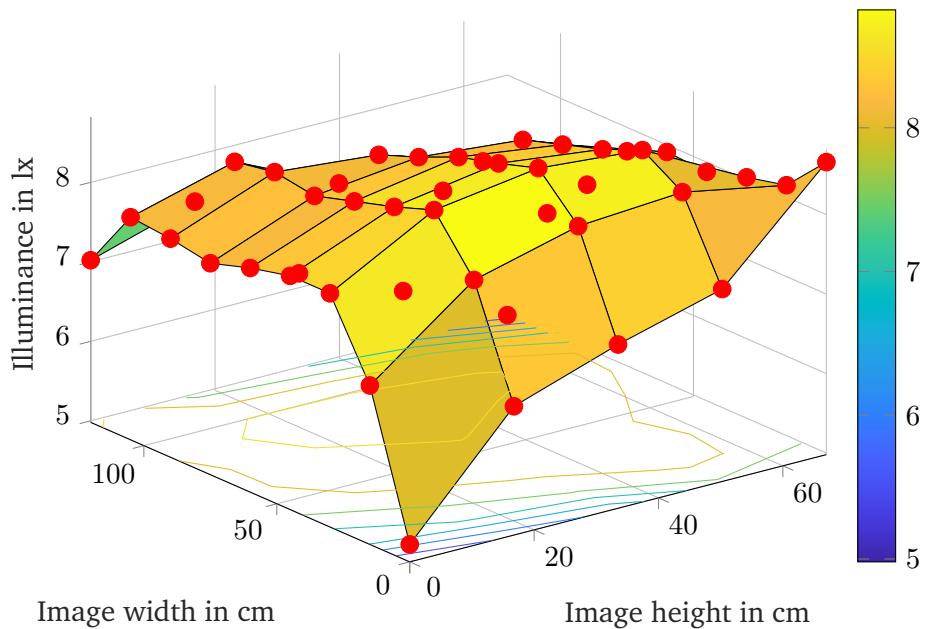


Figure C.3.: Illuminance surface plot of the projection on the ground of the maximal lit surface (1.2 m wide and 0.67 m height), which is illustrated schematically in Figure 3.8. In this case, the lit surface is projecting a black picture, which still adds some illuminance on the ground due to the technological limitations of the used LCD laser projector [127]. The red dots mark the measured illuminance data points.

## C.2. Measurements for the luminance coefficient and reflection of the surface materials

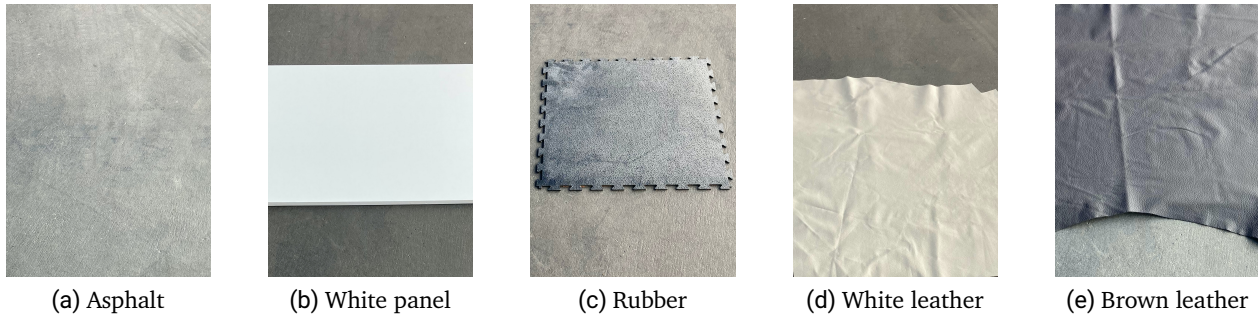


Figure C.4.: Appearance of the materials used for the luminance coefficient measurements and perception tests are listed above. The pictures are taken from a viewing distance of 1 m in the DLS.

Table C.1.: Measured target illuminance  $E_{\text{target}}$  and luminance  $L_{\text{target}}$  to obtain the luminance coefficient  $q$  of equation 5.2 for the PGS and DDS.

Scenario	Surface material	$E_{\text{target}}$ in lx	$L_{\text{target}, 0^\circ}$ in $\text{cd m}^{-2}$	$L_{\text{target}, 63.5^\circ}$ in $\text{cd m}^{-2}$
PGS	Asphalt	1585	43.86	44.22
	White panel	1609	633.1	592.5
	Rubber	1599	63.9	48.24
	Leather white	1599	237.1	232.7
	Leather brown	1599	27.72	27.73
DDS	Asphalt	1747	47.91	48.23
	White panel	1771	680.8	636.5
	Rubber	1761	65.98	50.85
	Leather white	1769	263.2	257.6
	Leather brown	1769	28.39	29.95

Table C.2.: Calculated luminance coefficient  $q$  for the measuring angles  $\gamma$  of  $0^\circ$  and  $63.5^\circ$  to obtain the reflection  $S$  with equation 5.2 for the PGS and DDS.

Scenario	Surface material	$q_{0^\circ, \text{scenario}}$ in $\text{cd m}^{-2} \text{lx}$	$q_{63.5^\circ, \text{scenario}}$ in $\text{cd m}^{-2} \text{lx}$	Reflection $S$
PGS	Asphalt	0,0277	0,0279	0,0896
	White panel	0,3935	0,3682	0,0831
	Rubber	0,0400	0,0302	0,0671
	Leather white	0,1483	0,1455	0,0872
	Leather brown	0,0173	0,0173	0,0889
DDS	Asphalt	0,0274	0,0276	0,0894
	White panel	0,3844	0,3594	0,0831
	Rubber	0,0375	0,0289	0,0685
	Leather white	0,1488	0,1456	0,0869
	Leather brown	0,0160	0,0169	0,0937

### C.3. Analysis of the perception test of the various surface materials

Table C.3.: Weber contrasts perceived in the pre-test for the perception of illuminance levels on various projection surfaces.

Intensity in %	White panel	Rubber	Asphalt	Leather brown	Leather white
<b>Weber contrast in 1 m</b>					
33.33	0.0270	0.0446	0.0255	0.0640	0.0746
34.51	0.0290	0.0451	0.0258	0.0655	0.0760
35.69	0.0305	0.0465	0.0290	0.0655	0.0774
36.86	0.0329	0.0479	0.0309	0.0676	0.0788
38.04	0.0337	0.0489	0.0296	0.0684	0.0802
39.22	0.0344	0.0504	0.0312	0.0690	0.0815
40.39	0.0368	0.0513	0.0322	0.0705	0.0843
41.57	0.0507	0.0532	0.0334	0.0719	0.0864
<b>Weber contrast in 5 m</b>					
33.33	0.0402	0.0803	0.0884	0.0053	0.0102
34.51	0.0405	0.0805	0.0886	0.0057	0.0106
35.69	0.0421	0.0808	0.0894	0.0065	0.0115
36.86	0.0438	0.0815	0.0912	0.0070	0.0125
38.04	0.0456	0.0818	0.0914	0.0078	0.0134
39.22	0.0466	0.0821	0.0918	0.0086	0.0134
40.39	0.0485	0.0834	0.0928	0.0090	0.0148
41.57	0.0504	0.0847	0.0929	0.0102	0.0161

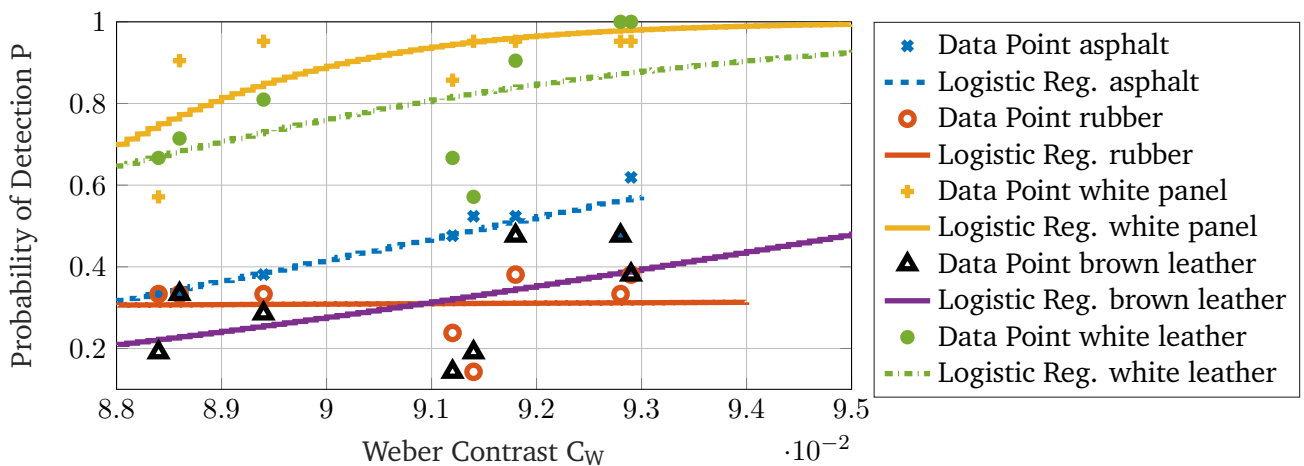


Figure C.5.: Analysis of the detection contrast of the test target for the five different projection surfaces at a 5 m viewing distance ( $N = 7$ ). The graph includes the detection probability for every contrast level for every projection material and the logistic regression fitted to the probability data (as indicated in equation 5.3). The tested projection materials are asphalt, rubber, a white panel (Figure 5.1c), and brown and white leather.



Table C.4.: Detection contrasts for a 90 %-threshold level of the fitted data in Figure 5.2 for a 5 m viewing distance of the five projection surfaces: asphalt, rubber, white panel, and brown and white leather.

Surface material	Weber contrast for a 90 %-threshold
Asphalt	0.10
Rubber	<b>42.18</b>
White panel	0.09
Brown leather	0.11
White leather	0.09

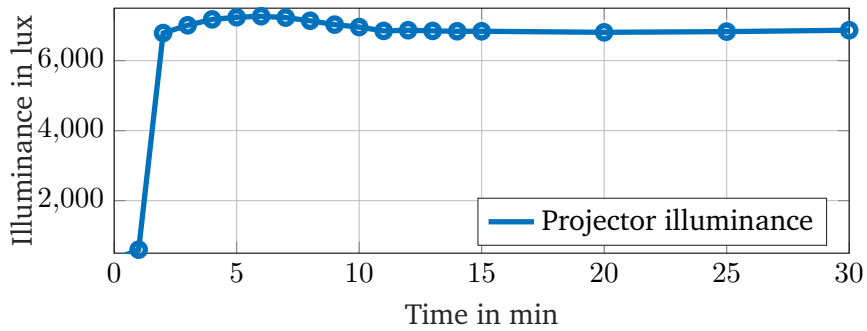


Figure C.6.: Burn-in behavior of the ambient lighting light sources (fluorescent lamps) of the testing environments for the DLS-dependent tests.

## C.4. Materials for the test procedure for direct and peripheral viewing of near-field projections



### Instruktion Wahrnehmung von Bodenprojektionen

In dieser Studie geht es um die Kontrastwahrnehmung einer Bodenprojektion im Nahfeld eines Fahrzeugs.

Die Studie gliedert sich in vier einzelne Versuche. Versuche Nr. 1A und Nr. 1B dienen der Detektionshäufigkeit. Bei Versuch Nr. 1C beurteilen Sie die subjektiv wahrgenommene Störung, die von einer Bodenprojektion ausgeht. Der gesamte Studienablauf gliedert sich in zwei Umgebungsbeleuchtungen: zuerst werden Versuche in dunklerer Umgebung und anschließend in hellerer Umgebung durchgeführt.

Vor Versuchsbeginn erhalten Sie einen ersten Fragebogen zur Angabe Ihrer persönlichen Daten. Damit sich Ihre Augen an die veränderte Umgebungsbeleuchtung gewöhnen, beantworten Sie diesen in einer dunkleren Umgebung.

Während des **Versuches Nr. 1A** werden Ihnen nacheinander Bodenprojektionen bei direktem Blick auf die Projektion und in verschiedenen Abständen präsentiert. Diese Projektionen befinden sich neben dem Fahrzeug auf der Beifahrerseite. Ihre Aufgabe ist es, anzugeben ob Sie eine Bodenprojektion detektieren konnten oder nicht. Die Detektion wird als erstmalige Wahrnehmung bzw. als das Bemerkten eines Lichteindrucks beschrieben. Es ist nicht relevant was bemerkt wurde, sondern ob etwas bemerkt wurde. Hierbei konzentrieren Sie sich nur darauf, ob Sie eine Projektion gesehen haben oder nicht. Die Wertigkeit der Projektion wird dabei außer Acht gelassen. Ihr Blick ist während des gesamten Versuchs auf die Bodenprojektion gerichtet. **Nachdem Sie den Signalton** gehört haben, geben Sie Ihre Antwort mit Hilfe der Ihnen vorliegenden Tastatur ein. Haben Sie die Bodenprojektion detektiert, drücken Sie die Taste „**Y**“ (**Ja**). Nehmen Sie nichts war, so drücken Sie die Taste „**N**“ (**Nein**). Für die Antworteingabe haben sie 1,5s lang Zeit. Dieser Versuch wird zu erst in dunklerer Umgebung und im späteren Versuchsablauf bei hellerer Umgebung durchgeführt.

**Versuch Nr. 1B** ist ähnlich zu Versuch Nr. 1A aufgebaut. Jedoch werden Ihnen hier Bodenprojektionen im äußeren, dem sogenannten peripheren Gesichtsfeld präsentiert. Während des Durchlaufs richten Sie Ihren Blick auf das rote Kreuz der jeweiligen Fixiermarke (A, B, C, D). Haben Sie die Bodenprojektion detektiert, drücken Sie nach dem Signalton die Taste „**Y**“ (**Ja**). Nehmen Sie nichts war, so drücken Sie die Taste „**N**“ (**Nein**). Dieser Versuch wird nur bei dunkler Umgebung durchgeführt.

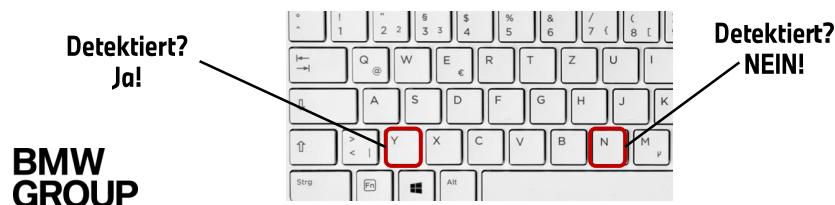


Figure C.7.: Illustration of the introduction text for the participants used in the contrast perception testing of the direct or peripheral location of the projection in the field of view in German.



## Instruktion

Ihre Aufgabe in diesem Teilversuch ist es, eine Bodenprojektion im peripheren Gesichtsfeld zu beurteilen. Diese subjektive Bewertung nehmen Sie unter Zuhilfenahme der untenstehenden Skala vor. Diese ermittelt die subjektiv wahrgenommene Störung und erstreckt sich über ein Intervall von 1 (unauffällig) bis 7 (störend).

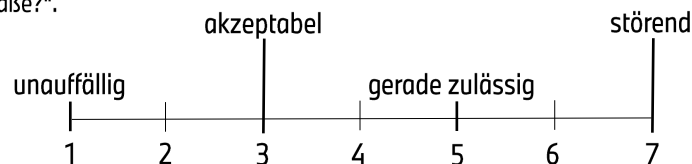
Vor Versuchsbeginn wird Ihnen eine Beispielprojektion gezeigt. Während des Versuchs werden Ihnen verschiedene Helligkeitsstufen einer Bodenprojektion präsentiert. Die Antwort geben Sie über die **obere Zahlenreihe der Tastatur** ein. Anschließend schauen Sie auf das rote Kreuz der entsprechenden Fixationsmarke (A, B, C, D). Der Versuch **startet nach drei aufeinander folgenden Tönen**. Im Versuchsablauf sehen Sie eine Bodenprojektion und im Anschluss hören Sie einen Ton. Nach diesem geben Sie Ihre Antwort ein. Dafür haben Sie etwa 8 Sekunden Zeit. Durchgeführt wird dieser Versuch bei dunklerer Umgebung.



Für die Bewertung der wahrgenommenen Störung stellen Sie sich bitte folgendes Szenario vor: Sie stehen an einem Zebrastreifen und möchten die Straße überqueren. In Ihrem Blickfeld befindet sich ein Auto mit geöffneter Türe, wobei ein Symbol auf die Straße projiziert wird. Sie können sich das Szenario wie in der nebenstehenden Abbildung vorstellen.



Bewerten Sie die Bodenprojektion im folgenden Versuch unter Berücksichtigung des folgenden Aspekts: „Stört mich die Bodenprojektion beim Überqueren der Straße?“.



**BMW  
GROUP**

Figure C.8.: Illustration of the introduction text for the participants used in the subjective contrast evaluation testing in German.

## C.5. Detailed illuminance, luminance and Weber contrast measurements for the contrast perception tests

Table C.5.: Used grayscale intensities with the resulting illuminances and Weber contrasts of the **symbol-based projections** in the **PGS** at viewing distances of 1 m and 5 m. Weber contrasts marked with a dash are not measured since these contrasts are not relevant to the conducted tests.

Grayscale intensity in %	Illuminance in lx	Weber contrast, 1 m	Weber contrast, 5 m
1.96	22.98	0.0319	-
2.35	23.15	0.0293	-
2.75	23.3	0.0268	0.0029
3.14	23.79	0.0084	0.0142
3.53	24.45	0.0162	0.0291
3.92	25.36	-	0.0453
4.31	26.55	0.0781	0.0748
5.10	28.21	0.1378	0.1131
5.88	30.9	0.2256	0.1563
6.67	34.6	0.3591	0.2445
7.45	39.1	-	0.3421
8.24	40.1	-	0.4127
13.33	79.3	2.07	1.434
20.00	180.2	5.84	3.906
26.67	317	10.42	7.135
27.84	351	-	7.575
29.02	386	-	8.437
30.20	423	-	8.967
31.37	452	-	9.817
32.55	477	-	10.61
33.33	500	15.96	11.09
33.73	512	-	12.24
34.90	541	-	12.08
40.00	729	22.14	16.02
46.67	1009	28.03	21.07
53.33	1341	33.85	26.13
60.00	1703	39.29	31.1
66.67	2093	44.05	35.97
73.33	2510	48.36	40.89
80.00	2980	52.57	45.59
86.67	3520	56.91	50.51
93.33	3970	60.24	54.21
100.00	4500	59.77	57.99

Table C.6.: Used grayscale intensities with the resulting illuminances and Weber contrasts of the **text-based projections** in the **PGS** at viewing distances of 1 m and 5 m. Weber contrasts marked with a dash are not measured since these contrasts are not relevant to the conducted tests.

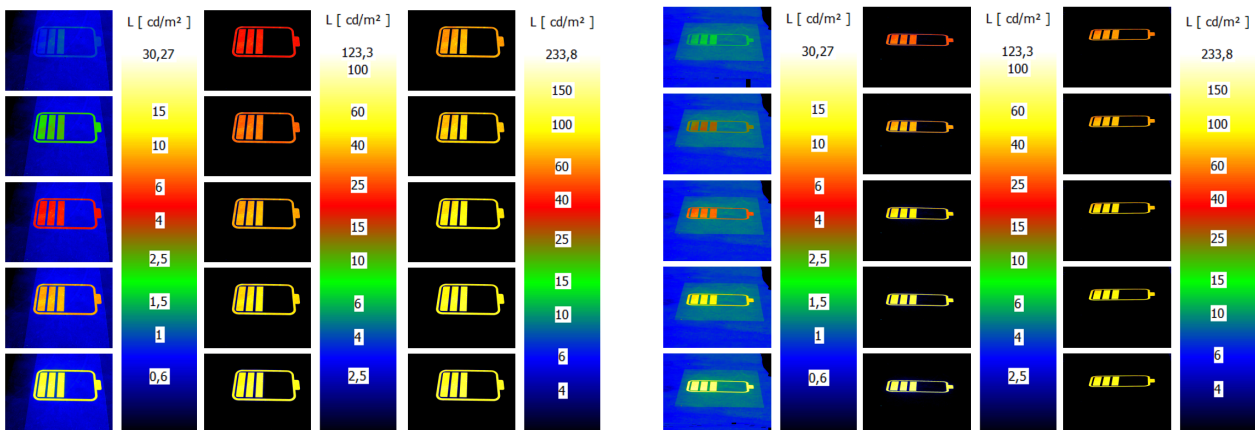
Grayscale intensity in %	Illuminance in lx	Weber contrast, 1 m	Weber contrast, 5 m
2.75	23.3	0.0365	-
3.14	23.79	0.0548	-
3.53	24.45	0.0765	0.0606
3.92	25.36	0.1034	0.0748
4.31	26.55	0.1394	0.0978
4.71	27.39	-	0.1191
5.10	28.21	0.2036	0.1296
5.88	30.9	0.2813	0.1644
6.67	34.6	0.4018	0.2328
7.45	39.1	-	0.3105
13.33	79.3	2.014	1.131
20.00	180.2	5.403	2.952
26.67	317	9.718	5.394
33.33	500	14.92	8.415
40.00	729	21.31	12.43
46.67	1009	27.98	16.7
53.33	1341	34.44	21.12
60.00	1703	40.8	25.95
66.67	2093	46.79	30.63
73.33	2510	52.78	35.13
80.00	2980	58.26	40.16
86.67	3520	64.47	45.38
93.33	3970	68.75	49.29
100.00	4500	73.06	53.59

Table C.7.: Used grayscale intensities with the resulting illuminances and Weber contrasts of the **symbol-based projections** in the **DLS** at viewing distances of 1 m and 5 m. Weber contrasts marked with a dash are not measured since these contrasts are not relevant to the conducted tests.

Grayscale intensity in %	Illuminance in lx	Weber contrast, 1 m	Weber contrast, 5 m
20.78	9440	0.0202	-
21.96	9470	0.0292	0.0404
23.14	9500	0.0260	0.0423
24.31	9520	0.0269	0.0376
25.49	9550	0.0338	0.0390
26.67	9580	0.0327	0.0404
27.84	9610	0.0347	0.0433
29.02	9650	0.0386	0.0455
30.20	9670	0.0412	0.0466
31.37	9720	0.0453	0.0489
32.55	9760	0.0411	0.0533
33.73	9800	-	0.0556
34.90	9840	-	0.0581
36.08	9880	-	0.0570
37.25	9930	-	0.0631
38.43	9970	-	0.0644
39.61	10020	-	0.0675
40.78	10060	-	0.0665
41.96	10120	-	0.0735
43.14	10170	-	0.0763
44.31	10220	-	0.0795
45.49	10166	-	0.0825
46.67	10268	-	0.0867
47.84	10324	-	0.0814

Table C.8.: Used grayscale intensities with the resulting illuminances and Weber contrasts of the **text-based projections** in the **DLS** at viewing distances of 1 m and 5 m. Weber contrasts marked with a dash are not measured since these contrasts are not relevant to the conducted tests.

Grayscale intensity in %	Illuminance in lx	Weber contrast, 1 m	Weber contrast, 5 m
21.57	9220	0.0539	-
22.75	9230	0.0731	-
23.92	9260	0.0759	-
25.10	9280	0.0891	-
26.27	9300	0.0911	-
27.45	9330	0.0938	-
28.63	9350	0.0959	-
29.80	9380	0.0993	0.0506
30.98	9400	0.1013	0.0514
32.16	9430	0.1047	0.0523
33.33	9460	0.1074	0.0532
34.51	9490	-	0.0542
35.69	9510	-	0.0555
36.86	9550	-	0.0568
38.04	9730	-	0.0543
39.22	9764	-	0.0697
40.39	9775	-	0.0753
41.57	9829	-	0.0787

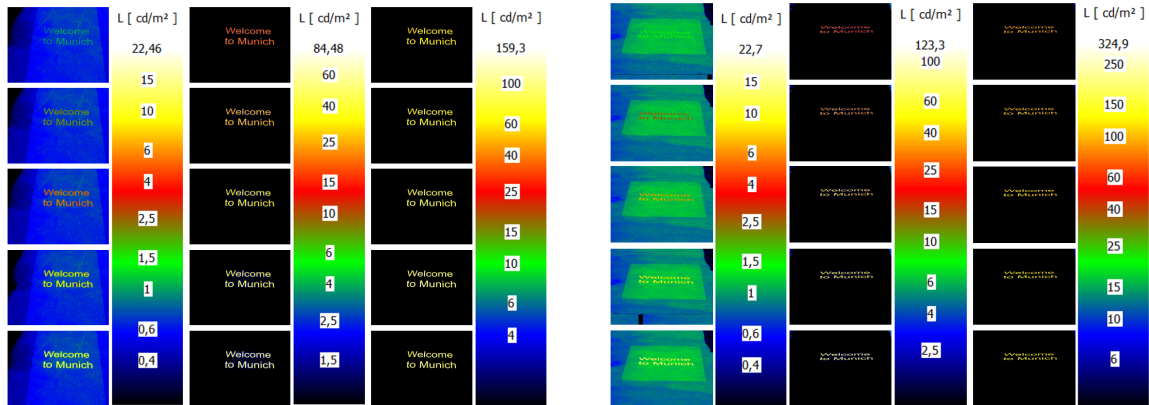


(a) Shown grayscale for symbol-based projection in % in 1 m, from top to bottom, from right column to left column: 6.67, 13.33, 20, 26.67, 33.33, 40, 46.67, 53.33, 60, 66.67, 73.33, 80, 81.57, 92.94, 100

(b) Shown grayscale for symbol-based projection in % in 5 m, from top to bottom, from right column to left column: 6.67, 13.33, 20, 26.67, 33.33, 40, 46.67, 53.33, 60, 66.67, 73.33, 80, 81.57, 92.94, 100

Figure C.9.: Luminance images of the symbol-based projection content for determining the contrast thresholds at the distances 1 m and 5 m in the PGS.

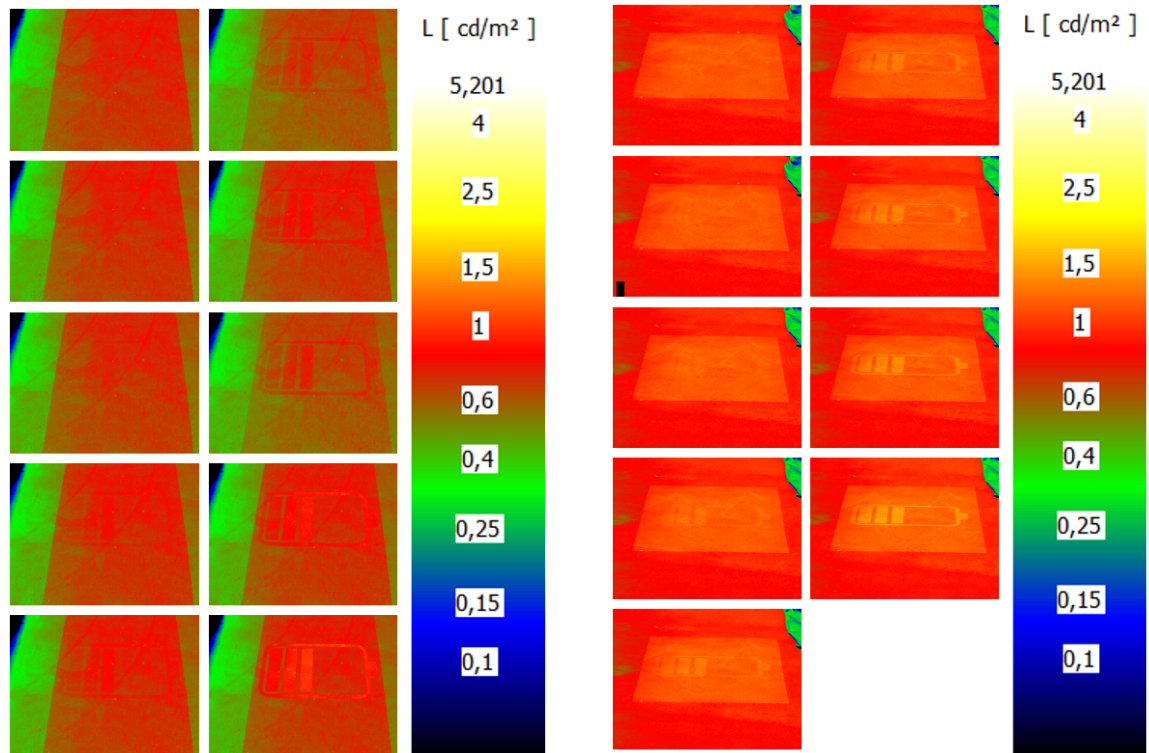




(a) Shown grayscale for text-based projection in % in 1 m, from top to bottom, from right column to left column: 6.67, 13.33, 20, 26.67, 33.33, 40, 46.67, 53.33, 60, 66.67, 73.33, 80, 81.57, 92.94, 100

(b) Shown grayscale for text-based projection in % in 5 m, from top to bottom, from right column to left column: 6.67, 13.33, 20, 26.67, 33.33, 40, 46.67, 53.33, 60, 66.67, 73.33, 80, 81.57, 92.94, 100

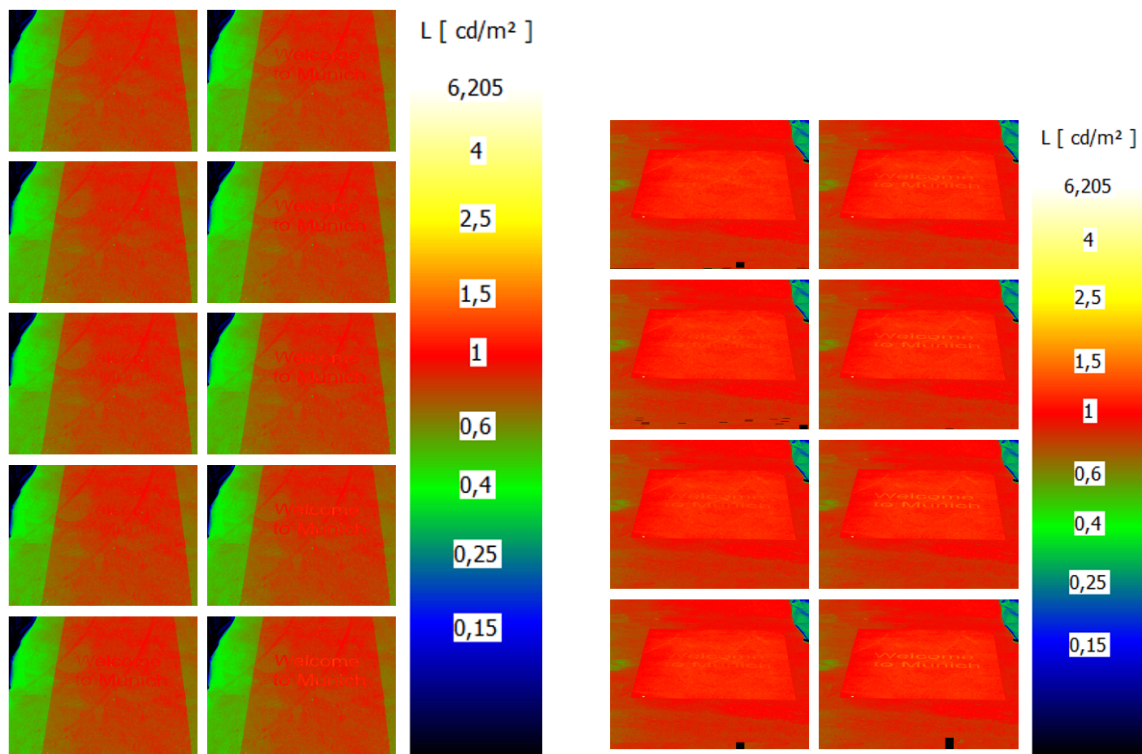
Figure C.10.: Luminance images of the text-based projection content for determining the contrast thresholds at the distances 1 m and 5 m in the PGS.



(a) Shown grayscale in %, from top to bottom, from right column to left column: 1.96, 2.35, 2.75, 3.14, 3.53, 3.92, 4.31, 4.71, 5.10 and 5.49

(b) Shown grayscale in %, from top to bottom, from right column to left column: 2.35, 2.75, 3.14, 3.53, 3.92, 4.31, 4.71, 5.10 and 5.49

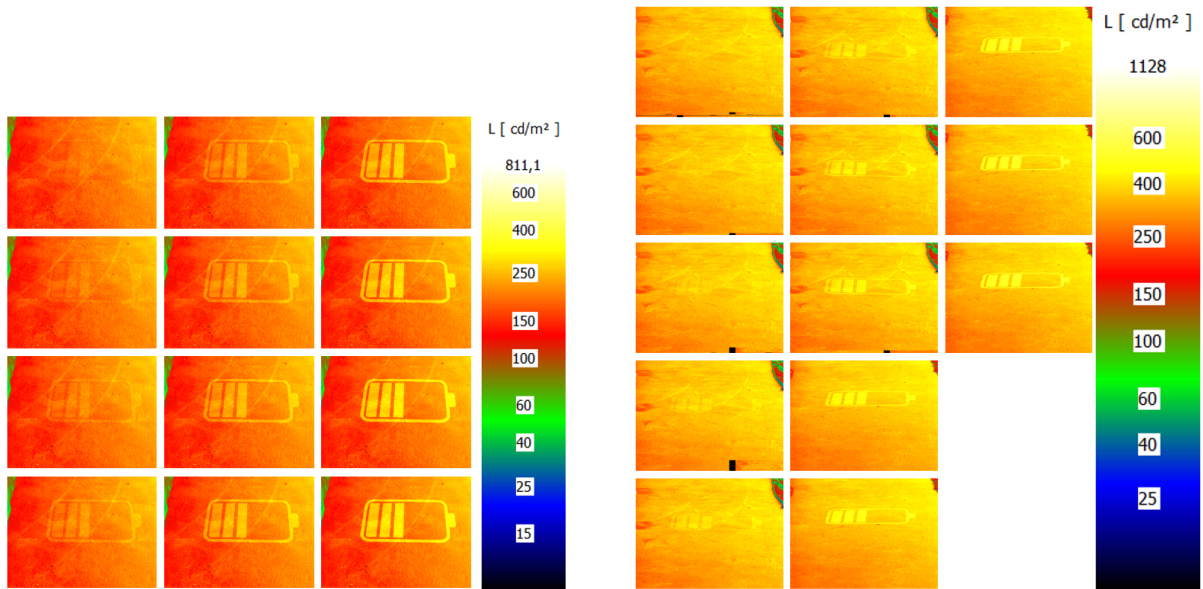
Figure C.11.: Luminance measurement of the symbol-based projection to determine the detection threshold at the viewing distances of 1 m (a) and 5 m (b) in the PGS.



(a) Shown grayscale in %, from top to bottom, from right column to left column: 2.35, 2.75, 3.14, 3.53, 3.92, 4.31, 4.71, 5.10, 5.49, and 5.88

(b) Shown grayscale in %, from top to bottom, from right column to left column: 3.14, 3.53, 3.92, 4.31, 4.71, 5.10, 5.49, and 5.88

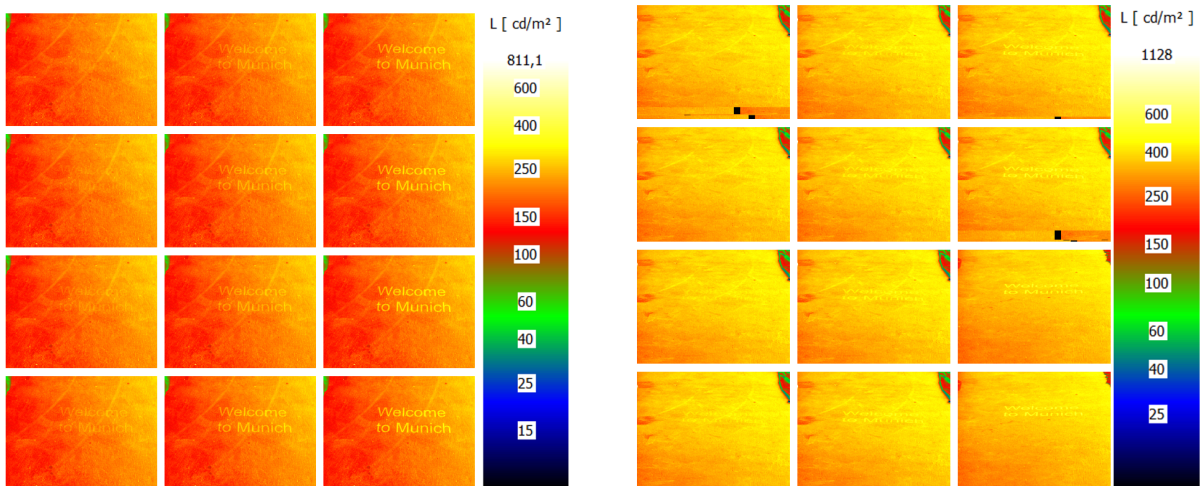
Figure C.12.: Luminance measurement of the text-based projection to determine the detection threshold at the viewing distances of 1 m (a) and 5 m (b) in the PGS.



(a) Shown grayscale for symbol-based projection in % in 1 m, from top to bottom, from right column to left column: 26.67, 33.33, 40, 46.67, 53.33, 60, 66.67, 73.33, 80, 81.57, 92.94, 100

(b) Shown grayscale for symbol-based projection in % in 5 m, from top to bottom, from right column to left column: 20, 26.67, 33.33, 40, 46.67, 53.33, 60, 66.67, 73.33, 80, 81.57, 92.94, 100

Figure C.13.: Luminance measurement of the symbol-based projection content for determining the contrast thresholds at the distances 1 m and 5 m in the DLS.



(a) Shown grayscale for text-based projection in % in 1 m, from top to bottom, from right column to left column: 26.67, 33.33, 40, 46.67, 53.33, 60, 66.67, 73.33, 80, 81.57, 92.94, 100

(b) Shown grayscale for text-based projection in % in 5 m, from top to bottom, from right column to left column: 26.67, 33.33, 40, 46.67, 53.33, 60, 66.67, 73.33, 80, 81.57, 92.94, 100

Figure C.14.: Luminance measurement of the text-based projection content for determining the contrast thresholds at the distances 1 m and 5 m in the DLS.

## D. Additional analysis for contrast and brightness perception testing of near-field projections

### D.1. Statistical analysis for dependencies of contrast perception testing

Table D.1.: Chi-square analysis defines the statistical effects of projection content, and viewing distance, for mesopic and photopic testing environments. The Table also includes the related effect size (Cramer's V).

Compared items		mesopic	photopic
Projection content	Text 1 m x Symbol 1 m	$\chi^2(7) = 83.73, p < 0.05,$ $V = 0.25$	$\chi^2(7) = 4.36, p > 0.05,$ $V = 0.05$
	Text 5 m x Symbol 5 m	$\chi^2(7) = 12.56, p > 0.05,$ $V = 0.09$	$\chi^2(7) = 1.38, p > 0.05,$ $V = 0.03$
		Text	Symbol
Viewing distance	1 m x 5 m mesopic	$\chi^2(7) = 7.33, p > 0.05,$ $V = 0.07$	$\chi^2(7) = 47.44, p < 0.05,$ $V = 0.19$
	1 m x 5 m photopic	$\chi^2(7) = 4.44, p > 0.05,$ $V = 0.06$	$\chi^2(7) = 0.56, p > 0.05,$ $V = 0.02$

Table D.2.: Chi-square analysis defines the statistical effects of projection's display mode in 1 m viewing distance for mesopic and photopic testing environments. The mode 3 Hz relates to the dynamic display of the projection for 2 s, and the other two variations are in static mode for either 350 ms and 2000 ms projection's display duration.

Compared items		mesopic	photopic
Display mode	3 Hz x 350 ms	$\chi^2(7) = 5.89, p > 0.05$	$\chi^2(7) = 1.37, p > 0.05$
	3 Hz x 2000 ms	$\chi^2(7) = 8.72, p > 0.05$	$\chi^2(7) = 1.12, p > 0.05$
	350 ms x 2000 ms	$\chi^2(7) = 3.03, p > 0.05$	$\chi^2(7) = 0.35, p > 0.05$

## D.2. Additional analysis for direct viewing of near-field projections

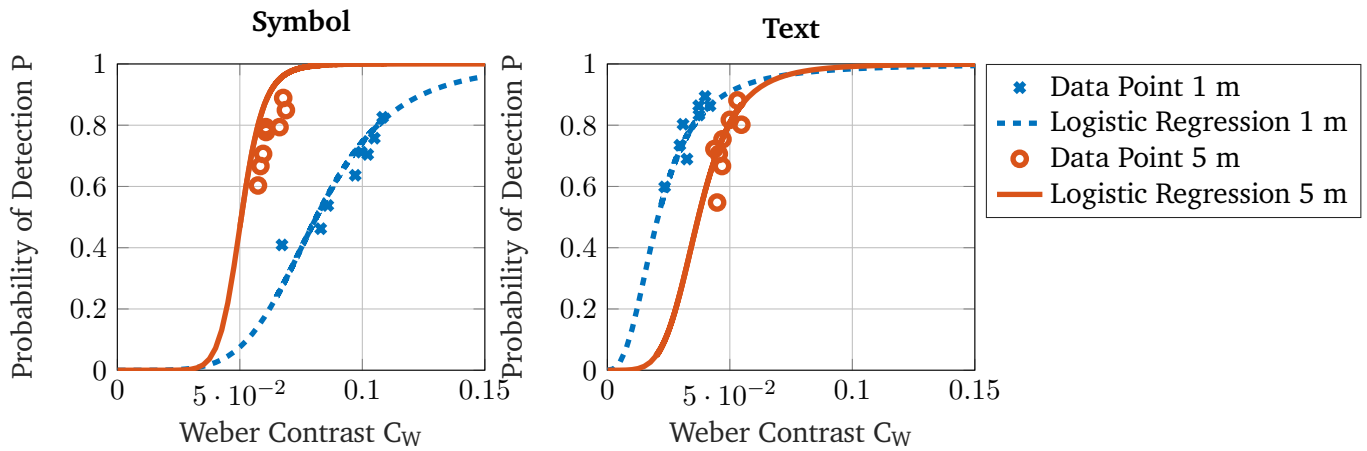


Figure D.1.: Logistic regression with the corresponding data points of the detection probability per Weber contrast value for the photopic setting ( $235 \text{ cd m}^{-2}$ ) of a symbol- (on the left) and text-based (on the right) projection analyzed for the Weber contrast of direct viewing. The graphs include the variation of 1 m and 5 m viewing distances.

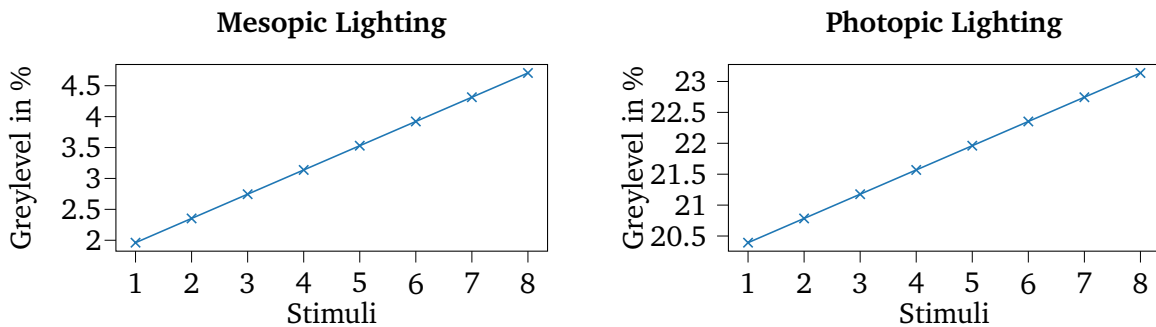


Figure D.2.: Overview of the eight stimuli presented in mesopic scenario ( $0.6 \text{ cd m}^{-2}$ ) on the left and photopic scenario ( $210 \text{ cd m}^{-2}$ ) on the right for the greyscale in % of the displayed content in section 6.1.4.

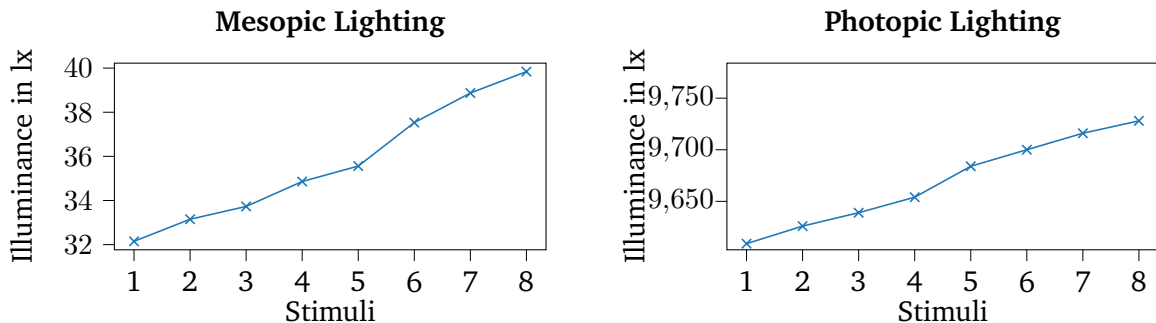


Figure D.3.: Overview of the eight stimuli presented in the mesopic scenario ( $0.6 \text{ cd m}^{-2}$ ) on the left and the photopic scenario ( $210 \text{ cd m}^{-2}$ ) on the right for the illuminance levels in lx of section 6.1.4.

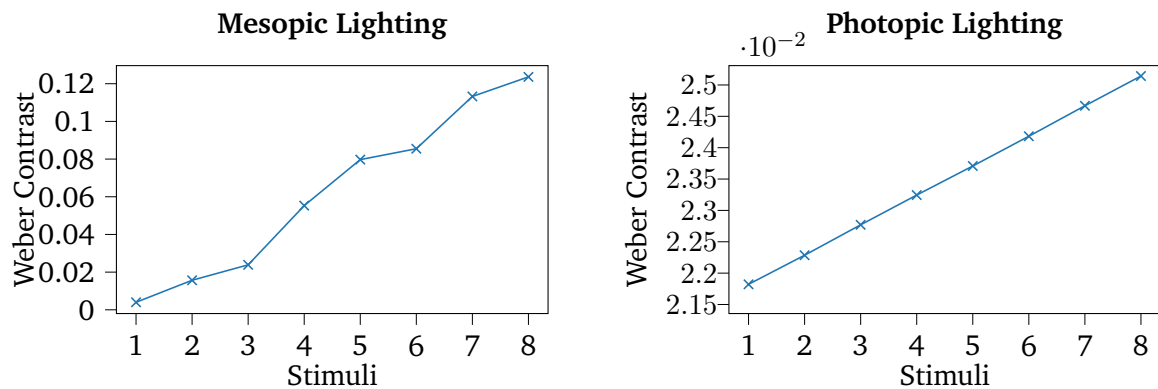


Figure D.4.: Overview of the eight stimuli presented in the mesopic scenario ( $0.6 \text{ cd m}^{-2}$ ) on the left and the photopic scenario ( $210 \text{ cd m}^{-2}$ ) on the right for the Weber contrast on the y-axis in section 6.1.4.

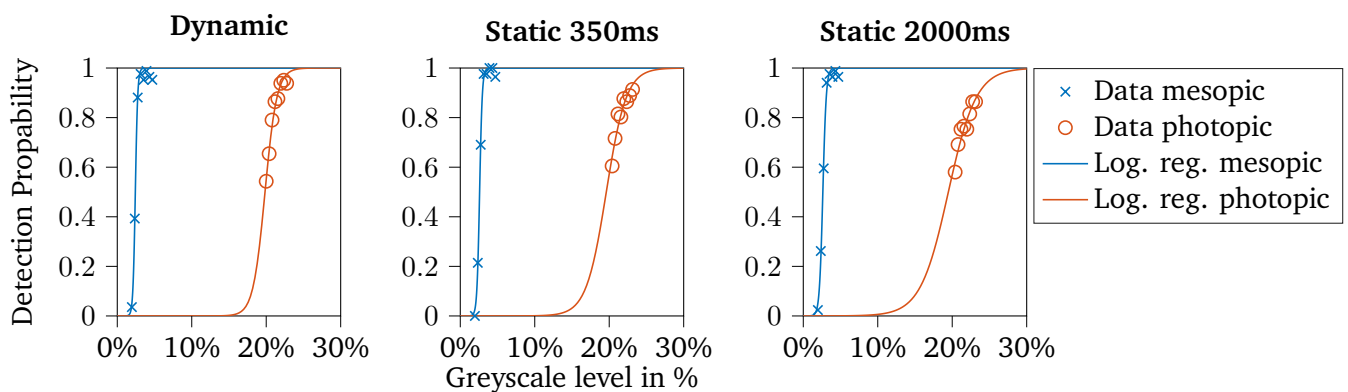


Figure D.5.: Logistic regression curves and data points of the detection probability percentages for the various environmental scenarios for the different presentation times, the graph on the top: dynamic, in the middle: static 2000 ms, and the lowest graph: 350 ms based on the greyscale percentages.

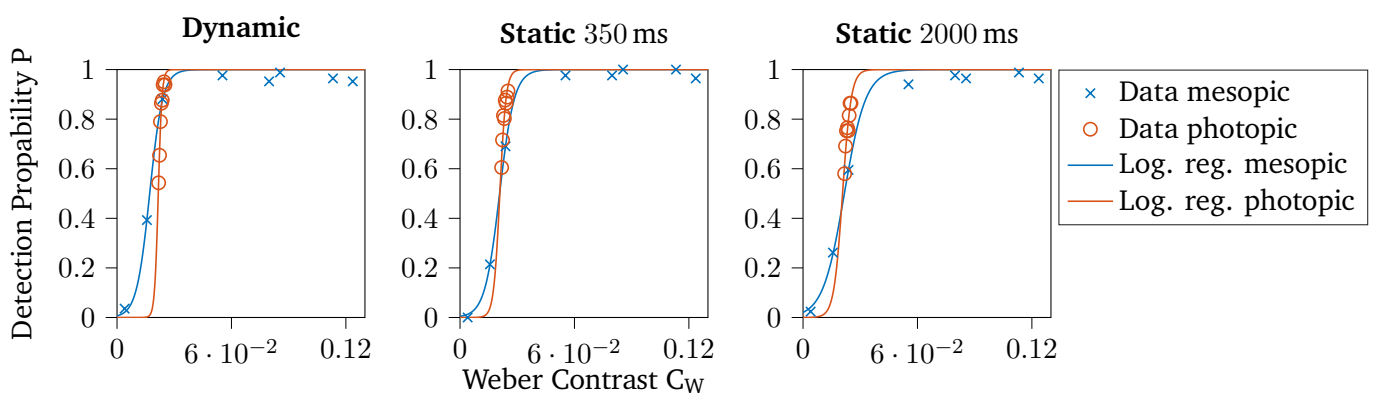


Figure D.6.: Logistic regression fits and data points for the detection probability percentages of the various environmental scenarios for the different presentation times, the graph on the top: dynamic, in the middle: static 2000 ms, and the lowest graph: 350 ms based on the Weber contrast.



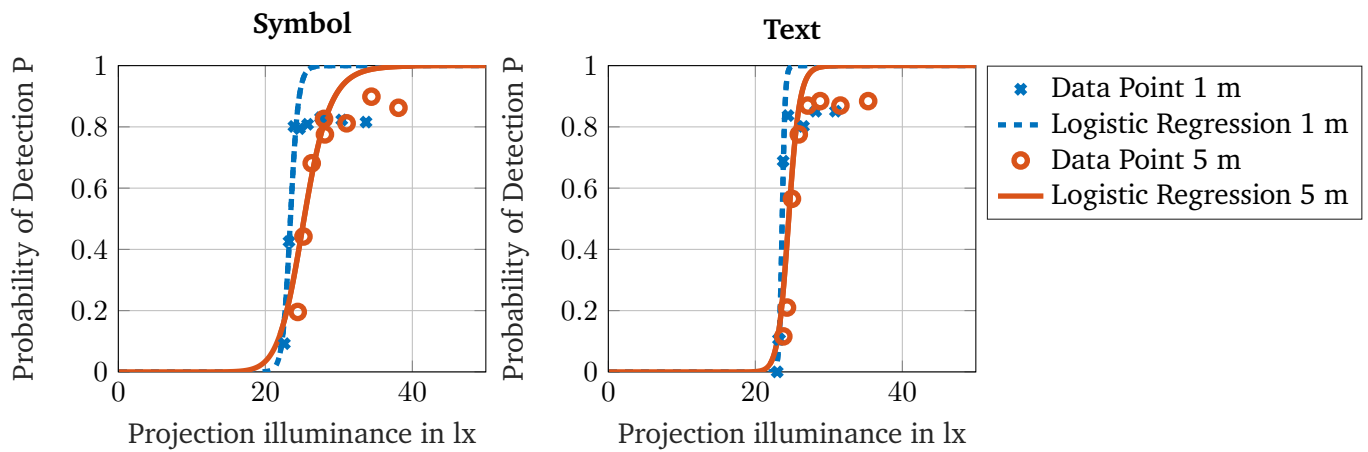


Figure D.7.: An applied logistic regression with the related data points of the detection probability per illuminance level of the projection for the mesopic (approx.  $0.6 \text{ cd m}^{-2}$ ) environmental setting of a symbol- and text-based projection. The x-axis displays the projection's illuminance level for direct viewing of the projection with the variation of 1 m and 5 m viewing distances.



---

## Publications and patents

---

The following is a list of my publications and patents, some of whose ideas and results have been incorporated into this thesis. Furthermore, some ideas and contents of this thesis may have already appeared in one of the publications listed below.

### Publications

- Corresponding author of **Challenges of Digital Projections in the Vehicle's Interior and Exterior** in *ISAL 2023* proceedings
- Co-author of **Near-field projections - How dynamic affects the detection threshold** in *ISAL 2023* proceedings
- Corresponding author of **An analysis of visibility requirements and reaction times of near-field projections** in *MDPI Applied Sciences* handed in on 5. August 2023 (currently in review)
- Corresponding author of **Resolution Aspects for Near-Field Projections** in *MDPI Applied Sciences*
- Corresponding author of **Review of user's evaluation and the needs for road projections around the vehicle** in *VISION 2022* proceedings
- Co-author of **Behaviour of Automated Vehicles in Critical Situations with Pedestrians** in *VISION 2021* proceedings
- Corresponding author of **Analysis and definition of resolution requirements for projections in the near field of a vehicle** in *ISAL 2021* proceedings
- Corresponding author of **Analysis and classification of road user behavior patterns in megacities and suggestions for additional light signals for automated vehicles in future mixed traffic scenarios** in *ISAL 2019* proceedings
- Corresponding author of **Analysis and definition of potential conflict situations between automated vehicles and other road users in megacities** in *IFAL 2019* proceedings
- Co-author of **Polymer materials for cost-efficient manufacturing of electrothermal actuators** in *ACTUATOR 2018* proceedings

---

## Patents

- **DE102021116678A1**: Kraftfahrzeug mit einer digitalen Projektionseinheit und Verfahren zum Betreiben eines Kraftfahrzeugs
- **DE102021116809A1**: Kraftfahrzeug mit einer Projektionseinheit und Verfahren zum Betreiben eines Kraftfahrzeugs
- **DE102021134193A1**: Projektionsvorrichtung und Fahrzeug
- **DE102022106328A1**: Fortbewegungsmittel, Vorrichtung und Verfahren zur Ausgabe einer Information an einen Anwender eines Fortbewegungsmittels
- **DE102022110004A1**: Fortbewegungsmittel und Anordnung zur Unterhaltung eines Insassen eines Fortbewegungsmittels
- **WO002023274704A1**: Motor vehicle comprising an digital projection unit, and method for operating a motor vehicle
- **WO002023174595A1**: Means of transportation, and device and method for outputting information to a user of a means of transportation